The Dissertation/Thesis/Capstone Committee for Anna Nia Certifies that this is the approved version of the following Dissertation:

Efficient Identification and Comprehension of Molecular Pathways Associated with Irradiation Induced Hepatic Carcinogenesis

Committee:

Mark Emmett, Ph.D., Supervisor

George Golovko, Ph.D., Chair

Daniel Jupiter

Daniel Jupiter, Ph.D.

Steven Widen, Ph.D.

Hosein Mohimani

Hosein Mohimani, Ph.D.

Efficient Identification and Comprehension of Molecular Pathways Associated with Irradiation Induced Hepatic Carcinogenesis

by

Anna Nia, B.S., M.S.

Dissertation

Presented to the Faculty of the Graduate School of

The University of Texas Medical Branch

in Partial Fulfillment

of the Requirements

for the Degree of

Doctor of Philosophy

The University of Texas Medical Branch

March 2020

Dedication

To my beloved parents, who have always been a source of inspiration, encouragement, and stamina to undertake my higher studies

Acknowledgements

I would like to acknowledge everyone who played a role in my academic accomplishments. First of all, my parents, and my brother, who supported me with love and understanding without whom I could not have accomplished this. Additionally, my committee members, each of whom has provided patient advice and guidance throughout the research process. Thank you all for your unwavering support.

My work has been supported by Ground-Based Studies in Space Radiobiology through the National Aeronautics and Space Administration NASA (NNX15AD65G). The funders did not participate in the design of the study, collection, analysis, or interpretation of data, or in writing of the current material.

Chapter 2 is a version of a manuscript published in *BMC Bioinformatics*. **Nia, A.M.**, Chen, T., Barnette, B.L., Khanipov, K., Ullrich, R.L., Bhavnani, S., Emmett, M.R. (2020), "Efficient Identification of Multiple Pathways: RNA-Seq Analysis of Livers from ^{56}Fe Ion Irradiated Mice", *BMC Bioinformatics*, DOI: 10.1186/s12859-020-3446-5.

Chapter 3 is a version of a manuscript currently in submission and under review at *BMC Genomics*. **Nia, A.M.**, Khanipov, K., Barnette, B.L., Ullrich, R.L., Golovko, G., Emmett, M.R. (2020), "Comparative RNA-Seq transcriptome analyses reveal dynamic time dependent effects of ^{56}Fe, ^{16}O, and ^{28}Si irradiation on the induction of murine hepatocellular carcinoma", *BMC Genomics*, DOI: 10.21203/rs.3.rs-17127/v1.

Chapter 4 is a version of a manuscript currently in preparation for submission to *Journal of the American Society for Mass Spectrometry (JASMS)*. **Nia, A.M.**, Shavkunov, A., Ullrich, R.L., Emmett, M.R. (2020), "^{137}Cs γ ray and ^{28}Si Irradiation Induced Murine

Hepatocellular Carcinoma Lipid Changes in Liver Assessed by MALDI-MSI Combined with Spatial Shrunken Centroid Clustering Algorithm", *Journal of the American Society for Mass Spectrometry (JASMS)*.

Efficient Identification and Comprehension of Molecular Pathways Associated with Irradiation Induced Hepatic Carcinogenesis

Publication No._____

Anna Nia, M.D., Ph.D.

The University of Texas Medical Branch, 2020

Supervisor: Mark R. Emmett

As human exploration into deep space continues to expand in the future, risk prediction for irradiation-induced diseases will become an increasingly important task. It will be critical to identify the biological effects of high-charge, high energy (HZE) and low energy ^{137}Cs γ rays, which are the major components of space irradiation on the human body during longer stay in deep space, including a mission to Mars. It has been shown that there is a significant increase in incidence of Hepatocellular carcinoma (HCC), after exposure to low dose HZE. There is, however, limited knowledge of the effects of low dose irradiation on the formation of HCC. To address this gap in knowledge, RNA-Seq and MALDI-MSI were used to assess the effects of space irradiation on the pathogenesis of HCC. In particular, RNA-seq was used to determine transcriptional changes, and MALDI-MSI to determine lipid changes, in the hepatic microenvironment of ion irradiated compared to non-irradiated controls, in two different strains of mice, at five different time points post-irradiation. For our RNA-Seq datasets, we first present a novel pipeline to perform gene co-expression network analysis, and use this to show that mitochondrial pathways are dysregulated in response to ^{56}Fe irradiation compared to non-irradiated

control, in the wildtype mouse strain (C57BL/6NCrl.) Next we performed a comparative transcriptomic analysis in a mouse model for irradiation-induced HCC (C3H/HeNCrl), in order to assess the carcinogenic effects of 600 MeV/n ^{56}Fe (0.2 Gy), 1 GeV/n ^{16}O (0.2 Gy), and 350 MeV/n ^{28}Si (0.2 Gy), compared to non-irradiated control. Our data demonstrated a clear difference in the effects of these HZE ions, particularly immunological, suggesting different molecular mechanisms of tumorigenesis for each ion. Additionally, we observed novel, functionally unannotated transcripts that were significantly affected by HZE. The biological functions of these transcripts were investigated using Self-Organizing Maps (SOMs). Finally, we used MALDI-MSI to identify lipid changes 12 months post-exposure to low dose ^{28}Si and ^{137}Cs γ rays' irradiation. We identified a number of lipid species; in particular, we have confirmed the identity of GSL; which is of special interest because its upregulation have been reported in patients with HCC.

Table of Contents

1 LIST OF TABLES

2 LIST OF FIGURES

3 LIST OF ABBREVIATIONS

GCR	Galactic Cosmic Ray
HZE	High Charge High Energy Ions
HCC	Hepatocellular Carcinoma
IPA	Ingenuity Pathway Analysis
LEO	Low Earth Orbit
MALDI-MSI	Matrix-Assisted Laser Desorption Ionization-Mass Spectrometry Imaging
SOM	Self Organizing Map
UTMB	University of Texas Medical Branch
WGCNA	Weighted Gene Co-Expression Network Analysis
WGCNA-M	Weighted Gene Co-Expression Network Analysis Modularity Maximization

4 CHAPTER 1: BACKGROUND

4.1 History

Apollo 17's twelve-day journey to the moon in 1972 remains the most recent time that humans have traveled beyond Earth's protective magnetic field. Space exploration is an important effort, with the potential for discoveries that will benefit humankind, [1] though these benefits come with certain risks for astronauts. A mission to Mars could last up to 3 years, which would lead to a significant amount of whole-body irradiation. Thus, as NASA now prepares for human exploration into deep space, risk prediction and intervention for irradiation-induced diseases will become increasingly important.

As of today, the main health concerns for manned deep space flights are exposure to galactic cosmic rays (GCR) and solar particle events (SPE), which can lead to late-occurring cancers and degenerative diseases. [2] Spacecraft in deep space are not shielded by the Earth's magnetic field or the solid shielding of the planet. Hence, they are exposed to transient irradiation from SPE and high-charge, high energy (HZE) radiation, which are considered to play important roles in the pathophysiology of irradiation-induced cancers. GCR include both low-linear-energy transfer (LET) such as γ rays, which are sparsely ionizing, as well as HZE ions (high LET) such as ^{56}Fe, ^{28}Si, and ^{16}O. [3] Long-duration space missions, such as a mission to Mars, are expected to expose astronauts to substantial cumulative low energy γ rays and HZE irradiation, that are serious health concerns. [4, 5] A necessary step to understanding and assessing these health concerns is investigating the molecular mechanisms instigated by these types of radiation, and which lead to carcinogenesis and degenerative processes that are part of cancer initiation and

progression. Elucidating mechanisms of carcinogenesis due to irradiation may allow the identification of countermeasures and treatments for disrupted pathways and molecular signaling. (Figure 1)

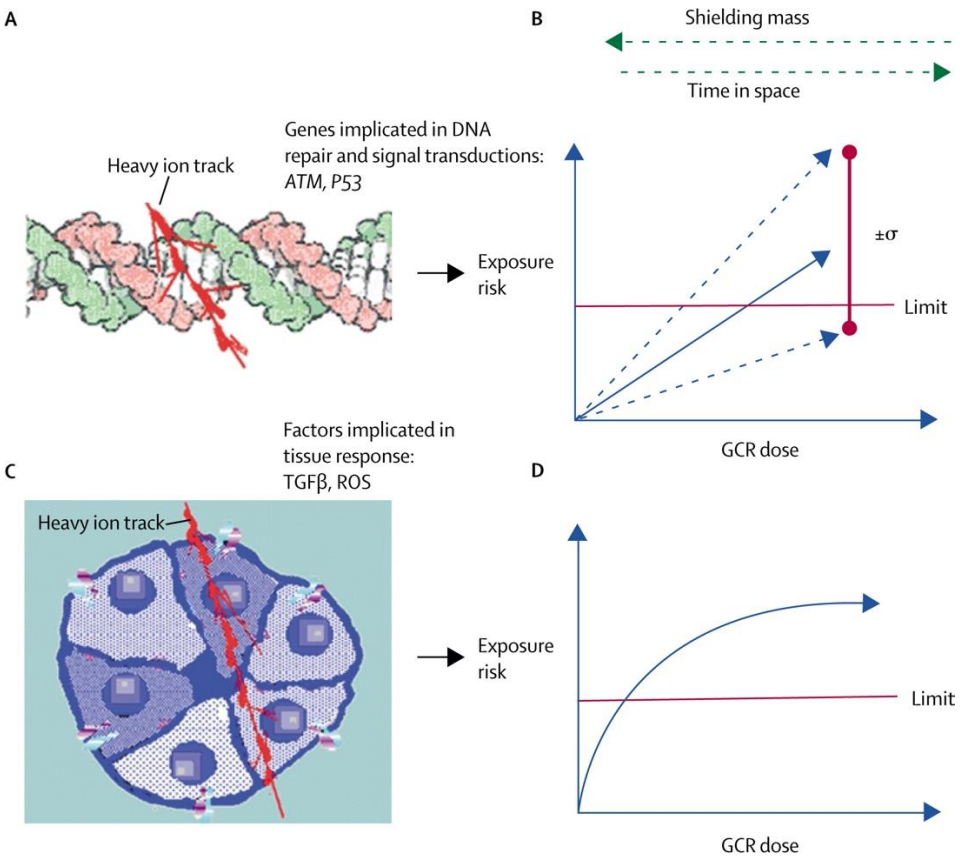

Figure 1. Importance of uncovering basic mechanisms of cancer induction by GCR.

[Reprinted with permission of Elsevier from: Cucinotta FA, Durante M: Cancer risk from exposure to galactic cosmic rays: implications for space exploration by human beings. The Lancet Oncology 2006, 7(5):431-435.][2]

4.2 Space Radiation Biology

Astronauts are exposed to HZE ions as well as low energy γ rays during deep space travel. Even at low doses, exposure to these irradiations can lead to cancer.[6] However, the effects of irradiation encountered in the space environment on the process of formation

of cancer are not well understood, because very few people have been exposed to space irradiation. Due to the non-availability of *in vivo* mechanistic data in humans for HZE exposure, studies in animal models aim to provide relevant information about molecular mechanisms involved in the carcinogenesis of various tumors. Studies generally show that HZE irradiation is more carcinogenic than low-LET γ rays' irradiation. [7-11] Ionizing irradiation affects mammalian cells in a variety of ways, such as DNA damage and chromosomal abnormalities. This damage is mostly due to energy deposition in the cell nucleus. Damage to DNA further leads to changes in transcription, translation, and post-translational modifications that ultimately affect all other cellular processes. [12-15] The relationship between ionizing irradiation and molecular damage is very complex, since not every interaction leads to identifiable DNA breakage and base damage. In fact, most mammalian cells have molecular machinery providing the capability to attempt DNA damage repair in order to promote cell survival. However, these processes may themselves result in mismatched bases, and activation of pathways controlling inflammation, cell death, etc. The downstream molecular effects of these processes, in the form of transcription, translation, secondary modifications, and lipid peroxidation, may lead to cancer initiation and progression over time.

4.3 Incidence of Hepatocellular Carcinoma (HCC) in Mice Irradiated with 1 GeV/nucleon ^{56}Fe Ions

The primary goal of NASA's space irradiation research is to assess the health effects of deep space irradiation on astronauts, in order to provide risk prediction and develop preventive measures against diseases that would slow space exploration. The irradiation

encountered in space is a form of galactic cosmic rays (GCR), which include low energy γ rays and particle nuclei of HZE, and other ions that are created during interactions with the spacecraft. [16] A study reported that a significant increase in hepatocellular carcinoma (HCC) was observed at doses as low as 0.1 Gy following 1 GeV/n ^{56}Fe irradiation. On the other hand, irradiation with γ rays had only a slight effect on HCC incidence, with doses as high as 3 Gy, as shown in Figure 2. The data estimated that the relative biological effectiveness (RBE) for the induction of HCC is on the order of 50 in ^{56}Fe irradiation, relative to ^{137}Cs γ rays. [7] Approximately 25% of those animals from the study which developed HCC had tumors that metastasized to their lungs. Figure 3 shows an increase in HCC metastasis to the lung following HZE-irradiation. [17] Additionally, an increased incidence of HCC has also been reported in animal studies using high-LET neutron exposures. [18] Due to this limited knowledge of the effects of irradiation on the formation of HCC, the development of effective countermeasures requires the characterization of HCC carcinogenesis in animal models using different types and dosages of irradiation. The aim of this research is to establish further mechanistic details on the molecular events that lead to irradiation-induced HCC initiation and progression.

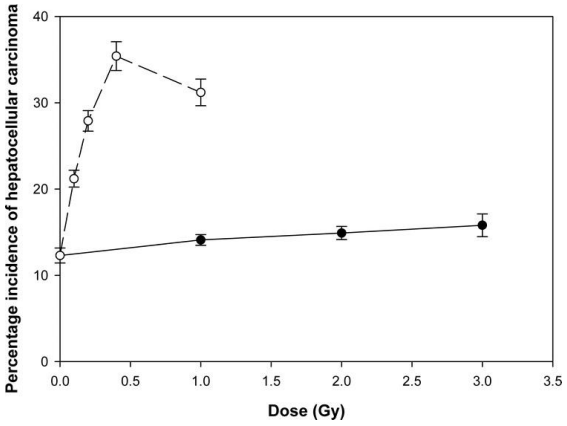

Figure 2. Incidence of HCC. Percentage incidence of hepatocellular carcinoma after exposure to 137Cs γ rays (solid circles) or 1 GeV/nucleon 56Fe ions (open circles) as a function of the dose.

[Open Access From: Weil MM, Bedford JS, Bielefeldt-Ohmann H, Ray FA, Genik PC, Ehrhart EJ, Fallgren CM, Hailu F, Battaglia CL, Charles B et al: Incidence of acute myeloid leukemia and hepatocellular carcinoma in mice irradiated with 1 GeV/nucleon 56Fe ions. Radiat Res 2009, 172(2):213-219.][7]

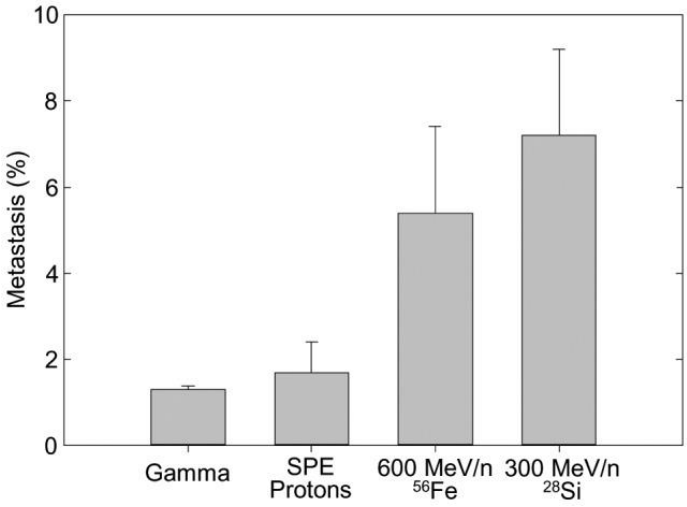

Figure 3. Incidence (%) of HCC with metastases after exposure to: ^{137}Cs γ rays, SPE1972 protons, 600 MeV/n ^{56}Fe, or 350 MeV/n ^{28}Si.

[Open Access From: Weil MM, Ray FA, Genik PC, Yu Y, McCarthy M, Fallgren CM, Ullrich RL: Effects of 28Si ions, 56Fe ions, and protons on the induction of murine acute myeloid leukemia and hepatocellular carcinoma. PLoS One 2014, 9(7):e104819.][17]

4.4 Overview of Following Chapters

In the following chapters, we discuss our findings regarding irradiation-induced transcriptional changes as well as irradiation-induced lipid changes.

4.4.1 IRRADIATION INDUCED TRANSCRIPTIONAL CHANGES

HCC carcinogenesis likely begins with the induction of genetic changes such as DNA mutations and/or methylation, that further result in transcriptional alterations leading to a premalignant state. Irradiation activates/inhibits a myriad of transcriptional pathways that are mainly involved in inflammation and oxidative changes. Chronic oxidative stress can lead to the progression of degenerative diseases, irradiation-induced tissue injury, and the development of HCC.[19-21] Profiling of mRNA transcription through RNA-Seq has become an increasingly common technique to understand biological phenomena at the molecular level. This method generates semi-quantitative expression data for all mRNAs present in each experiment. Our RNA-Seq analyses identified all transcript expression changes in response to a variety of irradiation types and dosages. Our data define key molecular components that are driving the HZE and γ rays' irradiation-induced transcriptional changes leading to HCC. In Chapters 2 and 3, we will describe these changes.

First, in Chapter 2, we present a novel pipeline (WGCNA-M) to perform gene co-expression analysis. For applicable RNA-Seq datasets, the pipeline can reduce the problem of parameter selection that occurs with the existing algorithm in Weighted Gene Co-expression Network Analysis (WGCNA). The WGCNA-M pipeline's (WGCNA combined with Modularity Maximization for community detection) robustness and efficacy were evaluated based on data from our RNA-Seq experiment of ^{56}Fe irradiated and non-irradiated control mice liver lobes to characterize the irradiation effects of deep space travel on the induction of HCC.

Next, in Chapter 3, we describe our findings regarding dynamic time-dependent effects of ^{56}Fe, ^{16}O, and ^{28}Si irradiation on the induction of murine HCC. Specifically, we discuss comparative RNA-Seq transcriptomic analysis to assess the carcinogenic effects of 600 MeV/n ^{56}Fe (0.2 Gy), 1 GeV/n ^{16}O (0.2 Gy), and 350 MeV/n ^{28}Si (0.2 Gy) ions in a mouse model for irradiation-induced HCC. Our findings not only led to a better understanding of the biological mechanisms of underlying risks for HCC after HZE irradiation, but also have important implications for the discovery of potential countermeasures to and identification of biomarkers for HZE-induced HCC.

4.4.2 IRRADIATION INDUCED LIPID CHANGES

Matrix assisted laser desorption ionization mass spectrometry imaging (MALDI-MSI) has been used for the identification of novel biomarkers, as well as early detection and recognition of microenvironmental changes in lipid profiles. [22-26] A high abundance of various lipids in biological tissues has rendered MALDI-MSI a suitable method to detect these changes. This technique has been used to identify and quantify (relative to control) polar lipids per sample, providing information on the structural integrity of cells and the potential state of cellular communication. [27-29] Changes in lipid expression have been shown to be involved in numerous pathological states. [30-34]

In Chapter 4, we demonstrate the use of MALDI-MSI combined with the Spatial Shrunken Centroid Clustering algorithm to define key lipid changes that are driving irradiation-induced HCC.

Finally, we conclude the dissertation in Chapter 5, where the contributions of the author of this dissertation are summarized. Our vision for future works in this area is also discussed.

5 CHAPTER 2: EFFICIENT IDENTIFICATION OF MULTIPLE PATHWAYS: RNA-SEQ ANALYSIS OF LIVERS FROM ^{56}FE ION IRRADIATED MICE

5.1 Abstract

Background: mRNA interaction with other mRNAs and other signaling molecules determine different biological pathways and functions. Gene co-expression network analysis methods have been widely used to identify correlation patterns between genes in various biological contexts (e.g., cancer, mouse genetics, yeast genetics). A challenge remains to identify an optimal partition of the networks where the individual modules (clusters) are neither too small to make any general inferences, nor too large to be biologically interpretable. Clustering thresholds for identification of modules are not systematically determined and depend on user-settable parameters requiring optimization. The absence of systematic threshold determination may result in suboptimal module identification and a large number of unassigned features.

Results: In this study, we propose a new pipeline to perform gene co-expression network analysis. The proposed pipeline employs WGCNA, a software widely used to perform different aspects of gene co-expression network analysis, and Modularity Maximization algorithm, to analyze novel RNA-Seq data to understand the effects of low-dose ^{56}Fe ion irradiation on the formation of hepatocellular carcinoma in mice. The network results, along with experimental validation, show that using WGCNA combined with Modularity Maximization, provides a more biologically interpretable network in our dataset, than that obtainable using WGCNA alone. The proposed pipeline showed better performance than

the existing clustering algorithm in WGCNA, and identified a module that was biologically validated by a mitochondrial complex I assay.

Conclusions: We present a pipeline that can reduce the problem of parameter selection that occurs with the existing algorithm in WGCNA, for applicable RNA-Seq datasets. This may assist in the future discovery of novel mRNA interactions, and elucidation of their potential downstream molecular effects.

Keywords: WGCNA, Modularity, Gene Expression Profiling, RNA-Seq, Sequence Analysis, Modularity Maximization, Network Visualization

5.2 Introduction

RNA-Seq, an approach to genome profiling that uses deep-sequencing technologies, has become an increasingly common technique to understand biological phenomena at the molecular level. This method generates quantitative count data on thousands of different mRNAs within each experiment. Comparing the expression of genes between different experimental conditions identifies hundreds of differentially expressed genes, but translating these lists into key functional distinctions between conditions has proved challenging. Since there are thousands of genes in each sample, many researchers filter their gene lists based on different criteria, in order to extract meaningful biological information. One such filtering criteria is based on differential gene expression analysis. Differential gene expression analysis has traditionally been used to determine genes that are statistically significantly differentially expressed between different experimental conditions based on different metrics, such as non-parametric generalized linear models, independent sample t-tests, and $\log_2$ fold changes. [35] Even though differential gene

expression analysis is one of the most common methods for identifying disease pathways in various experimental conditions, it does not take into consideration the interactions of genes that work as a system to coordinate cellular functions. As a result, using only differential gene expression analysis would limit mechanistic interpretations of the data. mRNAs never act in isolation, but rather in concert with each other and other signaling molecules to define a particular biological pathway and function. Interactions of these signaling molecules can be viewed as networks of interconnected genes and their partners, that are up/down regulated under certain chemical or environmental conditions.

Many algorithms that utilize network theory have found applications in identifying and analyzing these molecular interactions. [36-38] Correlation networks are an example of such algorithms, and describe the co-expression of many genes in response to changing conditions, which can ultimately provide information about the underlying molecular mechanisms or biochemical pathways. [39, 40] In particular, the Weighted Gene Co-expression Network Analysis (WGCNA) method, which is provided as an R software package, has been widely used for performing different aspects of weighted correlation network analysis. [41] The co-expression networks used in WGCNA are constructed based on correlations between the quantitative measurements of each gene, and can be described by an $n \times m$ matrix $X = [x_{ij}]$. Here the row indices ($i = 1,\ldots,n$) correspond to different genes, and the column indices ($j = 1,\ldots,m$) correspond to different sample measurements. While co-expression networks integrate systems-level information to provide a mechanistic interpretation of the dataset, detecting modules (clusters) of closely related mRNAs within the co-expression networks has been a challenging problem. Significant pathways that are identified by different clustering methods often yield tens or hundreds of

genes, making biological interpretation and validation challenging. Further, many clustering techniques such as Dynamic Tree Cut utilized in WGCNA rely on user-settable parameters, including minimum module size, and are sensitive to cluster splitting. [42, 43] While many of these module detection methods perform optimally on some datasets, they may fail to effectively detect patterns in other datasets. A practical challenge in terms of discovering modules and determining the total number of modules is the identification of the optimal number of modules in the network, such that the individual modules are neither too large, preventing meaningful interpretation, nor too small, allowing little to no general inference. In general, characterizing and detecting community structures within networks has been a challenging problem in the study of networks. [44-46] One of the most commonly used metrics to investigate community structure is a quality index for clustering known as Modularity. [47-49] In spite of its popularity, Modularity does have drawbacks. The resolution limit (RL) problem is one of the most significant drawbacks, referring to the problem of maximizing Modularity while hindering one's ability to detect communities that contain fewer links. [50] To address this problem, several approaches have been introduced. [51-54] Of these approaches, Modularity Maximization, which utilizes modularity density measures, has been shown to eliminate rather than merely reduce the RL problem in a wide range of networks.[54]

In this study, we propose a pipeline using Modularity Maximization [54] to effectively detect and evaluate modules from co-expression networks obtained from the adjacency matrix, utilizing WGCNA. [38, 41] We employ the above technique to characterize the effects of ^{56}Fe irradiation on mice livers, in order to study the potential consequences of deep space travel. In particular, astronauts will be exposed to HZE during

deep space travel. Even at low doses, exposure to HZE can lead to cancer. [55, 56] However, the effects of ions found in the deep space environment on cancer formation is not well understood since very few people have been exposed to space irradiation. As human exploration into deep space increases in the future, characterization of and intervention in irradiation-induced diseases will become more important. Previous studies have shown that irradiation of mice with low-dose HZE, specifically ^{56}Fe ions, significantly increases the incidences of HCC. [7, 17] HCC is the most common type of liver cancer, and its formation has mainly been studied in the context of terrestrial risk factors such as chronic hepatitis B/C virus infection, exposure to aflatoxin, obesity, smoking, and heavy alcohol consumption. [57-59] However, there is limited knowledge of the effects of low-dose ^{56}Fe ion irradiation on the formation of HCC. To better understand the molecular mechanisms of low-dose ^{56}Fe induced HCC, we used RNA-Seq to determine gene expression changes in the hepatic micro-environment of ^{56}Fe ion irradiated compared to non-irradiated control mice at 5 different time points post-irradiation. We hypothesized that mitochondrial pathways could be significantly affected, since mitochondria represent a substantial cellular target volume (4-25% depending on the cell). [60] In this manuscript, we will describe how WGCNA can be integrated with Modularity Maximization to construct co-expression correlation networks of differentially expressed genes and detect modules using data obtained from RNA-Seq.

5.3 Methods

In this section, we describe the WGCNA combined with Modularity Maximization for community detection pipeline used in the RNA-Seq dataset. Our evaluation strategy

was targeted to analyze data from an RNA-Seq experiment of ^{56}Fe irradiated and non-irradiated control mice liver lobes, designed to characterize the microenvironmental changes induced by HZE irradiation (similar to HZE ions encountered in deep space travel,) and that lead to induction of HCC. Our aim is to detect modules (clusters of genes) that are related by correlation across samples, and differ between experimental conditions. The resulting co-expression networks were analyzed using functional enrichment analysis and experimentally validated.

5.3.1 Animal Experiments and Sample Preparation

C57BL/6NCrl mice purchased from Charles River (Wilmington, MA) were used in this experiment. Tumor induction studies and studies of molecular changes in the irradiated tissues can only be conducted in whole animals. Further, based on an extensive literature search and examination of studies previously approved by the institutional animal care and use committees (IACUCs), computer models or cell culture studies are not possible. The numbers of animals used were based on the expected numbers of irradiation-related tumors that would develop if animals were allowed to live out their lifespans. Power calculations for numbers in this study are based on the chi-square test for comparing two proportions, with a two-sided significance level set at 0.05 at 80% power.

The serial sacrifice study included 15 male mice with 3 mice per time point at five time-points (30, 60, 120, 270, and 360 days) post-exposure to HZE, specifically ^{56}Fe irradiation. Additionally, 15 mice were used as controls, at the same time points, resulting in a total of 30 mice for this study. The two groups were: 600 Me V/n ^{56}Fe (0.2 Gy) and non-irradiated/sham-irradiated control. The mice were shipped from the vendor to

Brookhaven National Laboratories (BNL) and housed at the BNL animal facility until the time of irradiation at the NASA Space Radiation Laboratory (NSRL). Following irradiation, the animals were shipped to the UTMB Animal Resources Center (ARC), quarantined for one month, and maintained in the ARC for the duration of the experiment. Animals were housed in sterile cages with free access to food and water. Facilities at both BNL and UTMB are fully AAALAC accredited, ensuring adequacy of animal care at both animal facilities.

At each of the five time-points, 3 animals from each group were randomly selected and euthanized using CO_2 asphyxiation, as per current AVMA guidelines for euthanasia. Prior to euthanasia, animals were weighed and weights recorded. Post euthanasia, tissues of the left lobe of livers were collected, snap-frozen on either dry ice or liquid nitrogen, and stored at -80ºC until tissues could be extracted for RNA analysis. Livers were sampled by taking two 40-µm thick slices using a cryotome at -20°C.

5.3.2 ACQUISITION OF RNA-SEQ DATA

Total RNA was isolated from the liver slices using RNAqueous™ Total RNA Isolation Kit (ThermoFisher Scientific, Waltham, MA), and rRNA was removed using the Ribo-Zero™ rRNA Removal Kit (Illumina, San Diego, CA), prior to library preparation with the Illumina TruSeq RNA Library kit. Samples were sequenced in a paired-end 50 base format on an Illumina HiSeq 1500. FastQC was utilized for the quality evaluation of FASTQ files. [61] All FastQC reports were examined prior to the analysis of RNA-Seq samples. The total number of reads used in analysis varied between 23-35 million. A complete list of samples, and related reads information is available in Table 1. Reads were

aligned to the mouse GRCm38 reference genome using the STAR alignment program, version 2.5.3a, with the recommended ENCODE options. [62] The -quantMode GeneCounts option was used to obtain read counts per gene based on the Gencode release M14 annotation file. [63]

Sample Information

Number	Sample	Treatment Type	Time	Biological Replicate	Total Sequences
1.	H2	Non-Irradiated Control	1 month	1	32,905,344
2.	H3	Non-Irradiated Control	1 month	2	28,318,081
3.	H4	Non-Irradiated Control	1 month	3	27,220,319
4.	H7	Non-Irradiated Control	2 months	1	31,264,466
5.	H8	Non-Irradiated Control	2 months	2	31,375,164
6.	H9	Non-Irradiated Control	2 months	3	34,782,071
7.	H11	Non-Irradiated Control	4 months	1	24,449,063
8.	H12	Non-Irradiated Control	4 months	2	27,944,559
9.	H13	Non-Irradiated Control	4 months	3	23,137,137
10.	H16	Non-Irradiated Control	9 months	1	34,216,914
11.	H17	Non-Irradiated Control	9 months	2	30,149,494
12.	H18	Non-Irradiated Control	9 months	3	29,855,702
13.	H21	Non-Irradiated Control	12 months	1	26,910,777
14.	H22	Non-Irradiated Control	12 months	2	31,877,754
15.	H23	Non-Irradiated Control	12 months	3	33,432,277
16.	K2	^{56}Fe Irradiated	1 month	1	31,868,688
17.	K3	^{56}Fe Irradiated	1 month	2	37,890,611

18.	K4	^{56}Fe Irradiated	1 month	3	25,953,453
19.	K6	^{56}Fe Irradiated	2 months	1	47,994,834
20.	K7	^{56}Fe Irradiated	2 months	2	34,603,257
21.	K8	^{56}Fe Irradiated	2 months	3	32,128,695
22.	K12	^{56}Fe Irradiated	4 months	1	27,386,313
23.	K13	^{56}Fe Irradiated	4 months	2	29,914,981
24.	K14	^{56}Fe Irradiated	4 months	3	28,626,258
25.	K16	^{56}Fe Irradiated	9 months	1	24,669,187
26.	K17	^{56}Fe Irradiated	9 months	2	24,014,552
27.	K18	^{56}Fe Irradiated	9 months	3	28,179,114
28.	K23	^{56}Fe Irradiated	12 months	1	28,350,658
29.	K24	^{56}Fe Irradiated	12 months	2	31,439,904
30.	K25	^{56}Fe Irradiated	12 months	3	25,132,399

Table 1. Sample List and Total Reads.

5.3.3 DIFFERENTIAL GENE EXPRESSION ANALYSIS

Raw RNA-Seq data of 51,826 mRNAs from 15 non-irradiated control and 15 ^{56}Fe irradiated C57 mice liver tissue samples were subjected to differential gene expression analysis. All calculations and statistics were performed using statistical software R (R Foundation for Statistical Computing, Vienna, Austria) (version 3.5.1). [64] Differential gene expression analysis was conducted using R software package edgeR. [65, 66] First, normalization factors were calculated to scale the raw library sizes. In addition, dispersion parameters based on generalized linear models (GLM) were estimated; in particular, the common dispersion for negative binomial GLMs, trended dispersion for negative binomial GLMs using the power method, and empirical Bayes tagwise dispersions for negative binomial GLMs. [66, 67] Statistical tests were then conducted for every time point, to compare between ^{56}Fe irradiated and non-irradiated control samples, using a quasi-likelihood negative binomial generalized log-linear model for count data. [68-70] The

Benjamini-Hochberg correction was applied, and genes with FDR≤0.05 & fold change ≥1.5 (|($\log_2$(Fold Change)|≥0.59—up/down regulated) were extracted.

5.3.4 FEATURE SELECTION (FS)

Final differential gene expression analyses for all time points were combined. For genes differentially expressed at multiple time points, the lowest FDR was kept. The list was further filtered to keep only genes with FDR≤10^{-5}. For the final selected gene list, raw variance stabilized normalized count data were retrieved from every RNA-Seq sample (n=30) using the R package DESeq2. [71] This variance stabilized normalization method was specifically selected because it has proven useful for network construction using WGCNA methodology (The WGCNA FAQ).

5.3.5 WGCNA

The gene expression profiles were comprised of 51,826 genes from 30 samples. Constructing a co-expression network on this original list without filtering could not meet a power threshold that corresponded to (R^2=0.9) as recommended by WGCNA, and did not yield any biologically interpretable network. As a result, we first performed the feature selection based on differential gene expression analysis and FDR rank list (step 1-2 in Figure 4, and described above) and then constructed the WGCNA network on genes given by this feature selection (step 3 in Figure 4). WGCNA was performed on differentially expressed genes with FDR≤10^{-5} & fold change ≥1.5 (up/down-regulated). WGCNA analysis was performed per the methodology publication (step 4-7 in Figure 4). [41]

5.3.6 WGCNA WITH MODULARITY MAXIMIZATION

To evaluate the effect of feature selection on the median cluster size, we performed Modularity Maximization analysis on co-expression data derived by WGCNA applied to gene lists filtered over a range of FDR values. As shown in Figure 5, the FDR value of 10^{-5} led to the largest median cluster size, in this particular dataset. The features' significance threshold can be optimized by plotting median cluster sizes at different FDR values. To derive clusters, the following steps were used. An adjacency matrix based on the Pearson correlation with the soft threshold was calculated by WGCNA. [41] The power threshold parameter was set to 16, corresponding to an R^2 value of 0.9, which reflects a scale-free topology in which adjacency between all differential genes was calculated by a power function (step 3 in Figure 4). The adjacency matrix was then filtered to only keep pairs of genes with a Pearson correlation of ≥ 0.7 (step 4 in Figure 4). Then, module identification was performed using the Modularity Maximization clustering method (step 5 in Figure 4). [54, 72] Final modules were visualized using the ExplodeLayout algorithm (step 6 in Figure 4). [73]

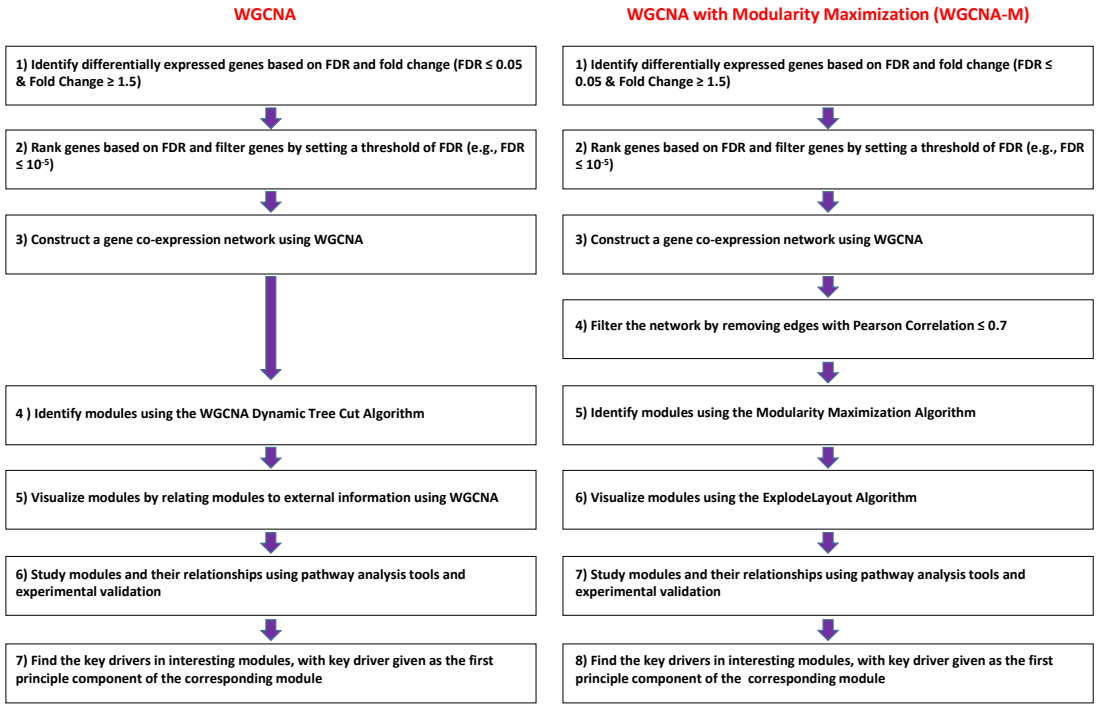

Figure 4. An overview of the WGCNA and WGCNA with Modularity Maximization (WGCNA-M) workflows.

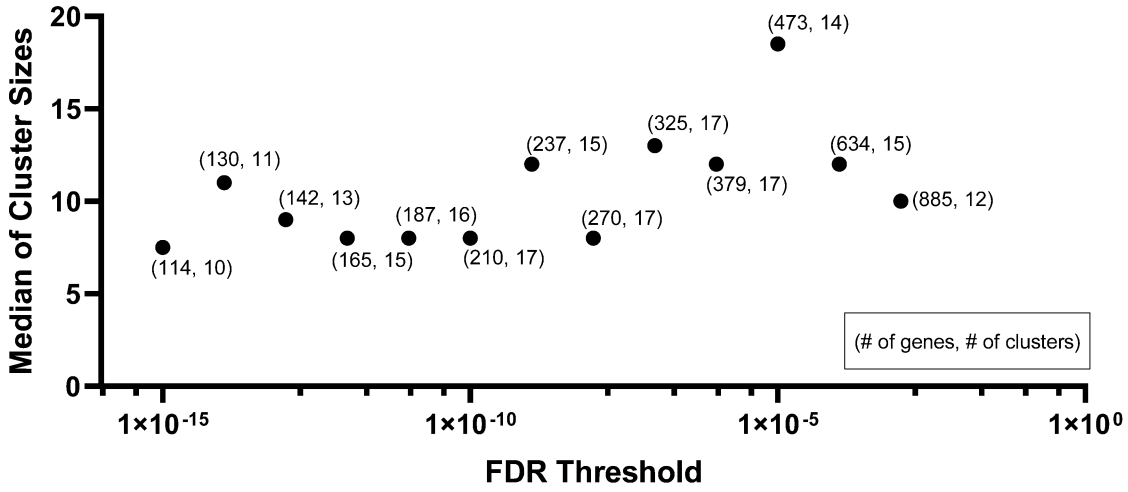

Figure 5. Plot to visualize different FDR thresholds using the Modularity Maximization Algorithm.

The plot shows the change in the median number of clusters detected using Modularity, as the FDR cutoff is varied. The numbers next to each point designate the number of

genes and the number of modules in the corresponding network. The module with the largest median size was chosen for further analysis, since small clusters are difficult to interpret.

5.3.7 MODULE STATISTICAL ANALYSIS

To determine whether the modules were observed by chance, the significance of the results was evaluated by comparing them to the average modularity of 1000 permutations of the weighted and thresholded co-expression network adjacency matrix. Each permutation of the network would preserve the number and weight of all the links but randomly shuffle them; thus it should still meet the scale-free network distribution criteria. Based on the 1000 permutations, we obtained a z-score of 86.8 for our modularity, indicating a strongly significant modular structure in the co-expression network as compared to random.

5.3.8 MITOCHONDRIAL COMPLEX I ENZYME ACTIVITY ASSAY

The mitochondria isolation kit for tissue (Abcam, ab110168) was used to isolate mitochondria from mice liver lobes. Complex 1 enzyme activity was monitored with a colorimetric microplate assay (Abcam, ab110168) using the isolated mitochondria from the liver.

5.3.9 FUNCTIONAL ENRICHMENT ANALYSIS

To determine whether the co-expression modules were biologically meaningful, functional enrichment analysis was performed separately on every module. Significant

functional pathways ($-\log_{10}(p\text{-}value) \geq 1.3$) for each module were evaluated using Ingenuity Pathway Analysis (IPA) (QIAGEN Inc., Hilden, Germany). [74]

5.4 Results

5.4.1 Differential Gene Expression Analysis

Results of differential gene expression analysis are shown in Table 2, which includes the total number of differentially expressed genes at each time point, as well as whether genes are up/down-regulated.

Differentially Expressed Genes

Comparison	Time	Total # of Differentially Expressed Transcripts	Up Regulated	Down Regulated
^{56}Fe Irradiated/Non-Irradiated Control	1 month	645	322	323
^{56}Fe Irradiated/Non-Irradiated Control	2 months	914	637	277
^{56}Fe Irradiated/Non-Irradiated Control	4 months	497	259	238
^{56}Fe Irradiated/Non-Irradiated Control	9 months	704	498	206
^{56}Fe Irradiated/Non-Irradiated Control	12 months	285	75	210
^{56}Fe Irradiated/Non-Irradiated Control	Sum	3045	1791	1254

Table 2. Results of differential gene expression analysis of RNA-Seq data from ^{56}Fe Irradiated and non-Irradiated control mice livers at various time points analyzed using edgeR package.

5.4.2 FEATURE SELECTION

A total of unique 2,273 differentially expressed genes were identified in comparison between ^{56}Fe irradiated and non-irradiated controls. Genes that were statistically significant with FDR$\leq 10^{-5}$ were used for downstream network analysis; 487 unique genes met the filtration criteria. The significance cut off can be adjusted to a higher value if a researcher decides to investigate more genes, depending on the study goals, experimental conditions, and data variability.

5.4.3 WGCNA

We initially used the WGCNA Dynamic Tree Cut algorithm [41] to identify modules within the selected differentially expressed genes. Module identification with this algorithm requires two parameters to be determined prior to network construction: deepSplit, and minClusterSize. deepSplit can be either logical or an integer in the range 0 to 4. It controls the sensitivity to cluster splitting. Higher values result in smaller clusters. minClusterSize represents the minimum number of genes needed in a module to be considered a separate module. Table 3 shows the results of WGCNA module identification using different minClusterSize values, with a default deepSplit value of 2. As minClusterSize increases, the total number of modules decreases. These values produce different types of networks with differing numbers of unassigned genes. If a gene does not belong to a specific module, it is assigned to the Grey/Unassigned Module. The number of unassigned genes varied between 36-73 (shown in the last column of Table 3). At the same time, the total number of modules needs to be within a reasonable range, in order to be able to meaningfully investigate the relationship between genes; 70 different modules each

containing a few genes may not provide meaningful information about these co-expression patterns. In our dataset, networks with a total of 11-18 modules provided interpretable co-expression patterns for further investigation, using pathway analysis tools as well as experimental validation. However, these clustering parameters resulted in 61-69 unassigned genes, representing ~12-14 percent of the 487 selected highly significant features.

WGCNA Results

minClusterSize	deepSplit	Total Number of Modules	Number of Transcripts in Unassigned Module (Grey)
2	2	70	36
3	2	49	37
4	2	37	46
5	2	31	49
6	2	25	57
7	2	20	60
8	2	18	61
9	2	17	65
10	2	15	67
11	2	15	67
12	2	11	69
13	2	11	69
14	2	9	73

Table 3. WGCNA Results with Dynamic Tree Cut Algorithm: deepSplit provides a rough control over the sensitivity to cluster splitting. The higher the value (or if TRUE), the more and smaller clusters will be produced. The Dynamic Tree Cut may identify modules whose expression profiles are very similar. The parameter minClusterSize allows one to control the minimum number of genes in a module, helping to avoid having similar clusters of few genes. As shown in the table, the lower values of minClusterSize increase the 'Total Number of Modules'. Moreover, as this number increases, the 'Number of Genes in Unassigned Module (Grey)' increases as well.

5.4.4 WGCNA WITH MODULARITY MAXIMIZATION

To optimize the number and size of identified modules as well as reduce the number of unassigned genes (~12-14%), we exploited the concept of Modularity Maximization, to assist in finding community structures, as an alternative to utilizing the Dynamic Tree Cut algorithm employed in the standard WGCNA pipeline. Dynamic Tree Cut relies on hierarchical clustering, which is based on the relative distance between genes and samples. Modules are detected by "cutting" these trees, which can lead to many different small modules or a few large modules, depending on the selection of the minClusterSize and deepSplit parameters. Using Modularity Maximization, we were able to identify modules without the need to set these parameters empirically. In particular, the adjacency matrix with a soft threshold beta of 16 (corresponding to R^2=0.9) was first computed using WGCNA, then a clustering algorithm based on Modularity Maximization was used to automatically find community structures in our dataset. We chose the Modularity Maximization method, since the metric of Modularity has been widely used to detect and assess community structures in social and biological networks since its inception. [54, 74-77]

Utilizing the modularity-based clustering algorithm to identify modules, 14 modules were discovered, and only 14 individual genes were unassigned. The final modularity score was Q=0.696, which is indicative of a strong modular structure in the network. Figure 6 depicts the 14 modules in the network, and Table 4 shows the number of genes included in each module along with the enriched molecular pathways, as discussed below.

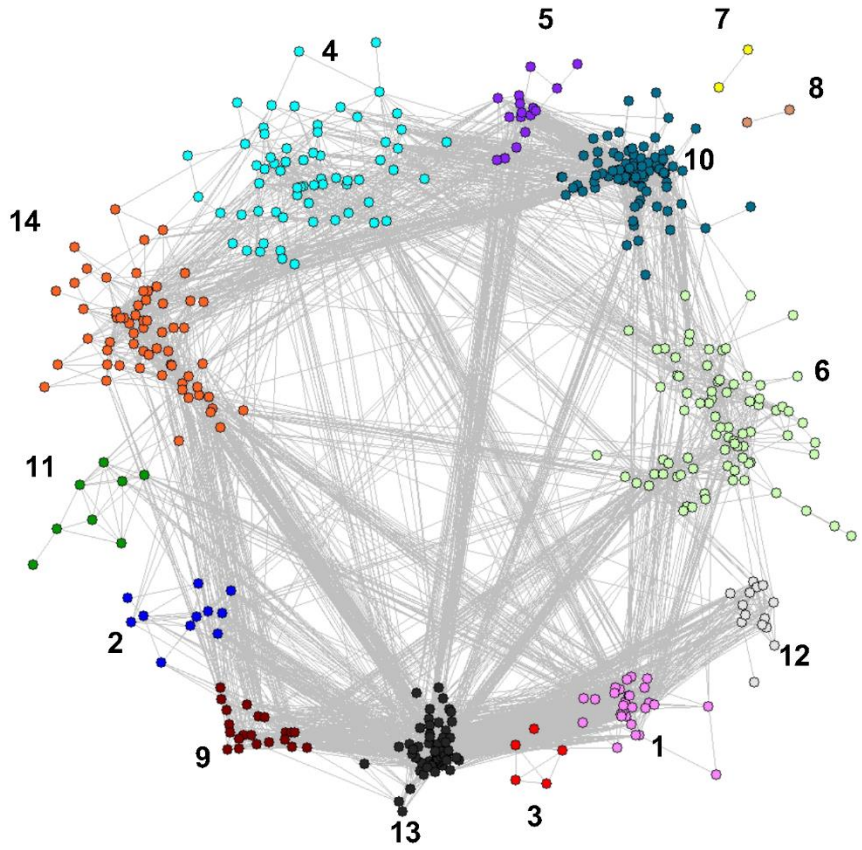

Figure 6. Modularity Maximization Network.

Modules identified by performing Modularity Maximization on the network obtained from WGCNA. The module numbers on the network correspond to the modules shown in Table 4. A total of 14 genes were unassigned.

Pathway Analysis

Module #	**Genes #**	**Molecular Pathways Identified as Enriched (*p*-value ≤ 0.05) in Each Module**
1	**28**	Sirtuin Signaling Pathway, Mitochondrial Dysfunction, Oxidative Phosphorylation, LXR/RXR Activation, FXR/RXR Activation, NAD Biosynthesis III, Oleate Biosynthesis II, Histamine Degradation

2	**11**	IL-9 Signaling, Transcriptional Network in Embryonic Stem Cells, Mitotic Roles of Polo-Like Kinase, GM-CSF Signaling, Growth Hormone Signaling, JAK/STAT Signaling, STAT3 Pathway
3	**5**	No Pathway. 3 transcripts in this module are not Identified. Specifically, Gm28437, Gm28661, Gm29216. The other two are mir-122 (microRNA 122) and Gm10925 (ATP Synthase F0 subunit 6)
4	**65**	Acyl-CoA Hydrolysis, Stearate Biosynthesis I, Pregnenolone Biosynthesis, Histidine Degradation VI, Ubiquinol-10-Biosynthesis, Asparagine Biosynthesis I, a-tocopherol Degradation, LSP/IL-1 Mediated Inhibition of RXR Function, FXR/RXR Activation
5	**16**	Toll-like Receptor Signaling, Heme Degradation, IL-12 Signaling and Production in Macrophages, Acute Phase Response Signaling, Granulocyte Adhesion and Diapedesis, NF-kB Signaling, Agranulocyte Adhesion and Diapedesis, Production of Nitric oxide and ROS in Macrophages
6	**80**	Nicotine Degradation II, Glutathione-mediated Detoxification, Circadian Rhythm Signaling, LPS/IL-1 Mediated Inhibition of RXR Function, Nicotine Degradation III, Adipogenesis Pathway, PXR/RXR Activation, Melatonin Degradation I
7	**2**	No Pathway. Two transcripts (CYP26A1 and CYP26B1) are both part of cytochrome P450 family 26 subfamily A member 1 and subfamily B member 1. They are involved in Pregnenolone Biosynthesis, Histidine Degradation VI, Ubiquinol-10 Biosynthesis and RAR Activation
8	**2**	No Pathway. Two transcripts (ANGPTL8 and HES1). HES1 is involved in Notch Signaling, VDR/RXR Activation.
9	**21**	Unfolded protein response, Protein Ubiquitination Pathway, eNOS Signaling, Glucocorticoid Receptor Signaling, Endoplasmic Reticulum Stress Pathway (6 Transcripts are heat shock proteins)

10	**89**	Acute Phase Response Signaling, IL-10 Signaling, IL-6 Signaling, Role of Macrophage, Fibroblasts and Endothelial Cells in Rheumatoid Arthritis, LXR/RXR Activation, B Cell Receptor Signaling, Altered T Cell and B Cell Signaling in Rheumatoid Arthritis, Hepatic Cholestatis
11	**8**	No Pathway. 4 unidentified transcripts (Cm23935, Gm24187, Rn 18s-rs5, Gm155644) and other 4 (Leucyl-tRNA synthetase 2, microRNA 6236, s-rRNA, l-rRNA)
12	**14**	No Pathway, basic helix-loop-helix family involved in Circadian Rhythm Signaling, Mir17hg, Small nuclear RNA (Snora57, Snora78) and 10 unidentified transcripts,
13	**69**	Estrogen-mediated S-phase Entry, Cell Cycle Regulation, Chronic Myeloid Leukemia Signaling, a-tocopherol Degradation
14	**63**	NRF2-mediated Oxidative Stress Pathway, Endoplasmic Reticulum Stress Pathway, Unfolded Protein Response, Death Receptor Signaling, RhoA Signaling, FXR/RXR Activation.

Table 4. Ingenuity Pathway Analysis on individual modules.

5.4.5 MODULE VALIDATION AND PROPERTIES

To explore the biological relevance of the modules, each module was investigated by Ingenuity Pathway Analysis (IPA). Specifically, module 1 was shown to be significant ($-\log_{10}(p\text{-}value)\geq 1.3$) in mitochondrial pathways, such as the Sirtuin Signaling Pathway, Mitochondrial Dysfunction, and Oxidative Phosphorylation. [74] All the genes involved in mitochondrial dysfunction in our dataset were contained in module 1. In particular, Figure

7 shows that 5 of these genes express different subunits of mitochondrial complex I and III. To validate these results, we performed an additional experimental technique to determine whether complex I activity is reduced in response to ^{56}Fe irradiation. Complex I activity was observed to be decreased in response to exposure to ^{56}Fe HZE ion across all time points as measured by mitochondrial complex I enzyme activity (Figure 8). The downstream effects of irradiation on mitochondrial functions have been emphasized [78], as mitochondria have been shown to occupy a substantial fraction of the cell volume. [60] Therefore, they may be fairly easily targeted by irradiation as the ^{56}Fe nuclei traverse the cell. The electron transport chain in the mitochondrion is composed of five protein complexes (I-V) that perform a series of oxidation-reduction reactions, in which O_2 is the final electron acceptor and is reduced to a water molecule. One of the consequences of this process is the formation of reactive oxygen species (ROS), which is thought to arise from the leakage of electrons, specifically from complex I and III, and to a minor extent complex II. [79-81] Using oxygen as the final electron acceptor causes mitochondria to consume about 90% of the body's oxygen but also become the richest source of ROS. [81-84] The upregulation of mitochondrial genes shown in Figure 7, specifically in complex I and complex III, suggests that leakage of electrons from these two complexes results in increased Complex I and III enzyme activity. This leads to further the overexpression of these genes in response to ^{56}Fe irradiation. Other modules could potentially be validated in future experimental designs, involving live animals and more fresh tissues. For example, module 2 can be tested for JAK/STAT signaling. STATs are ubiquitously expressed and mainly activated after stimulation of cytokine receptors. STATs function in the nucleus, but they are first activated in the cytoplasm and have then to be transported into the nuclear

compartment. [85] This translocation can be assessed by indirect immunofluorescence. Additionally, STAT signaling can be experimentally validated by pharmacologically inhibiting STAT pathways with specific STAT inhibitors. Similarly, module 9 could be tested for Endoplasmic Reticulum (ER) stress pathways. Several molecular indicators of ER stress could be examined by Western Blots and/or proteomic analysis, which could demonstrate increased or decreased phosphorylation of ER stress proteins.

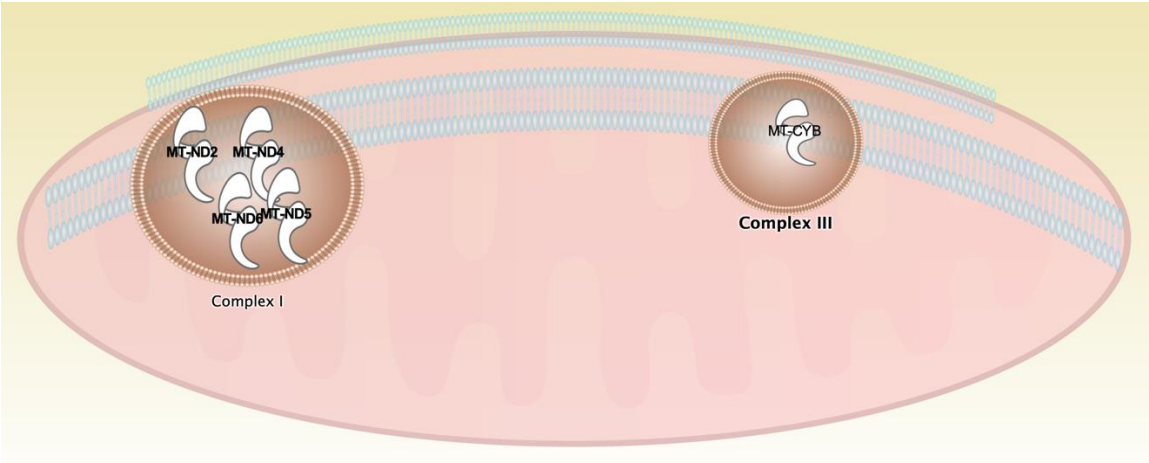

Figure 7. Mitochondrial Dysfunction Pathway Genes.

Five of the genes from module 1 are involved in the mitochondrial dysfunction pathway. Specifically, 4 of them, MT-ND2, MT-ND4, MT-ND5, and MT-ND6 are different subunits of Complex I. MT-CYB, or cytochrome b is part of Complex III/bc which also regulates Complex I. Figure was made using Ingenuity Pathway Analysis (IPA), (QIAGEN Inc., Hilden, Germany).

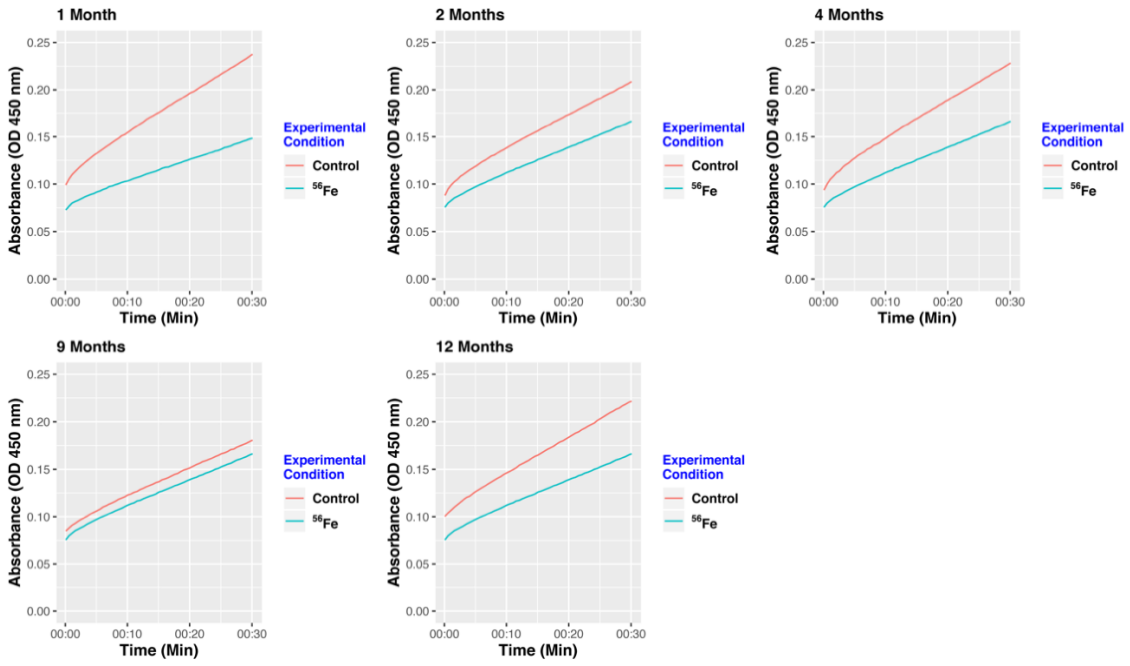

Figure 8. Results of Mitochondrial Complex I Functional Assay performed for each time point.

Complex 1 activity was decreased after exposure to 56Fe irradiation as compared to non-irradiated control at each time point.

5.5 Discussion

One of the current statistical challenges in identifying co-expression patterns in RNA-Seq data is a robust determination of the number and size of modules appropriate, across a variety of datasets. The choice of an appropriate clustering algorithm that yields the most biologically interpretable networks has been studied using different datasets and methods. For example, a study has investigated Recursive Indirect-Paths Modularity (RIP-M) for module detection in an RNA-Seq co-expression network. Using an influenza vaccine response study, the authors showed that RIP-M had higher cluster assignment accuracy as compared to Newman Modularity, and similar results to WGCNA. [86] We

compared WGCNA, RIP-M, and the combined WGCNA-M method based on the Rand Index (RI). [75] In calculating the RIs, we considered every unassigned gene, as a cluster by itself, since such genes are viewed as not being similar to each other. The RIs for WGCNA-M versus WGCNA, WGCNA-M versus RIP-M, and WGCNA versus RIP-M were 0.909, 0.892, 0.936, respectively. The numbers of genes unassigned to a cluster for WGCNA-M, WGCNA, and RIP-M were 14, 108, and 0, respectively. All of the 14 genes which were unassigned in WGCNA-M were also unassigned in WGCNA. Based on our observed RIs, RIP-M and WGCNA were the most similar when applied to our dataset. Like WGCNA, RIP-M also requires the parameter minModuleSize (minClusterSize) as well as an additional parameter, maxModuleSize, which specifies a target range of module sizes. All genes assigned to a module below minModuleSize are then grouped together and merged into a further module. Modules above maxModuleSize are split in subsequent iterations to arrive at the target range. RIP-M forces all genes to be assigned to a cluster; the 14 genes unassigned by WGCNA and the WGCNA-M approach for our dataset were placed into cluster 1 by RIP-M. Community detection method selection is an important issue in cluster analysis and may greatly influence the results of a study and their biological interpretability. Therefore, it is imperative to select the most suitable method for each specific experimental design, and for the nature of the data being investigated. A complete list of gene cluster-assignments for each method is provided in Table 5.

Utilizing Modularity Maximization to detect community structures provides an additional way to construct a network and explore various RNA-Seq datasets; however, WGCNA-M is not limited to this application domain, and can be applied to detect co-expression patterns amongst other omics studies. Protein or lipids can be linked together

in networks via a defined functional relationship in a similar fashion. Methodologically, MS-based proteomics and lipidomics tend to have consistency, and coverage issues [87-92] as compared to RNA-based high throughput methods. As a result, some network analysis methods as applied to proteomic data may not capture the complexity and nuances underlying biological processes, and alternative approaches may be needed to complement the existing analytical tools. Similar to any other analytical method, the network-based WGCNA-M analysis method must be applied appropriately based on the inherent quality and nature of each dataset. This will allow us to gain robust biological insight and decipher the unique patterns in our data from which we can further understand the complexity and coordinated function of the system being investigated. In the current study, utilization of WGCNA with Modularity Maximization resulted in the identification of biologically interpretable and relevant modules, without the need for parameter optimization.

	Cluster Assignment		
Gene ID	WGCNA	WGCNA-M	RIP-M
ENSMUSG00000000204	13	10	7
ENSMUSG00000000303	9	4	15
ENSMUSG00000000385	13	10	7
ENSMUSG00000000567	Unassigned	6	8
ENSMUSG00000001473	8	14	11
ENSMUSG00000001995	Unassigned	6	4
ENSMUSG00000002992	4	1	2
ENSMUSG00000003477	10	6	8
ENSMUSG00000004359	3	10	9
ENSMUSG00000004460	7	9	4
ENSMUSG00000004951	7	14	4
ENSMUSG00000005232	1	1	2
ENSMUSG00000005413	3	5	10
ENSMUSG00000005483	7	14	4
ENSMUSG00000005514	11	6	14
ENSMUSG00000005547	10	6	8
ENSMUSG00000005968	9	4	15
ENSMUSG00000006522	12	10	6

ENSMUSG00000006641	11	6	14
ENSMUSG00000007872	Unassigned	Unassigned	1
ENSMUSG00000008384	Unassigned	6	14
ENSMUSG00000008496	3	10	9
ENSMUSG00000009092	Unassigned	4	13
ENSMUSG00000009633	10	10	8
ENSMUSG00000012428	3	5	10
ENSMUSG00000014905	7	9	4
ENSMUSG00000015357	1	6	4
ENSMUSG00000015451	13	10	8
ENSMUSG00000015656	7	9	4
ENSMUSG00000016024	12	10	6
ENSMUSG00000016028	Unassigned	6	14
ENSMUSG00000018171	8	14	11
ENSMUSG00000018427	11	6	14
ENSMUSG00000019139	12	10	6
ENSMUSG00000019850	3	5	10
ENSMUSG00000020000	10	4	8
ENSMUSG00000020027	Unassigned	4	15
ENSMUSG00000020048	7	9	4
ENSMUSG00000020102	9	4	17
ENSMUSG00000020108	6	10	8
ENSMUSG00000020255	3	5	10
ENSMUSG00000020423	3	5	10
ENSMUSG00000020429	13	10	7
ENSMUSG00000020431	13	10	7
ENSMUSG00000020484	8	14	11
ENSMUSG00000020572	4	1	18
ENSMUSG00000020580	8	14	11
ENSMUSG00000020593	7	9	4
ENSMUSG00000020656	Unassigned	4	8
ENSMUSG00000020715	8	14	4
ENSMUSG00000020776	Unassigned	Unassigned	1
ENSMUSG00000020893	Unassigned	10	13
ENSMUSG00000020901	3	10	9
ENSMUSG00000020941	13	10	7
ENSMUSG00000021091	12	10	6
ENSMUSG00000021226	10	4	8
ENSMUSG00000021228	9	4	15
ENSMUSG00000021250	Unassigned	10	7
ENSMUSG00000021268	9	4	15
ENSMUSG00000021270	7	9	4
ENSMUSG00000021365	8	14	11

ENSMUSG00000021453	13	10	8
ENSMUSG00000021670	8	14	11
ENSMUSG00000021701	Unassigned	10	8
ENSMUSG00000021750	Unassigned	10	7
ENSMUSG00000021765	Unassigned	14	11
ENSMUSG00000022000	13	10	9
ENSMUSG00000022010	13	10	8
ENSMUSG00000022032	13	10	7
ENSMUSG00000022126	3	10	9
ENSMUSG00000022218	Unassigned	14	10
ENSMUSG00000022346	5	13	3
ENSMUSG00000022389	11	6	14
ENSMUSG00000022528	Unassigned	8	13
ENSMUSG00000022615	Unassigned	6	14
ENSMUSG00000022651	13	10	7
ENSMUSG00000022769	7	9	4
ENSMUSG00000022863	Unassigned	4	8
ENSMUSG00000022899	Unassigned	Unassigned	1
ENSMUSG00000022951	7	14	4
ENSMUSG00000023043	8	14	11
ENSMUSG00000023067	Unassigned	6	14
ENSMUSG00000023073	2	14	4
ENSMUSG00000023078	3	10	9
ENSMUSG00000023087	Unassigned	14	11
ENSMUSG00000023243	Unassigned	14	11
ENSMUSG00000023272	7	9	4
ENSMUSG00000023905	8	14	11
ENSMUSG00000024029	13	10	7
ENSMUSG00000024036	13	10	7
ENSMUSG00000024222	3	5	7
ENSMUSG00000024365	13	10	9
ENSMUSG00000024427	Unassigned	4	11
ENSMUSG00000024526	9	4	15
ENSMUSG00000024561	7	9	4
ENSMUSG00000024589	11	6	8
ENSMUSG00000024807	Unassigned	4	4
ENSMUSG00000024843	11	6	19
ENSMUSG00000024986	6	2	12
ENSMUSG00000024987	Unassigned	7	13
ENSMUSG00000025004	Unassigned	5	10
ENSMUSG00000025185	10	6	18
ENSMUSG00000025229	11	6	17
ENSMUSG00000025586	Unassigned	6	14

ENSMUSG00000025612	8	14	11
ENSMUSG00000025823	7	9	4
ENSMUSG00000025981	11	6	18
ENSMUSG00000026072	13	10	7
ENSMUSG00000026077	11	6	18
ENSMUSG00000026107	7	14	4
ENSMUSG00000026249	7	6	4
ENSMUSG00000026390	3	10	9
ENSMUSG00000026435	Unassigned	6	4
ENSMUSG00000026475	4	1	2
ENSMUSG00000026542	12	10	6
ENSMUSG00000026614	7	6	4
ENSMUSG00000026773	Unassigned	10	8
ENSMUSG00000026822	12	10	6
ENSMUSG00000026839	11	6	14
ENSMUSG00000026864	7	9	4
ENSMUSG00000026981	3	10	10
ENSMUSG00000026986	4	1	2
ENSMUSG00000027035	3	10	10
ENSMUSG00000027068	8	14	4
ENSMUSG00000027346	Unassigned	6	12
ENSMUSG00000027351	8	14	4
ENSMUSG00000027381	8	14	11
ENSMUSG00000027397	11	6	17
ENSMUSG00000027690	10	6	8
ENSMUSG00000027995	3	5	10
ENSMUSG00000028051	10	6	8
ENSMUSG00000028240	Unassigned	6	5
ENSMUSG00000028359	13	10	6
ENSMUSG00000028410	7	14	4
ENSMUSG00000028655	4	1	15
ENSMUSG00000028671	Unassigned	6	4
ENSMUSG00000028680	Unassigned	2	12
ENSMUSG00000028715	10	4	8
ENSMUSG00000028862	13	10	7
ENSMUSG00000028957	11	6	14
ENSMUSG00000029009	11	6	14
ENSMUSG00000029188	Unassigned	6	14
ENSMUSG00000029304	Unassigned	10	8
ENSMUSG00000029352	12	10	6
ENSMUSG00000029380	13	10	7
ENSMUSG00000029482	10	6	5
ENSMUSG00000029552	8	14	11

ENSMUSG00000029657	7	9	4
ENSMUSG00000029700	Unassigned	6	4
ENSMUSG00000029752	10	4	15
ENSMUSG00000030103	14	12	17
ENSMUSG00000030244	11	6	14
ENSMUSG00000030256	11	6	14
ENSMUSG00000030364	Unassigned	5	13
ENSMUSG00000030474	3	10	9
ENSMUSG00000030650	13	10	10
ENSMUSG00000030659	Unassigned	4	8
ENSMUSG00000030847	7	9	4
ENSMUSG00000030852	13	10	8
ENSMUSG00000031016	11	6	14
ENSMUSG00000031024	11	6	14
ENSMUSG00000031271	4	1	2
ENSMUSG00000031278	8	14	4
ENSMUSG00000031381	7	9	4
ENSMUSG00000031441	12	10	6
ENSMUSG00000031594	12	10	6
ENSMUSG00000031722	12	10	6
ENSMUSG00000031762	13	10	7
ENSMUSG00000031765	13	10	7
ENSMUSG00000031770	7	9	4
ENSMUSG00000031824	7	9	4
ENSMUSG00000031906	Unassigned	Unassigned	1
ENSMUSG00000032010	11	6	14
ENSMUSG00000032012	Unassigned	6	14
ENSMUSG00000032068	8	14	11
ENSMUSG00000032220	8	14	11
ENSMUSG00000032271	3	13	1
ENSMUSG00000032285	8	14	11
ENSMUSG00000032300	8	14	11
ENSMUSG00000032311	13	10	7
ENSMUSG00000032348	10	6	8
ENSMUSG00000032353	7	9	4
ENSMUSG00000032369	8	14	10
ENSMUSG00000032511	12	10	6
ENSMUSG00000032575	7	9	4
ENSMUSG00000032578	6	2	12
ENSMUSG00000032624	8	14	4
ENSMUSG00000032715	Unassigned	4	11
ENSMUSG00000032724	Unassigned	Unassigned	1
ENSMUSG00000032786	Unassigned	6	14

ENSMUSG00000032802	8	14	4
ENSMUSG00000033318	11	6	5
ENSMUSG00000034610	Unassigned	4	11
ENSMUSG00000034640	3	5	10
ENSMUSG00000034645	5	13	3
ENSMUSG00000034765	8	14	11
ENSMUSG00000034936	Unassigned	Unassigned	1
ENSMUSG00000035184	8	14	11
ENSMUSG00000035202	Unassigned	11	16
ENSMUSG00000035385	3	5	10
ENSMUSG00000035686	4	1	2
ENSMUSG00000036885	13	10	8
ENSMUSG00000036957	11	6	14
ENSMUSG00000037071	4	1	2
ENSMUSG00000037405	13	10	7
ENSMUSG00000037411	Unassigned	5	10
ENSMUSG00000037440	9	4	19
ENSMUSG00000037447	13	10	9
ENSMUSG00000037583	Unassigned	14	11
ENSMUSG00000037621	Unassigned	14	11
ENSMUSG00000037847	Unassigned	6	14
ENSMUSG00000038037	Unassigned	14	10
ENSMUSG00000038155	8	14	11
ENSMUSG00000038415	Unassigned	2	8
ENSMUSG00000038418	Unassigned	10	7
ENSMUSG00000038508	Unassigned	4	15
ENSMUSG00000038550	11	6	14
ENSMUSG00000038599	10	4	8
ENSMUSG00000038754	Unassigned	6	14
ENSMUSG00000039457	8	14	11
ENSMUSG00000039519	9	4	15
ENSMUSG00000039633	Unassigned	6	4
ENSMUSG00000039835	9	4	15
ENSMUSG00000039956	8	14	4
ENSMUSG00000039958	Unassigned	14	15
ENSMUSG00000040017	12	10	6
ENSMUSG00000040026	12	10	6
ENSMUSG00000040599	7	9	4
ENSMUSG00000040613	Unassigned	4	8
ENSMUSG00000040660	9	4	15
ENSMUSG00000040891	8	14	4
ENSMUSG00000041229	9	4	15
ENSMUSG00000041293	9	4	15

ENSMUSG00000041324	5	13	3
ENSMUSG00000041481	3	5	10
ENSMUSG00000041567	7	14	4
ENSMUSG00000041596	2	13	1
ENSMUSG00000041920	11	6	8
ENSMUSG00000042041	8	14	4
ENSMUSG00000042834	10	6	8
ENSMUSG00000043013	6	2	12
ENSMUSG00000044197	Unassigned	14	11
ENSMUSG00000045775	9	4	17
ENSMUSG00000046179	1	13	3
ENSMUSG00000046223	8	14	11
ENSMUSG00000046688	3	10	7
ENSMUSG00000046794	Unassigned	6	4
ENSMUSG00000047109	3	5	10
ENSMUSG00000047492	10	10	8
ENSMUSG00000047822	Unassigned	8	13
ENSMUSG00000047881	8	14	11
ENSMUSG00000049303	13	10	9
ENSMUSG00000049791	11	6	14
ENSMUSG00000049922	8	14	11
ENSMUSG00000050069	Unassigned	4	15
ENSMUSG00000050423	Unassigned	Unassigned	1
ENSMUSG00000050440	Unassigned	1	2
ENSMUSG00000051361	Unassigned	14	4
ENSMUSG00000051495	Unassigned	6	14
ENSMUSG00000052271	Unassigned	4	13
ENSMUSG00000052305	1	13	2
ENSMUSG00000052392	9	4	15
ENSMUSG00000052512	4	14	2
ENSMUSG00000052560	13	10	7
ENSMUSG00000052632	11	6	14
ENSMUSG00000052837	13	10	7
ENSMUSG00000052957	13	10	8
ENSMUSG00000053113	13	10	7
ENSMUSG00000053175	13	10	7
ENSMUSG00000053553	8	14	11
ENSMUSG00000053846	10	4	8
ENSMUSG00000055116	11	6	14
ENSMUSG00000055370	5	13	3
ENSMUSG00000055491	13	10	8
ENSMUSG00000055782	9	4	15
ENSMUSG00000055866	11	6	14

ENSMUSG00000056054	13	10	7
ENSMUSG00000056071	13	10	7
ENSMUSG00000056313	2	14	4
ENSMUSG00000056749	11	6	5
ENSMUSG00000056973	10	6	8
ENSMUSG00000057425	8	14	11
ENSMUSG00000057465	12	10	6
ENSMUSG00000057729	12	10	6
ENSMUSG00000057933	10	6	8
ENSMUSG00000058260	9	4	15
ENSMUSG00000058672	7	6	4
ENSMUSG00000058934	5	13	3
ENSMUSG00000059743	Unassigned	Unassigned	1
ENSMUSG00000059824	11	6	14
ENSMUSG00000060317	2	14	1
ENSMUSG00000060803	9	4	15
ENSMUSG00000061175	11	6	14
ENSMUSG00000061540	12	10	6
ENSMUSG00000061906	9	4	15
ENSMUSG00000062432	1	13	1
ENSMUSG00000062825	8	14	4
ENSMUSG00000063388	Unassigned	Unassigned	1
ENSMUSG00000063415	Unassigned	7	13
ENSMUSG00000063838	8	14	11
ENSMUSG00000063919	13	10	8
ENSMUSG00000063929	7	13	4
ENSMUSG00000064337	Unassigned	11	16
ENSMUSG00000064339	Unassigned	11	16
ENSMUSG00000064345	4	1	18
ENSMUSG00000064363	4	1	18
ENSMUSG00000064367	4	1	18
ENSMUSG00000064368	4	1	18
ENSMUSG00000064370	4	1	18
ENSMUSG00000064655	14	12	17
ENSMUSG00000064853	14	12	17
ENSMUSG00000065304	14	12	17
ENSMUSG00000065402	4	3	18
ENSMUSG00000065637	14	12	17
ENSMUSG00000065778	14	12	17
ENSMUSG00000065822	14	12	17
ENSMUSG00000066072	10	4	8
ENSMUSG00000066170	13	10	7
ENSMUSG00000066363	3	5	10

ENSMUSG00000066477	9	4	15
ENSMUSG00000066687	Unassigned	6	14
ENSMUSG00000067144	9	4	15
ENSMUSG00000067219	Unassigned	14	11
ENSMUSG00000068877	9	4	15
ENSMUSG00000069516	3	5	10
ENSMUSG00000070167	14	12	17
ENSMUSG00000070284	7	9	4
ENSMUSG00000070348	Unassigned	Unassigned	1
ENSMUSG00000070576	8	14	4
ENSMUSG00000071369	8	14	7
ENSMUSG00000071551	10	6	8
ENSMUSG00000072623	Unassigned	4	13
ENSMUSG00000072849	9	4	15
ENSMUSG00000073830	9	4	15
ENSMUSG00000073834	9	4	15
ENSMUSG00000073842	9	4	15
ENSMUSG00000074115	12	10	6
ENSMUSG00000074469	12	10	6
ENSMUSG00000074472	2	13	1
ENSMUSG00000074794	13	10	9
ENSMUSG00000075015	Unassigned	Unassigned	1
ENSMUSG00000075511	Unassigned	6	14
ENSMUSG00000076258	Unassigned	11	16
ENSMUSG00000076569	Unassigned	Unassigned	1
ENSMUSG00000076612	13	10	10
ENSMUSG00000076613	13	10	10
ENSMUSG00000076614	12	10	6
ENSMUSG00000077505	14	12	17
ENSMUSG00000078612	8	4	11
ENSMUSG00000078672	9	4	15
ENSMUSG00000078674	Unassigned	4	4
ENSMUSG00000078675	9	4	15
ENSMUSG00000078686	7	4	4
ENSMUSG00000078687	9	4	15
ENSMUSG00000078866	Unassigned	6	14
ENSMUSG00000079550	1	13	3
ENSMUSG00000081208	5	13	3
ENSMUSG00000081257	1	13	3
ENSMUSG00000081988	1	13	1
ENSMUSG00000082361	8	14	4
ENSMUSG00000082570	5	13	3
ENSMUSG00000083168	1	13	3

ENSMUSG00000083478	Unassigned	6	14
ENSMUSG00000083592	1	13	2
ENSMUSG00000083992	Unassigned	4	8
ENSMUSG00000084309	9	4	15
ENSMUSG00000084415	2	13	1
ENSMUSG00000084543	1	13	3
ENSMUSG00000084744	14	12	17
ENSMUSG00000084981	5	13	3
ENSMUSG00000085006	9	4	15
ENSMUSG00000085091	5	13	3
ENSMUSG00000085439	1	13	3
ENSMUSG00000085445	Unassigned	10	8
ENSMUSG00000085499	5	13	3
ENSMUSG00000085834	Unassigned	1	13
ENSMUSG00000085977	1	13	3
ENSMUSG00000086141	1	13	1
ENSMUSG00000086165	Unassigned	10	8
ENSMUSG00000086324	4	11	18
ENSMUSG00000086391	1	13	1
ENSMUSG00000086447	Unassigned	Unassigned	1
ENSMUSG00000086819	4	1	2
ENSMUSG00000086868	1	13	1
ENSMUSG00000087695	2	13	1
ENSMUSG00000087819	14	12	17
ENSMUSG00000087950	1	13	1
ENSMUSG00000088609	Unassigned	11	16
ENSMUSG00000089255	14	12	17
ENSMUSG00000089542	14	12	17
ENSMUSG00000089635	2	13	1
ENSMUSG00000089675	7	6	4
ENSMUSG00000089726	Unassigned	12	17
ENSMUSG00000089774	7	14	4
ENSMUSG00000089827	3	10	10
ENSMUSG00000089873	9	4	4
ENSMUSG00000090124	7	6	4
ENSMUSG00000090306	Unassigned	14	11
ENSMUSG00000090386	2	13	1
ENSMUSG00000090555	9	4	15
ENSMUSG00000090877	7	9	4
ENSMUSG00000090925	1	13	3
ENSMUSG00000092021	6	2	12
ENSMUSG00000092075	9	4	15
ENSMUSG00000094156	Unassigned	1	15

ENSMUSG00000094786	Unassigned	6	14
ENSMUSG00000096160	1	13	2
ENSMUSG00000096391	5	13	3
ENSMUSG00000096688	Unassigned	4	15
ENSMUSG00000096954	1	6	3
ENSMUSG00000097039	10	4	8
ENSMUSG00000097073	5	4	11
ENSMUSG00000097451	9	4	15
ENSMUSG00000097762	11	4	5
ENSMUSG00000098290	2	13	1
ENSMUSG00000098330	Unassigned	Unassigned	1
ENSMUSG00000098741	2	13	1
ENSMUSG00000098864	2	13	2
ENSMUSG00000098973	Unassigned	11	16
ENSMUSG00000098980	5	13	3
ENSMUSG00000099242	2	13	1
ENSMUSG00000099343	2	6	4
ENSMUSG00000100862	Unassigned	3	18
ENSMUSG00000101111	Unassigned	3	13
ENSMUSG00000101122	1	6	4
ENSMUSG00000101249	Unassigned	3	13
ENSMUSG00000101397	1	13	2
ENSMUSG00000101596	5	13	3
ENSMUSG00000102070	Unassigned	3	13
ENSMUSG00000102319	Unassigned	4	11
ENSMUSG00000102750	4	1	2
ENSMUSG00000102758	11	6	14
ENSMUSG00000102854	2	13	1
ENSMUSG00000102967	5	13	3
ENSMUSG00000103233	Unassigned	10	8
ENSMUSG00000103560	13	10	8
ENSMUSG00000103642	2	13	1
ENSMUSG00000104030	1	13	3
ENSMUSG00000104253	4	1	18
ENSMUSG00000104664	6	2	12
ENSMUSG00000104798	5	13	3
ENSMUSG00000104802	6	13	3
ENSMUSG00000105192	6	2	12
ENSMUSG00000105374	4	1	3
ENSMUSG00000105703	13	10	7
ENSMUSG00000105909	2	13	1
ENSMUSG00000106106	Unassigned	11	16
ENSMUSG00000106185	5	13	3

ENSMUSG00000106303	6	2	12
ENSMUSG00000106397	6	2	12
ENSMUSG00000106538	4	1	18
ENSMUSG00000106619	1	13	2
ENSMUSG00000106815	4	1	2
ENSMUSG00000107304	1	13	1
ENSMUSG00000107390	1	13	3
ENSMUSG00000108709	4	1	3
ENSMUSG00000109612	6	10	7
ENSMUSG00000109679	1	13	3
ENSMUSG00000109708	1	13	1
ENSMUSG00000109709	1	13	3
ENSMUSG00000109807	6	2	12
ENSMUSG00000109904	11	6	14
ENSMUSG00000110088	1	13	3
ENSMUSG00000110151	1	13	1
ENSMUSG00000110384	Unassigned	6	18
ENSMUSG00000110386	13	10	7
ENSMUSG00000110439	4	1	2
ENSMUSG00000110488	2	13	1
ENSMUSG00000110494	1	13	3
ENSMUSG00000110496	11	6	14
ENSMUSG00000110520	1	13	1
ENSMUSG00000110537	Unassigned	14	11
ENSMUSG00000110588	13	10	7
ENSMUSG00000110757	1	13	1
ENSMUSG00000111250	Unassigned	4	15
ENSMUSG00000111424	1	13	3
ENSMUSG00000111631	1	13	2
ENSMUSG00000112090	1	13	3
ENSMUSG00000112744	1	13	3
ENSMUSG00000112774	Unassigned	6	14
ENSMUSG00000112873	Unassigned	6	14
ENSMUSG00000113387	4	1	18
ENSMUSG00000113399	13	10	8
ENSMUSG00000113544	4	1	2
ENSMUSG00000113986	4	1	2
ENSMUSG00000113987	1	13	3
ENSMUSG00000114131	1	13	3

Table 5. Gene cluster-assignment comparison. Complete list of gene cluster-assignments using Recursive Indirect-Paths Modularity (RIP-M), Weighted Gene Co-Expression Network Analysis (WGCNA), and Weighted Gene Co-Expression Network Analysis with Modularity Maximization (WGCNA-M).

5.6 Conclusions

In this study, we proposed a new pipeline that combines the adjacency matrix notion of WGCNA with Modularity Maximization to find modules that are involved in specific biological pathways. To show the validity of the identified modules, we conducted gene enrichment analysis and experimental validation. Our results showed that mitochondrial pathways that were changed in response to irradiation were contained in the same module. Further, our data indicates that even after performing stringent feature selection focusing on significant genes (FDR$\leq 10^{-5}$), WGCNA-M was still able to identify biologically relevant modules. The use of the WGCNA Dynamic Tree Cut clustering algorithm in our dataset resulted in a high number of unassigned genes (61-69). On the other hand, WGCNA-M reduced the number of unassigned genes to 14 while maintaining an optimal number of modules/specific pathways. The proposed pipeline enables the identification of network and community structures without requiring optimization of the minClusterSize and deepSplit parameters. The increasing number of high throughput genomic datasets, together with the use of appropriate network pipelines, will enable researchers to efficiently investigate molecular mechanisms and pathways involved in different disease processes.

5.7 Availability of Data and Materials

The data discussed in this chapter have been deposited in NCBI's Gene Expression Omnibus (Nia et al., 2020) and are accessible through GEO Series accession number GSE136165 (https://www.ncbi.nlm.nih.gov/geo/query/acc.cgi?acc=GSE136165). The R and C scripts written for this dissertation are accessible through https://github.com/annamnia/Efficient-Identification-of-Multiple-Pathways-RNA-Seq-Analysis-of-Livers-from-56Fe-Ion-Irradiated-M

5.8 Tutorial for WGCNA-M

5.8.1 Adjacency Matrix Tutorial

This script takes the user through a practical example of generating an adjacency matrix from expression data using WCGNA, which can then be used for further calculations using the modularity algorithm.

Dependencies:

- gdata
- dplyr
- Biobase
- convert
- IRanges
- edgeR
- GenomicRanges
- DESeq2

- limma
- rJava
- xlsx
- biomaRt
- enrichR
- devtools
- WGCNA

Input file requirements:

1. **Expression data**
    a. table of integer read counts, with rows corresponding to genes and columns to independent libraries. The counts represent the total number of reads aligning to each gene (or other genomic locus).
2. **Phenotype data**
    a. Phenotypic data summarizes information about the samples (e.g., sex, age, and treatment status; referred to as 'covariates'). The information describing the samples can be represented as a table with S rows and V columns, where V is the number of covariates, and S the number of samples.

In this example we will analyze the gene expression of ^{56}Fe irradiated C57 mice liver tissue samples. Reads were aligned to the mouse GRCm38 reference genome using the STAR alignment program, version 2.5.3a, with the recommended ENCODE options. The -quantMode GeneCounts option was used to obtain read counts per gene, based on the Gencode release M14 annotation file.

The following files will be used as inputs

Expression Data File	Phenotype Data File	Description
raw_exprsData_Control_C57_1mo.txt	pData_Fe_Control_C57_1mo.txt	Month 1
raw_exprsData_Control_C57_2mo.txt	pData_Fe_Control_C57_2mo.txt	Month 2
raw_exprsData_Control_C57_4mo.txt	pData_Fe_Control_C57_4mo.txt	Month 4
raw_exprsData_Control_C57_9mo.txt	pData_Fe_Control_C57_9mo.txt	Month 9
raw_exprsData_Control_C57_12mo.txt	pData_Fe_Control_C57_12mo.txt	Month 12
raw_exprsData_Control_C57.txt	pData_Fe_Control_C57.txt	Combined Months 1-12
	pData3.txt	Experimental conditions

1. On line 22, change the working directory path to the location where all of the example files are located.
2. For every time point differential gene expression analysis is conducted using R software package edgeR. First, normalization factors are calculated to scale the raw library sizes. In addition, dispersion parameters based on generalized linear models (GLM) are estimated; in particular, common dispersion for negative binomial

GLMs, trended dispersion for negative binomial GLMs using the power method, and empirical bayes tagwise dispersions for negative binomial GLMs. Pairwise statistical tests are then conducted between ^{56}Fe irradiated and non-irradiated control samples (at every time point) using a quasi-likelihood negative binomial generalized log-linear model applied to count data. Benjamini-Hochberg correction is applied and genes with FDR≤0.05 & fold change ≥1.5 are extracted.

3. The expression values of genes identified as differentially expressed by edgeR are extracted from the "Combined Months 1-12" files. List of differentially expressed genes are merged across time points and deduplicated, leaving the lowest FDR value for each trascript. The final list of differentially expressed genes can be re-filtered to a lower FDR, as desired. The raw counts for the selected genes are re-normalized using DESeq. (see edgeR, DESeq)
4. DESeq normalized expression values of differentially expressed genes are loaded into WGCNA for adjacency matrix calculation.
5. By inspection, remove any obvious outliers using a semi-automatic code that only requires a choice of a height cut. (see Tutorial for the WGCNA package for R)

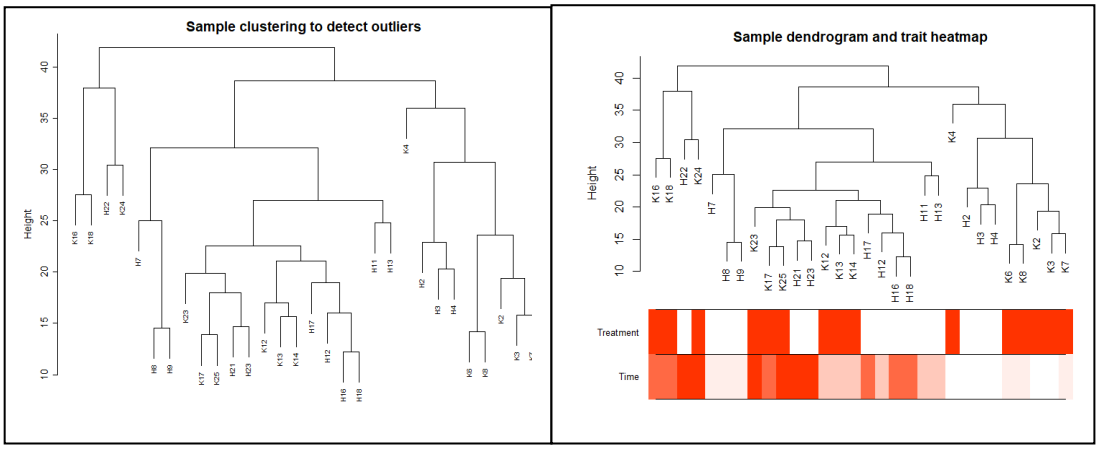

6. We now read in the trait data or experimental conditions and match the samples for which they were measured to the samples in the expression data. We choose the power 16, which is the lowest power for which the scale-free topology fit index curve flattens out upon reaching a high value (in this case, roughly 0.90).

Choosing the soft-thresholding power: analysis of network topology

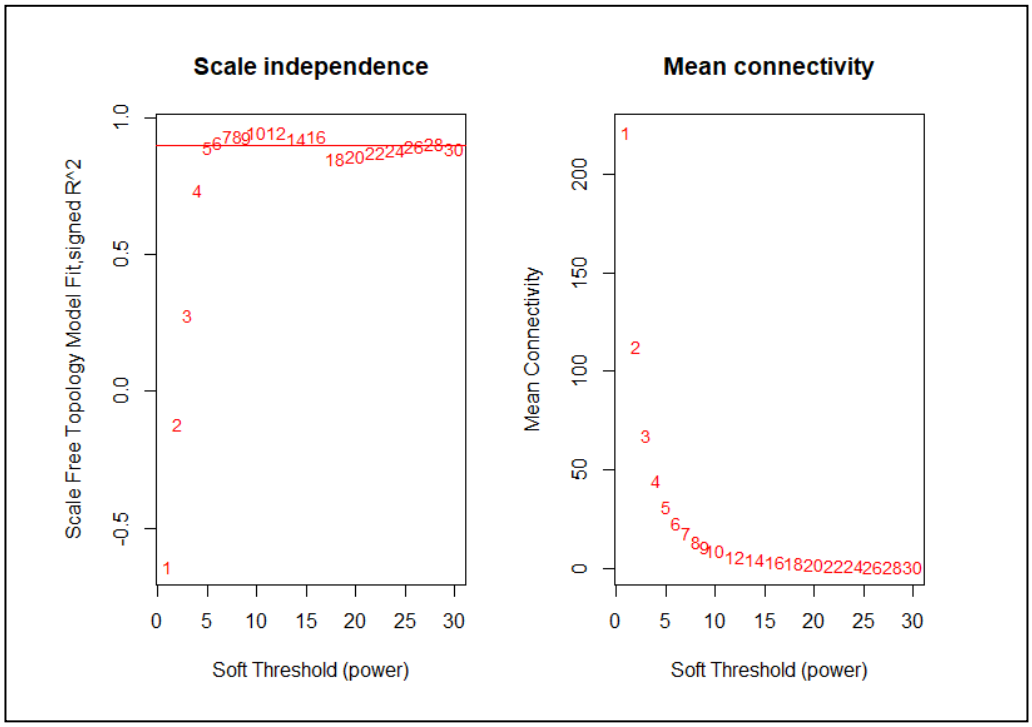

7. Adjacency matrix at the selected soft-thresholding power threshold is written out as "adjancency_matrix.txt"

5.8.2 MANUAL: WGCNA-M

This code performs unipartite network community detection, using modularity.

Dependencies:

- svDialogs

Input file requirements:

3. **Adjacency Matrix from WGCNA**

Running:

1. Run WGCNA-M.R script
2. Select the directory where the R script is located with the necessary library files as shown below

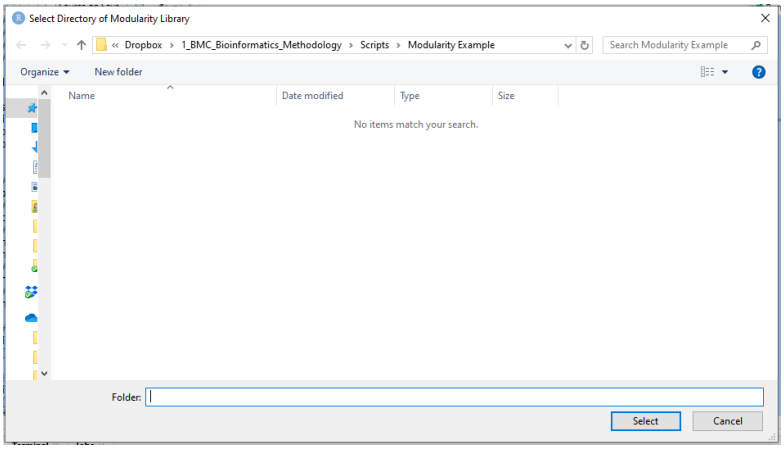

R_uni.c	8/22/2019 10:53 PM	C File	1 KB
R_uni.dll	8/22/2019 10:53 PM	Application exten...	49 KB
R_uni.h	8/22/2019 10:53 PM	H File	1 KB
R_uni.so	8/22/2019 10:53 PM	SO File	35 KB
uni_ft2.c	8/22/2019 10:53 PM	C File	16 KB
uni2.h	8/22/2019 10:53 PM	H File	2 KB

3. Select the Adjacency Matrix File:
    a. In the example dataset it is “adjacency_1e5.txt”

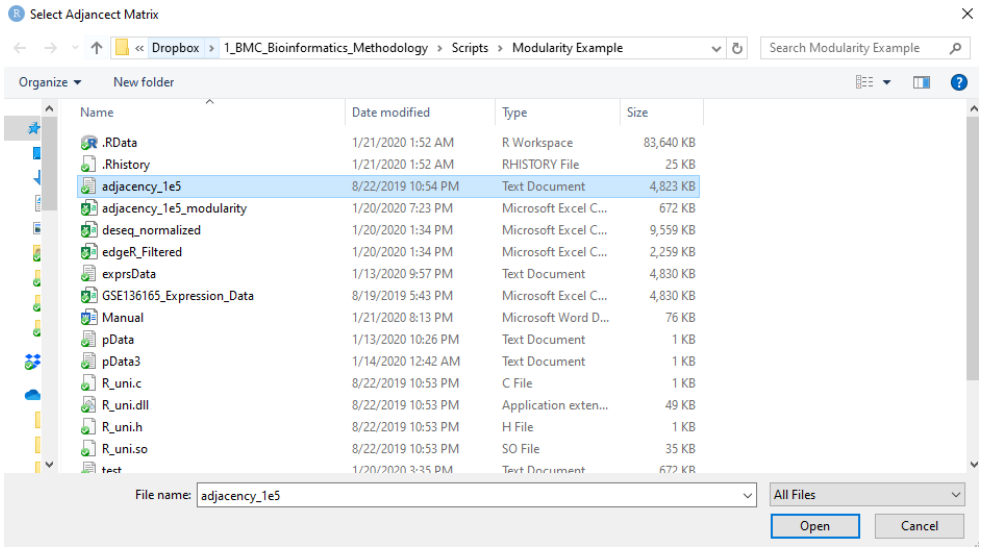

4. Select a File Name to Save the Modularity Network Algorithm Output in a comma separated values file format.

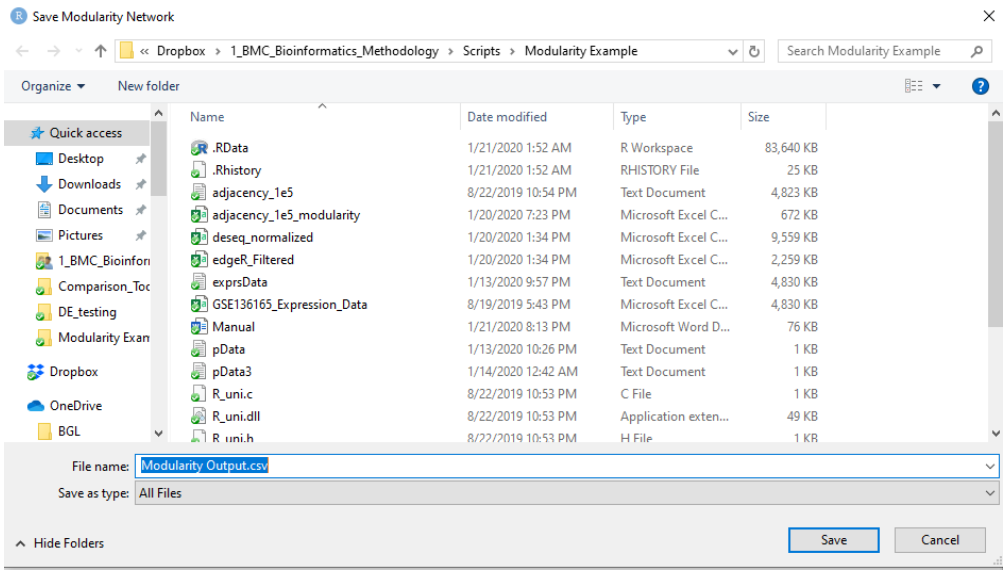

5. Pick the Soft Power Number based on how the adjacency matrix was generated by WCGNA

    a. A soft power threshold of 16 was chosen as optimal for the example dataset

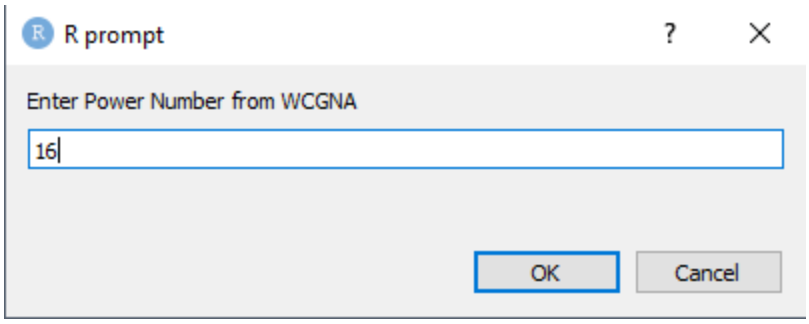

6. Pick the Pearson Correlation Threshold
    a. A Pearson correlation threshold of 0.7 was chosen as optimal for the example dataset

7.

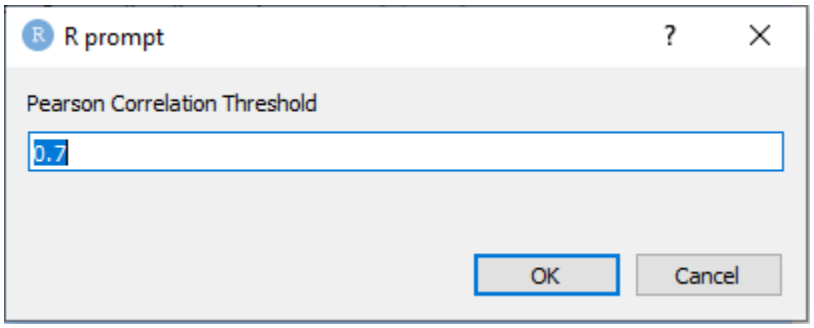

8. Pick the number of times to run the modularity algorithm

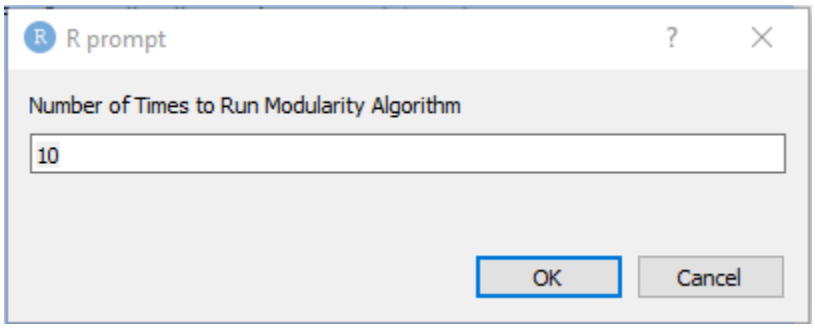

9. When the algorithm finishes running it will print a summary

```
> #print network size
> print(n)
[1] 634
> #print modularity score
> print(modRes[[4]])
[1] 0.4829613
> #print number of clusters
> print(max(modRes[[5]]))
[1] 5
> #print median of cluster size
> print(median(table(modRes[[5]])))
[1] 128
> #print average cluster size
> print(mean(table(modRes[[5]])))
[1] 126.8
```

6 Chapter 3: Comparative RNA-Seq Transcriptome Analyses Reveal Dynamic Time-Dependent Effects of ^{56}Fe, ^{16}O, and ^{28}Si Irradiation on the Induction of Murine Hepatocellular Carcinoma

6.1 Abstract

Background: One of the health risks posed to astronauts during deep space flights is exposure to high charge, high-energy (HZE) ions (Z>13), which can lead to induction of hepatocellular carcinoma (HCC). However, little is known on the molecular mechanisms of HZE irradiation induced HCC.

Results: We performed comparative RNA-Seq transcriptomic analyses to assess the carcinogenic effects of 600 MeV/n ^{56}Fe (0.2 Gy), 1 GeV/n ^{16}O (0.2 Gy), and 350 MeV/n ^{28}Si (0.2 Gy) ions in a mouse model for irradiation-induced HCC. C3H/HeNCrl mice were subjected to total body irradiation to simulate space environment HZE-irradiation, and liver tissues were extracted at five different time points post-irradiation to investigate the time-dependent carcinogenic response at the transcriptomic level. Our data demonstrated a clear difference in the biological effects of these HZE ions, particularly immunological, such as Acute Phase Response Signaling, B Cell Receptor Signaling, IL-8 Signaling, and ROS Production in Macrophages. Also seen in this study were novel unannotated transcripts that were significantly affected by HZE. To investigate the biological functions of these novel transcripts, we used a machine learning technique known as self-organizing maps (SOMs) to characterize the transcriptome expression profiles of 60 samples (45 HZE-irradiated, 15 non-irradiated control) from liver tissues. A handful of localized modules in the maps

emerged as groups of co-regulated and co-expressed transcripts. The functional context of these modules was discovered using overrepresentation analysis. We found that these spots typically contained enriched populations of transcripts related to specific immunological molecular processes (e.g., Acute Phase Response Signaling, B Cell Receptor Signaling, IL-3 Signaling), and RNA Transcription/Expression.

Conclusions: A large number of transcripts were found differentially expressed post-HZE irradiation. These results provide valuable information for uncovering the differences in molecular mechanisms underlying HZE specific induced HCC carcinogenesis. Additionally, a handful of novel differentially expressed unannotated transcripts were discovered for each HZE ion. Taken together, these findings may provide a better understanding of biological mechanisms underlying risks for HCC after HZE irradiation, and may also have important implications for discovery of potential countermeasures against and identification of biomarkers for HZE-induced HCC.

Keywords: RNA-Seq, Self-Organizing Maps, Novel Transcripts, Carcinogenesis, Tumor Microenvironment

6.2 Introduction

An important goal for the National Aeronautics and Space Administration (NASA) is to identify the effects of spaceflight-like conditions on irradiation-induced cancer. However, understanding the mechanisms of irradiation-induced cancer is impeded by the fact that there are no quantitative data from human populations exposed to the specific types of irradiation encountered during missions beyond low-earth orbit (LEO) or in deep space. During these missions, astronauts will be continuously exposed to low dose ionizing

irradiation (LDR). In particular, HZE ions such as ^{56}Fe, ^{16}O, and ^{28}Si are the major high linear energy transfer (LET) sources in deep space. [55, 93, 94] Previous studies have shown that irradiation of mice with low dose HZE, specifically ^{56}Fe ions, significantly increases the incidences of HCC, but there is a limited understanding of potential mechanisms. [7] Previous studies by multiple investigators have shown that irradiation of mice with HZE particles induces oxidative damage, and micro-environmental changes that are thought to play a role in the carcinogenic processes, yet a detailed analysis of these processes has not been undertaken. [6-8, 19, 21, 93, 95-97] The main goal of these studies was to establish an association between HZE irradiation and a specific response such as oxidative stress, microenvironmental changes, and/or apoptosis.

The pathogenic process involved in the development of HCC and other cancers following irradiation exposure likely begins with the induction of mutagenic, and/or epigenetic changes and production of oncometabolites that further results in transcriptional alterations leading to a premalignant state. Irradiation can activate and/or inhibit a myriad of transcriptional pathways that are mainly involved in inflammation and oxidative changes that may play a role in the subsequent development of irradiation-related cancers, which involves chronic oxidative stress leading to irradiation-induced tissue injury, and the subsequent development of HCC. [19-21] Use of RNA-Seq, an approach to transcriptome profiling, which utilizes the deep-sequencing technologies, has become an increasingly common technique to study biological phenomena at the molecular level. This approach generates quantitative data of thousands of different messenger RNAs (mRNAs) with each experiment. To better understand the molecular mechanisms of HZE induced hepatic carcinogenesis, we performed RNA isolation and sequencing of the livers of male

C3H/HeNCrl mice. This strain has been shown to be susceptible to induction of low-dose HZE-induced spontaneous HCC. [7] Low dose irradiation induces micro-environmental changes that lead to carcinogenesis and potentially tumor development. We conducted transcriptomic analyses to identify altered transcript expression in response to different types of HZE irradiation. The results of the present study confirm previous observations of significant differences between ^{56}Fe irradiation and non-irradiated control with respect to the induction of HCC. [7, 8]

Additionally, the alignment of RNA-Seq reads to the reference set of transcripts usually highlights a small but significant fraction of novel transcripts. Such transcripts are usually unexplored due to their unmappability to the genome sequence and/or the fact that they are missing functional gene annotations. In recent years, there has been an increased attention paid to the unannotated transcript expression data as a potentially valuable resource to identify novel transcripts missing from the existing transcriptome annotations. [98-103] The functionally unannotated transcripts from RNA-Seq in our experiments offered us an opportunity to find novel transcripts that are significantly affected by HZE and potentially associated with irradiation induced HCC.

To gain biological knowledge about the scope of the cellular processes involved in the irradiation induced HCC, we analyzed quantitative transcriptional changes in the livers of C3H/HeNCrl mice after irradiation with ^{56}Fe, ^{16}O, and ^{28}Si compared with those from non-irradiated control. These analyses helped us define key molecular components that are driving the HZE induced transcriptional changes leading to HCC as well as functional roles of unannotated transcripts.

6.3 Methods

6.3.1 Animal Experiments and Sample Preparation

C3H/HeNCrl mice purchased from Charles River (Wilmington, MA) were used in this experiment since they have been shown to be a suiTable experimental model for liver carcinogenesis. The C3H/HeNCrl strain was used based on previous studies demonstrating that these mice are sensitive to induction of HCC after exposure to a dose of 0.2 Gy of 600 MeV/n ^{56}Fe. [7] Tumor induction studies and characterization of molecular changes in the irradiated tissues need to be conducted in whole animals to study the microenvironmental effects of HZE exposure because computer models or cell culture are inadequate based on extensive literature searches. Conducted studies were approved by the institutional animal care and use committees (IACUCs). The numbers of animals used were based on the expected numbers of irradiation-related tumors that would develop if animals were allowed to live out their lifespans. Power calculations for numbers in this study are based on chi-square test for comparing two proportions, with a two-sided significance level set at 0.05, and at 80% power.

The serial sacrifice study included 15 male mice with 3 mice per time point at five time-points consisting of 30, 60, 120, 270, and 360 days post-exposure to HZE: ^{56}Fe, ^{16}O, and ^{28}Si irradiation. Additionally, 15 mice were used as controls, at the same time points, resulting in a total of 60 eight to ten-week-old male mice for this study. The 4 groups included 3 treatments (600 MeV/n ^{56}Fe (0.2 Gy), 1 GeV/n ^{16}O (0.2 Gy), and 350 MeV/n ^{28}Si (0.2 Gy)) and control (non-irradiated/sham irradiated). The mice were shipped from the vendor to Brookhaven National Laboratories (BNL) and housed at the BNL animal

facility until the time of irradiation at the NASA Space Radiation Laboratory (NSRL). Following irradiation, the animals were shipped to the UTMB Animal Resources Center (ARC), quarantined for one month, and maintained in the ARC for the duration of the experiment. Animals were housed in sterile cages with free access to food and water. Facilities at both BNL and UTMB are fully AAALAC accredited, ensuring adequacy of animal care at both animal facilities.

At each of the five time-points, 3 animals from each treatment group were randomly selected and euthanized using CO_2 asphyxiation, as per current AVMA guidelines for euthanasia. Prior to euthanasia, animals were weighed and weights recorded. Post euthanasia tissues of the left lobe of livers were collected, snap-frozen on either dry ice or liquid nitrogen, and stored at -80ºC until tissues could be extracted for RNA analyses. Livers were sampled by taking two 40 μm thick slices using a cryotome at -20°C.

6.3.2 ACQUISITION OF RNA-SEQ DATA

Total RNA was isolated from the liver slices using RNAqueous™ Total RNA Isolation Kit (ThermoFisher Scientific, Waltham, MA) and rRNA was removed using the Ribo-Zero™ rRNA Removal Kit (Illumina, San Diego, CA), prior to library preparation with the Illumina TruSeq RNA Library kit. Samples were sequenced in a paired-end 50 base format on an Illumina HiSeq 1500. CLC Genomics Workbench v12.0.3 was used for bioinformatical quality control and mapping of the RNA-Seq data. Sequencing data was initially trimmed using the CLC's "Trim Reads" module. Reads containing nucleotides below the quality threshold of 0.05 (using the modified Richard Mott algorithm), those with two or more unknown nucleotides or sequencing adapters were trimmed out.

Additionally, all reads have been trimmed by 14 bases from the 5' end of each read. The total number of reads used in analysis varied between 33 and 114 million. A complete list of samples, and related reads information is available in Table 6. Filtered sequencing reads were then processed using the "RNA-Seq Analysis" module. Reads were mapped using a global alignment strategy against the mouse GRCm38 reference genome with 95% length fraction and similarity fraction scores with annotation version GRCm38.97.

Sample Information

Sample Name	Mouse Strain	Treatment	Time Point (month)	Number of Reads Before Trimming	Number of Reads After Trimming
B1	C3H/HeNCrl	Control	1	27,803,741	27,593,600
B2	C3H/HeNCrl	Control	1	38,763,374	38,434,949
B3	C3H/HeNCrl	Control	1	28,647,253	28,446,327
B6	C3H/HeNCrl	Control	2	33,847,556	33,597,495
B7	C3H/HeNCrl	Control	2	29,461,708	29,284,111
B8	C3H/HeNCrl	Control	2	26,203,039	26,043,238
B11	C3H/HeNCrl	Control	4	25,414,881	25,244,281
B12	C3H/HeNCrl	Control	4	27,215,741	27,074,514
B13	C3H/HeNCrl	Control	4	16,715,026	16,620,010
B16	C3H/HeNCrl	Control	9	28,872,035	28,674,962
B17	C3H/HeNCrl	Control	9	18,012,784	17,922,314
B18	C3H/HeNCrl	Control	9	25,465,333	25,310,404
B21	C3H/HeNCrl	Control	12	21,304,222	21,204,760
B22	C3H/HeNCrl	Control	12	21,714,727	21,593,313

B25	C3H/HeNCrl	Control	12	18,375,391	18,252,464
E1	C3H/HeNCrl	^{56}Fe	1	34,592,008	34,438,044
E2	C3H/HeNCrl	^{56}Fe	1	34,515,771	34,332,528
E3	C3H/HeNCrl	^{56}Fe	1	29,559,903	29,429,351
E6	C3H/HeNCrl	^{56}Fe	2	35,947,917	35,794,507
E7	C3H/HeNCrl	^{56}Fe	2	31,131,612	30,924,067
E8	C3H/HeNCrl	^{56}Fe	2	30,078,715	29,907,978
E11	C3H/HeNCrl	^{56}Fe	4	27,971,374	27,880,383
E12	C3H/HeNCrl	^{56}Fe	4	28,131,345	28,050,475
E13	C3H/HeNCrl	^{56}Fe	4	27,783,844	27,693,338
E17	C3H/HeNCrl	^{56}Fe	9	29,265,273	29,165,791
E18	C3H/HeNCrl	^{56}Fe	9	28,164,125	28,072,094
E19	C3H/HeNCrl	^{56}Fe	9	24,831,462	24,609,209
E21	C3H/HeNCrl	^{56}Fe	12	31,486,613	31,311,847
E22	C3H/HeNCrl	^{56}Fe	12	20,517,771	20,428,583
E23	C3H/HeNCrl	^{56}Fe	12	24,249,471	24,096,544
F3	C3H/HeNCrl	^{16}O	1	34,033,641	33,940,904
F4	C3H/HeNCrl	^{16}O	1	37,051,878	36,906,215
F5	C3H/HeNCrl	^{16}O	1	39,026,140	38,877,220
F6	C3H/HeNCrl	^{16}O	2	29,096,350	28,991,895
F7	C3H/HeNCrl	^{16}O	2	32,159,425	32,069,211
F8	C3H/HeNCrl	^{16}O	2	30,669,033	30,547,830
F11	C3H/HeNCrl	^{16}O	4	57,549,867	57,397,802

F12	C3H/HeNCrl	^{16}O	4	40,188,169	40,073,955
F13	C3H/HeNCrl	^{16}O	4	24,642,593	24,562,846
F18	C3H/HeNCrl	^{16}O	9	23,183,122	23,115,690
F19	C3H/HeNCrl	^{16}O	9	22,468,806	22,404,440
F20	C3H/HeNCrl	^{16}O	9	24,030,796	23,952,028
F23	C3H/HeNCrl	^{16}O	12	26,614,330	26,470,972
F24	C3H/HeNCrl	^{16}O	12	28,651,764	28,448,632
F25	C3H/HeNCrl	^{16}O	12	22,993,406	22,857,177
A1	C3H/HeNCrl	^{28}Si	1	29,448,912	29,337,599
A2	C3H/HeNCrl	^{28}Si	1	35,982,178	35,803,291
A3	C3H/HeNCrl	^{28}Si	1	34,578,327	34,357,243
A6	C3H/HeNCrl	^{28}Si	2	23,769,566	23,636,132
A7	C3H/HeNCrl	^{28}Si	2	39,750,054	39,502,602
A8	C3H/HeNCrl	^{28}Si	2	38,280,772	37,980,706
A11	C3H/HeNCrl	^{28}Si	4	35,824,821	35,612,832
A12	C3H/HeNCrl	^{28}Si	4	28,437,483	28,194,876
A13	C3H/HeNCrl	^{28}Si	4	32,749,059	32,566,960
A16	C3H/HeNCrl	^{28}Si	9	26,257,484	26,082,882
A17	C3H/HeNCrl	^{28}Si	9	18,513,436	18,429,411
A20	C3H/HeNCrl	^{28}Si	9	34,911,295	34,691,357
A21	C3H/HeNCrl	^{28}Si	12	33,510,740	33,239,692
A23	C3H/HeNCrl	^{28}Si	12	27,988,794	27,809,886
A25	C3H/HeNCrl	^{28}Si	12	32,278,179	32,036,538

Table 6. Sample List and Total Reads.

6.3.3 DIFFERENTIAL TRANSCRIPT EXPRESSION ANALYSIS

Raw abundance counts of 107,319 mRNAs from 15 non-irradiated control, 15 ^{56}Fe irradiated, 15 ^{16}O irradiated, and 15 ^{28}Si irradiated C3H/HeNCrl male mice liver tissue samples were subjected to differential transcript expression analysis. All calculations and statistics were performed using statistical software R (R Foundation for Statistical Computing, Vienna, Austria) (version 3.5.1). [64] Differential gene expression analysis was conducted using R software package edgeR. [65, 66] First, normalization factors were calculated to scale the raw library sizes. In addition, dispersion parameters based on generalized linear models (GLM) were estimated; in particular, the common dispersion for negative binomial GLMs, trended dispersion for negative binomial GLMs using the power method, and empirical Bayes tagwise dispersions for negative binomial GLMs. [66, 67] Statistical tests were then conducted at every time point, to compare between ^{56}Fe irradiated and non-irradiated control, ^{16}O irradiated and non-irradiated control, and ^{28}Si irradiated and non-irradiated control samples using a quasi-likelihood negative binomial generalized log-linear model for count data. [68-70] The Benjamini-Hochberg correction was applied, and transcripts with FDR≤0.05 & fold change≥2 (both up and down regulated) were extracted and utilized in further analyses.

6.3.4 FUNCTIONAL ENRICHMENT ANALYSIS

To determine the biological functions of significantly differentially expressed (DE) transcripts, functional enrichment analysis was performed separately for the DE transcripts at each time point using Ingenuity Pathway Analysis (IPA), (QIAGEN Inc., Hilden, Germany). [74] The most significant functional pathways (-log10(*p-value*)≥1.3) at each time point were then evaluated and reported. A complete list of all identified statistically significant pathways is provided in Tables 8-12, 15-19, and 21-25.

6.3.5 SOM ANALYSIS

Self-Organizing Map (SOM) analysis was performed to identify clusters of transcripts with similar expression patterns, and was conducted for every time point analyzing pairwise comparisons of ^{56}Fe irradiated and non-irradiated control, ^{16}O irradiated and non-irradiated control, and ^{28}Si irradiated and non-irradiated control samples. SOMs were created using the algorithm implemented in the MATLAB software Neural Networking Toolbox [www.mathworks.com] version R2018b based on inputs of Log_2(Fold Change) from the differential transcript expression analyses data. In order to scale network inputs and outputs, we normalized our input matrix so that they had zero mean and unity standard deviation. We then processed the input matrix using principal component analysis (PCA) to reduce dimensionality. The SOM algorithm was then used to cluster the data based on similarity and topology using 100,000 training epochs. The SOM translates the differentially expressed transcriptome profile into a two-dimensional quadratic 7x7 pixel map and a color code for similarity values.

Next, we performed functional pathway analysis using IPA (QIAGEN Inc., Hilden, Germany) [74], on selected adjacent modules (clusters selected for IPA analysis are

numbered and shown in circles on SOM maps) that contained the reported functionally unannotated transcripts by IPA to explore their functionality based on the annotated transcripts contained within those modules (available activation z-scores, shared enriched functions of interest, and similar transcript expression patterns). Activation z-score is statistically computed by IPA for each functional pathway and is used to infer biological functions and predict implicated functional pathways. The activation z-score is predicted by assessing the consistency of the pattern between the observed gene-regulation pattern and the activation/inhibition pattern given by the network relative to a random pattern. Activation z-score calculations are accomplished independently from associated p-values and is based upon the match results from up/down regulation. Given the observed differential regulation of a transcript in the dataset, the activation state is determined for each specific functional pathway, and the directionality effect is then assigned. If an activation z-score can't be predicted for a significant pathway based on the available data and after bias correction, NA (white color) is assigned for that specific pathway. [74]

6.4 Results

6.4.1 DIFFERENTIAL EXPRESSION ANALYSIS OF ^{56}FE REVEALS DYNAMIC TIME-DEPENDENT CHANGES IN INFLAMMATORY RESPONSE AT THE WHOLE TRANSCRIPTOME LEVEL

Transcriptional changes and altered pathways associated with ^{56}Fe induced hepatic carcinogenesis were evaluated using differential expression analysis of RNA-Seq data in ^{56}Fe irradiated compared to non-irradiated control mice at 5 different time points (1mo, 2mo, 4mo, 9mo, and 12mo). Table 7 shows the total number of differentially expressed transcripts at each time point. IPA was used to functionally annotate and map the biological processes involving these differentially expressed transcripts (Figure 9). Inflammatory pathways and their temporal importance in irradiation induced tissue injury are poorly understood. In this regard, the analyses revealed a significant activation of acute phase response signaling at 1 month, followed by significant inhibition of this pathway at 2, 4, 9, and 12 months. The microenvironment present early after ^{56}Fe irradiation is proinflammatory and results in activation of inflammatory pathways, such as acute phase response signaling. This is a rapid inflammatory response that provides protection against noxious stimuli using non-specific defense mechanisms. [104-106] Tissue inflammation can naturally subside overtime, but a significant suppression of inflammatory genes, which we see in our data, is characteristic of induced capillary remodeling and angiogenesis. [107] The prominent inhibition of acute phase response signaling at later time points compared to non-irradiated animals suggests that impaired immune response and regulation are involved in accelerated hepatic carcinogenesis in these mice. Similarly, the peroxisome proliferator activated receptor α (PPARα), a ligand activated transcription factor that

belongs to the family of nuclear receptors, is significantly affected at 1 month (activated), 2 months (inhibited), 4 months (inhibited), 9 months (inhibited), and 12 months (activated). PPARα has a prominent role in fatty acid oxidation, where it can exert an anti-inflammatory and anti-oxidative effect. Its activation at 1 month and 12 months suggests that there is an early inflammatory response, that recurs later due to the progression of carcinogenic processes. [108-110]

B cell receptor signaling (BCR) is significantly affected at months 2 (directionality unknown), 4 (inhibited), 9 (inhibited), and 12 (activated). Activation of BCR signaling inhibits apoptosis in B cells. [111] This observation is supported in a previous study, which demonstrated that ^{56}Fe irradiation increased the incidence of murine acute myeloid leukemia (AML) and HCC. [7] Furthermore, PI3K/AKT signaling is significantly affected at 2 months (inhibited), 4 months (directionality unknown), 9 months (activated) and 12 months (inhibited). AKT has two distinct mechanisms of action. First, it can have an inhibitory role, such as inhibiting apoptosis, and allowing for cell survival. Second, it can have an activating role, by activating IKK which in turn leads to NF-κB activation and cell survival. [112-114] The analysis also revealed a significant activation of the Liver X receptor (LXR)/Retinoid X Receptor (RXR) pathway at 1 and 9 months accompanied by an inhibition at 2- and 4-months post ^{56}Fe irradiation. Previous studies have shown LXRs to be key modulators of both lipid metabolism and inflammatory signaling [115], as well as inducers of genes involved in the inhibition of inflammatory pathways. [116] The presence of this complex and coordinated time-dependent interplay between pro- and anti-inflammatory signaling pathways post ^{56}Fe irradiation could play a significant role in ^{56}Fe

irradiated induced hepatic carcinogenesis. A complete list of significant pathways ($-\log_{10}$(p-value)≥1.3) is provided in Tables 8, 9, 10, 11, and 12.

Ion	Time	Total DE	Upregulated	Downregulated
^{56}Fe	**1 mo**	695	304	391
^{56}Fe	**2 mo**	662	300	362
^{56}Fe	**4 mo**	679	325	354
^{56}Fe	**9 mo**	718	374	344
^{56}Fe	**12 mo**	564	304	260
^{16}O	**1 mo**	710	384	326
^{16}O	**2 mo**	615	298	317
^{16}O	**4 mo**	588	328	260
^{16}O	**9 mo**	602	332	270
^{16}O	**12 mo**	796	504	292
^{28}Si	**1 mo**	849	407	442
^{28}Si	**2 mo**	699	319	380
^{28}Si	**4 mo**	902	400	502
^{28}Si	**9 mo**	679	381	298
^{28}Si	**12 mo**	628	328	300

Table 7. Differentially Expressed Transcripts. Total DE shows the total number of differentially expressed transcripts (FDR≤0.05 & fold change ≥2) for each HZE ion at 5 different time points.

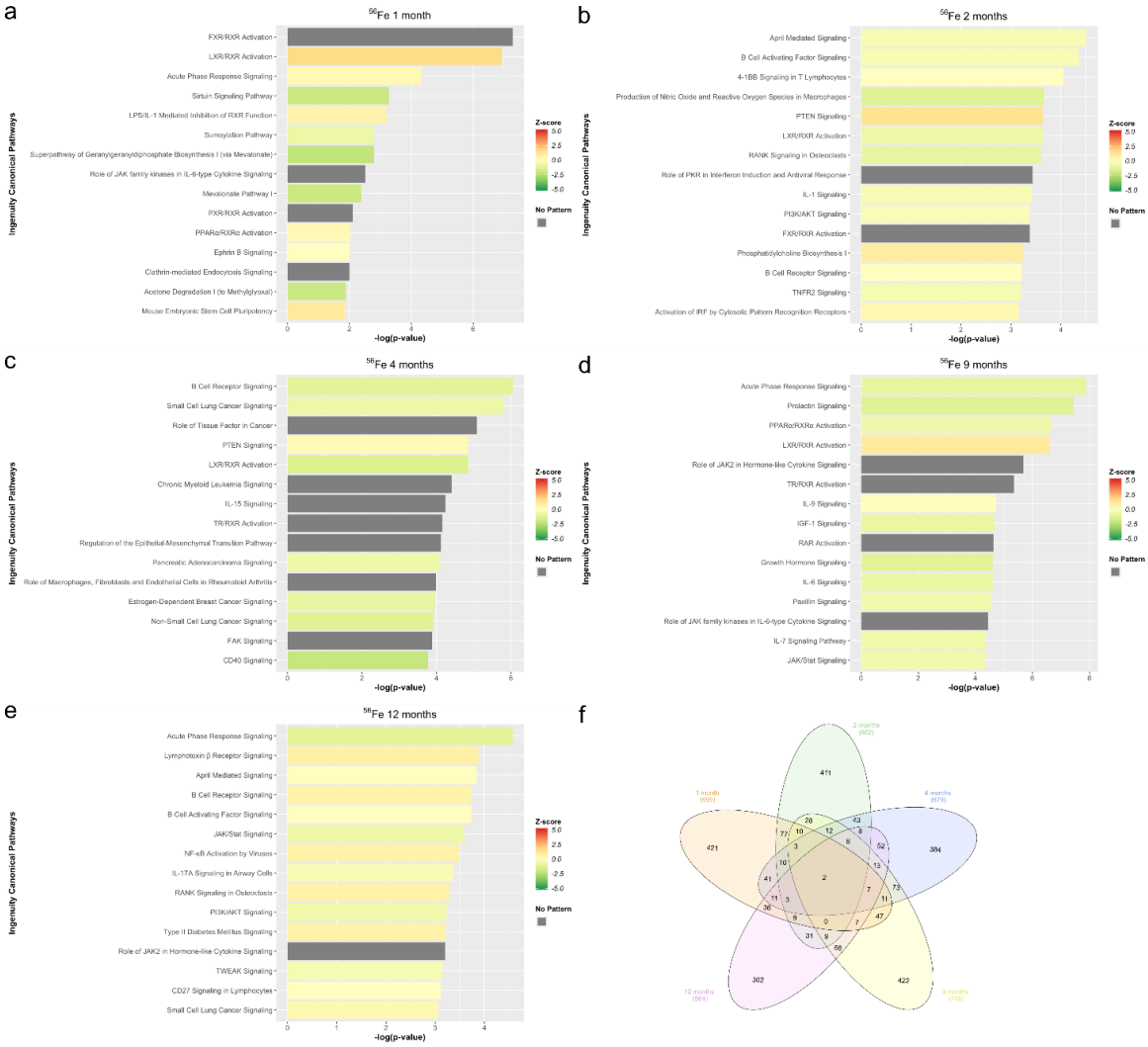

Figure 9. IPA of differentially expressed transcripts in ^{56}Fe.

(a) Top pathways enrichment analysis at 1 month. **(b)** Top pathways enrichment analysis at 2 months. **(c)** Top pathways enrichment analysis at 4 months. **(d)** Top pathways enrichment analysis at 9 months. **(e)** Top pathways enrichment analysis at 12 months. **(f)** The Venn Diagram shows shared and unique differentially expressed transcripts for all time points, in ^{56}Fe irradiation compared to control.

Ingenuity Canonical Pathways	**-log$_{10}$(p-value)**	**z-score**	**Molecules**
FXR/RXR Activation	7.27	NA	ABCB11,APOA2,BAAT,C4A/C4B,C9,CLU,FASN,FETUB,KNG1,NR0B2,NR1H3,NR1H4,PLTP,SAA1,SDC1,SERPINF1,VTN
LXR/RXR Activation	6.92	1.732	APOA2,C4A/C4B,C9,CLU,FASN,FDFT1,HMGCR,KNG1,NC

			OR2,NR1H3,NR1H4,PLTP,SAA1,SERPINF1,TLR3,VTN
Acute Phase Response Signaling	4.32	0.333	APOA2,C1R,C4A/C4B,C9,CP,ECSIT,FN1,HNRNPK,HP,IL6ST,MAPK14,MAPK3,SAA1,SERPINF1,TCF3
Sirtuin Signaling Pathway	3.28	-2	ATG13,GLUD1,MAP1LC3A,MAPK3,MAPK7,MT-ATP6,MT-CYB,MT-ND2,MT-ND3,MT-ND4,MT-ND4L,MT-ND5,MT-ND6,NR1H3,NR1H4,PFKFB3,RARB,SIRT5,TUBA4A
LPS/IL-1 Mediated Inhibition of RXR Function	3.2	0.632	ABCB11,ALAS1,ALDH2,CYP2B6,CYP2C8,CYP3A5,CYP4A11,ECSIT,FMO1,FMO2,HMGCS1,NR0B2,NR1H3,NR1H4,PLTP
Sumoylation Pathway	2.8	-0.816	RCC1,RFC1,RHOBTB1,SENP5,SENP7,SERBP1,SP3,XIAP,ZNF217
Superpathway of Geranylgeranyldiphosphate Biosynthesis I (via Mevalonate)	2.79	-2.236	FDPS,HADHB,HMGCR,HMGCS1,MVD
Role of JAK family kinases in IL-6-type Cytokine Signaling	2.51	NA	IL6ST,MAPK14,MAPK3,TYK2
Mevalonate Pathway I	2.38	-2	HADHB,HMGCR,HMGCS1,MVD
PXR/RXR Activation	2.11	NA	ABCB11,ALAS1,CYP2B6,CYP2C8,CYP3A5,NR0B2
PPARα/RXRα Activation	2.02	0.333	ADCY9,APOA2,CYP2C8,FASN,GPD2,MAPK14,MAPK3,MED12,NCOR2,NOTUM,NR0B2
Clathrin-mediated Endocytosis Signaling	2	NA	AP1B1,AP1G2,APOA2,ARRB1,CD2AP,CLU,MYO1E,NUMB,PICALM,SH3GLB2,TFRC
Ephrin B Signaling	2	0	ABI1,CAP1,CTNNB1,EPHB4,HNRNPK,MAPK3
Acetone Degradation I (to Methylglyoxal)	1.89	-2	CYP2B6,CYP2C8,CYP3A5,CYP4A11
Mouse Embryonic Stem Cell Pluripotency	1.85	1.134	CTNNB1,IL6ST,MAPK14,MAPK3,TCF3,TYK2,XIAP
Complement System	1.85	NA	C1R,C4A/C4B,C8A,C9
Superpathway of Cholesterol Biosynthesis	1.72	-2.449	FDFT1,FDPS,HADHB,HMGCR,HMGCS1,MVD
α-tocopherol Degradation	1.71	NA	CYP4A11,CYP4F3
HIPPO signaling	1.7	1	AMOT,DLG1,DLG5,MOB1A,PARD3,TEAD1
IL-22 Signaling	1.68	NA	MAPK14,MAPK3,TYK2
Endocannabinoid Developing Neuron Pathway	1.59	0.378	ADCY9,CDKN1B,CREB1,CTNNB1,MAPK14,MAPK3,MAPK7
Lipid Antigen Presentation by CD1	1.59	NA	AP1B1,AP1G2,PSAP
Bupropion Degradation	1.55	NA	CYP2B6,CYP2C8,CYP3A5
RAR Activation	1.54	NA	ADCY9,CYP26A1,DHRS4,MAPK14,NCOR2,PRKD3,RARB,SDR9C7,TNIP1,ZBTB16
Oxidative Phosphorylation	1.54	2.646	MT-ATP6,MT-CYB,MT-ND2,MT-ND3,MT-ND4,MT-ND4L,MT-ND5

Phenylalanine Degradation I (Aerobic)	1.54	NA	PCBD2,QDPR
Xenobiotic Metabolism Signaling	1.53	NA	ALDH2,CAMK2D,CYP2B6,CYP2C8,CYP3A5,FMO1,FMO2,HDAC4,MAPK14,MAPK3,MAPK7,NCOR2,PRKD3
Systemic Lupus Erythematosus Signaling	1.49	NA	C8A,C9,CREM,EFTUD2,HNRNPA2B1,HNRNPC,KNG1,MAPK3,NFAT5,PRPF40B,PRPF8
Endocannabinoid Cancer Inhibition Pathway	1.47	-2.828	ADCY9,CDKN1B,CREB1,CTNNB1,MAPK14,MAPK3,SMPD4,TCF3
UVC-Induced MAPK Signaling	1.43	-2	MAPK14,MAPK3,PRKD3,SMPD4
Gap Junction Signaling	1.42	NA	ADCY9,CTNNB1,GJB1,MAPK3,MAPK7,NOTUM,PRKD3,SP3,TUBA4A,TUBB2A
Nicotine Degradation II	1.41	-1.342	CYP2B6,CYP2C8,CYP3A5,FMO1,FMO2
Epithelial Adherens Junction Signaling	1.4	NA	CTNNB1,EPN2,MYH10,PARD3,RAPGEF1,TCF3,TUBA4A,TUBB2A
Tetrapyrrole Biosynthesis II	1.4	NA	ALAS1,UROS
Glycerol Degradation I	1.4	NA	Gk,GPD2
14-3-3-mediated Signaling	1.38	-1.342	CDKN1B,MAPK3,NOTUM,PRKD3,TSC1,TUBA4A,TUBB2A
Triacylglycerol Biosynthesis	1.38	-2	AGPAT3,LPIN1,LPIN3,PLPP5
Apelin Cardiomyocyte Signaling Pathway	1.35	-1.633	MAPK14,MAPK3,MAPK7,NOTUM,PRKD3,SLC9A8
Mitochondrial Dysfunction	1.34	NA	GPD2,MT-ATP6,MT-CYB,MT-ND2,MT-ND3,MT-ND4,MT-ND4L,MT-ND5,MT-ND6

Table 8. Significant Pathways for differentially expressed transcripts in ^{56}Fe vs. non-irradiated control at 1 month.

Ingenuity Canonical Pathways	**-log$_{10}$(p-value)**	**z-score**	**Molecules**
April Mediated Signaling	4.51	-0.378	CHUK,IKBKB,IKBKG,MAPK14,MAPK9,NFAT5,NFATC1
B Cell Activating Factor Signaling	4.36	-0.378	CHUK,IKBKB,IKBKG,MAPK14,MAPK9,NFAT5,NFATC1
4-1BB Signaling in T Lymphocytes	4.05	0	ATF2,CHUK,IKBKB,IKBKG,MAPK14,MAPK9
Production of Nitric Oxide and Reactive Oxygen Species in Macrophages	3.66	-1.387	APOB,APOE,CAT,CHUK,CLU,IKBKB,IKBKG,Map3k7,MAPK14,MAPK9,PIK3CD,PTPA,RHOBTB1,SIRPA
LXR/RXR Activation	3.64	-0.707	APOB,APOE,C4A/C4B,CLU,ECHS1,NCOR1,NCO

			R2,NR1H2,SAA1,TLR3, VTN
PTEN Signaling	3.64	1.508	CDKN1B,CHUK,FGFR2, FGFR3,GSK3A,IKBKB,I KBKG,MAGI1,MAST2,P IK3CD,SYNJ1
RANK Signaling in Osteoclasts	3.6	-1	CHUK,IKBKB,IKBKG,M ap3k7,MAPK14,MAPK9, NFATC1,PIK3CD,XIAP
Role of PKR in Interferon Induction and Antiviral Response	3.43	NA	ATF2,CHUK,IKBKB,IK BKG,MAPK14,TLR3
IL-1 Signaling	3.42	-0.378	ADCY9,CHUK,GNB2,IK BKB,IKBKG,IRAK1,MA PK14,MAPK9,TOLLIP
FXR/RXR Activation	3.38	NA	APOB,APOE,BAAT,C4A /C4B,CLU,FETUB,LIPC, MAPK9,SAA1,SDC1,VT N
PI3K/AKT Signaling	3.38	-0.302	CDKN1B,CHUK,CTNNB 1,GSK3A,HSP90AB1,IK BKB,IKBKG,PIK3CD,PT PA,SYNJ1,TSC1
Phosphatidylcholine Biosynthesis I	3.24	1	CHKA,CHPT1,PCYT1A, PHKA1
B Cell Receptor Signaling	3.22	0	ATF2,CHUK,GSK3A,IK BKB,IKBKG,Map3k7,M APK14,MAPK9,NFAT5, NFATC1,PIK3CD,SYNJ1 ,TCF3
TNFR2 Signaling	3.2	-0.447	CHUK,IKBKB,IKBKG,T BK1,XIAP
Activation of IRF by Cytosolic Pattern Recognition Receptors	3.16	0.378	ADAR,ATF2,CHUK,IKB KB,IKBKG,MAPK9,TBK 1
Huntington's Disease Signaling	3.15	0	ATF2,ATP5F1B,ATP5F1 C,ATP5PB,DNM2,GNB2, HDAC5,MAPK9,NCOR1, NCOR2,PIK3CD,PLCB4, PSME1,RASA1,SGK1
Protein Kinase A Signaling	3.08	-1.941	ADCY9,AKAP1,AKAP12 ,AKAP8,ANAPC5,ATF2, CHUK,CTNNB1,EYA3,F LNA,GNB2,GSK3A,NFA T5,NFATC1,PHKA2,PLC B4,PTPN21,PTPRJ,SIRP A,TCF3,TTN
Epithelial Adherens Junction Signaling	2.94	NA	ACTR3,BAIAP2,CLIP1,C TNNB1,KEAP1,MAGI1, MET,MYH14,PARD3,RA PGEF1,TCF3
Adipogenesis pathway	2.86	NA	CTNNB1,FGFR2,FGFR3, HDAC5,KAT2A,KAT6A, RPS6KA1,SAP130,SENP 2,SMAD5
Neuroinflammation Signaling Pathway	2.85	-0.728	ATF2,BIRC6,CHUK,CT NNB1,IKBKB,IKBKG,IR AK1,MAPK14,MAPK6, MAPK9,NFAT5,NFATC1 ,NOX4,PIK3CD,TBK1,T LR3,XIAP

Antioxidant Action of Vitamin C	2.84	0.378	ABHD3,CHUK,GLRX,IKBKB,IKBKG,MAPK14,MAPK9,PLCB4,TXNRD2
Xenobiotic Metabolism Signaling	2.81	NA	ABCC3,CAT,ESD,FMO2,HDAC5,HSP90AB1,KEAP1,Map3k7,MAPK14,MAPK9,NCOR2,NDST1,NRIP1,PIK3CD,PTGES3,PTPA
Endocannabinoid Developing Neuron Pathway	2.76	0.333	ADCY9,ATF2,CDKN1B,CTNNB1,MAPK14,MAPK6,MAPK9,MGLL,PIK3CD
Sirtuin Signaling Pathway	2.71	0.832	ACLY,ATP5F1B,ATP5F1C,ATP5PB,GABARAPL1,GLUD1,KAT2A,MAPK6,MYCN,NDUFA10,NR1H2,PFKFB3,PFKM,PGK1,POLR3D,SCNN1A,STK11
Toll-like Receptor Signaling	2.65	-0.816	CHUK,IKBKB,IKBKG,IRAK1,MAPK14,TLR3,TOLLIP
Cdc42 Signaling	2.64	0.707	ACTR3,ATF2,BAIAP2,CLIP1,DIAPH1,H2-T22,MAPK14,MAPK9,PARD3,RASA1,TNK2
PPARα/RXRα Activation	2.62	-1.667	ACOX1,ADCY9,CHUK,CKAP5,HSP90AB1,IKBKB,IKBKG,MAPK14,MED24,NCOR1,NCOR2,PLCB4
Clathrin-mediated Endocytosis Signaling	2.61	NA	ACTR3,AP1B1,AP2A1,APOB,APOE,CLU,DNM2,MET,MYO6,PIK3CD,SH3GLB2,SYNJ1
Assembly of RNA Polymerase III Complex	2.5	NA	GTF3A,GTF3C4,POLR3D
LPS-stimulated MAPK Signaling	2.49	-0.378	ATF2,CHUK,IKBKB,IKBKG,MAPK14,MAPK9,PIK3CD
Apelin Cardiomyocyte Signaling Pathway	2.49	-1.414	ATP2A3,CAT,MAPK14,MAPK6,MAPK9,PIK3CD,PLCB4,SLC9A8
Glucocorticoid Receptor Signaling	2.48	NA	CHUK,HSP90AB1,IKBKB,IKBKG,MAPK14,MAPK9,NCOR1,NCOR2,NFAT5,NFATC1,NRIP1,PBRM1,PIK3CD,PTGES3,SGK1,TAF1,TAT
NF-κB Signaling	2.44	-1.508	AZI2,CHUK,FGFR2,FGFR3,IKBKB,IKBKG,IRAK1,PIK3CD,TBK1,TLR3,TNIP1
Role of RIG1-like Receptors in Antiviral Innate Immunity	2.44	-1.342	CHUK,IKBKB,IKBKG,TBK1,TRIM25
Acute Phase Response Signaling	2.41	-1.667	C4A/C4B,CHUK,FN1,IKBKB,IKBKG,IRAK1,MAPK14,MAPK9,PIK3CD,SAA1,TCF3

CD40 Signaling	2.37	-1.633	CHUK,IKBKB,IKBKG,MAPK14,MAPK9,PIK3CD
IL-17A Signaling in Airway Cells	2.34	-1.633	CHUK,IKBKB,IKBKG,MAPK14,MAPK9,PIK3CD
IL-12 Signaling and Production in Macrophages	2.3	NA	APOB,APOE,CHUK,CLU,IKBKB,IKBKG,MAPK14,MAPK9,PIK3CD
iNOS Signaling	2.27	-1.342	CHUK,IKBKB,IKBKG,IRAK1,MAPK14
Remodeling of Epithelial Adherens Junctions	2.24	-1	ACTR3,CBLL1,CLIP1,CTNNB1,DNM2,MET
TNFR1 Signaling	2.2	0.447	CHUK,IKBKB,IKBKG,MAP4K2,XIAP
PI3K Signaling in B Lymphocytes	2.16	-0.707	ATF2,CD81,CHUK,IKBKB,IKBKG,NFAT5,NFATC1,PIK3CD,PLCB4
NGF Signaling	2.12	0.707	ATF2,CHUK,IKBKB,IKBKG,Map3k7,MAPK9,PIK3CD,RPS6KA1
Role of Osteoblasts, Osteoclasts and Chondrocytes in Rheumatoid Arthritis	2.12	NA	CHUK,CTNNB1,IKBKB,IKBKG,MAPK14,MAPK9,NFAT5,NFATC1,PIK3CD,SMAD5,TCF3,XIAP
Cardiac Hypertrophy Signaling (Enhanced)	2.1	-0.655	ADCY9,ATF2,ATP2A3,CHUK,CTNNB1,DIAPH1,DLG1,FGFR2,FGFR3,GSK3A,HDAC5,IKBKB,IKBKG,Map3k7,MAPK14,MAPK9,NFAT5,NFATC1,PIK3CD,PKN1,PLCB4
ATM Signaling	2.09	0.447	ATF2,BRAT1,MAPK14,MAPK9,PTPA,SMC2,TRRAP
CD27 Signaling in Lymphocytes	2.09	0.447	CHUK,IKBKB,IKBKG,Map3k7,MAPK9
RAR Activation	2.07	NA	ADCY9,MAPK14,MAPK9,NCOR1,NCOR2,NRIP1,PBRM1,PIK3CD,SMAD5,TNIP1,TRIM24
LPS/IL-1 Mediated Inhibition of RXR Function	2.07	0.378	ABCC3,ACOX1,ACSL4,ALAS1,APOE,CAT,FMO2,IRAK1,LIPC,MAPK9,NDST1,NR1H2
Pyridoxal 5'-phosphate Salvage Pathway	2.07	0	GRK6,IRAK1,MAPK6,MAPK9,PKN1,SGK1
Role of Macrophages, Fibroblasts and Endothelial Cells in Rheumatoid Arthritis	2.05	NA	ATF2,CHUK,CTNNB1,FN1,IKBKB,IKBKG,IRAK1,MAPK14,MAPK9,NFAT5,NFATC1,PIK3CD,PLCB4,TCF3,TLR3
TWEAK Signaling	2.05	-1	CHUK,IKBKB,IKBKG,XIAP
IL-17A Signaling in Fibroblasts	2.05	NA	CHUK,IKBKB,IKBKG,MAPK14
CD28 Signaling in T Helper Cells	2.02	-0.707	ACTR3,CHUK,IKBKB,IKBKG,MAPK9,NFAT5,NFATC1,PIK3CD
Angiopoietin Signaling	2.02	0.447	CHUK,IKBKB,IKBKG,PIK3CD,RASA1,TNIP1
Role of IL-17A in Arthritis	1.99	NA	ATF2,MAPK14,MAPK9,PIK3CD,RPS6KA1

Chronic Myeloid Leukemia Signaling	1.95	NA	CDKN1B,CHUK,HDAC5,IKBKB,IKBKG,PIK3CD,RBL2
14-3-3-mediated Signaling	1.94	-0.707	CDKN1B,GSK3A,MAPK9,PIK3CD,PLCB4,RPS6KA1,STK11,TSC1
PPAR Signaling	1.94	-0.378	CHUK,HSP90AB1,IKBKB,IKBKG,NCOR1,NCOR2,NRIP1
IL-7 Signaling Pathway	1.94	-2.449	CDKN1B,GSK3A,MAPK14,MET,NFATC1,PIK3CD
Apelin Adipocyte Signaling Pathway	1.91	0.816	ADCY9,CAT,MAPK14,MAPK6,MAPK9,NOX4
Inhibition of Angiogenesis by TSP1	1.88	NA	CD47,MAPK14,MAPK9,SDC1
Role of NFAT in Regulation of the Immune Response	1.87	-1	ATF2,CHUK,GNB2,GSK3A,IKBKB,IKBKG,NFAT5,NFATC1,PIK3CD,PLCB4
Signaling by Rho Family GTPases	1.86	-0.707	ACTR3,ARHGEF12,BAIAP2,CLIP1,GNB2,MAPK9,NOX4,PARD3,PIK3CD,PKN1,RDX,RHOBTB1
Mitochondrial Dysfunction	1.85	NA	ATP5F1B,ATP5F1C,ATP5MC2,ATP5PB,CAT,CYB5A,FURIN,MAPK9,NDUFA10,TXNRD2
Induction of Apoptosis by HIV1	1.84	-0.447	CHUK,IKBKB,IKBKG,MAPK9,XIAP
3-phosphoinositide Degradation	1.83	-0.333	MTM1,PPP1R16B,PPP4R1,PTPA,PTPRJ,RASA1,SET,SIRPA,SYNJ1
NRF2-mediated Oxidative Stress Response	1.82	0.378	CAT,CDC34,DNAJA3,DNAJB11,GCLM,KEAP1,MAPK14,MAPK9,PIK3CD,SQSTM1
D-myo-inositol-5-phosphate Metabolism	1.81	-1	PLCB4,PPP1R16B,PPP4R1,PTPA,PTPRJ,RASA1,SET,SIRPA,SYNJ1
T Cell Receptor Signaling	1.81	NA	CHUK,IKBKB,IKBKG,NFAT5,NFATC1,PIK3CD,RASA1
ILK Signaling	1.78	0.707	ATF2,CTNNB1,FLNA,FN1,GSK3A,MAPK9,MYH14,PIK3CD,PTPA,RHOBTB1
Glycolysis I	1.77	1	ENO3,GPI,PFKM,PGK1
Superpathway of Inositol Phosphate Compounds	1.76	-1.508	PIK3CD,PLCB4,PPP1R16B,PPP4R1,PTPA,PTPRJ,RASA1,SEC16A,SET,SIRPA,SYNJ1
FGF Signaling	1.75	-1.633	ATF2,FGFR2,FGFR3,MAPK14,MET,PIK3CD
Choline Biosynthesis III	1.74	NA	CHPT1,PCYT1A,PHKA1
Salvage Pathways of Pyrimidine Ribonucleotides	1.73	-0.378	AK4,GRK6,IRAK1,MAPK6,MAPK9,PKN1,SGK1
Regulation of IL-2 Expression in Activated and Anergic T Lymphocytes	1.68	NA	CHUK,IKBKB,IKBKG,MAPK9,NFAT5,NFATC1
Fatty Acid β-oxidation I	1.67	0	ACSL4,ECHS1,HADHB,SCP2

Insulin Receptor Signaling	1.66	-0.378	ACLY,GSK3A,PIK3CD,RAPGEF1,SCNN1A,SGK1,SYNJ1,TSC1
IL-8 Signaling	1.64	-1.414	CHUK,GNB2,IKBKB,IKBKG,IRAK1,ITGAV,MAPK9,NOX4,PIK3CD,RHOBTB1
Antiproliferative Role of TOB in T Cell Signaling	1.64	NA	CDC34,CDKN1B,RPS6KA1
Factors Promoting Cardiogenesis in Vertebrates	1.64	NA	ATF2,CTNNB1,MAPK14,NOX4,SMAD5,TCF3
FAT10 Cancer Signaling Pathway	1.64	0	CHUK,CTNNB1,IKBKB,IKBKG
D-myo-inositol (1,4,5,6)-Tetrakisphosphate Biosynthesis	1.61	-0.707	PPP1R16B,PPP4R1,PTPA,PTPRJ,RASA1,SET,SIRPA,SYNJ1
D-myo-inositol (3,4,5,6)-tetrakisphosphate Biosynthesis	1.61	-0.707	PPP1R16B,PPP4R1,PTPA,PTPRJ,RASA1,SET,SIRPA,SYNJ1
Prostate Cancer Signaling	1.6	NA	ATF2,CDKN1B,CHUK,CTNNB1,HSP90AB1,PIK3CD
Aryl Hydrocarbon Receptor Signaling	1.6	0.707	CDKN1B,HSP90AB1,NCOR2,NFIA,NFIX,NRIP1,PTGES3,RBL2
3-phosphoinositide Biosynthesis	1.59	-1	PIK3CD,PPP1R16B,PPP4R1,PTPA,PTPRJ,RASA1,SET,SIRPA,SYNJ1
Phenylalanine Degradation I (Aerobic)	1.58	NA	PAH,QDPR
fMLP Signaling in Neutrophils	1.57	-1.633	ACTR3,GNB2,NFAT5,NFATC1,NOX4,PIK3CD,PLCB4
RhoA Signaling	1.54	-0.378	ACTR3,ARHGAP1,ARHGEF12,BAIAP2,PKN1,RDX,TTN
Molecular Mechanisms of Cancer	1.54	NA	ADCY9,ARHGEF12,CDK13,CDKN1B,CTNNB1,GSK3A,MAPK14,MAPK9,PIK3CD,PLCB4,RAPGEF1,RASA1,RHOBTB1,SMAD5,TCF3,XIAP
Apoptosis Signaling	1.53	0.816	BIRC6,CHUK,IKBKB,IKBKG,RPS6KA1,XIAP
Role of p14/p19ARF in Tumor Suppression	1.52	NA	PIK3CD,POLR3D,UBTF
Small Cell Lung Cancer Signaling	1.52	-1.342	CDKN1B,CHUK,IKBKB,IKBKG,PIK3CD
Hypoxia Signaling in the Cardiovascular System	1.52	NA	ATF2,BIRC6,CDC34,COPS5,HSP90AB1
Dendritic Cell Maturation	1.51	-0.333	ATF2,CHUK,IKBKB,IKBKG,MAPK14,MAPK9,PIK3CD,PLCB4,TLR3
Mouse Embryonic Stem Cell Pluripotency	1.45	-0.816	CTNNB1,MAPK14,PIK3CD,SMAD5,TCF3,XIAP
SAPK/JNK Signaling	1.45	0.447	ATF2,MAP4K2,MAPK8IP3,MAPK9,NFATC1,PIK3CD
Gα12/13 Signaling	1.44	0.378	CHUK,CTNNB1,IKBKB,IKBKG,MAPK9,PIK3CD,RASA1
BER pathway	1.44	NA	LIG3,PNKP

Reelin Signaling in Neurons	1.43	NA	APOE,ARHGEF12,MAPK8IP3,MAPK9,PIK3CD
Transcriptional Regulatory Network in Embryonic Stem Cells	1.42	NA	CDYL,KAT6A,SET,TRIM24
Actin Cytoskeleton Signaling	1.4	-0.707	ACTR3,ARHGEF12,BAIAP2,DIAPH1,FLNA,FN1,MYH14,PIK3CD,RDX,TTN
Lymphotoxin β Receptor Signaling	1.39	-1	CHUK,IKBKB,IKBKG,PIK3CD
Sertoli Cell-Sertoli Cell Junction Signaling	1.39	NA	ATF2,CTNNB1,DLG1,EPB41,GSK3A,KEAP1,Map3k7,MAPK14,MAPK9
Gαq Signaling	1.37	-1.633	CHUK,GNB2,IKBKB,IKBKG,NFATC1,PIK3CD,PLCB4,RHOBTB1
Estrogen Receptor Signaling	1.36	NA	MED15,MED24,NCOR1,NCOR2,NRIP1,TAF1,TRRAP
PEDF Signaling	1.35	-1.342	CHUK,IKBKB,IKBKG,MAPK14,PIK3CD
DNA Methylation and Transcriptional Repression Signaling	1.34	NA	ARID4B,MTA1,SAP130
AMPK Signaling	1.34	0	AK4,ATF2,MAPK14,PBRM1,PFKFB3,PFKM,PIK3CD,PTPA,STK11,TSC1
NF-κB Activation by Viruses	1.33	-1.342	CHUK,IKBKB,IKBKG,ITGAV,PIK3CD
Human Embryonic Stem Cell Pluripotency	1.32	NA	CTNNB1,FGFR2,FGFR3,GSK3A,PIK3CD,SMAD5,TCF3
HER-2 Signaling in Breast Cancer	1.31	NA	CDKN1B,GSK3A,PARD3,PIK3CD,TSC1
Valine Degradation I	1.31	NA	BCKDHB,ECHS1,HADHB
Type I Diabetes Mellitus Signaling	1.31	-0.816	CHUK,IKBKB,IKBKG,IRAK1,MAPK14,MAPK9

Table 9. Significant Pathways for differentially expressed transcripts in ^{56}Fe vs. non-irradiated control at 2 months.

Ingenuity Canonical Pathways	**-log$_{10}$(p-value)**	**z-score**	**Molecules**
B Cell Receptor Signaling	6.04	-1.213	AKT3,ATF2,BCL6,Calm1 (includes others),CREB1,EGR1,FCGR2A,IKBKG,INPP5B,MAP3K13,MAPK14,MAPK3,NFAT5,PIK3C2G,PIK3CA,SYK,SYNJ1,SYNJ2
Small Cell Lung Cancer Signaling	5.8	-0.816	AKT3,BIRC2,IKBKG,PA2G4,PIAS3,PIK3C2G,PIK3CA,RXRA,RXRB,SIN3A,TRAF3
Role of Tissue Factor in Cancer	5.08	NA	AKT3,ARRB1,EGFR,EGR1,ITGA3,ITGAV,JAK2,MAPK14,

			MAPK3,PIK3C2G,PIK3CA,STAT5A,STAT5B
LXR/RXR Activation	4.85	-1.508	APOE,C4A/C4B,CYP7A1,HMGCR,NR1H2,NR1H3,NR1H4,RXRA,RXRB,SAA1,SCD,SERPINF1,TLR3
PTEN Signaling	4.85	0.277	AKT3,EGFR,FGFR3,IKBKG,INPP5B,ITGA3,MAGI1,MAPK3,MAST2,PIK3CA,SYNJ1,SYNJ2,TGFBR1
Chronic Myeloid Leukemia Signaling	4.4	NA	AKT3,IKBKG,MAPK3,MDM2,PA2G4,PIK3C2G,PIK3CA,SIN3A,STAT5A,STAT5B,TGFBR1
IL-15 Signaling	4.24	NA	AKT3,JAK2,MAPK14,MAPK3,PIK3C2G,PIK3CA,STAT5A,STAT5B,SYK
TR/RXR Activation	4.16	NA	AKT3,CYP7A1,G6PC,HP,MDM2,PIK3C2G,PIK3CA,RXRA,RXRB,THRA
Regulation of the Epithelial-Mesenchymal Transition Pathway	4.12	NA	ADAM17,AKT3,APC,DVL2,EGFR,EGR1,FGF21,FGFR3,FZD6,JAK2,MAPK3,PIK3C2G,PIK3CA,TGFBR1,ZEB2
Pancreatic Adenocarcinoma Signaling	4.1	-0.707	AKT3,EGFR,JAK2,MAPK3,MDM2,PA2G4,PIK3C2G,PIK3CA,RALBP1,SIN3A,TGFBR1
Role of Macrophages, Fibroblasts and Endothelial Cells in Rheumatoid Arthritis	3.98	NA	AKT3,APC,ATF2,C5AR1,Calm1 (includes others),CEBPA,CREB1,CSNK1A1,DAAM1,FN1,FZD6,IKBKG,JAK2,MAPK14,MAPK3,NFAT5,PIK3C2G,PIK3CA,TLR3,TRAF3
Estrogen-Dependent Breast Cancer Signaling	3.96	-1	AKT3,ATF2,CREB1,EGFR,MAPK3,PIK3C2G,PIK3CA,STAT5A,STAT5B
Non-Small Cell Lung Cancer Signaling	3.92	-1.342	AKT3,EGFR,MAPK3,PA2G4,PIK3C2G,PIK3CA,RXRA,RXRB,SIN3A
FAK Signaling	3.88	NA	AKT3,ASAP1,CAPNS1,EGFR,ITGA3,MAPK3,PIK3C2G,PIK3CA,PXN,TNS1
CD40 Signaling	3.78	-2.121	IKBKG,MAPK14,MAPK3,PIK3C2G,PIK3CA,TANK,TNFAIP3,TRAF3
FLT3 Signaling in Hematopoietic Progenitor Cells	3.75	-1	AKT3,ATF2,CREB1,MAPK14,MAPK3,PIK3C2G,PIK3CA,STAT5A,STAT5B
Colorectal Cancer Metastasis Signaling	3.71	0.277	ADCY6,AKT3,APC,ARRB1,EGFR,FZD6,GNB1,GNB2,GRK2,JAK2,MAPK3,PIK3C2G,PIK3CA,RHOBTB1,RHOT1,TGFBR1,TLR3
IL-22 Signaling	3.63	-0.447	AKT3,MAPK14,MAPK3,STAT5A,STAT5B
SPINK1 General Cancer Pathway	3.6	0	AKT3,EGFR,JAK2,MAPK3,Mt1,Mt2,PIK3C2G,PIK3CA
FGF Signaling	3.56	-1.667	AKT3,ATF2,CREB1,FGF21,FGFR3,MAPK14,MAPK3,PIK3C2G,PIK3CA

Role of JAK family kinases in IL-6-type Cytokine Signaling	3.54	NA	JAK2,MAPK14,MAPK3,STAT5A,STAT5B
RANK Signaling in Osteoclasts	3.52	-1	AKT3,BIRC2,Calm1 (includes others),IKBKG,MAP3K13,MAPK14,MAPK3,PIK3C2G,PIK3CA
Lymphotoxin β Receptor Signaling	3.46	-0.816	AKT3,BIRC2,IKBKG,MAPK3,PIK3C2G,PIK3CA,TRAF3
Growth Hormone Signaling	3.35	1.134	CEBPA,JAK2,MAPK3,ONECUT1,PIK3C2G,PIK3CA,STAT5A,STAT5B
Prostate Cancer Signaling	3.31	NA	AKT3,ATF2,CREB1,MAPK3,MDM2,PA2G4,PIK3C2G,PIK3CA,SIN3A
FXR/RXR Activation	3.29	NA	AKT3,APOE,C4A/C4B,CYP7A1,FETUB,G6PC,NR1H3,NR1H4,RXRA,SAA1,SERPINF1
p53 Signaling	3.21	0.816	AKT3,ATR,COQ8A,GADD45G,MAPK14,MDM2,PIK3C2G,PIK3CA,PML
Role of NFAT in Regulation of the Immune Response	3.19	-0.905	AKT3,ATF2,Calm1 (includes others),CSNK1A1,FCGR2A,GNB1,GNB2,IKBKG,MAPK3,NFAT5,PIK3C2G,PIK3CA,SYK
JAK/Stat Signaling	3.16	0	AKT3,JAK2,MAPK3,PIAS3,PIK3C2G,PIK3CA,STAT5A,STAT5B
IL-7 Signaling Pathway	3.16	-0.378	AKT3,BCL6,MAPK14,MAPK3,PIK3C2G,PIK3CA,STAT5A,STAT5B
TNFR2 Signaling	3.16	1	BIRC2,IKBKG,TANK,TBK1,TNFAIP3
Neuroinflammation Signaling Pathway	3.15	-1.414	ACVR2B,AKT3,APP,ATF2,BIRC2,CREB1,IKBKG,JAK2,MAPK14,MAPK3,NFAT5,PIK3C2G,PIK3CA,SYK,TBK1,TGFBR1,TLR3,TRAF3
Neuregulin Signaling	3.12	0	ADAM17,AKT3,EGFR,ERBB4,ERRFI1,ITGA3,MAPK3,STAT5A,STAT5B
IL-2 Signaling	3.1	-0.378	AKT3,MAPK3,PIK3C2G,PIK3CA,STAT5A,STAT5B,SYK
PEDF Signaling	3.09	-0.707	AKT3,IKBKG,MAPK14,MAPK3,PIK3C2G,PIK3CA,SERPINF1,TCF12
Mouse Embryonic Stem Cell Pluripotency	3.05	-1.667	AKT3,APC,DVL2,FZD6,JAK2,MAPK14,MAPK3,PIK3C2G,PIK3CA
Production of Nitric Oxide and Reactive Oxygen Species in Macrophages	3.04	0	AKT3,APOE,IKBKG,JAK2,MAP3K13,MAPK14,MAPK3,PIK3C2G,PIK3CA,PPP1R3C,RHOBTB1,RHOT1,SIRPA
Phagosome Formation	3.03	NA	C5AR1,FCGR2A,FN1,ITGA3,PIK3C2G,PIK3CA,RHOBTB1,RHOT1,SYK,TLR3
IL-17A Signaling in Airway Cells	2.98	-1.134	AKT3,IKBKG,JAK2,MAPK14,MAPK3,PIK3C2G,PIK3CA
Cardiac Hypertrophy Signaling (Enhanced)	2.94	0	ACVR2B,ADCY6,AKT3,ATF2,Calm1 (includes others),DVL2,FGF21,FGFR3,FZD6,GNB1,IKBKG,IL17RB,I

			TGA3,JAK2,MAP3K13,MAPK14,MAPK3,NFAT5,PDE1A,PDE4B,PDK1,PIK3C2G,PIK3CA,TGFBR1
Germ Cell-Sertoli Cell Junction Signaling	2.93	NA	EPN2,ITGA3,KEAP1,MAP3K13,MAPK14,MAPK3,PIK3C2G,PIK3CA,PXN,RHOBTB1,RHOT1,TGFBR1
IL-4 Signaling	2.92	NA	AKT3,INPP5B,JAK2,NFAT5,PIK3C2G,PIK3CA,SYNJ1,SYNJ2
Protein Ubiquitination Pathway	2.91	NA	ANAPC5,BIRC2,DNAJB2,DNAJC12,HSPH1,MDM2,NEDD4L,PAN2,UBE4A,USP19,USP2,USP21,USP34,USP36,USP45,USP8
Role of JAK2 in Hormone-like Cytokine Signaling	2.9	NA	JAK2,SH2B1,SIRPA,STAT5A,STAT5B
Role of Osteoblasts, Osteoclasts and Chondrocytes in Rheumatoid Arthritis	2.9	NA	ADAM17,AKT3,APC,BIRC2,Calm1 (includes others),CSNK1A1,FZD6,IKBKG,ITGA3,MAPK14,MAPK3,NFAT5,PIK3C2G,PIK3CA
Role of JAK1 and JAK3 in γc Cytokine Signaling	2.86	NA	JAK2,MAPK3,PIK3C2G,PIK3CA,STAT5A,STAT5B,SYK
Epithelial Adherens Junction Signaling	2.85	NA	ACVR2B,AKT3,APC,BAIAP2,EGFR,EPN2,KEAP1,MAGI1,MYH11,PARD3,TGFBR1
NF-κB Signaling	2.85	-0.905	AKT3,EGFR,FGFR3,IKBKG,PIK3C2G,PIK3CA,TANK,TBK1,TGFBR1,TLR3,TNFAIP3,TRAF3
PXR/RXR Activation	2.83	NA	AKT3,ALAS1,CES3,CYP7A1,G6PC,RXRA,SCD
Amyloid Processing	2.81	-1	AKT3,APP,CAPNS1,CSNK1A1,MAPK14,MAPK3
Acute Phase Response Signaling	2.81	-1.414	AKT3,C4A/C4B,FN1,HP,IKBKG,JAK2,MAPK14,MAPK3,PIK3CA,SAA1,Saa3,SERPINF1
Ephrin Receptor Signaling	2.77	-0.302	ABI1,AKT3,ATF2,CREB1,EPHB4,GNB1,GNB2,ITGA3,JAK2,MAPK3,PIK3C2G,PXN
Relaxin Signaling	2.76	0	ADCY6,AKT3,CREB1,GNB1,GNB2,MAPK3,NPR2,PDE1A,PDE4B,PIK3C2G,PIK3CA
Acute Myeloid Leukemia Signaling	2.76	-0.707	AKT3,CEBPA,MAPK3,PIK3C2G,PIK3CA,PML,STAT5A,STAT5B
PI3K/AKT Signaling	2.73	0	AKT3,IKBKG,INPP5B,ITGA3,JAK2,MAPK3,MDM2,PIK3CA,SYNJ1,SYNJ2
Endocannabinoid Developing Neuron Pathway	2.69	-1.667	ADCY6,AKT3,ATF2,CREB1,GNB1,MAPK14,MAPK3,PIK3C2G,PIK3CA
Glioma Signaling	2.64	-1.633	AKT3,Calm1 (includes others),EGFR,MAPK3,MDM2,PA2G4,PIK3C2G,PIK3CA,SIN3A
Ovarian Cancer Signaling	2.64	-0.816	AKT3,APC,ARRB1,EGFR,FZD6,MAPK3,PA2G4,PIK3C2G,PIK3CA,SIN3A

Gαq Signaling	2.64	-0.333	AKT3,Calm1 (includes others),GNB1,GNB2,GRK2,IKBKG,MAPK3,PIK3C2G,PIK3CA,RHOBTB1,RHOT1
Integrin Signaling	2.64	0.302	AKT3,ASAP1,CAPNS1,GIT1,ITGA3,ITGAV,MAPK3,PIK3C2G,PIK3CA,PXN,RHOBTB1,RHOT1,TNK2
Huntington's Disease Signaling	2.6	0	AKT3,ATF2,ATP5F1C,CAPNS1,CREB1,EGFR,GNB1,GNB2,MAPK3,NAPA,PIK3C2G,PIK3CA,SIN3A,ZDHHC17
EGF Signaling	2.53	-1.633	AKT3,EGFR,MAPK14,MAPK3,PIK3C2G,PIK3CA
Role of PKR in Interferon Induction and Antiviral Response	2.53	NA	ATF2,IKBKG,MAPK14,TLR3,TRAF3
Erythropoietin Signaling	2.52	NA	AKT3,JAK2,MAPK3,PIK3C2G,PIK3CA,STAT5A,STAT5B
IL-3 Signaling	2.52	0.378	AKT3,JAK2,MAPK3,PIK3C2G,PIK3CA,STAT5A,STAT5B
Fc Epsilon RI Signaling	2.52	-1.667	AKT3,INPP5B,MAPK14,MAPK3,PIK3C2G,PIK3CA,SYK,SYNJ1,SYNJ2
Cardiac Hypertrophy Signaling	2.51	0	ADCY6,ATF2,Calm1 (includes others),CREB1,GNB1,GNB2,MAP3K13,MAPK14,MAPK3,PIK3C2G,PIK3CA,RHOBTB1,RHOT1,TGFBR1
Natural Killer Cell Signaling	2.49	NA	AKT3,FCGR2A,INPP5B,MAPK3,PIK3C2G,PIK3CA,SYK,SYNJ1,SYNJ2
IL-17 Signaling	2.49	NA	AKT3,ATF2,JAK2,MAPK14,MAPK3,PIK3C2G,PIK3CA
Systemic Lupus Erythematosus In B Cell Signaling Pathway	2.45	-1.291	AKT3,Calm1 (includes others),FCGR2A,INPP5B,JAK2,MAPK3,NFAT5,PIK3C2G,PIK3CA,SYK,SYNJ1,SYNJ2,TBK1,TLR3,TRAF3
CXCR4 Signaling	2.44	0.333	ADCY6,AKT3,EGR1,GNB1,GNB2,MAPK3,PIK3C2G,PIK3CA,PXN,RHOBTB1,RHOT1
LPS-stimulated MAPK Signaling	2.43	-1.134	ATF2,CREB1,IKBKG,MAPK14,MAPK3,PIK3C2G,PIK3CA
NF-κB Activation by Viruses	2.4	-0.378	AKT3,IKBKG,ITGA3,ITGAV,MAPK3,PIK3C2G,PIK3CA
Docosahexaenoic Acid (DHA) Signaling	2.39	NA	AKT3,APP,PIK3C2G,PIK3CA,SERPINF1
Molecular Mechanisms of Cancer	2.37	NA	ADCY6,AKT3,APC,ATR,BIRC2,FZD6,ITGA3,JAK2,MAPK14,MAPK3,MDM2,PA2G4,PIK3C2G,PIK3CA,RALBP1,RHOBTB1,RHOT1,SIN3A,TGFBR1
GNRH Signaling	2.37	0	ADCY6,ATF2,Calm1 (includes others),CREB1,EGFR,EGR1,GNB1,MAP3K13,MAPK14,MAPK3,PXN
Cancer Drug Resistance By Drug Efflux	2.32	NA	ABCC10,AKT3,MAPK3,MDM2,PDK1,PIK3CA

Dendritic Cell Maturation	2.28	-0.905	AKT3,ATF2,CREB1,FCGR2A,IKBKG,JAK2,MAPK14,MAPK3,PIK3C2G,PIK3CA,TLR3
Thrombopoietin Signaling	2.25	0.816	JAK2,MAPK3,PIK3C2G,PIK3CA,STAT5A,STAT5B
Thrombin Signaling	2.22	-1.667	ADCY6,AKT3,CREB1,EGFR,GNB1,GNB2,MAPK14,MAPK3,PIK3C2G,PIK3CA,RHOBTB1,RHOT1
P2Y Purigenic Receptor Signaling Pathway	2.21	-0.707	ADCY6,AKT3,ATF2,CREB1,GNB1,GNB2,MAPK3,PIK3C2G,PIK3CA
HGF Signaling	2.19	0	AKT3,ATF2,ITGA3,MAP3K13,MAPK3,PIK3C2G,PIK3CA,PXN
ErbB4 Signaling	2.16	-0.447	ADAM17,ERBB4,MAPK3,PIK3C2G,PIK3CA,YAP1
PDGF Signaling	2.16	0.378	INPP5B,JAK2,MAPK3,PIK3C2G,PIK3CA,SYNJ1,SYNJ2
TNFR1 Signaling	2.15	0	BIRC2,IKBKG,MADD,TANK,TNFAIP3
4-1BB Signaling in T Lymphocytes	2.15	-1	ATF2,IKBKG,MAPK14,MAPK3
GM-CSF Signaling	2.13	0	AKT3,JAK2,MAPK3,PIK3C2G,PIK3CA,STAT5B
Phosphatidylcholine Biosynthesis I	2.13	NA	CHKA,PCYT1A,PHKA1
ILK Signaling	2.13	-0.632	AKT3,ATF2,CREB1,FN1,MAPK3,MYH11,PIK3C2G,PIK3CA,PXN,RHOBTB1,RHOT1
Tec Kinase Signaling	2.12	1.89	GNB1,GNB2,ITGA3,JAK2,PIK3C2G,PIK3CA,RHOBTB1,RHOT1,STAT5A,STAT5B
IL-9 Signaling	2.1	1	PIK3C2G,PIK3CA,STAT5A,STAT5B
PI3K Signaling in B Lymphocytes	2.09	-2.333	AKT3,ATF2,Calm1 (includes others),CREB1,IKBKG,MAPK3,NFAT5,PIK3CA,SYK
White Adipose Tissue Browning Pathway	2.09	-1	ADCY6,ATF2,CREB1,FGF21,FGFR3,MAPK14,RXRA,RXRB,THRA
Melanoma Signaling	2.08	-0.447	AKT3,MAPK3,MDM2,PIK3C2G,PIK3CA
UVB-Induced MAPK Signaling	2.08	-1.342	EGFR,MAPK14,MAPK3,PIK3C2G,PIK3CA
Actin Cytoskeleton Signaling	2.08	0	APC,BAIAP2,CYFIP1,FGF21,FN1,GIT1,ITGA3,MAPK3,MYH11,PIK3C2G,PIK3CA,PXN
Glioblastoma Multiforme Signaling	2.07	-0.333	AKT3,APC,EGFR,FZD6,MAPK3,MDM2,PIK3C2G,PIK3CA,RHOBTB1,RHOT1
NGF Signaling	2.06	-0.707	AKT3,ATF2,CREB1,IKBKG,MAP3K13,MAPK3,PIK3C2G,PIK3CA
Insulin Receptor Signaling	2.06	-0.333	AKT3,INPP5B,JAK2,MAPK3,PIK3C2G,PIK3CA,PPP1R3C,SYNJ1,SYNJ2
Ephrin B Signaling	2.05	-1	ABI1,EPHB4,GNB1,GNB2,MAPK3,PXN
ATM Signaling	2.04	-0.447	ATF2,ATR,CREB1,GADD45G,MAPK14,MDM2,TRRAP

Bladder Cancer Signaling	2.04	NA	EGFR,FGF21,FGFR3,MAPK3,MDM2,PA2G4,SIN3A
Glioma Invasiveness Signaling	2.02	-0.447	ITGAV,MAPK3,PIK3C2G,PIK3CA,RHOBTB1,RHOT1
Circadian Rhythm Signaling	2.01	NA	ATF2,CREB1,NR1D1,PER3
IL-17A Signaling in Fibroblasts	2.01	NA	IKBKG,LCN2,MAPK14,MAPK3
RAR Activation	2	NA	ADCY6,AKT3,JAK2,MAPK14,PIK3CA,PML,PRMT1,RXRA,RXRB,STAT5A,STAT5B
TREM1 Signaling	1.99	0	AKT3,JAK2,MAPK3,STAT5A,STAT5B,TLR3
IL-8 Signaling	1.97	-0.333	AKT3,EGFR,GNB1,GNB2,IKBKG,ITGAV,MAPK3,PIK3C2G,PIK3CA,RHOBTB1,RHOT1
Angiopoietin Signaling	1.97	0	AKT3,IKBKG,PIK3C2G,PIK3CA,STAT5A,STAT5B
Opioid Signaling Pathway	1.96	-1.941	ADCY6,AKT3,ARRB1,ATF2,Calm1 (includes others),CREB1,GNB1,GRK2,GRK6,MAPK3,PDE1A,PDK1,PIK3C2G
Role of IL-17A in Arthritis	1.95	NA	ATF2,MAPK14,MAPK3,PIK3C2G,PIK3CA
Leptin Signaling in Obesity	1.94	-0.447	ADCY6,AKT3,JAK2,MAPK3,PIK3C2G,PIK3CA
Protein Kinase A Signaling	1.93	-0.5	ADCY6,ANAPC5,ATF2,Calm1 (includes others),CREB1,GNB1,GNB2,MAPK3,MTMR3,NFAT5,PDE1A,PDE4B,PPP1R3C,PTPN21,PTPRG,PXN,SIRPA,TGFBR1
T Cell Exhaustion Signaling Pathway	1.92	0.333	ACVR2B,AKT3,BCL6,JAK2,MAPK3,NFAT5,PDK1,PIK3C2G,PIK3CA,TGFBR1
Phospholipase C Signaling	1.89	-0.632	ADCY6,ATF2,Calm1 (includes others),CREB1,FCGR2A,GNB1,GNB2,ITGA3,MAPK3,NFAT5,RHOBTB1,RHOT1,SYK
Antiproliferative Role of Somatostatin Receptor 2	1.86	0	GNB1,GNB2,MAPK3,NPR2,PIK3C2G,PIK3CA
April Mediated Signaling	1.85	-1	IKBKG,MAPK14,NFAT5,TRAF3
PD-1, PD-L1 cancer immunotherapy pathway	1.82	-0.378	AKT3,JAK2,PIK3C2G,PIK3CA,STAT5A,STAT5B,YAP1
D-myo-inositol (1,4,5)-trisphosphate Degradation	1.81	NA	INPP5B,SYNJ1,SYNJ2
PCP pathway	1.8	-2.236	ATF2,DAAM1,DVL2,FZD6,LGR4
Prolactin Signaling	1.79	0.816	JAK2,MAPK3,PIK3C2G,PIK3CA,STAT5A,STAT5B
HER-2 Signaling in Breast Cancer	1.79	NA	AKT3,EGFR,MDM2,PARD3,PIK3C2G,PIK3CA
Regulation of eIF4 and p70S6K Signaling	1.78	-0.447	AKT3,EIF4G1,EIF4G3,ITGA3,MAPK14,MAPK3,PIK3C2G,PIK3CA,RPS19
B Cell Activating Factor Signaling	1.77	-1	IKBKG,MAPK14,NFAT5,TRAF3

IL-12 Signaling and Production in Macrophages	1.75	NA	AKT3,APOE,IKBKG,MAPK14,MAPK3,PIK3C2G,PIK3CA,RXRA
STAT3 Pathway	1.75	-0.707	EGFR,FGFR3,IL17RB,JAK2,MAPK14,MAPK3,PIAS3,TGFBR1
Activation of IRF by Cytosolic Pattern Recognition Receptors	1.74	0.447	ATF2,IKBKG,TANK,TBK1,TRAF3
Gαs Signaling	1.74	-0.816	ADCY6,ATF2,CREB1,GNB1,GNB2,MAPK3,RAPGEF4
Th2 Pathway	1.74	1.414	ACVR2B,IL17RB,JAK2,PIK3C2G,PIK3CA,STAT5A,STAT5B,TGFBR1
Role of NFAT in Cardiac Hypertrophy	1.72	-0.333	ADCY6,AKT3,Calm1 (includes others),CSNK1A1,GNB1,GNB2,MAPK14,MAPK3,PIK3C2G,PIK3CA,TGFBR1
D-myo-inositol (1,3,4)-trisphosphate Biosynthesis	1.71	NA	INPP5B,SYNJ1,SYNJ2
Oncostatin M Signaling	1.7	1	JAK2,MAPK3,STAT5A,STAT5B
ErbB2-ErbB3 Signaling	1.69	0.447	MAPK3,PIK3C2G,PIK3CA,STAT5A,STAT5B
Wnt/Ca+ pathway	1.69	-2.236	ATF2,CREB1,DVL2,FZD6,NFAT5
Autophagy	1.69	NA	ATG13,BECN1,CTSH,NBR1,SQSTM1
PPARα/RXRα Activation	1.69	-0.333	ACVR2B,ADCY6,CKAP5,IKBKG,JAK2,MAPK14,MAPK3,RXRA,STAT5B,TGFBR1
Rac Signaling	1.68	0	BAIAP2,CYFIP1,ITGA3,MAPK3,PARD3,PIK3C2G,PIK3CA
Role of RIG1-like Receptors in Antiviral Innate Immunity	1.67	1	IKBKG,TANK,TBK1,TRAF3
IL-23 Signaling Pathway	1.67	0	AKT3,JAK2,PIK3C2G,PIK3CA
IL-17A Signaling in Gastric Cells	1.66	NA	EGFR,MAPK14,MAPK3
Regulation of Cellular Mechanics by Calpain Protease	1.64	0	CAPNS1,EGFR,ITGA3,MAPK3,PXN
LPS/IL-1 Mediated Inhibition of RXR Function	1.62	0	ACSL1,ACSL4,ALAS1,APOE,CYP7A1,FMO1,FMO2,NR1H2,NR1H3,NR1H4,RXRA
1D-myo-inositol Hexakisphosphate Biosynthesis II (Mammalian)	1.62	NA	INPP5B,SYNJ1,SYNJ2
FAT10 Cancer Signaling Pathway	1.61	0	ACVR2B,AKT3,IKBKG,TGFBR1
Factors Promoting Cardiogenesis in Vertebrates	1.6	NA	ACVR2B,APC,ATF2,FZD6,MAPK14,TGFBR1
Role of NANOG in Mammalian Embryonic Stem Cell Pluripotency	1.59	-0.447	AKT3,APC,FZD6,JAK2,MAPK3,PIK3C2G,PIK3CA
Wnt/β-catenin Signaling	1.59	0	ACVR2B,AKT3,APC,CSNK1A1,DVL2,FZD6,MDM2,SOX6,TGFBR1
ErbB Signaling	1.58	-0.816	EGFR,ERBB4,MAPK14,MAPK3,PIK3C2G,PIK3CA
IL-15 Production	1.56	NA	EGFR,EPHB4,ERBB4,FGFR3,JAK2,SYK,TNK2
Sphingosine-1-phosphate Signaling	1.56	-0.816	ADCY6,AKT3,MAPK3,PIK3C2G,PIK3CA,RHOBTB1,RHOT1

Adrenomedullin signaling pathway	1.55	-0.632	ADCY6,AKT3,Calm1 (includes others),MAPK14,MAPK3,NPR2,PIK3C2G,PIK3CA,RXRA,RXRB
iNOS Signaling	1.55	NA	Calm1 (includes others),IKBKG,JAK2,MAPK14
Melanocyte Development and Pigmentation Signaling	1.54	-0.816	ADCY6,ATF2,CREB1,MAPK3,PIK3C2G,PIK3CA
Endocannabinoid Cancer Inhibition Pathway	1.53	0	ADCY6,AKT3,ATF2,CREB1,MAPK14,MAPK3,PIK3C2G,PIK3CA
fMLP Signaling in Neutrophils	1.52	-0.816	Calm1 (includes others),GNB1,GNB2,MAPK3,NFAT5,PIK3C2G,PIK3CA
Cholecystokinin/Gastrin-mediated Signaling	1.51	-0.816	ATF2,EGFR,MAPK14,MAPK3,PXN,RHOBTB1,RHOT1
Role of p14/p19ARF in Tumor Suppression	1.49	NA	MDM2,PIK3C2G,PIK3CA
CD28 Signaling in T Helper Cells	1.49	-1.134	AKT3,Calm1 (includes others),IKBKG,NFAT5,PIK3C2G,PIK3CA,SYK
IL-6 Signaling	1.49	-0.378	AKT3,IKBKG,JAK2,MAPK14,MAPK3,PIK3C2G,PIK3CA
Cleavage and Polyadenylation of Pre-mRNA	1.48	NA	CPSF1,PAPOLA
PAK Signaling	1.48	0.816	GIT1,ITGA3,MAPK3,PIK3C2G,PIK3CA,PXN
UVA-Induced MAPK Signaling	1.48	-1	EGFR,MAPK14,MAPK3,PARP16,PIK3C2G,PIK3CA
Fcγ Receptor-mediated Phagocytosis in Macrophages and Monocytes	1.46	0	AKT3,FCGR2A,MAPK3,PIK3C2G,PXN,SYK
UVC-Induced MAPK Signaling	1.46	NA	ATR,EGFR,MAPK14,MAPK3
Renin-Angiotensin Signaling	1.46	-0.816	ADCY6,ATF2,JAK2,MAPK14,MAPK3,PIK3C2G,PIK3CA
Signaling by Rho Family GTPases	1.44	0.378	BAIAP2,CYFIP1,GNB1,GNB2,ITGA3,MAPK3,PARD3,PIK3C2G,PIK3CA,RHOBTB1,RHOT1
CREB Signaling in Neurons	1.43	-1.414	ADCY6,AKT3,ATF2,Calm1 (includes others),CREB1,GNB1,GNB2,MAPK3,PIK3C2G,PIK3CA
CCR3 Signaling in Eosinophils	1.43	-1	Calm1 (includes others),GNB1,GNB2,MAPK14,MAPK3,PIK3C2G,PIK3CA
mTOR Signaling	1.42	0	AKT3,ATG13,EIF4G1,EIF4G3,MAPK3,PIK3C2G,PIK3CA,RHOBTB1,RHOT1,RPS19
BER pathway	1.42	NA	LIG1,LIG3
SAPK/JNK Signaling	1.41	0	ATF2,GNB1,MAP3K13,MAP4K5,PIK3C2G,PIK3CA
Glucocorticoid Receptor Signaling	1.4	NA	AKT3,CEBPA,CREB1,IKBKG,JAK2,MAPK14,MAPK3,NFAT5,PIK3C2G,PIK3CA,STAT5A,STAT5B,TAT,TGFBR1
G-Protein Coupled Receptor Signaling	1.4	NA	ADCY6,AKT3,ATF2,CREB1,GRK2,IKBKG,MAPK3,PDE1A,PDE4B,PIK3C2G,PIK3CA,RAPGEF4

Reelin Signaling in Neurons	1.39	NA	APOE,APP,ITGA3,PIK3C2G,PIK3CA
PPAR Signaling	1.39	0	IKBKG,MAPK3,NR1H3,RXRA,STAT5A,STAT5B
Superpathway of D-myo-inositol (1,4,5)-trisphosphate Metabolism	1.38	NA	INPP5B,SYNJ1,SYNJ2
NRF2-mediated Oxidative Stress Response	1.38	-0.816	DNAJB2,FMO1,KEAP1,MAPK14,MAPK3,PIK3C2G,PIK3CA,PRDX1,SQSTM1
Agrin Interactions at Neuromuscular Junction	1.37	0.447	EGFR,ERBB4,ITGA3,MAPK3,PXN
GDNF Family Ligand-Receptor Interactions	1.37	-1.342	CREB1,GFRA1,MAPK3,PIK3C2G,PIK3CA
Amyotrophic Lateral Sclerosis Signaling	1.36	1.342	AKT3,BIRC2,CAPNS1,GPX1,PIK3C2G,PIK3CA
IGF-1 Signaling	1.36	0	AKT3,JAK2,MAPK3,PIK3C2G,PIK3CA,PXN
Adipogenesis pathway	1.34	NA	CEBPA,FGFR3,FZD6,LPIN1,NOCT,SIN3A,STAT5B
Neurotrophin/TRK Signaling	1.33	-1.342	ATF2,CREB1,MAPK3,PIK3C2G,PIK3CA
G Protein Signaling Mediated by Tubby	1.32	NA	GNB1,GNB2,JAK2
Paxillin Signaling	1.31	0.447	ITGA3,ITGAV,MAPK14,PIK3C2G,PIK3CA,PXN
Sumoylation Pathway	1.31	NA	CEBPA,MDM2,PML,RANGAP1,RHOBTB1,RHOT1
Clathrin-mediated Endocytosis Signaling	1.31	NA	APOE,ARRB1,CD2AP,FGF21,MDM2,MYO6,PIK3C2G,PIK3CA,SYNJ1
EIF2 Signaling	1.3	-1.633	AKT3,EIF4G1,EIF4G3,MAPK3,PIK3C2G,PIK3CA,PTBP1,RPL37,RPL38,RPS19
Xenobiotic Metabolism Signaling	1.3	NA	CES3,ESD,FMO1,FMO2,KEAP1,MAP3K13,MAPK14,MAPK3,PIK3C2G,PIK3CA,RXRA,UGT2B28
ERK/MAPK Signaling	1.3	-1	ATF2,CREB1,ITGA3,MAPK3,PIK3C2G,PIK3CA,PPP1R3C,PXN,RAPGEF4

Table 10. Significant Pathways for differentially expressed transcripts in ^{56}Fe vs. non-irradiated control at 4 months.

Ingenuity Canonical Pathways	-log$_{10}$(p-value)	z-score	Molecules
Acute Phase Response Signaling	7.89	-1.069	C1R,C4A/C4B,GRB2,HMOX2,HP,HRAS,IL1R1,IL33,MAPK14,MAPK9,NR3C1,PIK3CD,SAA1,SERPINA1,SERPINF1,SOCS1,SOCS2,SOCS3,STAT3,TCF3,TF
Prolactin Signaling	7.45	-1.387	FYN,GRB2,HRAS,NR3C1,PIK3C2G,PIK3C3,PIK3CD,PRKCB,PRLR,SOCS1,SOCS2,SOCS3,STAT3,STAT5A
PPARα/RXRα Activation	6.65	-0.688	ADCY3,ADCY7,AIP,CD36,CYP2C18,CYP2C8,FASN,GHR,GRB2,HELZ2,HRAS,HS

			P90AB1,IL1R1,LPL,MAPK14,MEF2C,PRKAA1,PRKACA,PRKCB,RXRA
LXR/RXR Activation	6.61	1.155	ACACA,APOA4,C4A/C4B,CD36,FASN,IL1R1,IL33,LPL,PON3,RXRA,RXRB,SAA1,SCD,SERPINA1,SERPINF1,TF
Role of JAK2 in Hormone-like Cytokine Signaling	5.68	NA	GHR,PRLR,SIRPA,SOCS1,SOCS2,SOCS3,STAT3,STAT5A
TR/RXR Activation	5.35	NA	ACACA,COL6A3,FASN,HP,ME1,PIK3C2G,PIK3C3,PIK3CD,RXRA,RXRB,TBL1XR1,THRSP
IL-9 Signaling	4.72	0	PIK3C2G,PIK3C3,PIK3CD,SOCS2,SOCS3,STAT3,STAT5A
IGF-1 Signaling	4.67	-0.905	GRB2,HRAS,IGFBP2,PIK3C2G,PIK3C3,PIK3CD,PRKACA,PXN,SOCS1,SOCS2,SOCS3,STAT3
RAR Activation	4.63	NA	ADCY3,ADCY7,GTF2H1,MAPK14,MAPK9,PBRM1,PIK3CD,PML,PRKACA,PRKCB,RDH16,RXRA,RXRB,SMARCA2,SMARCA4,STAT5A,TNIP1
IL-6 Signaling	4.6	-0.832	GRB2,HRAS,IL1R1,IL33,MAPK14,MAPK9,MCL1,PIK3C2G,PIK3C3,PIK3CD,SOCS1,SOCS3,STAT3
Growth Hormone Signaling	4.6	-1.265	GHR,PIK3C2G,PIK3C3,PIK3CD,PRKCB,SOCS1,SOCS2,SOCS3,STAT3,STAT5A
Paxillin Signaling	4.54	-0.632	ACTN4,DOCK1,GRB2,HRAS,ITGAV,ITGB2,MAPK14,MAPK9,PIK3C2G,PIK3C3,PIK3CD,PXN
Role of JAK family kinases in IL-6-type Cytokine Signaling	4.44	NA	MAPK14,MAPK9,SOCS1,SOCS3,STAT3,STAT5A
JAK/Stat Signaling	4.35	-0.632	GRB2,HRAS,PIK3C2G,PIK3C3,PIK3CD,SOCS1,SOCS2,SOCS3,STAT3,STAT5A
IL-7 Signaling Pathway	4.35	-0.632	FYN,GRB2,GSK3A,MAPK14,MCL1,PIK3C2G,PIK3C3,PIK3CD,SOCS1,STAT5A
HGF Signaling	4.35	-0.302	DOCK1,ELF4,GRB2,HRAS,Map3k7,MAPK9,PIK3C2G,PIK3C3,PIK3CD,PRKCB,PXN,STAT3
FXR/RXR Activation	4.19	NA	APOA4,C4A/C4B,FASN,IL33,LPL,MAPK9,PKLR,PON3,RXRA,SAA1,SERPINA1,SERPINF1,TF
HER-2 Signaling in Breast Cancer	4.17	NA	GRB2,GSK3A,HRAS,ITGB2,PARD3,PIK3C2G,PIK3C3,PIK3CD,PRKCB,TSC1
Role of JAK1 and JAK3 in γc Cytokine Signaling	4.12	NA	GRB2,HRAS,PIK3C2G,PIK3C3,PIK3CD,SOCS1,SOCS3,STAT3,STAT5A

PXR/RXR Activation	4.07	NA	ALAS1,ALDH3A2,CES3,CYP2A6 (includes others),CYP2C8,NR3C1,PRKACA,RXRA,SCD
Xenobiotic Metabolism Signaling	4.06	NA	AIP,ALDH3A2,CAMK2G,CES3,CYP2C8,ESD,FMO1,GSTM5,HDAC5,HRAS,HSP90AB1,Map3k7,MAPK14,MAPK9,MGST1,PIK3C2G,PIK3C3,PIK3CD,PRKCB,RXRA
Apelin Endothelial Signaling Pathway	4.02	-0.577	ADCY3,ADCY7,GNAI2,HDAC5,HRAS,MAPK9,MEF2C,PIK3C2G,PIK3C3,PIK3CD,PRKAA1,PRKCB
Adrenomedullin signaling pathway	3.97	0	ADCY3,ADCY7,CFH,GRB2,GSK3A,GUCY2C,HRAS,IL33,MAPK14,MAPK9,PIK3C2G,PIK3C3,PIK3CD,PRKACA,RXRA,RXRB
Insulin Receptor Signaling	3.93	-2.111	ACLY,FYN,GRB2,GSK3A,HRAS,PIK3C2G,PIK3C3,PIK3CD,PRKACA,SOCS3,SYNJ1,TRIP10,TSC1
Renin-Angiotensin Signaling	3.89	-1	ADCY3,ADCY7,GRB2,HRAS,MAPK14,MAPK9,PIK3C2G,PIK3C3,PIK3CD,PRKACA,PRKCB,STAT3
Acute Myeloid Leukemia Signaling	3.83	0	GRB2,HRAS,KIT,PIK3C2G,PIK3C3,PIK3CD,PML,STAT3,STAT5A,TCF3
B Cell Receptor Signaling	3.82	-1.387	CAMK2G,GRB2,GSK3A,HRAS,Map3k7,MAPK14,MAPK9,MEF2C,PIK3C2G,PIK3C3,PIK3CD,PRKCB,PTPRC,SYNJ1,TCF3
Leptin Signaling in Obesity	3.7	0	ADCY3,ADCY7,GRB2,PIK3C2G,PIK3C3,PIK3CD,PRKACA,SOCS3,STAT3
Erythropoietin Signaling	3.66	NA	GRB2,HRAS,PIK3C2G,PIK3C3,PIK3CD,PRKCB,SOCS1,SOCS3,STAT5A
Endocannabinoid Developing Neuron Pathway	3.63	-0.632	ADCY3,ADCY7,GNAI2,HRAS,MAPK14,MAPK9,PIK3C2G,PIK3C3,PIK3CD,PRKACA,STAT3
Role of NFAT in Cardiac Hypertrophy	3.6	-0.775	ADCY3,ADCY7,CACNA1A,CAMK2G,GNAI2,GRB2,HDAC5,HRAS,MAPK14,MAPK9,MEF2C,PIK3C2G,PIK3C3,PIK3CD,PRKACA,PRKCB
Apelin Adipocyte Signaling Pathway	3.58	-0.333	ADCY3,ADCY7,GNAI2,GPX1,MAPK14,MAPK9,MGST1,PRKAA1,PRKACA
ErbB2-ErbB3 Signaling	3.55	0	GRB2,GSK3A,HRAS,PIK3C2G,PIK3C3,PIK3CD,STAT3,STAT5A
IL-22 Signaling	3.47	-0.447	MAPK14,MAPK9,SOCS3,STAT3,STAT5A
Thrombopoietin Signaling	3.45	0	GRB2,HRAS,PIK3C2G,PIK3C3,PIK3CD,PRKCB,STAT3,STAT5A

Type II Diabetes Mellitus Signaling	3.43	-2.121	ACSL1,CACNA1A,CD36,MAPK9,PIK3C2G,PIK3C3,PIK3CD,PKLR,PRKAA1,PRKCB,SOCS1,SOCS2,SOCS3
LPS/IL-1 Mediated Inhibition of RXR Function	3.43	0.447	ACSL1,ALAS1,ALDH3A2,Cyp2a12/Cyp2a22,CYP2A6 (includes others),CYP2C8,CYP4A11,FABP2,FMO1,GSTM5,IL1R1,IL33,MAPK9,MGST1,RXRA,XPO1
IL-4 Signaling	3.34	NA	GRB2,HLA-A,HRAS,NR3C1,PIK3C2G,PIK3C3,PIK3CD,SOCS1,SYNJ1
FGF Signaling	3.31	-1	FGFR2,FGFR3,GRB2,HRAS,MAPK14,PIK3C2G,PIK3C3,PIK3CD,STAT3
GM-CSF Signaling	3.28	-0.707	CAMK2G,GRB2,HRAS,PIK3C2G,PIK3C3,PIK3CD,PRKCB,STAT3
14-3-3-mediated Signaling	3.23	-1.265	GRB2,GSK3A,HRAS,MAPK9,PIK3C2G,PIK3C3,PIK3CD,PRKCB,STK11,TSC1,TUBB2A
Axonal Guidance Signaling	3.22	NA	ABLIM1,ADAM17,ADAM23,ADAM9,ARPC1A,DOCK1,EPHB4,FYN,GIT1,GNAI2,GRB2,HERC2,HRAS,NRP2,PIK3C2G,PIK3C3,PIK3CD,PLXNB1,PRKACA,PRKCB,PXN,RTN4,SEMA4B,SEMA4C,SEMA6D,TUBB2A
Clathrin-mediated Endocytosis Signaling	3.17	NA	APOA4,ARPC1A,EPS15,GRB2,ITGB2,MYO6,PICALM,PIK3C2G,PIK3C3,PIK3CD,SERPINA1,SH3GL1,SYNJ1,TF
Germ Cell-Sertoli Cell Junction Signaling	3.14	NA	ACTN4,CDH1,HRAS,Map3k7,MAPK14,MAPK9,PIK3C2G,PIK3C3,PIK3CD,PXN,RHOBTB1,SORBS1,TUBB2A
Macropinocytosis Signaling	3.08	-1.633	ABI1,ACTN4,HRAS,ITGB2,PIK3C2G,PIK3C3,PIK3CD,PRKCB
EGF Signaling	3.07	-0.378	GRB2,HRAS,MAPK14,PIK3C2G,PIK3C3,PIK3CD,STAT3
Adipogenesis pathway	3.06	NA	EZH2,FGFR2,FGFR3,GTF2H1,HDAC5,Kat6b,KAT7,KMT2B,LPL,SETDB1,TBL1XR1
GNRH Signaling	3.05	-0.577	ADCY3,ADCY7,CACNA1A,CAMK2G,GNAI2,GRB2,HRAS,Map3k7,MAPK14,MAPK9,PRKACA,PRKCB,PXN
NF-κB Signaling	3.05	-1.387	FGFR2,FGFR3,GHR,HRAS,IL1R1,IL33,PIK3C2G,PIK3C3,PIK3CD,PRKACA,PRKCB,TNFAIP3,TNIP1
STAT3 Pathway	3.04	-2.53	FGFR2,FGFR3,GHR,HRAS,IL1R1,MAPK14,MAPK9,SOCS1,SOCS2,SOCS3,STAT3

Melanocyte Development and Pigmentation Signaling	3.03	-0.333	ADCY3,ADCY7,GRB2,HRAS,KIT,PIK3C2G,PIK3C3,PIK3CD,PRKACA
Leukocyte Extravasation Signaling	3	-1.941	ACTN4,ARHGAP4,CLDN12,GNAI2,ITGB2,MAPK14,MAPK9,PIK3C2G,PIK3C3,PIK3CD,PRKCB,PXN,RAPGEF4,RASGRP1
FcγRIIB Signaling in B Lymphocytes	2.97	-0.378	CACNA1A,DOK1,GRB2,HRAS,MAPK9,PIK3C2G,PIK3C3,PIK3CD
IL-3 Signaling	2.97	0	GRB2,HRAS,PIK3C2G,PIK3C3,PIK3CD,PRKCB,STAT3,STAT5A
Non-Small Cell Lung Cancer Signaling	2.97	-0.447	CDK4,GRB2,HRAS,PIK3C2G,PIK3C3,PIK3CD,RXRA,RXRB
Apelin Pancreas Signaling Pathway	2.97	0	MAPK9,PIK3C2G,PIK3C3,PIK3CD,PRKAA1,PRKACA
p53 Signaling	2.97	1.342	ATR,CDK4,COQ8A,GADD45G,MAPK14,PIK3C2G,PIK3C3,PIK3CD,PML
G-Protein Coupled Receptor Signaling	2.94	NA	ADCY3,ADCY7,CAMK2G,FYN,GNAI2,GRB2,GRK2,HRAS,PIK3C2G,PIK3C3,PIK3CD,PRKACA,PRKCB,RAPGEF4,RASGRP1,RGS16,STAT3
IL-2 Signaling	2.9	-0.378	GRB2,HRAS,PIK3C2G,PIK3C3,PIK3CD,SOCS1,STAT5A
Hereditary Breast Cancer Signaling	2.89	NA	ATR,CDK4,GADD45G,HDAC5,HRAS,PBRM1,PIK3C2G,PIK3C3,PIK3CD,SMARCA2,SMARCA4
Fc Epsilon RI Signaling	2.83	-1.897	FYN,GRB2,HRAS,MAPK14,MAPK9,PIK3C2G,PIK3C3,PIK3CD,PRKCB,SYNJ1
FLT3 Signaling in Hematopoietic Progenitor Cells	2.83	0	GRB2,HRAS,MAPK14,PIK3C2G,PIK3C3,PIK3CD,STAT3,STAT5A
CD40 Signaling	2.82	-1.134	MAPK14,MAPK9,PIK3C2G,PIK3C3,PIK3CD,STAT3,TNFAIP3
Chronic Myeloid Leukemia Signaling	2.82	NA	CDK4,GRB2,HDAC5,HRAS,PIK3C2G,PIK3C3,PIK3CD,RBL2,STAT5A
NRF2-mediated Oxidative Stress Response	2.81	-1.134	DNAJB2,FMO1,GSTM5,HERPUD1,HRAS,MAPK14,MAPK9,MGST1,PIK3C2G,PIK3C3,PIK3CD,PRKCB,SQSTM1
Integrin Signaling	2.78	-1.155	ACTN4,ARPC1A,DOCK1,FYN,GIT1,GRB2,HRAS,ITGAV,ITGB2,PIK3C2G,PIK3C3,PIK3CD,PXN,RHOBTB1
VEGF Signaling	2.73	0	ACTN4,EIF2S3,GRB2,HRAS,PIK3C2G,PIK3C3,PIK3CD,PRKCB,PXN
Aryl Hydrocarbon Receptor Signaling	2.72	-1.414	AIP,ALDH3A2,ATR,CDK4,GSTM5,HSP90AB1,MGST1,RBL2,RXRA,RXRB,SMARCA4

eNOS Signaling	2.71	-0.707	ADCY3,ADCY7,AQP4,AQP8,CHRNA4,HSP90AB1,PIK3C2G,PIK3C3,PIK3CD,PRKAA1,PRKACA,PRKCB
Telomerase Signaling	2.7	0	ELF4,GRB2,HDAC5,HRAS,HSP90AB1,PIK3C2G,PIK3C3,PIK3CD,TERT
PTEN Signaling	2.7	1.897	FGFR2,FGFR3,GHR,GRB2,GSK3A,HRAS,MAGI1,MAST2,PIK3CD,SYNJ1
Endocannabinoid Cancer Inhibition Pathway	2.69	0.302	ADCY3,ADCY7,CDH1,GNAI2,MAPK14,PIK3C2G,PIK3C3,PIK3CD,PRKAA1,PRKACA,TCF3
Molecular Mechanisms of Cancer	2.67	NA	ADCY3,ADCY7,ATR,CAMK2G,CDH1,CDK4,FYN,GNAI2,GRB2,GSK3A,HRAS,MAPK14,MAPK9,PIK3C2G,PIK3C3,PIK3CD,PRKACA,PRKCB,RASGRP1,RHOBTB1,TCF3
ERK/MAPK Signaling	2.67	-0.277	DOCK1,ELF4,FYN,GRB2,HRAS,PIK3C2G,PIK3C3,PIK3CD,PRKACA,PRKCB,PXN,RAPGEF4,STAT3
CXCR4 Signaling	2.64	-0.905	ADCY3,ADCY7,DOCK1,GNAI2,HRAS,MAPK9,PIK3C2G,PIK3C3,PIK3CD,PRKCB,PXN,RHOBTB1
Melanoma Signaling	2.64	-0.447	CDH1,CDK4,HRAS,PIK3C2G,PIK3C3,PIK3CD
UVB-Induced MAPK Signaling	2.64	-1.633	MAPK14,MAPK9,PIK3C2G,PIK3C3,PIK3CD,PRKCB
ErbB4 Signaling	2.63	-1.134	ADAM17,GRB2,HRAS,PIK3C2G,PIK3C3,PIK3CD,PRKCB
Cardiac Hypertrophy Signaling	2.61	0	ADCY3,ADCY7,CACNA1A,GNAI2,GRB2,HRAS,Map3k7,MAPK14,MAPK9,MEF2C,PIK3C2G,PIK3C3,PIK3CD,PRKACA,RHOBTB1
Acetone Degradation I (to Methylglyoxal)	2.58	-1.342	CYP2A6 (includes others),CYP2C18,CYP2C8,CYP4A11,POR
Nitric Oxide Signaling in the Cardiovascular System	2.56	1	CACNA1A,GUCY2C,HSP90AB1,PIK3C2G,PIK3C3,PIK3CD,PRKAA1,PRKACA,PRKCB
IL-15 Signaling	2.56	NA	HRAS,MAPK14,PIK3C2G,PIK3C3,PIK3CD,STAT3,STAT5A
PDGF Signaling	2.55	0	GRB2,HRAS,PIK3C2G,PIK3C3,PIK3CD,PRKCB,STAT3,SYNJ1
Virus Entry via Endocytic Pathways	2.54	NA	FLNA,FYN,HLA-A,HRAS,ITGB2,PIK3C2G,PIK3C3,PIK3CD,PRKCB
Complement System	2.53	NA	C1R,C4A/C4B,C6,CFH,ITGB2
AMPK Signaling	2.53	0.632	ACACA,CHRNA4,FASN,MAPK14,PBRM1,PIK3C2G,PI

			K3C3,PIK3CD,PRKAA1,PRKACA,SMARCA2,SMARCA4,STK11,TSC1
Breast Cancer Regulation by Stathmin1	2.5	NA	ADCY3,ADCY7,CAMK2G,GNAI2,GRB2,HRAS,PIK3C2G,PIK3C3,PIK3CD,PRKACA,PRKCB,TUBB2A,UHMK1
ErbB Signaling	2.49	-1.414	GRB2,HRAS,MAPK14,MAPK9,PIK3C2G,PIK3C3,PIK3CD,PRKCB
Ephrin Receptor Signaling	2.48	-0.905	ABI1,ARPC1A,DOK1,EPHB4,FYN,GNAI2,GRB2,HRAS,PIK3C2G,PXN,SORBS1,STAT3
Inhibition of Angiogenesis by TSP1	2.48	-2.236	CD36,CD47,FYN,MAPK14,MAPK9
Glioma Signaling	2.41	-1.134	CAMK2G,CDK4,GRB2,HRAS,PIK3C2G,PIK3C3,PIK3CD,PRKCB,RBL2
Angiopoietin Signaling	2.4	1	GRB2,HRAS,PIK3C2G,PIK3C3,PIK3CD,STAT5A,TNIP1
Glucocorticoid Receptor Signaling	2.38	NA	BAG1,GRB2,GTF2H1,HRAS,HSP90AB1,MAPK14,MAPK9,NR3C1,PBRM1,PIK3C2G,PIK3C3,PIK3CD,PRKAA1,PRKACA,SMARCA2,SMARCA4,STAT3,STAT5A
FAK Signaling	2.38	NA	DOCK1,FYN,GRB2,HRAS,PIK3C2G,PIK3C3,PIK3CD,PXN
HMGB1 Signaling	2.38	-1	HRAS,IL1R1,IL33,Kat6b,KAT7,MAPK14,MAPK9,PIK3C2G,PIK3C3,PIK3CD,RHOBTB1
Reelin Signaling in Neurons	2.37	NA	FYN,ITGB2,MAPK8IP3,MAPK9,PIK3C2G,PIK3C3,PIK3CD
Stearate Biosynthesis I (Animals)	2.36	-1.633	ACOT1,ACOT2,ACSL1,CYP4A11,ELOVL6,FASN
White Adipose Tissue Browning Pathway	2.35	0.632	ADCY3,ADCY7,CACNA1A,FGFR2,FGFR3,MAPK14,PRKAA1,PRKACA,RXRA,RXRB
PAK Signaling	2.35	-1.414	GIT1,GRB2,HRAS,MAPK9,PIK3C2G,PIK3C3,PIK3CD,PXN
Tec Kinase Signaling	2.34	-0.333	FYN,GNAI2,GTF2I,MAPK9,PIK3C2G,PIK3C3,PIK3CD,PRKCB,RHOBTB1,STAT3,STAT5A
GDNF Family Ligand-Receptor Interactions	2.34	-1.134	DOK1,GRB2,HRAS,MAPK9,PIK3C2G,PIK3C3,PIK3CD
CNTF Signaling	2.33	0	GRB2,HRAS,PIK3C2G,PIK3C3,PIK3CD,STAT3
ILK Signaling	2.3	-0.632	ACTN4,CDH1,DOCK1,FLNA,GSK3A,ITGB2,MAPK9,PIK3C2G,PIK3C3,PIK3CD,PXN,RHOBTB1
Regulation of the Epithelial-Mesenchymal Transition Pathway	2.3	NA	ADAM17,CDH1,FGFR2,FGFR3,GRB2,HRAS,PIK3C2G,PI

			K3C3,PIK3CD,STAT3,TCF3, ZEB2
Bupropion Degradation	2.3	-1	CYP2A6 (includes others),CYP2C18,CYP2C8,POR
Th1 Pathway	2.29	-0.707	GRB2,HLA-A,ITGB2,PIK3C2G,PIK3C3,PIK3CD,SOCS1,SOCS3,STAT3
Sertoli Cell-Sertoli Cell Junction Signaling	2.28	NA	ACTN4,CDH1,CLDN12,EPB41,GSK3A,HRAS,Map3k7,MAPK14,MAPK9,PRKACA,SORBS1,TUBB2A
Cholecystokinin/Gastrin-mediated Signaling	2.27	-1.414	GRB2,HRAS,IL33,MAPK14,MAPK9,MEF2C,PRKCB,PXN,RHOBTB1
Endometrial Cancer Signaling	2.25	-0.816	CDH1,GRB2,HRAS,PIK3C2G,PIK3C3,PIK3CD
CD28 Signaling in T Helper Cells	2.25	-1.414	ARPC1A,FYN,GRB2,HLA-A,MAPK9,PIK3C2G,PIK3C3,PIK3CD,PTPRC
Docosahexaenoic Acid (DHA) Signaling	2.25	NA	GSK3A,PIK3C2G,PIK3C3,PIK3CD,SERPINF1
IL-23 Signaling Pathway	2.25	-0.447	PIK3C2G,PIK3C3,PIK3CD,SOCS3,STAT3
Mouse Embryonic Stem Cell Pluripotency	2.25	0	GRB2,HRAS,MAPK14,PIK3C2G,PIK3C3,PIK3CD,STAT3,TCF3
SAPK/JNK Signaling	2.25	-1.134	GRB2,HRAS,MAP4K5,MAPK8IP3,MAPK9,PIK3C2G,PIK3C3,PIK3CD
LPS-stimulated MAPK Signaling	2.25	-1.89	HRAS,MAPK14,MAPK9,PIK3C2G,PIK3C3,PIK3CD,PRKCB
Th1 and Th2 Activation Pathway	2.22	NA	GRB2,HLA-A,IL33,ITGB2,PIK3C2G,PIK3C3,PIK3CD,SOCS1,SOCS3,STAT3,STAT5A
PPAR Signaling	2.22	-0.707	AIP,GRB2,HRAS,HSP90AB1,IL1R1,IL33,RXRA,STAT5A
Apelin Cardiomyocyte Signaling Pathway	2.22	-1.414	GNAI2,MAPK14,MAPK9,PIK3C2G,PIK3C3,PIK3CD,PRKCB,SLC9A6
NF-κB Activation by Viruses	2.22	-1.89	HRAS,ITGAV,ITGB2,PIK3C2G,PIK3C3,PIK3CD,PRKCB
Cardiac Hypertrophy Signaling (Enhanced)	2.19	-0.853	ADCY3,ADCY7,CACNA1A,CAMK2G,FGFR2,FGFR3,GHR,GNAI2,GSK3A,HDAC5,HRAS,IL1R1,IL33,Map3k7,MAPK14,MAPK9,MEF2C,PIK3C2G,PIK3C3,PIK3CD,PRKACA,PRKCB,STAT3
Protein Ubiquitination Pathway	2.18	NA	ANAPC5,BAG1,BIRC6,DNAJB2,HLA-A,HSP90AB1,PAN2,PSMD13,PSMD2,UBE2M,UBE4B,USO1,USP19,USP24,USP36
Endothelin-1 Signaling	2.16	-1.155	ADCY3,ADCY7,GNAI2,GRB2,GUCY2C,HRAS,MAPK1

			4,MAPK9,PIK3C2G,PIK3C3,PIK3CD,PRKCB
Myc Mediated Apoptosis Signaling	2.15	NA	GRB2,HRAS,MAPK9,PIK3C2G,PIK3C3,PIK3CD
IL-17A Signaling in Airway Cells	2.12	-0.816	MAPK14,MAPK9,PIK3C2G,PIK3C3,PIK3CD,STAT3
Epithelial Adherens Junction Signaling	2.11	NA	ACTN4,ARPC1A,CDH1,CLIP1,HRAS,MAGI1,PARD3,SORBS1,TCF3,TUBB2A
T Cell Receptor Signaling	2.08	NA	FYN,GRB2,HRAS,PIK3C2G,PIK3C3,PIK3CD,PTPRC,RASGRP1
Colorectal Cancer Metastasis Signaling	2.08	0	ADCY3,ADCY7,CDH1,GRB2,GRK2,HRAS,MAPK9,PIK3C2G,PIK3C3,PIK3CD,PRKACA,RHOBTB1,STAT3,TCF3
PKCθ Signaling in T Lymphocytes	2.04	-1	CACNA1A,CAMK2G,FYN,GRB2,HLA-A,HRAS,Map3k7,PIK3C2G,PIK3C3,PIK3CD
SPINK1 General Cancer Pathway	2.03	-0.816	HRAS,Mt2,PIK3C2G,PIK3C3,PIK3CD,STAT3
VEGF Family Ligand-Receptor Interactions	2.03	-0.816	GRB2,HRAS,NRP2,PIK3C2G,PIK3C3,PIK3CD,PRKCB
IL-12 Signaling and Production in Macrophages	2.02	NA	APOA4,MAPK14,MAPK9,PIK3C2G,PIK3C3,PIK3CD,PRKCB,RXRA,SERPINA1
Gap Junction Signaling	2	NA	ADCY3,ADCY7,GNAI2,GRB2,GUCY2C,HRAS,PIK3C2G,PIK3C3,PIK3CD,PRKACA,PRKCB,TUBB2A
Regulation of eIF4 and p70S6K Signaling	2	-0.447	EIF2S3,EIF4G1,EIF4G3,GRB2,HRAS,MAPK14,PABPC1,PIK3C2G,PIK3C3,PIK3CD
HOTAIR Regulatory Pathway	2	-0.632	ATXN1,CDH1,EZH2,KMT2A,PIK3C2G,PIK3C3,PIK3CD,SETDB1,STAT3,TCF3
P2Y Purigenic Receptor Signaling Pathway	2	-1	ADCY3,ADCY7,GNAI2,HRAS,PIK3C2G,PIK3C3,PIK3CD,PRKACA,PRKCB
Th2 Pathway	2	0.816	GRB2,HLA-A,IL33,ITGB2,PIK3C2G,PIK3C3,PIK3CD,SOCS3,STAT5A
Role of NFAT in Regulation of the Immune Response	1.98	-0.632	FYN,GNAI2,GRB2,GSK3A,HLA-A,HRAS,MEF2C,PIK3C2G,PIK3C3,PIK3CD,XPO1
Retinol Biosynthesis	1.98	0.447	CES3,DDHD2,ESD,LPL,PNPLA5
UVC-Induced MAPK Signaling	1.98	-2	ATR,HRAS,MAPK14,MAPK9,PRKCB
Thrombin Signaling	1.96	-0.905	ADCY3,ADCY7,CAMK2G,GNAI2,GRB2,HRAS,MAPK14,PIK3C2G,PIK3C3,PIK3CD,PRKCB,RHOBTB1
CREB Signaling in Neurons	1.94	-0.302	ADCY3,ADCY7,CACNA1A,CAMK2G,GNAI2,GRB2,HRAS,PIK3C2G,PIK3C3,PIK3CD,PRKACA,PRKCB

Thyroid Cancer Signaling	1.94	NA	CDH1,HRAS,RXRA,RXRB,TCF3
IL-1 Signaling	1.93	0	ADCY3,ADCY7,GNAI2,IL1R1,MAPK14,MAPK9,PRKACA
mTOR Signaling	1.93	-1.667	ATG13,EIF4G1,EIF4G3,HRAS,PIK3C2G,PIK3C3,PIK3CD,PRKAA1,PRKCB,RHOBTB1,STK11,TSC1
GADD45 Signaling	1.9	NA	ATR,CDK4,GADD45G
Small Cell Lung Cancer Signaling	1.89	0	CDK4,PIK3C2G,PIK3C3,PIK3CD,RXRA,RXRB
Production of Nitric Oxide and Reactive Oxygen Species in Macrophages	1.87	-0.632	APOA4,Map3k7,MAPK14,MAPK9,PIK3C2G,PIK3C3,PIK3CD,PRKCB,RHOBTB1,SERPINA1,SIRPA
Caveolar-mediated Endocytosis Signaling	1.86	NA	ARCN1,FLNA,FYN,HLA-A,ITGAV,ITGB2
ATM Signaling	1.86	-0.447	ATR,GADD45G,HERC2,MAPK14,MAPK9,TLK2,TRRAP
Glioma Invasiveness Signaling	1.86	-1.342	HRAS,ITGAV,PIK3C2G,PIK3C3,PIK3CD,RHOBTB1
Superpathway of Inositol Phosphate Compounds	1.83	0	INPP5E,PI4KB,PIK3C2G,PIK3C3,PIK3CD,PPP1R16B,PPP4C,PTPRC,SEC16A,SIRPA,SOCS3,SYNJ1
Role of Tissue Factor in Cancer	1.82	NA	FYN,HRAS,ITGAV,MAPK14,PIK3C2G,PIK3C3,PIK3CD,STAT5A
Role of IL-17A in Arthritis	1.81	NA	MAPK14,MAPK9,PIK3C2G,PIK3C3,PIK3CD
Natural Killer Cell Signaling	1.79	NA	FYN,GRB2,HRAS,PIK3C2G,PIK3C3,PIK3CD,PRKCB,SYNJ1
Estrogen-Dependent Breast Cancer Signaling	1.79	-0.447	HRAS,PIK3C2G,PIK3C3,PIK3CD,STAT5A,TERT
Agrin Interactions at Neuromuscular Junction	1.76	-1.342	AGRN,HRAS,ITGB2,MAPK9,PKLR,PXN
Triacylglycerol Degradation	1.75	-0.447	Ces2e,CES3,DDHD2,LPL,PNPLA5
IL-8 Signaling	1.74	-1.667	CDH1,GNAI2,HRAS,ITGAV,ITGB2,MAPK9,PIK3C2G,PIK3C3,PIK3CD,PRKCB,RHOBTB1
IL-17 Signaling	1.74	NA	HRAS,MAPK14,MAPK9,PIK3C2G,PIK3C3,PIK3CD
D-myo-inositol (1,4,5)-trisphosphate Degradation	1.72	NA	INPP5E,SEC16A,SYNJ1
3-phosphoinositide Biosynthesis	1.72	0	PI4KB,PIK3C2G,PIK3C3,PIK3CD,PPP1R16B,PPP4C,PTPRC,SIRPA,SOCS3,SYNJ1
Opioid Signaling Pathway	1.7	-0.832	ADCY3,ADCY7,CACNA1A,CAMK2G,FYN,GNAI2,GRK2,GRK6,HRAS,PIK3C2G,PRKACA,PRKCB,RGS16
PEDF Signaling	1.69	-1.633	HRAS,MAPK14,PIK3C2G,PIK3C3,PIK3CD,SERPINF1
Systemic Lupus Erythematosus Signaling	1.68	NA	C6,CD2BP2,GRB2,HLA-A,HRAS,IL33,PIK3C2G,PIK3C3,PIK3CD,PRPF3,PRPF40B,PTPRC

Corticotropin Releasing Hormone Signaling	1.68	0.333	ADCY3,ADCY7,CACNA1A,GNAI2,GUCY2C,MAPK14,MEF2C,PRKACA,PRKCB
α-tocopherol Degradation	1.66	NA	CYP4A11,CYP4F12
Gα12/13 Signaling	1.66	-1.414	CDH1,HRAS,MAPK9,MEF2C,PIK3C2G,PIK3C3,PIK3CD,PXN
Synaptogenesis Signaling Pathway	1.66	-0.775	ADCY3,ADCY7,ARPC1A,CAMK2G,CDH1,EPHB4,FYN,GRB2,HRAS,MAPK14,PIK3C2G,PIK3C3,PIK3CD,PRKACA,RASGRP1
PD-1, PD-L1 cancer immunotherapy pathway	1.65	1.134	CBLB,HLA-A,PIK3C2G,PIK3C3,PIK3CD,RASGRP1,STAT5A
Phagosome Maturation	1.65	NA	CANX,Dync1i2,DYNC2H1,HLA-A,M6PR,PIK3C3,TCIRG1,TUBB2A,VPS39
Chemokine Signaling	1.64	-1.633	CAMK2G,GNAI2,HRAS,MAPK14,PIK3C2G,PRKCB
D-myo-inositol (1,3,4)-trisphosphate Biosynthesis	1.62	NA	INPP5E,SEC16A,SYNJ1
BMP signaling pathway	1.6	-0.816	CHRD,GRB2,HRAS,MAPK14,MAPK9,PRKACA
Oncostatin M Signaling	1.59	1	GRB2,HRAS,STAT3,STAT5A
Maturity Onset Diabetes of Young (MODY) Signaling	1.57	NA	CACNA1A,FABP2,PKLR
Pancreatic Adenocarcinoma Signaling	1.57	-0.378	CDK4,GRB2,MAPK9,PIK3C2G,PIK3C3,PIK3CD,STAT3
2-ketoglutarate Dehydrogenase Complex	1.57	NA	DLST,OGDH
Acetate Conversion to Acetyl-CoA	1.57	NA	ACSL1,ACSS3
Autophagy	1.56	NA	ATG13,NBR1,PIK3C3,SQSTM1,VPS39
PI3K/AKT Signaling	1.56	0.378	GRB2,GSK3A,HRAS,HSP90AB1,MCL1,PIK3CD,SYNJ1,TSC1
CDK5 Signaling	1.55	1.134	ADCY3,ADCY7,CACNA1A,HRAS,MAPK14,MAPK9,PRKACA
Type I Diabetes Mellitus Signaling	1.55	-1.633	HLA-A,IL1R1,MAPK14,MAPK9,SOCS1,SOCS2,SOCS3
CTLA4 Signaling in Cytotoxic T Lymphocytes	1.53	NA	FYN,GRB2,HLA-A,PIK3C2G,PIK3C3,PIK3CD
RANK Signaling in Osteoclasts	1.53	-0.816	Map3k7,MAPK14,MAPK9,PIK3C2G,PIK3C3,PIK3CD
1D-myo-inositol Hexakisphosphate Biosynthesis II (Mammalian)	1.53	NA	INPP5E,SEC16A,SYNJ1
Salvage Pathways of Pyrimidine Ribonucleotides	1.52	0.378	APOBEC1,CDADC1,CDK4,DMPK,GRK6,MAPK9,PRKAA1
Regulation of Cellular Mechanics by Calpain Protease	1.51	NA	ACTN4,CDK4,GRB2,HRAS,PXN
Cell Cycle: G1/S Checkpoint Regulation	1.51	-1	ATR,CDK4,FBXL5,HDAC5,RBL2
iCOS-iCOSL Signaling in T Helper Cells	1.48	-0.816	CAMK2G,GRB2,HLA-A,PIK3C2G,PIK3C3,PIK3CD,PTPRC

Actin Cytoskeleton Signaling	1.48	0	ACTN4,ARPC1A,DOCK1,FLNA,GIT1,GRB2,HRAS,PIK3C2G,PIK3C3,PIK3CD,PXN
Remodeling of Epithelial Adherens Junctions	1.46	NA	ACTN4,ARPC1A,CDH1,CLIP1,TUBB2A
Glioblastoma Multiforme Signaling	1.45	-0.378	CDK4,GRB2,HRAS,PIK3C2G,PIK3C3,PIK3CD,RHOBTB1,TCF3,TSC1
GPCR-Mediated Nutrient Sensing in Enteroendocrine Cells	1.43	-0.378	ADCY3,ADCY7,CACNA1A,GNAI2,PRKACA,PRKCB,RAPGEF4
EIF2 Signaling	1.43	0.378	EIF2S3,EIF4G1,EIF4G3,GRB2,HRAS,PABPC1,PIK3C2G,PIK3C3,PIK3CD,RPL18A,RPL38
NGF Signaling	1.42	-0.378	GRB2,HRAS,Map3k7,MAPK9,PIK3C2G,PIK3C3,PIK3CD
Prostate Cancer Signaling	1.41	NA	GRB2,HRAS,HSP90AB1,PIK3C2G,PIK3C3,PIK3CD
Ephrin A Signaling	1.41	NA	FYN,PIK3C2G,PIK3C3,PIK3CD
Role of p14/p19ARF in Tumor Suppression	1.41	NA	PIK3C2G,PIK3C3,PIK3CD
Sphingosine-1-phosphate Signaling	1.4	0	ADCY3,ADCY7,GNAI2,PIK3C2G,PIK3C3,PIK3CD,RHOBTB1
TGF-β Signaling	1.4	-1	GRB2,HRAS,MAPK14,MAPK9,RNF111,TFE3
Role of Macrophages, Fibroblasts and Endothelial Cells in Rheumatoid Arthritis	1.38	NA	CAMK2G,HRAS,IL1R1,IL33,MAPK14,MAPK9,PIK3C2G,PIK3C3,PIK3CD,PRKCB,SOCS1,SOCS3,STAT3,TCF3
IL-10 Signaling	1.37	NA	IL1R1,IL33,MAPK14,SOCS3,STAT3
fMLP Signaling in Neutrophils	1.37	-1.134	ARPC1A,GNAI2,HRAS,PIK3C2G,PIK3C3,PIK3CD,PRKCB
Ephrin B Signaling	1.35	-0.447	ABI1,EPHB4,GNAI2,HRAS,PXN
GP6 Signaling Pathway	1.35	-1.134	COL6A3,FYN,GSK3A,PIK3C2G,PIK3C3,PIK3CD,PRKCB
UVA-Induced MAPK Signaling	1.34	-1	HRAS,MAPK14,MAPK9,PIK3C2G,PIK3C3,PIK3CD
Phagosome Formation	1.34	NA	ITGB2,MARCO,PIK3C2G,PIK3C3,PIK3CD,PRKCB,RHOBTB1
Oxidative Ethanol Degradation III	1.33	NA	ACSL1,ACSS3,ALDH3A2
Pyridoxal 5'-phosphate Salvage Pathway	1.33	1.342	CDK4,DMPK,GRK6,MAPK9,PRKAA1
Nicotine Degradation II	1.33	-0.447	CYP2A6 (includes others),CYP2C18,CYP2C8,FMO1,POR
Estrogen Biosynthesis	1.33	-1	CYP2A6 (includes others),CYP2C18,CYP2C8,POR
Fcγ Receptor-mediated Phagocytosis in Macrophages and Monocytes	1.32	-1.633	ARPC1A,DOCK1,FYN,PIK3C2G,PRKCB,PXN
Neuregulin Signaling	1.31	-0.447	ADAM17,GRB2,HRAS,HSP90AB1,PRKCB,STAT5A
Superpathway of D-myo-inositol (1,4,5)-trisphosphate Metabolism	1.3	NA	INPP5E,SEC16A,SYNJ1

Table 11. Significant Pathways for differentially expressed transcripts in ^{56}Fe vs. non-irradiated control at 9 months.

Ingenuity Canonical Pathways	-log$_{10}$(p-value)	z-score	Molecules
Acute Phase Response Signaling	4.57	-1.265	AKT3,C1R,IKBKB,IKBKG,JAK2,MAPK9,NFKB1,NR3C1,PIK3CD,SAA1,SOCS1,SOCS3,TCF3,TF
Lymphotoxin β Receptor Signaling	3.87	0.816	AKT3,BCL2L1,IKBKB,IKBKG,NFKB1,PIK3CD,TRAF3
April Mediated Signaling	3.85	0	IKBKB,IKBKG,MAPK9,NFAT5,NFKB1,TRAF3
B Cell Receptor Signaling	3.74	0.632	AKT3,BCL2L1,FCGR2A,IKBKB,IKBKG,MAP3K13,MAPK9,NFAT5,NFKB1,PIK3CD,PTPRC,SYNJ1,TCF3
B Cell Activating Factor Signaling	3.73	0	IKBKB,IKBKG,MAPK9,NFAT5,NFKB1,TRAF3
JAK/Stat Signaling	3.59	-0.707	AKT3,BCL2L1,JAK2,NFKB1,PIK3CD,PTPN1,SOCS1,SOCS3
NF-κB Activation by Viruses	3.48	0.707	AKT3,IKBKB,IKBKG,ITGA3,ITGAL,NFKB1,PIK3CD,PRKD3
IL-17A Signaling in Airway Cells	3.37	-0.378	AKT3,IKBKB,IKBKG,JAK2,MAPK9,NFKB1,PIK3CD
RANK Signaling in Osteoclasts	3.28	0.707	AKT3,IKBKB,IKBKG,MAP3K13,MAPK9,NFKB1,PIK3CD,XIAP
PI3K/AKT Signaling	3.23	-0.632	AKT3,BCL2L1,IKBKB,IKBKG,ITGA3,JAK2,NFKB1,PIK3CD,SYNJ1,TSC1
Type II Diabetes Mellitus Signaling	3.21	0.707	AKT3,IKBKB,IKBKG,MAPK9,NFKB1,PIK3CD,PRKAA1,PRKD3,SMPD4,SOCS1,SOCS3
Role of JAK2 in Hormone-like Cytokine Signaling	3.2	NA	JAK2,PTPN1,SH2B1,SOCS1,SOCS3
TWEAK Signaling	3.14	-0.447	IKBKB,IKBKG,NFKB1,TRAF3,XIAP
CD27 Signaling in Lymphocytes	3.11	0	BCL2L1,IKBKB,IKBKG,MAP3K13,MAPK9,NFKB1
Small Cell Lung Cancer Signaling	3.06	0.378	AKT3,BCL2L1,IKBKB,IKBKG,NFKB1,PIK3CD,TRAF3
Role of Osteoblasts, Osteoclasts and Chondrocytes in Rheumatoid Arthritis	3.03	NA	ADAM17,AKT3,APC,AXIN1,IKBKB,IKBKG,ITGA3,MAPK9,NFAT5,NFKB1,PIK3CD,TCF3,XIAP
p53 Signaling	3	0.378	AKT3,BCL2L1,COQ8A,GADD45G,MDM4,PIK3CD,PML,STAG1
IL-6 Signaling	2.92	-0.333	AKT3,IKBKB,IKBKG,JAK2,MAPK9,NFKB1,PIK3CD,SOCS1,SOCS3

Erythropoietin Signaling	2.9	NA	AKT3,JAK2,NFKB1,PIK3CD,PRKD3,SOCS1,SOCS3
Chronic Myeloid Leukemia Signaling	2.86	NA	AKT3,BCL2L1,HDAC10,HDAC6,IKBKB,IKBKG,NFKB1,PIK3CD
PTEN Signaling	2.84	-0.333	AKT3,BCL2L1,FGFR2,IKBKB,IKBKG,ITGA3,NFKB1,PIK3CD,SYNJ1
Induction of Apoptosis by HIV1	2.79	0	BCL2L1,IKBKB,IKBKG,MAPK9,NFKB1,XIAP
Role of JAK family kinases in IL-6-type Cytokine Signaling	2.79	NA	JAK2,MAPK9,SOCS1,SOCS3
Activation of IRF by Cytosolic Pattern Recognition Receptors	2.71	-0.816	DDX58,IKBKB,IKBKG,MAPK9,NFKB1,TRAF3
Role of RIG1-like Receptors in Antiviral Innate Immunity	2.68	0.447	DDX58,IKBKB,IKBKG,NFKB1,TRAF3
IL-23 Signaling Pathway	2.68	0.447	AKT3,JAK2,NFKB1,PIK3CD,SOCS3
IL-4 Signaling	2.65	NA	AKT3,JAK2,NFAT5,NR3C1,PIK3CD,SOCS1,SYNJ1
Glucocorticoid Receptor Signaling	2.65	NA	AKT3,BAG1,BCL2L1,ERCC3,GTF2A1,IKBKB,IKBKG,JAK2,MAPK9,NFAT5,NFKB1,NR3C1,PIK3CD,POLR2E,PRKAA1,TAF1
CD40 Signaling	2.64	-0.816	IKBKB,IKBKG,MAPK9,NFKB1,PIK3CD,TRAF3
Production of Nitric Oxide and Reactive Oxygen Species in Macrophages	2.6	0.302	AKT3,IKBKB,IKBKG,JAK2,MAP3K13,MAPK9,NFKB1,PIK3CD,PPARA,PPP1R10,PRKD3
FAT10 Cancer Signaling Pathway	2.59	0.447	ACVR1,AKT3,IKBKB,IKBKG,NFKB1
Role of Macrophages, Fibroblasts and Endothelial Cells in Rheumatoid Arthritis	2.55	NA	AKT3,APC,AXIN1,IKBKB,IKBKG,JAK2,MAPK9,NFAT5,NFKB1,PIK3CD,PRKD3,SOCS1,SOCS3,TCF3,TRAF3
TNFR2 Signaling	2.49	1	IKBKB,IKBKG,NFKB1,XIAP
RAR Activation	2.48	NA	ADCY4,AKR1C3,AKT3,ERCC3,JAK2,MAPK9,NFKB1,PIK3CD,PML,PRKD3,SDR9C7
NGF Signaling	2.44	0.707	AKT3,IKBKB,IKBKG,MAP3K13,MAPK9,NFKB1,PIK3CD,SMPD4
Leukocyte Extravasation Signaling	2.43	0	CLDN12,FER,ITGA3,ITGAL,MAPK9,PIK3CD,PRKD3,PXN,RAPGEF4,SIPA1,TEC
4-1BB Signaling in T Lymphocytes	2.38	0	IKBKB,IKBKG,MAPK9,NFKB1
Apelin Endothelial Signaling Pathway	2.38	1.414	ADCY4,AKT3,ARNT,MAPK9,NFKB1,PIK3CD,PRKAA1,PRKD3
Apoptosis Signaling	2.34	0.378	AIFM1,BCL2L1,CAPNS1,IKBKB,IKBKG,NFKB1,XIAP
CD28 Signaling in T Helper Cells	2.34	1.414	AKT3,IKBKB,IKBKG,MAPK9,NFAT5,NFKB1,PIK3CD,PTPRC
Reelin Signaling in Neurons	2.25	NA	ARHGEF2,ITGA3,ITGAL,MAPK8IP3,MAPK9,PIK3CD

Mouse Embryonic Stem Cell Pluripotency	2.24	1.134	AKT3,APC,AXIN1,JAK2,PIK3CD,TCF3,XIAP
SAPK/JNK Signaling	2.24	0	GNB1,MAP3K13,MAP4K5,MAPK8IP3,MAPK9,MINK1,PIK3CD
IL-17A Signaling in Fibroblasts	2.24	NA	IKBKB,IKBKG,LCN2,NFKB1
Gα12/13 Signaling	2.21	0.707	AKT3,IKBKB,IKBKG,MAPK9,NFKB1,PIK3CD,PXN,TEC
Amyotrophic Lateral Sclerosis Signaling	2.18	1.633	AKT3,BCL2L1,CAPNS1,GPX1,GRIK5,PIK3CD,XIAP
LPS-stimulated MAPK Signaling	2.14	0	IKBKB,IKBKG,MAPK9,NFKB1,PIK3CD,PRKD3
PEDF Signaling	2.14	1.633	AKT3,BCL2L1,IKBKB,IKBKG,NFKB1,PIK3CD
Sertoli Cell-Sertoli Cell Junction Signaling	2.12	NA	AKT3,AXIN1,CLDN12,EPB41,EPN2,ITGA3,MAP3K13,MAPK9,TJP2,TJP3
PPARα/RXRα Activation	2.11	0.707	ACVR1,ADCY4,CKAP5,HELZ2,IKBKB,IKBKG,JAK2,NFKB1,PPARA,PRKAA1
Colorectal Cancer Metastasis Signaling	2.1	0.577	ADCY4,AKT3,APC,ARRB1,AXIN1,BCL2L1,GNB1,JAK2,MAPK9,NFKB1,PIK3CD,TCF3
Prolactin Signaling	2.09	-0.447	JAK2,NR3C1,PIK3CD,PRKD3,SOCS1,SOCS3
T Cell Receptor Signaling	2.09	NA	IKBKB,IKBKG,NFAT5,NFKB1,PIK3CD,PTPRC,TEC
Pancreatic Adenocarcinoma Signaling	2.07	0.378	AKT3,BCL2L1,JAK2,MAPK9,NFKB1,PIK3CD,PLD2
Cardiac Hypertrophy Signaling (Enhanced)	2.07	1.147	ACVR1,ADCY4,AKT3,DIAPH1,FGFR2,GNB1,HDAC10,HDAC6,IKBKB,IKBKG,ITGA3,JAK2,MAP3K13,MAPK9,NFAT5,NFKB1,PIK3CD,PRKD3,RCAN1
Type I Diabetes Mellitus Signaling	2.05	-1.134	IKBKB,IKBKG,JAK2,MAPK9,NFKB1,SOCS1,SOCS3
HGF Signaling	2.01	0.378	AKT3,ITGA3,MAP3K13,MAPK9,PIK3CD,PRKD3,PXN
Role of PKR in Interferon Induction and Antiviral Response	2	NA	IKBKB,IKBKG,NFKB1,TRAF3
IL-8 Signaling	1.99	1	AKT3,BCL2L1,GNB1,IKBKB,IKBKG,MAPK9,NFKB1,PIK3CD,PLD2,PRKD3
iCOS-iCOSL Signaling in T Helper Cells	1.97	1.633	AKT3,IKBKB,IKBKG,NFAT5,NFKB1,PIK3CD,PTPRC
Insulin Receptor Signaling	1.96	-0.378	AKT3,JAK2,PIK3CD,PPP1R10,PTPN1,SOCS3,SYNJ1,TSC1
IL-22 Signaling	1.89	NA	AKT3,MAPK9,SOCS3
Role of JAK1, JAK2 and TYK2 in Interferon Signaling	1.89	NA	JAK2,NFKB1,SOCS1
Huntington's Disease Signaling	1.88	1.134	AKT3,BCL2L1,CAPNS1,DNM2,GNB1,HDAC10,HDAC6,MAPK9,PIK3CD,POLR2E,PRKD3
IL-15 Production	1.88	NA	AATK,DYRK1A,FER,FGFR2,JAK2,NFKB1,TEC

IL-1 Signaling	1.87	0	ADCY4,GNB1,IKBKB,IKBKG,MAPK9,NFKB1
Apelin Pancreas Signaling Pathway	1.85	1	MAPK9,NFKB1,PIK3CD,PRKAA1
Role of NFAT in Regulation of the Immune Response	1.78	2.121	AKT3,FCGR2A,GNB1,IKBKB,IKBKG,NFAT5,NFKB1,PIK3CD,RCAN1
IL-15 Signaling	1.77	NA	AKT3,BCL2L1,JAK2,NFKB1,PIK3CD
iNOS Signaling	1.76	0	IKBKB,IKBKG,JAK2,NFKB1
IL-10 Signaling	1.75	NA	FCGR2A,IKBKB,IKBKG,NFKB1,SOCS3
Fcγ Receptor-mediated Phagocytosis in Macrophages and Monocytes	1.74	1.633	AKT3,FCGR2A,PIP5K1A,PLD2,PRKD3,PXN
Sirtuin Signaling Pathway	1.72	-0.632	ADAM10,ATG13,CYC1,GADD45G,GLUD1,LDHA,NDUFAF1,NDUFV1,NFKB1,NR1H2,PPARA,PRKAA1,SIRT7
HOTAIR Regulatory Pathway	1.71	0	AEBP2,AKT3,NFKB1,PIK3CD,SETDB1,STK38,TCF3,XIAP
Regulation of the Epithelial-Mesenchymal Transition Pathway	1.7	NA	ADAM17,AKT3,APC,AXIN1,FGFR2,JAK2,NFKB1,PIK3CD,TCF3
Caveolar-mediated Endocytosis Signaling	1.7	NA	DNM2,FLOT1,ITGA3,ITGAL,PTPN1
Growth Hormone Signaling	1.7	-0.447	JAK2,PIK3CD,PRKD3,SOCS1,SOCS3
TNFR1 Signaling	1.7	1	IKBKB,IKBKG,NFKB1,XIAP
Assembly of RNA Polymerase II Complex	1.7	NA	ERCC3,GTF2A1,POLR2E,TAF1
Molecular Mechanisms of Cancer	1.68	NA	ADCY4,AKT3,APC,ARHGEF2,AXIN1,BCL2L1,CDK19,ITGA3,JAK2,MAPK9,NFKB1,PIK3CD,PRKD3,TCF3,XIAP
Phenylalanine Degradation I (Aerobic)	1.68	NA	PCBD2,QDPR
Angiopoietin Signaling	1.66	1	AKT3,IKBKB,IKBKG,NFKB1,PIK3CD
Gαq Signaling	1.65	2.121	AKT3,GNB1,IKBKB,IKBKG,NFKB1,PIK3CD,PLD2,PRKD3
Adipogenesis pathway	1.64	NA	ERCC3,FGFR2,HDAC10,HDAC6,PPIP5K1,SETDB1,TBL1XR1
Leptin Signaling in Obesity	1.64	0	ADCY4,AKT3,JAK2,PIK3CD,SOCS3
Phospholipase C Signaling	1.63	1.667	ADCY4,ARHGEF2,FCGR2A,GNB1,HDAC10,HDAC6,ITGA3,NFAT5,NFKB1,PLD2,PRKD3
IGF-1 Signaling	1.63	-0.816	AKT3,JAK2,PIK3CD,PXN,SOCS1,SOCS3
Hepatic Cholestasis	1.63	NA	ADCY4,IKBKB,IKBKG,MAPK9,NFKB1,PPARA,PPRC1,PRKD3,TJP2
IL-12 Signaling and Production in Macrophages	1.63	NA	AKT3,IKBKB,IKBKG,MAPK9,NFKB1,PIK3CD,PRKD3
Tec Kinase Signaling	1.63	0.378	GNB1,ITGA3,JAK2,MAPK9,NFKB1,PIK3CD,PRKD3,TEC

Agrin Interactions at Neuromuscular Junction	1.61	-1.342	AGRN,ITGA3,ITGAL,MAPK9,PXN
FXR/RXR Activation	1.61	NA	AKT3,FETUB,LIPC,MAPK9,PPARA,SAA1,TF
Tight Junction Signaling	1.61	NA	AKT3,ARHGEF2,CASK,CLDN12,EPB41,NFKB1,TJP2,TJP3
IL-17 Signaling	1.6	NA	AKT3,JAK2,MAPK9,NFKB1,PIK3CD
Sumoylation Pathway	1.58	NA	MAPK9,NFKB1,NR3C1,PML,RNF4,XIAP
Human Embryonic Stem Cell Pluripotency	1.57	NA	ACVR1,AKT3,APC,AXIN1,FGFR2,PIK3CD,TCF3
tRNA Charging	1.55	1.342	FARSA,IARS,LARS2,Qars,VARS
PI3K Signaling in B Lymphocytes	1.52	1.89	AKT3,IKBKB,IKBKG,NFAT5,NFKB1,PIK3CD,PTPRC
Germ Cell-Sertoli Cell Junction Signaling	1.52	NA	AXIN1,EPN2,FER,ITGA3,MAP3K13,MAPK9,PIK3CD,PXN
Virus Entry via Endocytic Pathways	1.52	NA	AP1G2,DNM2,ITGA3,ITGAL,PIK3CD,PRKD3
Antioxidant Action of Vitamin C	1.52	0	IKBKB,IKBKG,JAK2,MAPK9,NFKB1,PLD2
IL-9 Signaling	1.51	NA	NFKB1,PIK3CD,SOCS3
mTOR Signaling	1.43	0.378	AKT3,ATG13,EIF4G1,PIK3CD,PLD2,PRKAA1,PRKD3,RPS19,TSC1
MIF-mediated Glucocorticoid Regulation	1.42	NA	CD74,NFKB1,NR3C1
Dendritic Cell Maturation	1.41	0.707	AKT3,FCGR2A,IKBKB,IKBKG,JAK2,MAPK9,NFKB1,PIK3CD
TR/RXR Activation	1.39	NA	AKR1C3,AKT3,COL6A3,PIK3CD,TBL1XR1
Regulation of IL-2 Expression in Activated and Anergic T Lymphocytes	1.39	NA	IKBKB,IKBKG,MAPK9,NFAT5,NFKB1
Role of NFAT in Cardiac Hypertrophy	1.38	1.89	ADCY4,AKT3,GNB1,HDAC10,HDAC6,MAPK9,PIK3CD,PRKD3,RCAN1
Role of Tissue Factor in Cancer	1.38	NA	AKT3,ARRB1,BCL2L1,ITGA3,JAK2,PIK3CD
Acute Myeloid Leukemia Signaling	1.37	2.236	AKT3,NFKB1,PIK3CD,PML,TCF3
Factors Promoting Cardiogenesis in Vertebrates	1.35	NA	ACVR1,APC,AXIN1,PRKD3,TCF3
GP6 Signaling Pathway	1.35	1.633	ADAM10,AKT3,COL4A5,COL6A3,PIK3CD,PRKD3
Renin-Angiotensin Signaling	1.31	0.447	ADCY4,JAK2,MAPK9,NFKB1,PIK3CD,PRKD3
LPS/IL-1 Mediated Inhibition of RXR Function	1.3	0	CYP2A6 (includes others),CYP4A11,FMO1,FMO2,LIPC,MAPK9,NR1H2,PPARA,PPARGC1B

Table 12. Significant Pathways for differentially expressed transcripts in ^{56}Fe vs. non-irradiated control at 12 months.

6.4.2 IDENTIFICATION OF DYSREGULATED MOLECULAR PATHWAYS CORRESPONDING TO UNANNOTATED TRANSCRIPTS ASSOCIATED WITH ^{56}FE IRRADIATION, USING SOM

The above IPA analysis (Figure 9) resulted in a collection of 67 statistically significant high-quality functionally unannotated transcripts across all time points from ^{56}Fe irradiated mice (Table 13). To characterize the unannotated transcripts, we obtained the $\log_2$ (fold change) expression values of significantly differentially expressed transcripts from ^{56}Fe irradiation compared to non-irradiated control across 5 time points and applied the SOM machine learning algorithm. We next identified the modules from SOMs, which contained the majority of unannotated transcripts and combined them to form larger clusters of similar transcription patterns for functional analysis using IPA. We compared the identified 11 clusters across 5 time points and selected the most significant pathways across all clusters (Figure 10f). The activation z-scores were predicted for some of the clusters based on our observed data and the available literature. The Fe 1-month Clusters have an activated positive z-score for organismal death and an inhibited negative z-score for RNA transcription and cell neoplasia. These observations are in line with our current understanding of early cellular response to irradiation and production of reactive oxygen species at earlier time points and activation of neoplasia at later time points. Clusters of unannotated transcripts show inhibition of pathways involved in RNA expression and transcription at 1 month, and activation of these pathways at 9 and 12 months. A complete

list of unannotated transcript ENSMBL IDs with their corresponding module numbers is provided in Table 14.

Ion	1 month	2 months	4 months	9 months	12 months	Total
^{56}Fe	16	16	13	8	14	67
^{16}O	24	23	13	13	22	95
^{28}Si	19	14	17	12	19	81

Table 13. Number of unannotated transcripts analyzed by IPA.

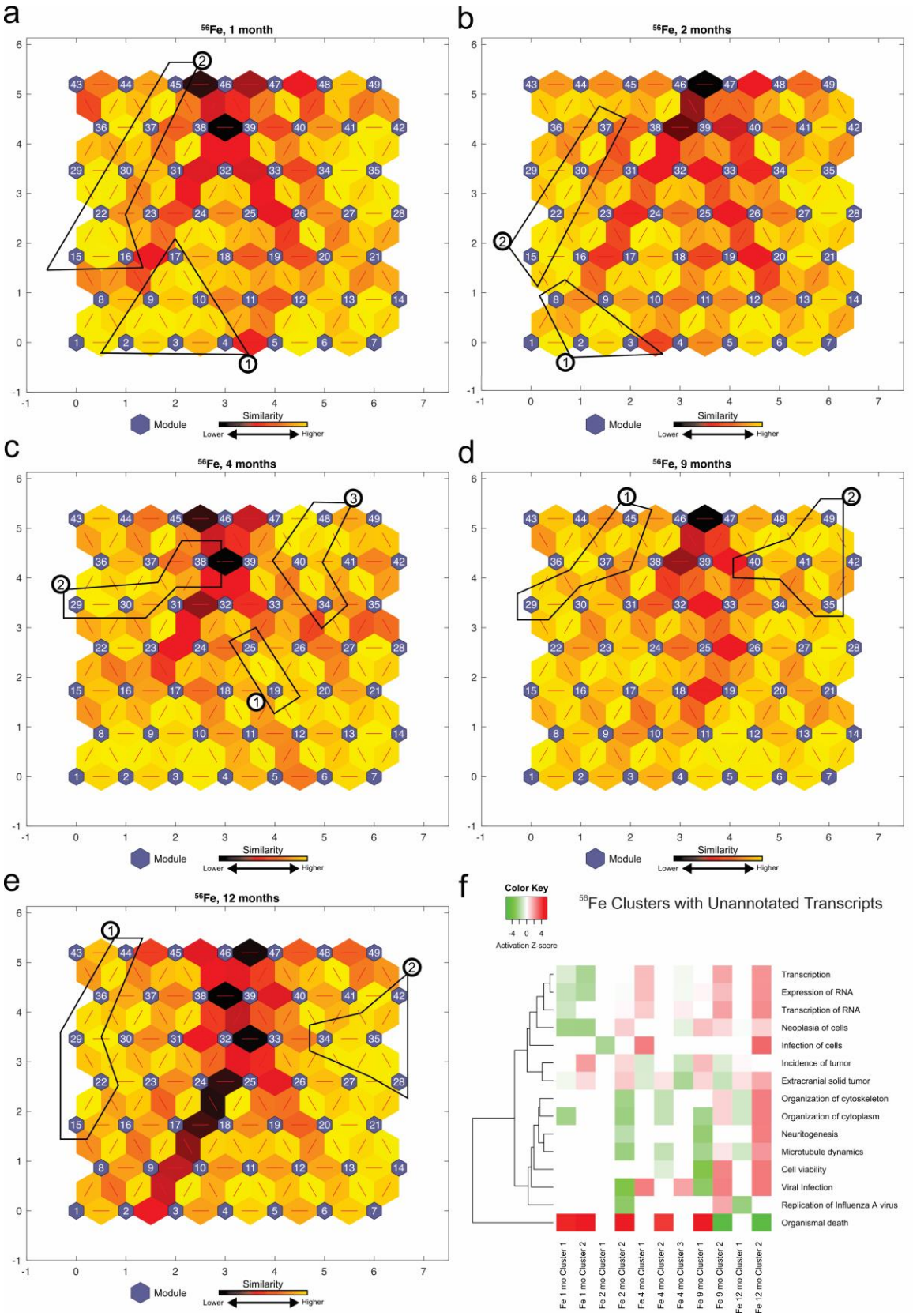
a
56Fe, 1 month
b
56Fe, 2 months
c
56Fe, 4 months
d
56Fe, 9 months
e
56Fe, 12 months
Module
Similarity
Lower
Higher
f
Color Key
-4 0 4
Activation Z-score
56Fe Clusters with Unannotated Transcripts
Transcription
Expression of RNA
Transcription of RNA
Neoplasia of cells
Infection of cells
Incidence of tumor
Extracranial solid tumor
Organization of cytoskeleton
Organization of cytoplasm
Neuritogenesis
Microtubule dynamics
Cell viability
Viral Infection
Replication of Influenza A virus
Organismal death
Fe 1 mo Cluster 1
Fe 1 mo Cluster 2
Fe 2 mo Cluster 1
Fe 2 mo Cluster 2
Fe 4 mo Cluster 1
Fe 4 mo Cluster 2
Fe 4 mo Cluster 3
Fe 9 mo Cluster 1
Fe 9 mo Cluster 2
Fe 12 mo Cluster 1
Fe 12 mo Cluster 2

Figure 10. ^{56}Fe analysis of self-organizing maps for each time point.

(a,b,c,d,e) Kohonen Self-Organizing Map (SOM) was applied to the differentially expressed (DE) transcripts obtained from the RNA-Seq data to identify coherent patterns of transcript expression at each time point, as well as patterns within the unannotated transcripts. The SOM clusters transcripts in each module according to $\log_2$(fold change) of the expression values. SOM clustering analysis demonstrates the distances between correlated transcript groups. The small blue hexagons are modules comprising transcripts with similar $\log_2$(fold change) expression patterns. The numbers of transcripts in each module are provided in Figure 11. Neighboring modules are connected with a red line. The colors of the lines connecting the modules indicate the similarity between modules: Lighter colors represent higher similarity, and darker colors represent lower similarity. **(f)** Expression patterns of unannotated transcripts were identified, and the corresponding modules (represented in circled numbers) were further analyzed by IPA. Only the most significant pathways across all clusters are shown with available color-coded activation z-scores. Inhibitory, activation, or unknown directionality z-scores correspond to green, red, and white, respectively. The entries with white color indicate the directionality could not be predicted based on the available data, yet the pathway is significantly identified by pathway analysis. The goal of the IPA downstream effects analysis is to identify functional pathways whose activity is expected to be increased or decreased, given the observed expression changes in a user's dataset (see Methods.)

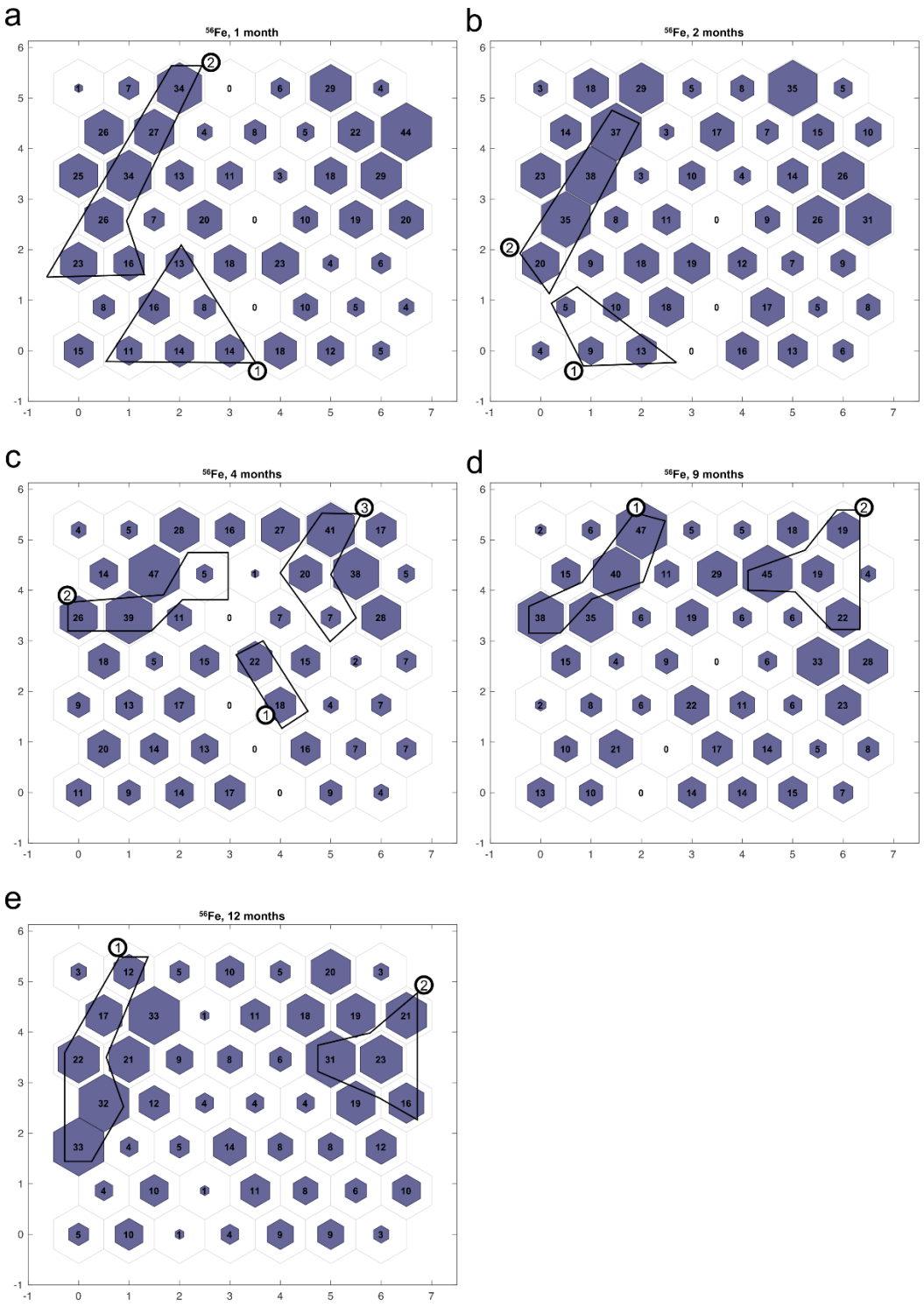

Figure 11. ^{56}Fe Analysis of self-organizing maps for each time point.

(a,b,c,d,e) Kohonen Self-Organizing Map (SOM) was applied to the differentially expressed (DE) transcripts obtained from the RNA-Seq data to identify coherent patterns

of transcript expression at each time point, as well as patterns within the unmapped transcripts. The mapping clusters transcripts in each unit according to log_2(fold change) expression values for the transcripts in that unit. SOM clustering analysis demonstrates the distances between correlated transcript groups. The small blue hexagons are modules comprising transcripts with similar log_2(fold change) expression pattern. The numbers inside hexagons correspond to the number of transcripts in each module.

^{56}Fe, 1 month		^{56}Fe, 2 months		^{56}Fe, 4 months		^{56}Fe, 9 months		^{56}Fe, 12 months	
Module	**Transcript Ensemble ID**	**Module**	**Transcript Ensemble ID**	**Module**	**Transcript Ensemble ID**	**Module**	**Transcript Ensemble ID**	**Module**	**Transcript Ensemble ID**
10	ENSMUST00000237602	13	ENSMUST00000237025	19	ENSMUST00000236950	18	ENSMUST00000235957	15	ENSMUST00000236171
15	ENSMUST00000237742	15	ENSMUST00000236006	25	ENSMUST00000237098	29	ENSMUST00000236217	22	ENSMUST00000236392
16	ENSMUST00000236727	19	ENSMUST00000236824	29	ENSMUST00000235915	35	ENSMUST00000235927	28	ENSMUST00000236217
17	ENSMUST00000236267	23	ENSMUST00000236209	29	ENSMUST00000236006	37	ENSMUST00000236006	29	ENSMUST00000235411
19	ENSMUST00000236403	28	ENSMUST00000236925	30	ENSMUST00000235764	40	ENSMUST00000237358	2	ENSMUST00000235318
20	ENSMUST00000238288	2	ENSMUST00000235947	34	ENSMUST00000237854	40	ENSMUST00000237862	32	ENSMUST00000235947
27	ENSMUST00000237170	30	ENSMUST00000236873	38	ENSMUST00000235411	45	ENSMUST00000236547	34	ENSMUST00000237874
2	ENSMUST00000238201	30	ENSMUST00000237472	40	ENSMUST00000237874	49	ENSMUST00000238729	35	ENSMUST00000235620
2	ENSMUST00000236186	30	ENSMUST00000237823	48	ENSMUST00000236209			35	ENSMUST00000236330
30	ENSMUST00000237167	33	ENSMUST00000237749	48	ENSMUST00000236046			42	ENSMUST00000235135
45	ENSMUST00000236268	37	ENSMUST00000235620	48	ENSMUST00000235207			42	ENSMUST00000238368
45	ENSMUST00000238271	38	ENSMUST00000238677	48	ENSMUST00000236850			44	ENSMUST00000238729
48	ENSMUST00000237472	3	ENSMUST00000235318	48	ENSMUST00000236687			44	ENSMUST00000236006
4	ENSMUST00000235304	42	ENSMUST00000237742					46	ENSMUST00000238731
4	ENSMUST00000235231	6	ENSMUST00000236480						
9	ENSMUST00000235929	8	ENSMUST00000238176						

Table 14. Unannotated differentially expressed transcripts in ^{56}Fe experiments at all time points. Each unannotated ENSEMBLE transcript ID is listed with the corresponding module number in the SOM Figure 10.

6.4.3 DIFFERENTIAL EXPRESSION ANALYSIS OF ^{16}O REVEALS DYNAMIC TIME-DEPENDENT CHANGES IN INFLAMMATORY RESPONSE AT THE WHOLE TRANSCRIPTOME LEVEL

Transcriptional changes and altered pathways associated with proposed ^{16}O induced hepatic carcinogenesis were evaluated using differential expression analysis of RNA-Seq data in ^{16}O irradiated compared to non-irradiated control mice at 5 different time points (1mo, 2mo, 4mo, 9mo, and 12mo). Table 7 shows the total number of differentially expressed transcripts at each time point. IPA was used to functionally annotate and map the biological processes involving these differentially expressed transcripts (Figure 12). The analyses revealed that the LXR/RXR pathway is significantly affected at all time points; specifically, at 1 month (activated), 2 months (directionality unknown), 4 months (activated), 9 months (activated), and 12 months (inhibited). These results indicate that ^{16}O irradiation shows a time-dependent inflammatory response, similar to that of ^{56}Fe. Similarly, PPARα is significantly affected at 1 month (activated), 4 months (directionality unknown), 9 months (activated), and 12 months (activated). This suggests that, even with a time-dependent inflammatory response, ^{16}O tend to exert a more potent activation of inflammatory pathways as compared to ^{56}Fe. Furthermore, Interleukin 8 (IL-8) signaling is significantly activated at 4 and 12 months, but inhibited at 1 and 2 months. IL-8 is a member of the C-X-C family of chemokines and plays a central role in angiogenesis, tumor growth, and inflammation. IL-8 upregulates the expression of genes involved in tumor growth, angiogenesis, and tumor invasion. IL-8 also enhances cell proliferation by activating cyclin D via a protein kinase B (PKB/Akt) mediated mechanism. [117-119]

Our results show activation of LPS/IL-1 mediated inhibition of RXR function pathway at 1, 2, 9, and 12 months. The RXR plays a role in the following cascade of biological events. Binding of the CD14/TRL4/MD2 receptor complex to toxins promotes the secretion of pro-inflammatory cytokines (IL-1, TNFα) in different cell types, but especially in macrophages. Liver tissue injury downregulates the expression of hepatic specific genes, known as negative hepatic acute phase response (APR). Most of these repressed genes are regulated by retinoid X receptors (RXRs), which dimerizes with LXR. RXRs undergo nuclear export and therefore inhibited in response to proinflammatory cytokines (i.e. IL-1) initiated by the stimuli, and this export leads to impaired lipid metabolism and signaling. [104, 120, 121] The impaired lipid metabolism induced by ^{16}O irradiation is furthered demonstrated by the adipogenesis pathway, which was significantly affected at 1, 2, 9, and 12 months (directionality/z-score unknown). Adipogenesis, adipocyte differentiation, is a complicated cellular process that is tightly regulated by a number of transcription factors, lipids, hormones, and signaling pathway molecules. [122-124] In addition, similar to the case with ^{56}Fe, BCR is affected at 1 month (directionality unknown), 2 months (inhibited), 4 months (activated), 9 months (inhibited) and 12 months (activated). Activation of BCR at 12 months reduces apoptosis, which could further play a role in hepatic carcinogenesis. This is bolstered by the significant activation of the chronic myeloid leukemia signaling (CML) pathway at all time points, triggered by expression of the BCR gene product. The transcriptional changes in CML involve genes that result in cell proliferation. [125-127] A complete list of statistically significant altered pathways ($-\log_{10}$(p-value)≥1.3) is provided in Tables 15, 16, 17, 18, and 19.

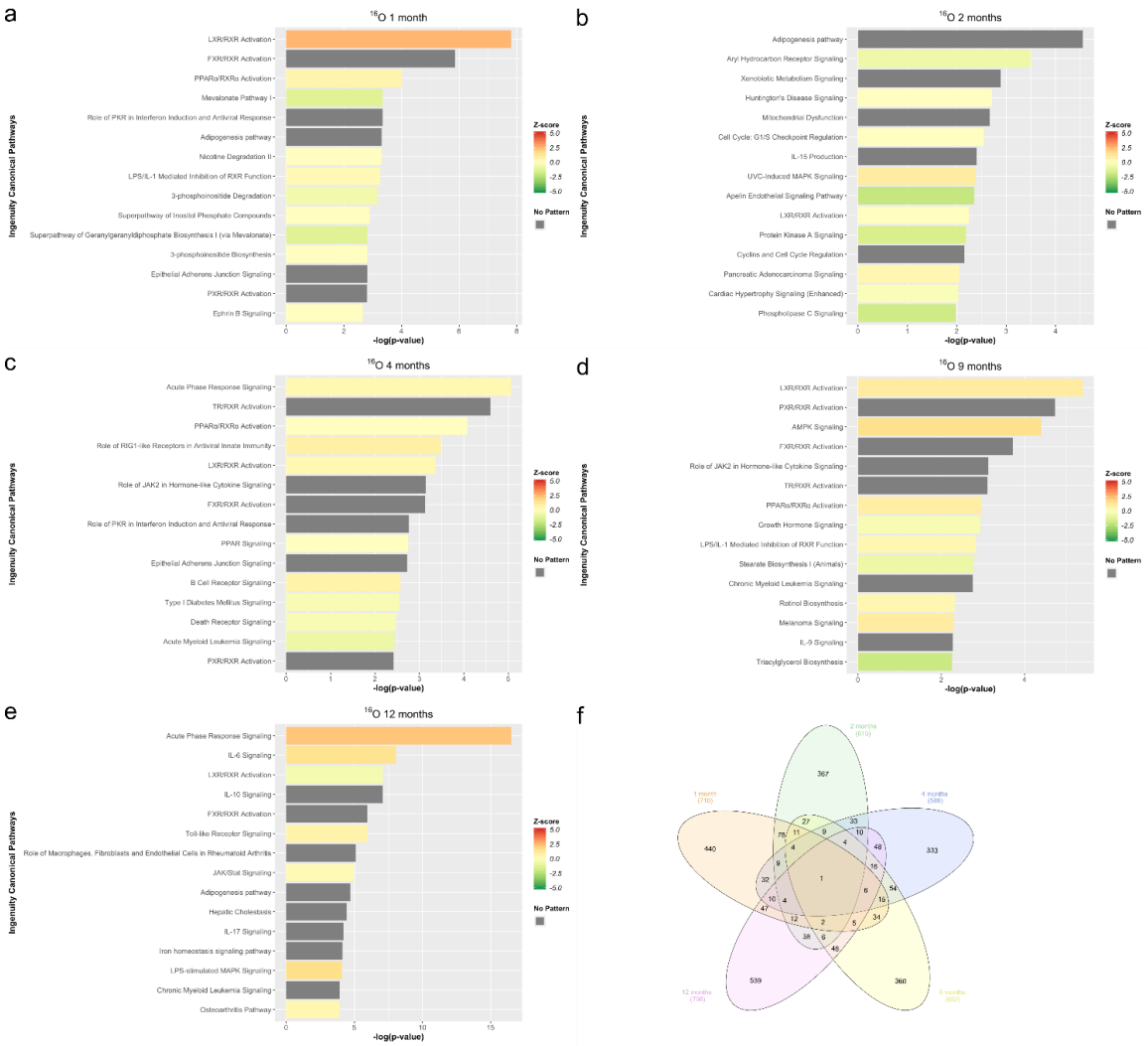

Figure 12. IPA of differentially expressed transcripts in ^{16}O.

(a) Top pathways enrichment analysis at 1 month. **(b)** Top pathways enrichment analysis at 2 months. **(c)** Top pathways enrichment analysis at 4 months. **(d)** Top pathways enrichment analysis at 9 months. **(e)** Top pathways enrichment analysis at 12 months. **(f)** The Venn Diagram shows shared and unique differentially expressed transcripts for all time points, in ^{16}O irradiation compared to control.

Ingenuity Canonical Pathways	-log$_{10}$(p-value)	z-score	Molecules
LXR/RXR Activation	7.8	2.53	ACACA,APOA2,C4A/C4B,C9,CD36,CLU,FASN,FDFT1,HMGCR,KNG1,MLXIPL,NCOR2,NR1H3,PLTP,SAA1,SCD,SERPINF1
FXR/RXR Activation	5.86	NA	APOA2,C4A/C4B,C9,CLU,FASN,FETUB,KNG1,MLXIPL,NR0B2,NR1H3,PLTP,S

			AA1,SCARB1,SDC1,SERPINF1
PPARα/RXRα Activation	4.01	0.577	APOA2,CD36,CKAP5,Cyp2c70,CYP2C8,FASN,GPD2,GRB2,IKBKB,IKBKG,MED23,NCOR2,NR0B2,PLCE1,TGFBR1
Mevalonate Pathway I	3.35	-1.342	ACAT2,HADHB,HMGCR,HMGCS1,MVD
Role of PKR in Interferon Induction and Antiviral Response	3.34	NA	ATF2,CASP8,IKBKB,IKBKG,STAT1,TRAF3
Nicotine Degradation II	3.31	0	CYP2A6 (includes others),CYP2C8,CYP3A5,FMO1,FMO2,FMO4,INMT,UGT2B28
Adipogenesis pathway	3.31	NA	CEBPA,CTNNB1,EZH2,FGFR2,FGFR3,HDAC10,LPIN1,NOCT,PPIP5K1,RPS6KA1,SMAD5
LPS/IL-1 Mediated Inhibition of RXR Function	3.26	0.333	ALAS1,CYP2A6 (includes others),CYP2C8,CYP3A5,CYP4A11,Cyp4a14,FMO1,FMO2,FMO4,HMGCS1,NR0B2,NR1H3,NR1I3,PLTP,SCARB1
3-phosphoinositide Degradation	3.18	-0.577	CA3,INPP4A,MTMR3,PPIP5K1,Ppp1cc,PPP1R16B,PTPA,PTPRF,PTPRJ,SET,SIRPA,SYNJ1
Superpathway of Inositol Phosphate Compounds	2.9	0	CA3,PI4K2B,PIP5K1A,PLCE1,PPIP5K1,Ppp1cc,PPP1R16B,PTPA,PTPRF,PTPRJ,SEC16A,SET,SIRPA,SYNJ1
3-phosphoinositide Biosynthesis	2.82	0	CA3,PI4K2B,PIP5K1A,PPIP5K1,Ppp1cc,PPP1R16B,PTPA,PTPRF,PTPRJ,SET,SIRPA,SYNJ1
Superpathway of Geranylgeranyldiphosphate Biosynthesis I (via Mevalonate)	2.82	-1.342	ACAT2,HADHB,HMGCR,HMGCS1,MVD
Epithelial Adherens Junction Signaling	2.81	NA	ACTN4,BAIAP2,CLIP1,CTNNB1,EPN2,MYH10,PARD3,TCF3,TGFBR1,TUBA4A,TUBB2A
PXR/RXR Activation	2.8	NA	ALAS1,CYP2A6 (includes others),CYP2C8,CYP3A5,NR0B2,NR1I3,SCD
Ephrin B Signaling	2.66	0	ABI1,AXIN1,CAP1,CTNNB1,EPHB4,GNB2,HNRNPK
D-myo-inositol-5-phosphate Metabolism	2.64	-0.302	CA3,PLCE1,PPIP5K1,Ppp1cc,PPP1R16B,PTPA,PTPRF,PTPRJ,SET,SIRPA,SYNJ1
Inhibition of Angiogenesis by TSP1	2.6	NA	CD36,CD47,HSPG2,SDC1,TGFBR1
D-myo-inositol (1,4,5,6)-Tetrakisphosphate Biosynthesis	2.45	0	CA3,PPIP5K1,Ppp1cc,PPP1R16B,PTPA,PTPRF,PTPRJ,SET,SIRPA,SYNJ1
D-myo-inositol (3,4,5,6)-tetrakisphosphate Biosynthesis	2.45	0	CA3,PPIP5K1,Ppp1cc,PPP1R16B,PTPA,PTPRF,PTPRJ,SET,SIRPA,SYNJ1

RAR Activation	2.39	NA	AKR1C4,CARM1,CYP26A1,DHRS4,NCOR2,PBRM1,PML,PRKD3,RARB,SDR9C7,SMAD5,TNIP1
Role of RIG1-like Receptors in Antiviral Innate Immunity	2.37	0.447	CASP8,IKBKB,IKBKG,TRAF3,TRIM25
Superpathway of Cholesterol Biosynthesis	2.32	-1.89	ACAT2,FDFT1,HADHB,HMGCR,HMGCS1,MVD,TM7SF2
Acute Phase Response Signaling	2.29	-1.342	APOA2,C1R,C4A/C4B,C9,GRB2,HNRNPK,IKBKB,IKBKG,SAA1,SERPINF1,TCF3
HIPPO signaling	2.29	0	DLG1,ITCH,MOB1A,PARD3,Ppp1cc,PTPA,SMAD5
Regulation of IL-2 Expression in Activated and Anergic T Lymphocytes	2.16	NA	Calm1 (includes others),GRB2,IKBKB,IKBKG,NFATC1,PPP3CB,TGFBR1
B Cell Receptor Signaling	2.14	0	ATF2,BCL6,Calm1 (includes others),GRB2,IKBKB,IKBKG,MAP3K13,NFATC1,PPP3CB,SYNJ1,TCF3
Phosphatidylcholine Biosynthesis I	2.12	NA	CHPT1,PCYT1A,PHKA1
Factors Promoting Cardiogenesis in Vertebrates	2.11	NA	ATF2,AXIN1,CTNNB1,PRKD3,SMAD5,TCF3,TGFBR1
Sertoli Cell-Sertoli Cell Junction Signaling	2.07	NA	ACTN4,ATF2,AXIN1,CTNNB1,DLG1,EPN2,MAP3K13,SPTAN1,TJP3,TUBA4A,TUBB2A
Cardiac Hypertrophy Signaling	2.06	-0.905	ADRA1B,ATF2,Calm1 (includes others),EIF2B4,GNB2,GRB2,MAP3K13,MEF2A,PLCE1,PPP3CB,RHOBTB1,RPS6KA1,TGFBR1
TWEAK Signaling	1.99	-1	CASP8,IKBKB,IKBKG,TRAF3
Ketogenesis	1.98	NA	ACAT2,HADHB,HMGCS1
Pregnenolone Biosynthesis	1.91	NA	CYP26A1,CYP26B1,CYP4A11
Cell Cycle Regulation by BTG Family Proteins	1.91	NA	E2F3,E2F5,NOCT,PTPA
Acetone Degradation I (to Methylglyoxal)	1.91	-1	CYP2A6 (includes others),CYP2C8,CYP3A5,CYP4A11
Breast Cancer Regulation by Stathmin1	1.89	NA	ARHGEF12,Calm1 (includes others),E2F3,E2F5,GNB2,GRB2,PRKD3,PTPA,TUBA4A,TUBB2A,UHMK1
Chronic Myeloid Leukemia Signaling	1.88	NA	E2F3,E2F5,GRB2,HDAC10,IKBKB,IKBKG,TGFBR1
SAPK/JNK Signaling	1.88	0	ATF2,GRB2,HNRNPK,MAP3K13,MAPK8IP3,MINK1,NFATC1
PTEN Signaling	1.87	0	BCL2L11,FGFR2,FGFR3,GRB2,IKBKB,IKBKG,SYNJ1,TGFBR1
Complement System	1.87	NA	C1R,C4A/C4B,C8A,C9

April Mediated Signaling	1.83	-1	IKBKB,IKBKG,NFATC1,TRAF3
B Cell Activating Factor Signaling	1.76	-1	IKBKB,IKBKG,NFATC1,TRAF3
Activation of IRF by Cytosolic Pattern Recognition Receptors	1.72	0.447	ATF2,IKBKB,IKBKG,STAT1,TRAF3
α-tocopherol Degradation	1.72	NA	CYP4A11,CYP4F3
Choline Biosynthesis III	1.7	NA	CHPT1,PCYT1A,PHKA1
Gαq Signaling	1.69	-1.134	ADRA1B,Calm1 (includes others),GNB2,IKBKB,IKBKG,NFATC1,PPP3CB,PRKD3,RHOBTB1
Production of Nitric Oxide and Reactive Oxygen Species in Macrophages	1.67	1	APOA2,CLU,IKBKB,IKBKG,MAP3K13,PRKD3,PTPA,RHOBTB1,SIRPA,STAT1
RANK Signaling in Osteoclasts	1.66	0	Calm1 (includes others),IKBKB,IKBKG,MAP3K13,NFATC1,PPP3CB
Histidine Degradation VI	1.65	NA	CYP26A1,CYP26B1,CYP4A11
Tetrahydrofolate Salvage from 5,10-methenyltetrahydrofolate	1.63	NA	GART,MTHFD1L
Glioblastoma Multiforme Signaling	1.61	-0.447	AXIN1,CTNNB1,E2F3,E2F5,GRB2,PLCE1,RHOBTB1,TCF3,TSC1
Protein Kinase A Signaling	1.6	-1.069	ATF2,Calm1 (includes others),CTNNB1,EYA3,GNB2,MTMR3,MYH10,NFATC1,PLCE1,Ppp1cc,PPP3CB,PRKD3,PTPRF,PTPRJ,SIRPA,TCF3,TGFBR1
Role of Macrophages, Fibroblasts and Endothelial Cells in Rheumatoid Arthritis	1.59	NA	ATF2,AXIN1,Calm1 (includes others),CEBPA,CTNNB1,IKBKB,IKBKG,NFATC1,PLCE1,PPP3CB,PRKD3,PROK1,TCF3,TRAF3
FAT10 Cancer Signaling Pathway	1.59	0	CTNNB1,IKBKB,IKBKG,TGFBR1
Insulin Receptor Signaling	1.58	0	ACLY,EIF2B4,GRB2,Ppp1cc,PTPRF,SYNJ1,TRIP10,TSC1
Remodeling of Epithelial Adherens Junctions	1.57	NA	ACTN4,CLIP1,CTNNB1,TUBA4A,TUBB2A
Xenobiotic Metabolism Signaling	1.57	NA	ARNT,CYP2C8,CYP3A5,ESD,FMO1,FMO2,FMO4,MAP3K13,NCOR2,NR1I3,PRKD3,PTPA,UGT2B28
Bupropion Degradation	1.56	NA	CYP2A6 (includes others),CYP2C8,CYP3A5
NGF Signaling	1.55	0.378	ATF2,GRB2,IKBKB,IKBKG,MAP3K13,RPS6KA1,SMPD4
Phenylalanine Degradation I (Aerobic)	1.55	NA	PCBD2,QDPR
Germ Cell-Sertoli Cell Junction Signaling	1.54	NA	ACTN4,AXIN1,CTNNB1,EPN2,MAP3K13,RHOBTB1,TGFBR1,TUBA4A,TUBB2A
IL-15 Production	1.53	NA	AXL,EPHB4,FGFR2,FGFR3,KIT,STAT1,TNK2

iNOS Signaling	1.53	NA	Calm1 (includes others),IKBKB,IKBKG,STAT1
TGF-β Signaling	1.52	NA	GRB2,RNF111,SMAD5,TFE3,TGFBR1,ZFYVE9
Phospholipase C Signaling	1.51	-1.265	ARHGEF12,ATF2,Calm1 (includes others),GNB2,GRB2,HDAC10,MEF2A,NFATC1,PLCE1,PPP3CB,PRKD3,RHOBTB1
NF-κB Signaling	1.49	-1	AZI2,CASP8,FGFR2,FGFR3,IKBKB,IKBKG,TGFBR1,TNIP1,TRAF3
TNFR1 Signaling	1.47	0	CASP8,IKBKB,IKBKG,MADD
Apoptosis Signaling	1.46	1.633	BCL2L11,CASP8,IKBKB,IKBKG,RPS6KA1,SPTAN1
Estrogen Biosynthesis	1.42	0	AKR1C4,CYP2A6 (includes others),CYP2C8,CYP3A5
14-3-3-mediated Signaling	1.4	-1.342	GRB2,PLCE1,PRKD3,RPS6KA1,TSC1,TUBA4A,TUBB2A
Integrin Signaling	1.4	-0.333	ACTN4,ARF5,ASAP1,GRB2,ITGA7,ITGAL,ITGAV,RHOBTB1,TLN2,TNK2
CD27 Signaling in Lymphocytes	1.39	0	CASP8,IKBKB,IKBKG,MAP3K13
mTOR Signaling	1.39	-0.447	DGKZ,EIF4G3,MT-RNR1,MT-RNR2,PRKD3,PROK1,PTPA,RHOBTB1,RPS6KA1,TSC1
Triacylglycerol Biosynthesis	1.39	0	AGPAT3,LPIN1,PLPP5,TAZ
Mouse Embryonic Stem Cell Pluripotency	1.39	0	AXIN1,CTNNB1,GRB2,LIFR,SMAD5,TCF3
Role of NFAT in Regulation of the Immune Response	1.39	-0.707	ATF2,Calm1 (includes others),GNB2,GRB2,IKBKB,IKBKG,MEF2A,NFATC1,PPP3CB
PPAR Signaling	1.37	0.816	GRB2,IKBKB,IKBKG,NCOR2,NR0B2,NR1H3
4-1BB Signaling in T Lymphocytes	1.37	NA	ATF2,IKBKB,IKBKG
Ubiquinol-10 Biosynthesis (Eukaryotic)	1.37	NA	CYP26A1,CYP26B1,CYP4A11
Unfolded protein response	1.32	NA	CEBPA,INSIG1,P4HB,SYVN1
Cyclins and Cell Cycle Regulation	1.32	NA	E2F3,E2F5,FBXL5,HDAC10,PTPA
Role of JAK2 in Hormone-like Cytokine Signaling	1.3	NA	SH2B2,SIRPA,STAT1

Table 15. Significant Pathways for differentially expressed transcripts in ^{16}O vs. non-irradiated control at 1 month.

Ingenuity Canonical Pathways	-log10(p-value)	z-score	Molecules
Adipogenesis pathway	4.55	NA	ATG7,CTNNB1,EZH2,FGFR2,HDAC10,HDAC5,LPIN1,NOCT,PPIP5K1,SAP130,SIN3A,TBL1XR1
Aryl Hydrocarbon Receptor Signaling	3.5	-0.707	ALDH2,ARNT,ATR,CDKN1B,GSTM4,HSP90AB1,MGST1,NCOR2,NFIA,NFKB1,RXRB
Xenobiotic Metabolism Signaling	2.89	NA	ALDH2,ANKRA2,ARNT,GSTM4,HDAC5,HSP90AB1,KEAP1,MAP3K13,Map3k7,MAPK9,MGST1,NCOR2,NFKB1,NR1I3,PRKD3
Huntington's Disease Signaling	2.71	0	ATF2,ATP5PB,DNM2,EGFR,GNB2,HDAC10,HDAC5,MAPK9,NCOR1,NCOR2,PRKD3,SGK1,SIN3A
Mitochondrial Dysfunction	2.67	NA	ATP5MC2,ATP5PB,CYB5A,CYC1,MAPK9,MT-ATP6,MT-ND4L,NCSTN,NDUFAF1,PINK1,TXNRD2
Cell Cycle: G1/S Checkpoint Regulation	2.55	0	ATR,CDKN1B,FBXL5,HDAC10,HDAC5,SIN3A
IL-15 Production	2.4	NA	CLK2,EGFR,EPHB4,FES,FGFR2,NFKB1,TEK,TNK2
UVC-Induced MAPK Signaling	2.38	1	ATR,EGFR,MAPK9,PRKD3,SMPD2
Apelin Endothelial Signaling Pathway	2.35	-2.121	ARNT,Calm1 (includes others),HDAC5,MAPK9,MEF2A,NFKB1,PRKD3,TEK
LXR/RXR Activation	2.25	0	APOE,C4A/C4B,CD36,NCOR1,NCOR2,NFKB1,RXRB,TLR3
Protein Kinase A Signaling	2.19	-1.667	AKAP1,AKAP13,ANAPC5,ATF2,Calm1 (includes others),CTNNB1,EYA3,FLNA,GNB2,NAPEPLD,NFKB1,PHKA2,PRKD3,PTPRC,SIRPA,TCF3,TTN
Cyclins and Cell Cycle Regulation	2.15	NA	ATR,CDKN1B,FBXL5,HDAC10,HDAC5,SIN3A
Pancreatic Adenocarcinoma Signaling	2.05	0.447	CDKN1B,EGFR,MAPK9,NAPEPLD,NFKB1,PROK1,SIN3A
Cardiac Hypertrophy Signaling (Enhanced)	2.03	-0.229	ADRA1B,AKAP13,ATF2,Calm1 (includes others),CTNNB1,DIAPH1,FGFR2,HDAC10,HDAC5,ITGA3,MAP3K13,Map3k7,MAPK9,MEF2A,MKNK1,NAPEPLD,NFKB1,PKN1,PRKD3
Phospholipase C Signaling	1.98	-1.897	ARHGEF2,ATF2,Calm1 (includes others),GNB2,HDAC10,HDAC5,ITGA3,MEF2A,MPRIP,NAPEPLD,NFKB1,PRKD3
RANK Signaling in Osteoclasts	1.95	-0.816	Calm1 (includes others),MAP3K13,Map3k7,MAPK9,NFKB1,XIAP
α-tocopherol Degradation	1.84	NA	CYP4F12,CYP4F3
Prostate Cancer Signaling	1.83	NA	ATF2,CDKN1B,CTNNB1,HSP90AB1,NFKB1,SIN3A
IL-17A Signaling in Gastric Cells	1.83	NA	EGFR,MAPK9,NFKB1
mTOR Signaling	1.79	-1	EIF4A2,EIF4G1,NAPEPLD,PRKD3,PROK1,RPS11,RPS13,RPS14,RPTOR,TSC1
ATM Signaling	1.79	0	ATF2,ATR,HERC2,MAPK9,MDM4,SMC2

RhoA Signaling	1.79	-0.378	ACTR3,ARHGAP12,BAIAP2,MPRIP,PKN1,RAPGEF6,TTN
Epithelial Adherens Junction Signaling	1.78	NA	ACTR3,BAIAP2,CTNNB1,EGFR,KEAP1,MYH14,SSX2IP,TCF3
PTEN Signaling	1.74	-0.378	BCAR1,CDKN1B,EGFR,FGFR2,INPP5D,ITGA3,NFKB1
NRF2-mediated Oxidative Stress Response	1.72	0.447	DNAJB11,DNAJC1,EPHX1,GSTM4,HERPUD1,KEAP1,MAPK9,MGST1,PRKD3
B Cell Receptor Signaling	1.72	-1.134	ATF2,Calm1 (includes others),INPP5D,MAP3K13,Map3k7,MAPK9,NFKB1,PTPRC,TCF3
Actin Cytoskeleton Signaling	1.71	0	ACTR3,BAIAP2,BCAR1,DIAPH1,FLNA,FN1,ITGA3,MPRIP,MYH14,TTN
Sirtuin Signaling Pathway	1.69	-1.667	ACLY,ATG7,ATP5PB,CYC1,HSF1,MT-ATP6,MT-ND4L,NDUFAF1,NFKB1,PFKFB3,PGK1,POLR3D,RPTOR
Regulation of eIF4 and p70S6K Signaling	1.69	NA	EIF2S2,EIF4A2,EIF4G1,ITGA3,MKNK1,RPS11,RPS13,RPS14
HOTAIR Regulatory Pathway	1.69	-0.707	ATG7,CTNNB1,EZH2,HSF1,JARID2,NFKB1,TCF3,XIAP
Caveolar-mediated Endocytosis Signaling	1.69	NA	DNM2,EGFR,FLNA,FLOT2,ITGA3
Pyridoxal 5'-phosphate Salvage Pathway	1.69	1.342	DMPK,GRK6,MAPK9,PKN1,SGK1
Sertoli Cell-Sertoli Cell Junction Signaling	1.67	NA	ATF2,BCAR1,CTNNB1,EPB41,ITGA3,KEAP1,MAP3K13,Map3k7,MAPK9
EIF2 Signaling	1.66	0	EIF2S2,EIF4A2,EIF4G1,NOX4,RPL10A,RPL19,RPS11,RPS13,RPS14,XIAP
Reelin Signaling in Neurons	1.62	NA	APOE,ARHGEF2,ITGA3,MAPK8IP3,MAPK9
TNFR2 Signaling	1.61	NA	NFKB1,TBK1,XIAP
CD27 Signaling in Lymphocytes	1.6	0	MAP3K13,Map3k7,MAPK9,NFKB1
VDR/RXR Activation	1.6	0	CDKN1B,NCOR1,NCOR2,PRKD3,RXRB
PI3K/AKT Signaling	1.59	1.134	CDKN1B,CTNNB1,HSP90AB1,INPP5D,ITGA3,NFKB1,TSC1
RAR Activation	1.58	NA	AKR1C4,MAPK9,NCOR1,NCOR2,NFKB1,PBRM1,PRKD3,RXRB,TNIP1
Cdc42 Signaling	1.58	0	ACTR3,ATF2,BAIAP2,DIAPH1,ITGA3,MAPK9,MPRIP,TNK2
IL-8 Signaling	1.55	-0.378	EGFR,GNB2,MAPK9,NAPEPLD,NFKB1,NOX4,PRKD3,PROK1,TEK
4-1BB Signaling in T Lymphocytes	1.54	NA	ATF2,MAPK9,NFKB1
Assembly of RNA Polymerase III Complex	1.53	NA	GTF3C4,POLR3D
HGF Signaling	1.48	0	ATF2,ITGA3,MAP3K13,Map3k7,MAPK9,PRKD3
Salvage Pathways of Pyrimidine Ribonucleotides	1.48	0.816	AK4,DMPK,GRK6,MAPK9,PKN1,SGK1
GNRH Signaling	1.45	0.378	ATF2,Calm1 (includes others),EGFR,MAP3K13,Map3k7,MAPK9,NFKB1,PRKD3
Induction of Apoptosis by HIV1	1.41	1	MAPK9,NFKB1,SLC25A3,XIAP
Endocannabinoid Cancer Inhibition Pathway	1.41	0.378	ATF2,CDKN1B,CTNNB1,PROK1,RPTOR,SMPD2,TCF3
Oxidative Phosphorylation	1.4	-0.816	ATP5MC2,ATP5PB,CYB5A,CYC1,MT-ATP6,MT-ND4L
Ephrin Receptor Signaling	1.4	0	ABI1,ACTR3,ATF2,BCAR1,EPHB4,GNB2,ITGA3,PROK1
NGF Signaling	1.39	0	ATF2,MAP3K13,Map3k7,MAPK9,NFKB1,SMPD2

TR/RXR Activation	1.37	NA	NCOR1,NCOR2,RCAN2,RXRB,TBL1XR1
Activation of IRF by Cytosolic Pattern Recognition Receptors	1.37	0	ATF2,MAPK9,NFKB1,TBK1
fMLP Signaling in Neutrophils	1.35	-2.236	ACTR3,Calm1 (includes others),GNB2,NFKB1,NOX4,PRKD3
Factors Promoting Cardiogenesis in Vertebrates	1.34	NA	ATF2,CTNNB1,NOX4,PRKD3,TCF3
Colorectal Cancer Metastasis Signaling	1.33	1.414	ARRB1,CTNNB1,EGFR,GNB2,MAPK9,MSH3,NFKB1,PROK1,TCF3,TLR3
Cholecystokinin/Gastrin-mediated Signaling	1.33	0	ATF2,BCAR1,EGFR,MAPK9,MEF2A,PRKD3
Autophagy	1.32	NA	ATG7,CTSS,NBR1,VPS33B
Inhibition of Angiogenesis by TSP1	1.32	NA	CD36,MAPK9,SDC1
Phosphatidylcholine Biosynthesis I	1.32	NA	CHKA,PHKA1

Table 16. Significant Pathways for differentially expressed transcripts in ^{16}O vs. non-irradiated control at 2 months.

Ingenuity Canonical Pathways	**-log$_{10}$(p-value)**	**z-score**	**Molecules**
Acute Phase Response Signaling	5.06	0.378	AHSG,C1R,C2,FN1,IKBKB,IKBKG,IL1R1,ITIH2,ITIH3,MAP2K3,NR3C1,SAA1,SOCS2,TCF3,TF
TR/RXR Activation	4.6	NA	F10,FASN,G6PC,MDM2,ME1,PIK3C2G,RXRB,SREBF1,TBL1XR1,THRSP
PPARα/RXRα Activation	4.08	0	ADCY6,ADCY9,AIP,CKAP5,FASN,HELZ2,HSP90AA1,IKBKB,IKBKG,IL1R1,MAP2K3,MAP4K4,SLC27A1,TGFBR1
Role of RIG1-like Receptors in Antiviral Innate Immunity	3.48	0.816	CASP8,IKBKB,IKBKG,TBK1,TRAF3,TRIM25
LXR/RXR Activation	3.36	0.378	AHSG,APOE,FASN,IL1R1,NR1H2,RXRB,SAA1,SCD,SREBF1,TF
Role of JAK2 in Hormone-like Cytokine Signaling	3.14	NA	SH2B1,SH2B3,SIRPA,SOCS2,STAT5A
FXR/RXR Activation	3.13	NA	AHSG,APOE,FASN,G6PC,LIPC,NR5A2,PKLR,SAA1,SREBF1,TF
Role of PKR in Interferon Induction and Antiviral Response	2.76	NA	CASP8,IKBKB,IKBKG,MAP2K3,TRAF3
PPAR Signaling	2.75	0	AIP,HSP90AA1,IKBKB,IKBKG,IL1R1,MAP4K4,PDGFRA,STAT5A
Epithelial Adherens Junction Signaling	2.72	NA	AFDN,CLIP1,JUP,KEAP1,MET,MYH10,MYH11,PARD3,TCF3,TGFBR1
B Cell Receptor Signaling	2.57	0.707	FCGR2A,IKBKB,IKBKG,INPP5K,MAP2K3,Map3k7,NFAT5,PIK3C2G,PTPRC,SYNJ1,TCF3

Type I Diabetes Mellitus Signaling	2.55	-0.378	CASP8,HLA-A,IFNGR1,IKBKB,IKBKG,IL1R1,MAP2K3,SOCS2
Death Receptor Signaling	2.47	-0.378	CASP8,IKBKB,IKBKG,LMNA,MAP4K4,SPTAN1,TBK1
Acute Myeloid Leukemia Signaling	2.44	-0.816	CEBPA,JUP,MAP2K3,PIK3C2G,PML,STAT5A,TCF3
PXR/RXR Activation	2.42	NA	ALAS1,G6PC,GSTM1,NR1I3,NR3C1,SCD
IL-1 Signaling	2.39	0	ADCY6,ADCY9,GNB1,IKBKB,IKBKG,IL1R1,MAP2K3
Cardiac β-adrenergic Signaling	2.33	-0.378	ADCY6,ADCY9,AKAP13,ATP2A3,GNB1,PDE1A,PDE4B,PPP1R10,PPP1R3C
IL-10 Signaling	2.33	NA	FCGR2A,IKBKB,IKBKG,IL1R1,MAP2K3,MAP4K4
NF-κB Signaling	2.27	0	CASP8,IKBKB,IKBKG,IL1R1,MAP4K4,PDGFRA,PIK3C2G,TBK1,TGFBR1,TRAF3
Apoptosis Signaling	2.27	-0.816	CAPNS1,CASP8,IKBKB,IKBKG,LMNA,MAP4K4,SPTAN1
CD27 Signaling in Lymphocytes	2.27	0.447	CASP8,IKBKB,IKBKG,MAP2K3,Map3k7
TWEAK Signaling	2.19	-1	CASP8,IKBKB,IKBKG,TRAF3
Production of Nitric Oxide and Reactive Oxygen Species in Macrophages	2.04	0	APOE,IFNGR1,IKBKB,IKBKG,Map3k7,PIK3C2G,PPP1R10,PPP1R3C,RHOT1,SIRPA
April Mediated Signaling	2.03	1	IKBKB,IKBKG,NFAT5,TRAF3
LPS/IL-1 Mediated Inhibition of RXR Function	1.97	-1.134	ALAS1,APOE,FMO1,GSTM1,IL1R1,LIPC,NR1H2,NR1I3,NR5A2,SLC27A1,SREBF1
IL-4 Signaling	1.96	NA	HLA-A,INPP5K,NFAT5,NR3C1,PIK3C2G,SYNJ1
Activation of IRF by Cytosolic Pattern Recognition Receptors	1.95	0.447	IKBKB,IKBKG,STAT2,TBK1,TRAF3
B Cell Activating Factor Signaling	1.95	1	IKBKB,IKBKG,NFAT5,TRAF3
Cellular Effects of Sildenafil (Viagra)	1.91	NA	ADCY6,ADCY9,GUCY2C,MPRIP,MYH10,MYH11,PDE1A,PDE4B
CD40 Signaling	1.9	-0.447	IKBKB,IKBKG,MAP2K3,PIK3C2G,TRAF3
Insulin Receptor Signaling	1.89	1.134	ACLY,INPP5K,PIK3C2G,PPP1R10,PPP1R3C,PTPRF,SYNJ1,TSC1
Sphingosine-1-phosphate Signaling	1.82	1.134	ADCY6,ADCY9,CASP8,PDGFRA,PIK3C2G,RHOT1,SMPD4
Protein Kinase A Signaling	1.79	0.535	ADCY6,ADCY9,AKAP13,GNB1,MYH10,NFAT5,PDE1A,PDE4B,PPP1R10,PPP1R3C,PTPN21,PTPRC,PTPRF,SIRPA,TCF3,TGFBR1

Role of Oct4 in Mammalian Embryonic Stem Cell Pluripotency	1.78	NA	JARID2,NR5A2,RXRB,TDRD7
p53 Signaling	1.73	0.447	ATR,MDM2,MDM4,PIK3C2G,PML,STAG1
PTEN Signaling	1.69	-1.134	IKBKB,IKBKG,INPP5K,MAST2,PDGFRA,SYNJ1,TGFBR1
Osteoarthritis Pathway	1.69	-0.632	ACVRL1,CASP8,FN1,IL1R1,LRP1,MTF1,PTH1R,SIK3,TCF3,TGFBR1
Cell Cycle: G2/M DNA Damage Checkpoint Regulation	1.69	0	ATR,FBXL5,MDM2,MDM4
Small Cell Lung Cancer Signaling	1.68	1	IKBKB,IKBKG,PIK3C2G,RXRB,TRAF3
Relaxin Signaling	1.67	0.816	ADCY6,ADCY9,GNB1,GUCY2C,NPR2,PDE1A,PDE4B,PIK3C2G
NRF2-mediated Oxidative Stress Response	1.67	NA	DNAJB12,DNAJC1,DNAJC5,DNAJC8,FMO1,GSTM1,KEAP1,MAP2K3,PIK3C2G
Hepatic Fibrosis / Hepatic Stellate Cell Activation	1.67	NA	COL4A1,FN1,IFNGR1,IL1R1,MET,MYH10,MYH11,PDGFRA,TGFBR1
TNFR1 Signaling	1.66	0	CASP8,IKBKB,IKBKG,MADD
Phenylalanine Degradation I (Aerobic)	1.66	NA	PCBD2,QDPR
Growth Hormone Signaling	1.65	2.236	CEBPA,PIK3C2G,RPS6KC1,SOCS2,STAT5A
HOTAIR Regulatory Pathway	1.64	0	DNMT3B,JARID2,MDM2,MET,PIK3C2G,SETDB1,STK38,TCF3
Chronic Myeloid Leukemia Signaling	1.63	NA	IKBKB,IKBKG,MDM2,PIK3C2G,STAT5A,TGFBR1
Clathrin-mediated Endocytosis Signaling	1.59	NA	APOE,CD2AP,MDM2,MET,PICALM,PIK3C2G,PIP5K1C,SYNJ1,TF
TNFR2 Signaling	1.59	NA	IKBKB,IKBKG,TBK1
CDP-diacylglycerol Biosynthesis I	1.55	NA	AGPAT3,CDS2,GPAM
PI3K/AKT Signaling	1.55	1.134	HSP90AA1,IKBKB,IKBKG,INPP5K,MDM2,SYNJ1,TSC1
Tight Junction Signaling	1.55	NA	AFDN,CEBPA,CPSF1,MYH10,MYH11,PARD6A,SPTAN1,TGFBR1
Systemic Lupus Erythematosus Signaling	1.53	NA	FCGR2A,HLA-A,HNRNPA2B1,HNRNPC,NFAT5,PIK3C2G,PRPF38B,PRPF40B,PRPF6,PTPRC
Sumoylation Pathway	1.53	-2	CEBPA,MDM2,NR3C1,PML,RFC1,RHOT1
Lymphotoxin β Receptor Signaling	1.52	1	IKBKB,IKBKG,PIK3C2G,TRAF3
Assembly of RNA Polymerase III Complex	1.52	NA	BDP1,GTF3C1
BER pathway	1.52	NA	LIG1,LIG3
PEDF Signaling	1.51	1.342	CASP8,IKBKB,IKBKG,PIK3C2G,TCF12
IL-9 Signaling	1.48	NA	PIK3C2G,SOCS2,STAT5A
HER-2 Signaling in Breast Cancer	1.47	NA	MDM2,PARD3,PARD6A,PIK3C2G,TSC1

Germ Cell-Sertoli Cell Junction Signaling	1.46	NA	AFDN,JUP,KEAP1,MAP2K3,Map3k7,PIK3C2G,RHOT1,TGFBR1
HIPPO signaling	1.43	NA	PARD3,PPP1R10,PPP1R3C,WWTR1,YAP1
IL-17A Signaling in Fibroblasts	1.42	NA	IKBKB,IKBKG,LCN2
iCOS-iCOSL Signaling in T Helper Cells	1.41	2.236	HLA-A,IKBKB,IKBKG,NFAT5,PIK3C2G,PTPRC
Systemic Lupus Erythematosus In B Cell Signaling Pathway	1.41	-0.302	Eda,FCGR2A,IFNGR1,INPP5K,MAP4K4,NFAT5,PIK3C2G,STAT2,SYNJ1,TBK1,TRAF3
Telomere Extension by Telomerase	1.4	NA	HNRNPA2B1,TERF2
Cardiac Hypertrophy Signaling (Enhanced)	1.39	0.5	ADCY6,ADCY9,AKAP13,ATP2A3,Eda,GNB1,IKBKB,IKBKG,IL1R1,MAP2K3,Map3k7,MKNK1,NFAT5,PDE1A,PDE4B,PIK3C2G,TGFBR1
Aryl Hydrocarbon Receptor Signaling	1.38	0.816	AIP,ATR,GSTM1,HSP90AA1,MDM2,NFIA,RXRB
Induction of Apoptosis by HIV1	1.38	-1	CASP8,IKBKB,IKBKG,SLC25A3
Role of Macrophages, Fibroblasts and Endothelial Cells in Rheumatoid Arthritis	1.38	NA	CEBPA,CSNK1A1,FN1,IKBKB,IKBKG,IL1R1,LRP1,MAP2K3,NFAT5,PIK3C2G,TCF3,TRAF3
Endocannabinoid Cancer Inhibition Pathway	1.37	-0.378	ADCY6,ADCY9,CASP8,MAP2K3,PIK3C2G,SMPD4,TCF3
Phosphatidylglycerol Biosynthesis II (Non-plastidic)	1.36	NA	AGPAT3,CDS2,GPAM
NGF Signaling	1.35	1.633	IKBKB,IKBKG,Map3k7,PIK3C2G,RPS6KC1,SMPD4
Iron homeostasis signaling pathway	1.34	NA	ATP6AP1,FBXL5,LRP1,NUBP2,PDGFRA,STAT5A,TF
Dopamine Receptor Signaling	1.34	NA	ADCY6,ADCY9,PPP1R10,PPP1R3C,QDPR
Role of NFAT in Regulation of the Immune Response	1.32	2.646	CSNK1A1,FCGR2A,GNB1,HLA-A,IKBKB,IKBKG,NFAT5,PIK3C2G
Phosphatidylcholine Biosynthesis I	1.3	NA	CHKA,PHKA1

Table 17. Significant Pathways for differentially expressed transcripts in ^{16}O vs. non-irradiated control at 4 months.

Ingenuity Canonical Pathways	**-log$_{10}$(p-value)**	**z-score**	**Molecules**
LXR/RXR Activation	5.4	1	ACACA,C4A/C4B,CD36,FASN,ITIH4,LPL,PLTP,PON3,SAA1,SCD,SERPINA1,TF,TLR3
PXR/RXR Activation	4.73	NA	ALAS1,ALDH3A2,CES3,CYP2A6 (includes

			others),CYP2C8,NR0B2,PRKACA,SCD,SLCO1B3
AMPK Signaling	4.4	1.604	ACACA,ACACB,ADRA2B,ARID1A,CHRNA4,FASN,PFKFB3,PFKM,PIK3C2G,PIK3CA,PPM1B,PRKAA1,PRKACA,RAB6A,STK11,TSC2
FXR/RXR Activation	3.72	NA	C4A/C4B,FASN,ITIH4,LPL,NR0B2,PLTP,PON3,SAA1,SERPINA1,SLCO1B3,TF
Role of JAK2 in Hormone-like Cytokine Signaling	3.13	NA	GHR,SIRPA,SOCS2,STAT5A,TYK2
TR/RXR Activation	3.11	NA	ACACA,FASN,MDM2,ME1,NCOA4,PIK3C2G,PIK3CA,THRSP
PPARα/RXRα Activation	2.96	0.905	ADCY3,CD36,CKAP5,CYP2C8,FASN,GHR,LPL,MAP4K4,MEF2C,NR0B2,PRKAA1,PRKACA
Growth Hormone Signaling	2.94	-0.378	CEBPA,GHR,PIK3C2G,PIK3CA,RPS6KA1,SOCS2,STAT5A
LPS/IL-1 Mediated Inhibition of RXR Function	2.84	0.447	ACSL1,ALAS1,ALDH3A2,Cyp2a12/Cyp2a22,CYP2A6 (includes others),CYP2C8,CYP4A11,FMO1,GSTP1,NR0B2,PLTP,SLCO1B3,XPO1
Stearate Biosynthesis I (Animals)	2.78	-0.816	ACOT1,ACSL1,CYP4A11,ELOVL1,ELOVL6,FASN
Chronic Myeloid Leukemia Signaling	2.76	NA	CDK4,CDKN1B,HDAC5,MDM2,PIK3C2G,PIK3CA,RBL2,STAT5A
Retinol Biosynthesis	2.33	0.447	CES3,ESD,LPL,PNPLA3,PNPLA5
Melanoma Signaling	2.29	1	CDH1,CDK4,MDM2,PIK3C2G,PIK3CA
IL-9 Signaling	2.28	NA	PIK3C2G,PIK3CA,SOCS2,STAT5A
Triacylglycerol Biosynthesis	2.26	-2	AGPAT3,ELOVL1,ELOVL6,PLPP2,PNPLA3
IL-7 Signaling Pathway	2.12	-0.447	BCL6,CDKN1B,MET,PIK3C2G,PIK3CA,STAT5A
Triacylglycerol Degradation	2.09	0.447	CES3,LPL,PNPLA3,PNPLA5,TARS2
B Cell Receptor Signaling	2.08	-1.265	BCL6,CAMK2D,CAMK2G,GAB1,Map3k7,MEF2C,PIK3C2G,PIK3CA,SYK,SYNJ1
Complement System	2.06	NA	C4A/C4B,C6,C8G,CFH
Adipogenesis pathway	2.05	NA	CEBPA,GTF2H1,HDAC5,Kat6b,KAT7,LPL,RBBP7,RPS6KA1
CNTF Signaling	2.03	0.447	LIFR,PIK3C2G,PIK3CA,RPS6KA1,TYK2
HER-2 Signaling in Breast Cancer	2.02	NA	CDKN1B,MDM2,PARD3,PIK3C2G,PIK3CA,TSC2
Xenobiotic Metabolism Signaling	1.98	NA	ALDH3A2,CAMK2D,CAMK2G,CES3,CYP2C8,ESD,FMO1,GSTP1,HDAC5,Map3k7,PIK3C2G,PIK3CA,UGT2B28

HGF Signaling	1.93	0	DOCK1,ELF2,GAB1,Map3k7,MET,PIK3C2G,PIK3CA
cAMP-mediated signaling	1.93	-1.667	ADCY3,ADRA2B,AKAP12,AKAP13,CAMK2D,CAMK2G,CREM,LPAR1,PDE5A,PRKACA,RPS6KA1
RAR Activation	1.92	NA	ADCY3,ARID1A,CARM1,GTF2H1,PIK3CA,PML,PRKACA,RDH16,STAT5A,TAF4
Systemic Lupus Erythematosus Signaling	1.89	NA	C6,C8G,CD2BP2,CD72,CREM,HLA-A,HNRNPA2B1,PIK3C2G,PIK3CA,PRPF3,PRPF40B
ErbB2-ErbB3 Signaling	1.89	1	CDKN1B,PIK3C2G,PIK3CA,STAT5A,TYK2
Insulin Receptor Signaling	1.88	-1.414	ACLY,GAB1,PIK3C2G,PIK3CA,PPP1R10,PRKACA,SYNJ1,TSC2
Glioma Signaling	1.86	-1	CAMK2D,CAMK2G,CDK4,MDM2,PIK3C2G,PIK3CA,RBL2
Breast Cancer Regulation by Stathmin1	1.85	NA	ADCY3,CAMK2D,CAMK2G,CDKN1B,GNB1,PIK3C2G,PIK3CA,PPP1R10,PRKACA,UHMK1
Cell Cycle: G1/S Checkpoint Regulation	1.84	-0.447	CDK4,CDKN1B,HDAC5,MDM2,RBL2
α-tocopherol Degradation	1.82	NA	CYP4A11,CYP4F12
Aryl Hydrocarbon Receptor Signaling	1.81	0	ALDH3A2,CDK4,CDKN1B,GSTP1,MDM2,NEDD8,NR0B2,RBL2
Apelin Pancreas Signaling Pathway	1.8	0	PIK3C2G,PIK3CA,PRKAA1,PRKACA
GM-CSF Signaling	1.74	-0.447	CAMK2D,CAMK2G,PIK3C2G,PIK3CA,RACK1
Acetate Conversion to Acetyl-CoA	1.73	NA	ACSL1,ACSS3
p53 Signaling	1.72	0.447	CDK4,COQ8A,MDM2,PIK3C2G,PIK3CA,PML
FAK Signaling	1.72	NA	ASAP1,CAPNS1,DOCK1,PIK3C2G,PIK3CA,TNS1
IL-15 Signaling	1.71	NA	PIK3C2G,PIK3CA,STAT5A,SYK,TYK2
Role of p14/p19ARF in Tumor Suppression	1.62	NA	MDM2,PIK3C2G,PIK3CA
Sirtuin Signaling Pathway	1.61	0.905	ACLY,ATG13,ATP5F1B,ATP5PF,CDH1,MT-ATP6,NDUFA10,NDUFA4,PFKFB3,PFKM,PRKAA1,SIRT4,STK11
Biotin-carboxyl Carrier Protein Assembly	1.58	NA	ACACA,ACACB
PD-1, PD-L1 cancer immunotherapy pathway	1.55	0	CDKN1B,HLA-A,PIK3C2G,PIK3CA,STAT5A,TYK2
CDP-diacylglycerol Biosynthesis I	1.55	NA	AGPAT3,CDS2,PNPLA3
Oxidative Ethanol Degradation III	1.55	NA	ACSL1,ACSS3,ALDH3A2
PI3K/AKT Signaling	1.54	0.816	CDKN1B,GAB1,MDM2,PIK3CA,SYNJ1,TSC2,TYK2
JAK/Stat Signaling	1.54	0.447	PIK3C2G,PIK3CA,SOCS2,STAT5A,TYK2
Antiproliferative Role of Somatostatin Receptor 2	1.52	-1	CDKN1B,GNB1,GUCY2C,PIK3C2G,PIK3CA
Apelin Adipocyte Signaling Pathway	1.52	1.342	ADCY3,GPX1,GSTP1,PRKAA1,PRKACA
Pancreatic Adenocarcinoma Signaling	1.48	-0.447	CDK4,CDKN1B,MDM2,PIK3C2G,PIK3CA,TYK2

eNOS Signaling	1.48	-0.816	ADCY3,AQP8,CHRNA4,LPAR1,PIK3C2G,PIK3CA,PRKAA1,PRKACA
Nitric Oxide Signaling in the Cardiovascular System	1.47	1.633	GUCY2C,PDE5A,PIK3C2G,PIK3CA,PRKAA1,PRKACA
Ethanol Degradation IV	1.44	NA	ACSL1,ACSS3,ALDH3A2
HIPPO signaling	1.42	1	AMOT,ITCH,PARD3,PPP1R10,WWTR1
Endocannabinoid Developing Neuron Pathway	1.4	-0.447	ADCY3,CDKN1B,GNB1,PIK3C2G,PIK3CA,PRKACA
IL-4 Signaling	1.4	NA	HLA-A,PIK3C2G,PIK3CA,SYNJ1,TYK2
Cardiac β-adrenergic Signaling	1.39	-1	ADCY3,AKAP12,AKAP13,GNB1,PDE5A,PPP1R10,PRKACA
Acute Phase Response Signaling	1.37	NA	C4A/C4B,ITIH3,ITIH4,PIK3CA,SAA1,SERPINA1,SOCS2,TF
Oxidative Phosphorylation	1.36	1.633	ATP5F1B,ATP5PF,MT-ATP6,NDUFA10,NDUFA4,SURF1
Endocannabinoid Cancer Inhibition Pathway	1.36	1.134	ADCY3,CDH1,CDKN1B,PIK3C2G,PIK3CA,PRKAA1,PRKACA
mTOR Signaling	1.35	-1.89	ATG13,EIF4G1,EIF4G3,PIK3C2G,PIK3CA,PRKAA1,RPS6KA1,STK11,TSC2
Phosphatidylglycerol Biosynthesis II (Non-plastidic)	1.35	NA	AGPAT3,CDS2,PNPLA3
Acetone Degradation I (to Methylglyoxal)	1.35	NA	CYP2A6 (includes others),CYP2C8,CYP4A11
IL-2 Signaling	1.33	0	PIK3C2G,PIK3CA,STAT5A,SYK
Acute Myeloid Leukemia Signaling	1.32	-0.447	CEBPA,PIK3C2G,PIK3CA,PML,STAT5A
Apelin Endothelial Signaling Pathway	1.3	0.816	ADCY3,HDAC5,MEF2C,PIK3C2G,PIK3CA,PRKAA1
Role of NFAT in Cardiac Hypertrophy	1.3	-0.707	ADCY3,CAMK2D,CAMK2G,GNB1,HDAC5,MEF2C,PIK3C2G,PIK3CA,PRKACA

Table 18. Significant Pathways for differentially expressed transcripts in ^{16}O vs. non-irradiated control at 9 months.

Ingenuity Canonical Pathways	**-log$_{10}$(p-value)**	**z-score**	**Molecules**
Acute Phase Response Signaling	16.5	2.2	A2M,AKT3,APOA2,CP,FGA,FN1,HMOX1,HP,HPX,IKBKG,IL18,IL1R1,IL1RN,IL33,ITIH3,ITIH4,JAK2,JUN,LBP,MAP2K6,MAPK9,NFKB1,OSMR,PIK3CD,SAA1,Saa3,SERPINA3,SERPINE1,SOCS1,SOCS3,TCF3,TF
IL-6 Signaling	8.05	1.5	A2M,AKT3,CD14,IKBKG,IL18,IL1R1,IL1RN,IL33,JAK2,JUN,LBP,MAP2K6,MAPK9,NFKB1,PIK3C3,PIK3CD,SOCS1,SOCS3
LXR/RXR Activation	7.1	-0.5	APOA2,CD14,FGA,HPX,IL18,IL1R1,IL1RN,IL33,ITIH4,LBP,NCOR1,NFKB1,NR1H2,NR1H4,RXRA,SAA1,TF

IL-10 Signaling	7.09	NA	CD14,FCGR2A,HMOX1,IKBKG,IL18,IL1R1,IL1RN,IL33,JUN,LBP,MAP2K6,NFKB1,SOCS3
FXR/RXR Activation	5.95	NA	ABCB11,AKT3,APOA2,FETUB,FGA,HPX,IL18,IL1RN,IL33,ITIH4,LIPC,MAPK9,NR1H4,RXRA,SAA1,TF
Toll-like Receptor Signaling	5.94	0.632	CD14,IKBKG,IL18,IL1RN,IL33,IRAK2,JUN,LBP,MAP2K6,NFKB1,TLR2,TNFAIP3
Role of Macrophages, Fibroblasts and Endothelial Cells in Rheumatoid Arthritis	5.09	NA	AKT3,ATF2,AXIN1,CEBPD,FN1,IKBKG,IL17RA,IL18,IL1R1,IL1RN,IL33,IRAK2,JAK2,JUN,MAP2K6,MAPK9,NFAT5,NFKB1,PIK3C3,PIK3CD,SOCS1,SOCS3,TCF3,TLR2
JAK/Stat Signaling	4.96	0.302	AKT3,BCL2L1,CDKN1A,JAK2,JUN,NFKB1,PIK3C3,PIK3CD,PTPN1,SOCS1,SOCS3
Adipogenesis pathway	4.69	NA	CEBPD,ERCC3,EZH2,FGFR2,FGFR3,HDAC3,HDAC6,HDAC7,KDM1A,KMT2B,PPIP5K1,SAP130,SETDB1,SOX9
Hepatic Cholestasis	4.45	NA	ABCB11,ADCY1,ADCY4,CD14,IKBKG,IL18,IL1R1,IL1RN,IL33,IRAK2,JUN,LBP,MAPK9,NFKB1,NR1H4,PPRC1,RXRA
IL-17 Signaling	4.2	NA	AKT3,ATF2,IL17RA,JAK2,JUN,MAP2K6,MAPK9,NFKB1,PIK3C3,PIK3CD
Iron homeostasis signaling pathway	4.12	NA	ARNT,ATP6AP1,ATP6V0A4,CP,FBXL5,HMOX1,HP,HPX,JAK2,SLC11A2,SLC39A14,TCIRG1,TF,TFR2
LPS-stimulated MAPK Signaling	4.1	1.667	ATF2,CD14,IKBKG,JUN,LBP,MAP2K6,MAPK9,NFKB1,PIK3C3,PIK3CD
Chronic Myeloid Leukemia Signaling	3.92	NA	AKT3,BCL2L1,CDKN1A,CDKN1B,HDAC3,HDAC6,HDAC7,IKBKG,NFKB1,PIK3C3,PIK3CD
Osteoarthritis Pathway	3.91	0.5	ACVRL1,ATF2,DDIT4,DDR2,FGFR3,FN1,H19,HDAC3,IL1R1,MTF1,MYBBP1A,NFKB1,PRKAA1,SLC39A8,SOX9,TCF3,TLR2
NF-κB Signaling	3.9	0.775	AKT3,FGFR2,FGFR3,IKBKG,IL18,IL1R1,IL1RN,IL33,MAP2K6,NFKB1,PIK3C3,PIK3CD,TBK1,TLR2,TNFAIP3
TNFR2 Signaling	3.86	1.342	IKBKG,JUN,NFKB1,TBK1,TNFAIP3,XIAP
RANK Signaling in Osteoclasts	3.8	1.897	AKT3,IKBKG,JUN,MAP2K6,MAP3K13,MAPK9,NFKB1,PIK3C3,PIK3CD,XIAP
Dendritic Cell Maturation	3.77	2.324	AKT3,ATF2,DDR2,FCGR2A,HLA-

			A,IKBKG,IL18,IL1RN,IL33,JAK2,MAPK9,NFKB1,PIK3C3,PIK3CD,TLR2
TR/RXR Activation	3.72	NA	AKT3,COL6A3,FGA,HDAC3,HP,NCOR1,PIK3C3,PIK3CD,RXRA,SYT12
Glucocorticoid Receptor Signaling	3.69	NA	A2M,AKT3,BAG1,BCL2L1,CDKN1A,ERCC3,FKBP5,IKBKG,IL1RN,JAK2,JUN,MAPK9,NCOR1,NFAT5,NFKB1,PIK3C3,PIK3CD,PRKAA1,SERPINE1,SMARCA2,SMARCA4,TAF1
B Cell Receptor Signaling	3.62	1.941	AKT3,ATF2,BCL2L1,FCGR2A,IKBKG,JUN,MAP2K6,MAP3K13,MAPK9,NFAT5,NFKB1,PIK3C3,PIK3CD,SYNJ1,TCF3
IL-1 Signaling	3.6	1.134	ADCY1,ADCY4,GNB1,IKBKG,IL1R1,IRAK2,JUN,MAP2K6,MAPK9,NFKB1
Activation of IRF by Cytosolic Pattern Recognition Receptors	3.51	0.707	ATF2,DDX58,IKBKG,JUN,MAPK9,MAVS,NFKB1,TBK1
iNOS Signaling	3.51	0.816	CD14,IKBKG,IRAK2,JAK2,JUN,LBP,NFKB1
IL-17A Signaling in Fibroblasts	3.47	NA	CEBPD,IKBKG,IL17RA,JUN,LCN2,NFKB1
CD40 Signaling	3.42	0.707	IKBKG,JUN,MAP2K6,MAPK9,NFKB1,PIK3C3,PIK3CD,TNFAIP3
IL-17A Signaling in Airway Cells	3.37	1.414	AKT3,IKBKG,IL17RA,JAK2,MAPK9,NFKB1,PIK3C3,PIK3CD
RAR Activation	3.35	NA	ADCY1,ADCY4,AKT3,CSF2RB,ERCC3,JAK2,JUN,MAPK9,NCOR1,NFKB1,PIK3CD,RXRA,SMARCA2,SMARCA4,ZBTB16
IL-15 Production	3.31	NA	AATK,CLK4,DDR2,EPHB4,FGFR2,FGFR3,JAK2,MAP2K6,NFKB1,ROR1,TEC
HOTAIR Regulatory Pathway	3.3	-0.832	AKT3,CDKN1A,DNMT3B,EZH2,HSF1,KDM1A,KMT2A,NFKB1,PIK3C3,PIK3CD,SETDB1,TCF3,XIAP
Role of JAK family kinases in IL-6-type Cytokine Signaling	3.3	NA	JAK2,MAPK9,OSMR,SOCS1,SOCS3
Role of Osteoblasts, Osteoclasts and Chondrocytes in Rheumatoid Arthritis	3.29	NA	AKT3,AXIN1,IKBKG,IL18,IL1R1,IL1RN,IL33,JUN,MAP2K6,MAPK9,NFAT5,NFKB1,PIK3C3,PIK3CD,TCF3,XIAP
SAPK/JNK Signaling	3.28	1.667	ATF2,DUSP8,GNB1,JUN,MAP3K13,MAPK8IP3,MAPK9,MINK1,PIK3C3,PIK3CD
Hereditary Breast Cancer Signaling	3.27	NA	AKT3,CDKN1A,GADD45G,HDAC3,HDAC6,HDAC7,MSH2,PIK3C3,PIK3CD,RAD50,SMARCA2,SMARCA4

CD27 Signaling in Lymphocytes	3.24	1.633	BCL2L1,IKBKG,JUN,MAP2K6,MAP3K13,MAPK9,NFKB1
LPS/IL-1 Mediated Inhibition of RXR Function	3.22	1.155	ABCB11,ABCC4,CD14,IL18,IL1R1,IL1RN,IL33,JUN,LBP,LIPC,MAPK9,NR1H2,NR1H4,PPARGC1B,RXRA,SLC27A1
Cardiac Hypertrophy Signaling (Enhanced)	3.2	1.961	ADCY1,ADCY4,AKT3,ATF2,CSF2RB,DIAPH1,FGFR2,FGFR3,GNB1,HDAC3,HDAC6,HDAC7,IKBKG,IL17RA,IL18,IL1R1,IL33,JAK2,JUN,MAP2K6,MAP3K13,MAPK9,NFAT5,NFKB1,PIK3C3,PIK3CD,RCAN1
PTEN Signaling	3.1	0.302	AKT3,BCL2L1,CDKN1A,CDKN1B,FGFR2,FGFR3,IKBKG,MAST2,NFKB1,PIK3CD,SYNJ1
Role of IL-17A in Arthritis	3.1	NA	ATF2,IL17RA,MAP2K6,MAPK9,NFKB1,PIK3C3,PIK3CD
Small Cell Lung Cancer Signaling	3.04	1.89	AKT3,BCL2L1,CDKN1B,IKBKG,NFKB1,PIK3C3,PIK3CD,RXRA
Pancreatic Adenocarcinoma Signaling	3.03	2.333	AKT3,BCL2L1,CDKN1A,CDKN1B,HMOX1,JAK2,MAPK9,NFKB1,PIK3C3,PIK3CD
PPARα/RXRα Activation	3.01	0.277	ADCY1,ADCY4,APOA2,CKAP5,IKBKG,IL1R1,JAK2,JUN,MAP2K6,NCOR1,NFKB1,PRKAA1,RXRA,SLC27A1
IL-23 Signaling Pathway	2.92	0.816	AKT3,JAK2,NFKB1,PIK3C3,PIK3CD,SOCS3
IL-12 Signaling and Production in Macrophages	2.89	NA	AKT3,APOA2,IKBKG,IL18,JUN,MAPK9,NFKB1,PIK3C3,PIK3CD,RXRA,TLR2
Endocannabinoid Developing Neuron Pathway	2.88	0.632	ADCY1,ADCY4,AKT3,ATF2,CDKN1B,GNB1,MAP2K6,MAPK9,PIK3C3,PIK3CD
Erythropoietin Signaling	2.85	NA	AKT3,JAK2,JUN,NFKB1,PIK3C3,PIK3CD,SOCS1,SOCS3
Adrenomedullin signaling pathway	2.8	2.138	ADCY1,ADCY4,AKT3,ARNT,IL18,IL1RN,IL33,MAP2K6,MAPK9,NFKB1,NPR2,PIK3C3,PIK3CD,RXRA
Molecular Mechanisms of Cancer	2.79	NA	ADCY1,ADCY4,AKT3,ARHGEF1,ARHGEF2,AXIN1,BCL2L1,CDK10,CDK9,CDKN1A,CDKN1B,CTNND1,FNBP1,JAK2,JUN,MAP2K6,MAPK9,NFKB1,PIK3C3,PIK3CD,TCF3,XIAP
4-1BB Signaling in T Lymphocytes	2.79	2.236	ATF2,IKBKG,JUN,MAPK9,NFKB1
HMGB1 Signaling	2.7	0.632	AKT3,FNBP1,IL18,IL1R1,IL33,JUN,MAP2K6,MAPK9,NFKB1,PIK3C3,PIK3CD,SERPINE1

Th1 Pathway	2.69	0	HLA-A,IL18,JAK2,MAP2K6,NFIL3,NFKB1,PIK3C3,PIK3CD,SOCS1,SOCS3
Apelin Endothelial Signaling Pathway	2.69	1.897	ADCY1,ADCY4,AKT3,ARNT,JUN,MAPK9,NFKB1,PIK3C3,PIK3CD,PRKAA1
Colorectal Cancer Metastasis Signaling	2.68	2.324	ADCY1,ADCY4,AKT3,AXIN1,BCL2L1,FNBP1,GNB1,JAK2,JUN,MAPK9,MSH2,NFKB1,PIK3C3,PIK3CD,TCF3,TLR2
Role of JAK2 in Hormone-like Cytokine Signaling	2.67	NA	JAK2,PTPN1,SH2B1,SOCS1,SOCS3
PPAR Signaling	2.66	-1	IKBKG,IL18,IL1R1,IL1RN,IL33,JUN,NCOR1,NFKB1,RXRA
IGF-1 Signaling	2.6	0.378	AKT3,IGFBP1,JAK2,JUN,PIK3C3,PIK3CD,SOCS1,SOCS3,YWHAZ
IL-4 Signaling	2.58	NA	AKT3,HLA-A,JAK2,NFAT5,PIK3C3,PIK3CD,SOCS1,SYNJ1
Aryl Hydrocarbon Receptor Signaling	2.57	0.302	ARNT,CDKN1A,CDKN1B,JUN,NFIA,NFIC,NFIX,NFKB1,RXRA,SMARCA4,TGM2
Sertoli Cell-Sertoli Cell Junction Signaling	2.57	NA	A2M,AKT3,ATF2,AXIN1,CLDN12,CLDN14,EPB41,EPN2,JUN,MAP3K13,MAPK9,MYO7A,SPTAN1
Neuroinflammation Signaling Pathway	2.56	2.357	AKT3,ATF2,HLA-A,HMOX1,IKBKG,IL18,IL1R1,IRAK2,JAK2,JUN,MAPK9,NFAT5,NFKB1,PIK3C3,PIK3CD,TBK1,TLR2,XIAP
Endocannabinoid Cancer Inhibition Pathway	2.55	-1.508	ADCY1,ADCY4,AKT3,ATF2,CDKN1A,CDKN1B,MAP2K6,PIK3C3,PIK3CD,PRKAA1,TCF3
Th1 and Th2 Activation Pathway	2.53	NA	HLA-A,IL18,IL33,JAK2,JUN,MAP2K6,NFIL3,NFKB1,PIK3C3,PIK3CD,SOCS1,SOCS3
Huntington's Disease Signaling	2.53	1.414	AKT3,ATF2,BCL2L1,CAPNS1,DNM2,GNB1,HDAC3,HDAC6,HDAC7,JUN,MAPK9,NCOR1,PIK3C3,PIK3CD,TGM2
Type I Diabetes Mellitus Signaling	2.44	0	HLA-A,IKBKG,IL1R1,JAK2,MAP2K6,MAPK9,NFKB1,SOCS1,SOCS3
Lymphotoxin β Receptor Signaling	2.42	2.236	AKT3,BCL2L1,IKBKG,NFKB1,PIK3C3,PIK3CD
Choline Biosynthesis III	2.42	0	CHPT1,HMOX1,PCYT1A,PHKA1
April Mediated Signaling	2.4	1.342	IKBKG,JUN,MAPK9,NFAT5,NFKB1
STAT3 Pathway	2.37	-1.134	CDKN1A,CSF2RB,FGFR2,FGFR3,IL17RA,IL1R1,JAK2,MAPK9,SOCS1,SOCS3

IL-17A Signaling in Gastric Cells	2.35	NA	IL17RA,JUN,MAPK9,NFKB1
P2Y Purigenic Receptor Signaling Pathway	2.35	3.162	ADCY1,ADCY4,AKT3,ATF2,GNB1,JUN,NFKB1,P2RY2,PIK3C3,PIK3CD
PI3K/AKT Signaling	2.35	1.265	AKT3,BCL2L1,CDKN1A,CDKN1B,IKBKG,JAK2,NFKB1,PIK3CD,SYNJ1,YWHAZ
B Cell Activating Factor Signaling	2.3	1.342	IKBKG,JUN,MAPK9,NFAT5,NFKB1
p53 Signaling	2.27	-1.134	AKT3,BCL2L1,CDKN1A,COQ8A,GADD45G,JUN,PIK3C3,PIK3CD
Leptin Signaling in Obesity	2.26	0.447	ADCY1,ADCY4,AKT3,JAK2,PIK3C3,PIK3CD,SOCS3
Role of NFAT in Regulation of the Immune Response	2.26	2.111	AKT3,ATF2,FCGR2A,GNB1,HLA-A,IKBKG,JUN,NFAT5,NFKB1,PIK3C3,PIK3CD,RCAN1
VDR/RXR Activation	2.23	1.342	CD14,CDKN1A,CDKN1B,IGFBP1,NCOR1,RXRA,THBD
Induction of Apoptosis by HIV1	2.2	0	BCL2L1,IKBKG,MAPK9,NFKB1,SLC25A3,XIAP
Phospholipase C Signaling	2.19	0.577	ADCY1,ADCY4,ARHGEF1,ARHGEF2,ATF2,FCGR2A,FNBP1,GNB1,HDAC3,HDAC6,HDAC7,HMOX1,NFAT5,NFKB1,TGM2
Tight Junction Signaling	2.18	NA	AKT3,ARHGEF2,CLDN12,CLDN14,CPSF1,EPB41,HSF1,JUN,NFKB1,PATJ,SPTAN1
Role of RIG1-like Receptors in Antiviral Innate Immunity	2.17	0.447	DDX58,IKBKG,MAVS,NFKB1,TBK1
PEDF Signaling	2.15	1.134	AKT3,BCL2L1,IKBKG,NFKB1,PIK3C3,PIK3CD,TCF12
Production of Nitric Oxide and Reactive Oxygen Species in Macrophages	2.14	1.732	AKT3,APOA2,FNBP1,IKBKG,JAK2,JUN,MAP3K13,MAPK9,NFKB1,PIK3C3,PIK3CD,TLR2
CD28 Signaling in T Helper Cells	2.13	2.121	AKT3,HLA-A,IKBKG,JUN,MAPK9,NFAT5,NFKB1,PIK3C3,PIK3CD
MIF Regulation of Innate Immunity	2.13	2.236	CD14,CD74,JUN,MAPK9,NFKB1
Apelin Pancreas Signaling Pathway	2.13	0.447	MAPK9,NFKB1,PIK3C3,PIK3CD,PRKAA1
Role of p14/p19ARF in Tumor Suppression	2.12	-2	PIK3C3,PIK3CD,POLR3D,UBTF
Renin-Angiotensin Signaling	2.09	1.89	ADCY1,ADCY4,ATF2,JAK2,JUN,MAPK9,NFKB1,PIK3C3,PIK3CD
Germ Cell-Sertoli Cell Junction Signaling	2.05	NA	A2M,AXIN1,CTNND1,EPN2,FNBP1,MAP2K6,MAP3K13,MAPK9,MYO7A,PIK3C3,PIK3CD
Cell Cycle: G1/S Checkpoint Regulation	2	0.447	CDKN1A,CDKN1B,FBXL5,HDAC3,HDAC6,HDAC7
Gα12/13 Signaling	2	2.333	AKT3,ARHGEF1,IKBKG,JUN,MAPK9,NFKB1,PIK3C3,PIK3CD,TEC

Sumoylation Pathway	2	0	DNMT3A,FNBP1,JUN,KDM1A,MAPK9,NFKB1,SP3,XIAP
IL-8 Signaling	1.99	2.111	AKT3,BCL2L1,FNBP1,GNB1,HMOX1,IKBKG,IRAK2,JUN,MAPK9,NFKB1,PIK3C3,PIK3CD
Phosphatidylcholine Biosynthesis I	1.98	NA	CHPT1,PCYT1A,PHKA1
FGF Signaling	1.98	0.378	AKT3,ATF2,FGFR2,FGFR3,MAP2K6,PIK3C3,PIK3CD
SPINK1 General Cancer Pathway	1.94	0	AKT3,JAK2,Mt1,Mt2,PIK3C3,PIK3CD
TNFR1 Signaling	1.94	2	IKBKG,JUN,NFKB1,TNFAIP3,XIAP
IL-9 Signaling	1.92	1	NFKB1,PIK3C3,PIK3CD,SOCS3
HGF Signaling	1.89	2.121	AKT3,ATF2,CDKN1A,JUN,MAP3K13,MAPK9,PIK3C3,PIK3CD
Acute Myeloid Leukemia Signaling	1.89	1.134	AKT3,CSF2RB,MAP2K6,NFKB1,PIK3C3,PIK3CD,TCF3
GM-CSF Signaling	1.89	1.633	AKT3,BCL2L1,CSF2RB,JAK2,PIK3C3,PIK3CD
DNA Methylation and Transcriptional Repression Signaling	1.87	NA	DNMT3A,DNMT3B,MTA1,SAP130
IL-15 Signaling	1.86	NA	AKT3,BCL2L1,JAK2,NFKB1,PIK3C3,PIK3CD
Type II Diabetes Mellitus Signaling	1.84	1.89	AKT3,IKBKG,MAPK9,NFKB1,PIK3C3,PIK3CD,PRKAA1,SLC27A1,SOCS1,SOCS3
Coagulation System	1.83	0	A2M,FGA,SERPINE1,THBD
Prostate Cancer Signaling	1.81	NA	AKT3,ATF2,CDKN1A,CDKN1B,NFKB1,PIK3C3,PIK3CD
Hepatic Fibrosis / Hepatic Stellate Cell Activation	1.8	NA	A2M,CD14,COL4A1,COL4A5,COL6A3,FGFR2,FN1,IL1R1,LBP,NFKB1,SERPINE1
p38 MAPK Signaling	1.8	0.707	ATF2,IL18,IL1R1,IL1RN,IL33,IRAK2,MAP2K6,TIFA
Growth Hormone Signaling	1.78	0	A2M,JAK2,PIK3C3,PIK3CD,SOCS1,SOCS3
NGF Signaling	1.76	2.828	AKT3,ATF2,IKBKG,MAP3K13,MAPK9,NFKB1,PIK3C3,PIK3CD
ILK Signaling	1.76	2.111	AKT3,ATF2,FLNA,FN1,FNBP1,JUN,MAP2K6,MAPK9,NFKB1,PIK3C3,PIK3CD
TREM1 Signaling	1.75	0.816	AKT3,IL18,JAK2,NFKB1,NLRP12,TLR2
Role of NFAT in Cardiac Hypertrophy	1.72	1.667	ADCY1,ADCY4,AKT3,GNB1,HDAC3,HDAC6,HDAC7,MAP2K6,MAPK9,PIK3C3,PIK3CD,RCAN1
Reelin Signaling in Neurons	1.7	NA	ARHGEF1,ARHGEF2,MAPK8IP3,MAPK9,PIK3C3,PIK3CD
Estrogen-Dependent Breast Cancer Signaling	1.7	2.449	AKT3,ATF2,JUN,NFKB1,PIK3C3,PIK3CD
Cholecystokinin/Gastrin-mediated Signaling	1.68	0.707	ATF2,FNBP1,IL18,IL1RN,IL33,JUN,MAP2K6,MAPK9

GP6 Signaling Pathway	1.68	2.121	ADAM10,AKT3,COL4A1,COL4A5,COL6A3,FGA,PIK3C3,PIK3CD
IL-3 Signaling	1.68	1.633	AKT3,CSF2RB,JAK2,JUN,PIK3C3,PIK3CD
Inhibition of Angiogenesis by TSP1	1.67	1	AKT3,CD47,JUN,MAPK9
Role of BRCA1 in DNA Damage Response	1.65	NA	BABAM2,CDKN1A,MSH2,RAD50,SMARCA2,SMARCA4
IL-7 Signaling Pathway	1.65	0	AKT3,CDKN1B,JUN,PIK3C3,PIK3CD,SOCS1
MSP-RON Signaling Pathway	1.65	NA	CSF2RB,JAK2,PIK3C3,PIK3CD,TLR2
Systemic Lupus Erythematosus In B Cell Signaling Pathway	1.65	0	AKT3,BCL2L1,FCGR2A,IL18,IL33,JAK2,JUN,MAVS,NFAT5,NFKB1,PIK3C3,PIK3CD,SYNJ1,TBK1
Mouse Embryonic Stem Cell Pluripotency	1.64	1.134	AKT3,AXIN1,JAK2,PIK3C3,PIK3CD,TCF3,XIAP
Antiproliferative Role of Somatostatin Receptor 2	1.63	0.447	CDKN1A,CDKN1B,GNB1,NPR2,PIK3C3,PIK3CD
Cyclins and Cell Cycle Regulation	1.63	NA	CDKN1A,CDKN1B,FBXL5,HDAC3,HDAC6,HDAC7
Apelin Cardiac Fibroblast Signaling Pathway	1.62	NA	AKT3,PRKAA1,SERPINE1
Role of PKR in Interferon Induction and Antiviral Response	1.6	NA	ATF2,IKBKG,MAP2K6,NFKB1
Role of Pattern Recognition Receptors in Recognition of Bacteria and Viruses	1.59	1.89	DDX58,IL18,IL33,MAPK9,MAVS,NFKB1,PIK3C3,PIK3CD,TLR2
Amyotrophic Lateral Sclerosis Signaling	1.58	0.816	AKT3,BCL2L1,CAPNS1,GRIK5,PIK3C3,PIK3CD,XIAP
IL-22 Signaling	1.57	NA	AKT3,MAPK9,SOCS3
Role of JAK1, JAK2 and TYK2 in Interferon Signaling	1.57	NA	JAK2,NFKB1,SOCS1
Prolactin Signaling	1.56	0	JAK2,JUN,PIK3C3,PIK3CD,SOCS1,SOCS3
HER-2 Signaling in Breast Cancer	1.56	NA	AKT3,CDKN1A,CDKN1B,PARD3,PIK3C3,PIK3CD
Telomerase Signaling	1.56	NA	AKT3,CDKN1A,HDAC3,HDAC6,HDAC7,PIK3C3,PIK3CD
PD-1, PD-L1 cancer immunotherapy pathway	1.56	-1.134	AKT3,BCL2L1,CDKN1B,HLA-A,JAK2,PIK3C3,PIK3CD
IL-2 Signaling	1.54	1	AKT3,JUN,PIK3C3,PIK3CD,SOCS1
Relaxin Signaling	1.51	2.333	ADCY1,ADCY4,AKT3,GNB1,JUN,NFKB1,NPR2,PIK3C3,PIK3CD
T Cell Receptor Signaling	1.5	NA	IKBKG,JUN,NFAT5,NFKB1,PIK3C3,PIK3CD,TEC
Docosahexaenoic Acid (DHA) Signaling	1.5	NA	AKT3,BCL2L1,PIK3C3,PIK3CD
Myc Mediated Apoptosis Signaling	1.49	NA	AKT3,MAPK9,PIK3C3,PIK3CD,YWHAZ
Wnt/Ca+ pathway	1.49	1.342	ATF2,AXIN1,NFAT5,NFKB1,ROR1
Th2 Pathway	1.46	1.342	HLA-A,IL33,JAK2,JUN,NFKB1,PIK3C3,PIK3CD,SOCS3

mTOR Signaling	1.45	0.378	AKT3,ATG13,DDIT4,EIF4G1,FNBP1,HMOX1,PIK3C3,PIK3CD,PRKAA1,RPS14,RPS19
NRF2-mediated Oxidative Stress Response	1.44	1.633	ABCC4,DNAJB2,FKBP5,HMOX1,JUN,JUNB,MAP2K6,MAPK9,PIK3C3,PIK3CD
Altered T Cell and B Cell Signaling in Rheumatoid Arthritis	1.43	NA	HLA-A,IL18,IL1RN,IL33,NFKB1,TLR2
Rac Signaling	1.43	1.633	ABI2,JUN,NFKB1,PARD3,PIK3C3,PIK3CD,PIP5K1C
HIF1α Signaling	1.41	NA	AKT3,ARNT,JUN,LDHA,MAPK9,PIK3C3,PIK3CD
Death Receptor Signaling	1.41	0.816	IKBKG,NFKB1,SPTAN1,TBK1,TIPARP,XIAP
Regulation of the Epithelial-Mesenchymal Transition Pathway	1.4	NA	AKT3,AXIN1,FGFR2,FGFR3,JAK2,MAP2K6,NFKB1,PIK3C3,PIK3CD,TCF3
iCOS-iCOSL Signaling in T Helper Cells	1.4	1.89	AKT3,HLA-A,IKBKG,NFAT5,NFKB1,PIK3C3,PIK3CD
Role of JAK1 and JAK3 in γc Cytokine Signaling	1.39	NA	JAK2,PIK3C3,PIK3CD,SOCS1,SOCS3
Tec Kinase Signaling	1.39	0.707	FNBP1,GNB1,GTF2I,JAK2,MAPK9,NFKB1,PIK3C3,PIK3CD,TEC
Th17 Activation Pathway	1.38	0	IL1R1,IRAK2,JAK2,NFAT5,NFKB1,SOCS3
PI3K Signaling in B Lymphocytes	1.37	2.121	AKT3,ATF2,ATF5,IKBKG,JUN,NFAT5,NFKB1,PIK3CD
White Adipose Tissue Browning Pathway	1.37	1.414	ADCY1,ADCY4,ATF2,FGFR2,FGFR3,LDHA,PRKAA1,RXRA
Actin Cytoskeleton Signaling	1.36	0.707	ABI2,ARHGEF1,CD14,DIAPH1,FLNA,FN1,GIT1,LBP,PIK3C3,PIK3CD,PIP5K1C
Graft-versus-Host Disease Signaling	1.35	NA	HLA-A,IL18,IL1RN,IL33
Cell Cycle: G2/M DNA Damage Checkpoint Regulation	1.35	1	CDKN1A,FBXL5,TRIP12,YWHAZ
Assembly of RNA Polymerase III Complex	1.32	NA	GTF3C1,POLR3D
TGF-β Signaling	1.32	1.633	INHBB,JUN,MAP2K6,MAPK9,SERPINE1,SKI
ATM Signaling	1.3	2	ATF2,CDKN1A,GADD45G,JUN,MAPK9,RAD50

Table 19. Significant Pathways for differentially expressed transcripts in ^{16}O vs. non-irradiated control at 12 months.

6.4.4 IDENTIFICATION OF DYSREGULATED MOLECULAR PATHWAYS CORRESPONDING TO UNANNOTATED TRANSCRIPTS ASSOCIATED WITH ^{16}O IRRADIATION, USING SOM

The above IPA analyses (Figure 12) resulted in a collection of 95 statistically significant high-quality functionally unannotated transcripts across all time points from ^{16}O irradiated mice (Table 13). To characterize the unannotated transcripts, we obtained the $\log_2$(fold change) expression values of differentially expressed transcripts from ^{16}O irradiation compared to non-irradiated control across 5 time points and applied the SOM machine learning algorithm. We next identified the modules from SOMs which contained the majority of unannotated transcripts and combined them to form larger clusters of similar transcription patterns for functionality analysis using IPA. We compared the identified 13 clusters across 5 time points using IPA (Figure 13f). Figure 4f shows the most significant pathways across all clusters. The activation z-scores were predicted for some of the clusters based on our observed data and the available literature. The clusters of unannotated transcripts tended to show inhibitory responses with negative z-scores at 1 and 2 months, and activation at later time points. Even though the directionality could not be determined for some of these pathways, some of the identified significant pathways are similar to those previously observed in Figure 3, and are involved in immune response (B cell receptor signaling and acute phase response signaling), cholesterol biosynthesis, and the hepatic fibrosis signaling pathway. A complete list of unannotated transcript ENSMBL IDs with their corresponding module numbers is provided in Table 20.

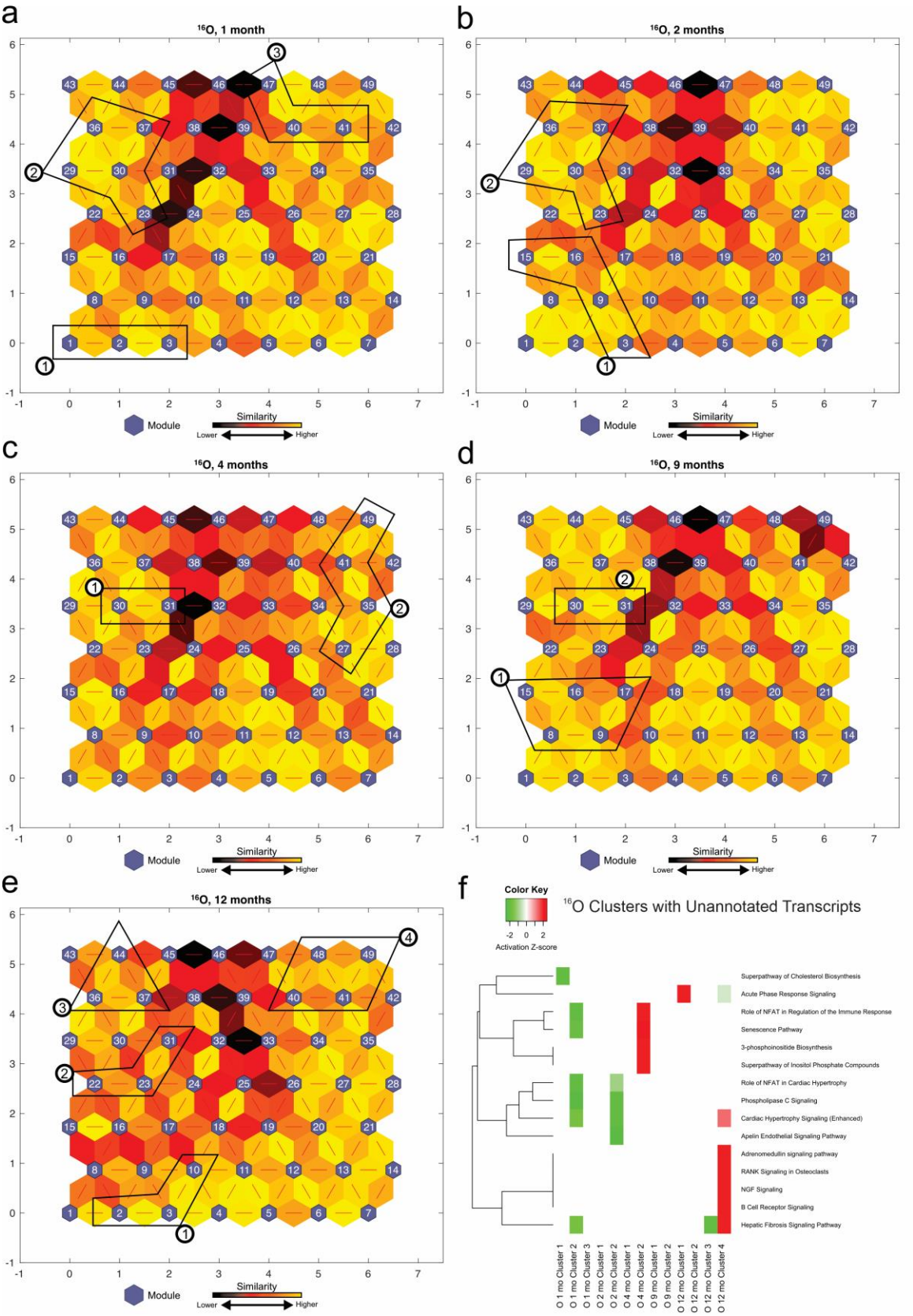
a
16O, 1 month
b
16O, 2 months
c
16O, 4 months
d
16O, 9 months
e
16O, 12 months
Module
Similarity
Lower
Higher
f
Color Key
-2 0 2
Activation Z-score
16O Clusters with Unannotated Transcripts
Superpathway of Cholesterol Biosynthesis
Acute Phase Response Signaling
Role of NFAT in Regulation of the Immune Response
Senescence Pathway
3-phosphoinositide Biosynthesis
Superpathway of Inositol Phosphate Compounds
Role of NFAT in Cardiac Hypertrophy
Phospholipase C Signaling
Cardiac Hypertrophy Signaling (Enhanced)
Apelin Endothelial Signaling Pathway
Adrenomedullin signaling pathway
RANK Signaling in Osteoclasts
NGF Signaling
B Cell Receptor Signaling
Hepatic Fibrosis Signaling Pathway
O 1 mo Cluster 1
O 1 mo Cluster 2
O 1 mo Cluster 3
O 2 mo Cluster 1
O 2 mo Cluster 2
O 4 mo Cluster 1
O 4 mo Cluster 2
O 9 mo Cluster 1
O 9 mo Cluster 2
O 12 mo Cluster 1
O 12 mo Cluster 2
O 12 mo Cluster 3
O 12 mo Cluster 4

Figure 13. ^{16}O analysis of self-organizing maps for each time point.

(a,b,c,d,e) Kohonen Self-Organizing Map (SOM) was applied to the differentially expressed (DE) transcripts obtained from the RNA-Seq data to identify coherent patterns of transcript expression at each time point, as well as patterns within the unannotated transcripts. The SOM clusters transcripts in each module according to $\log_2$(fold change) of the expression values. SOM clustering analysis demonstrates the distances between correlated transcript groups. The small blue hexagons are modules comprising transcripts with similar $\log_2$(fold change) expression patterns. The numbers of transcripts in each module are provided in Figure 14. Neighboring modules are connected with a red line. The colors of the lines connecting the modules indicate the similarity between modules: Lighter colors represent higher similarity, and darker colors represent lower similarity. **(f)** Expression patterns of unannotated transcripts were identified, and the corresponding modules (represented in circled numbers) were further analyzed by IPA. Only the most significant pathways across all clusters are shown with available color-coded activation z-scores. Inhibitory, activation, or unknown directionality z-scores corresponds to green, red, and white respectively. The entries with white color indicate the directionality could not be predicted based on the available data, yet the pathway is significantly identified by pathway analysis. The goal of the IPA downstream effects analysis is to identify functional pathways whose activity is expected to be increased or decreased, given the observed expression changes in a user's dataset (see Methods.)

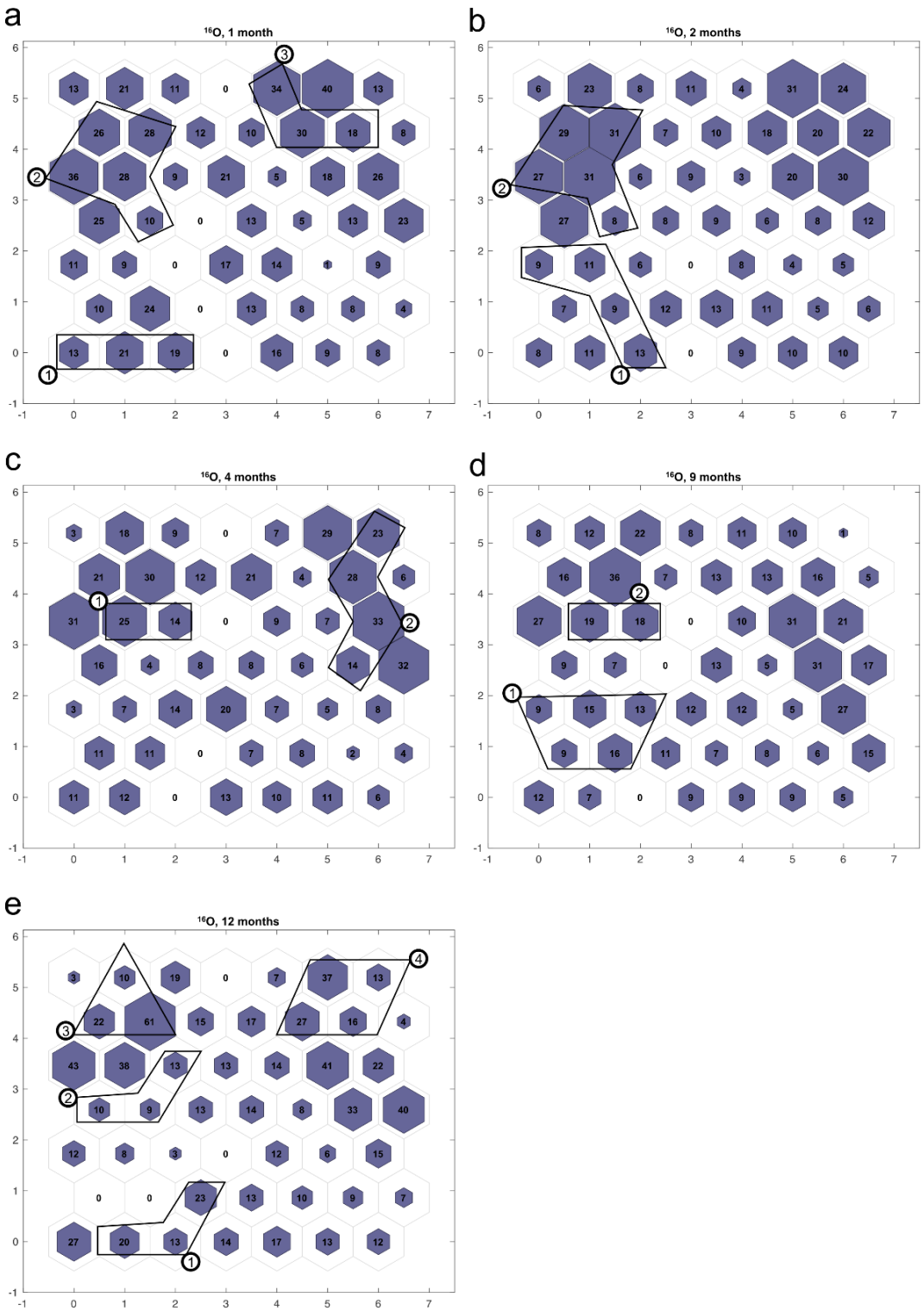

Figure 14. ^{16}O Analysis of self-organizing maps for each time point.

(a,b,c,d,e) Kohonen Self-Organizing Map (SOM) was applied to the differentially expressed (DE) transcripts obtained from the RNA-Seq data to identify coherent patterns

of transcript expression at each time point, as well as patterns within the unmapped transcripts. The mapping clusters transcripts in each unit according to log_2(fold change) expression values for the transcripts in that unit. SOM clustering analysis demonstrates the distances between correlated transcript groups. The small blue hexagons are modules comprising transcripts with similar log_2(fold change) expression pattern. The numbers inside hexagons correspond to the number of transcripts in each module.

^{16}O, 1 month		^{16}O, 2 months		^{16}O, 4 months		^{16}O, 9 months		^{16}O, 12 months	
Module	**Transcript Ensemble ID**	**Module**	**Transcript Ensemble ID**	**Module**	**Transcript Ensemble ID**	**Module**	**Transcript Ensemble ID**	**Module**	**Transcript Ensemble ID**
19	ENSMUST00000237265	11	ENSMUST00000235160	17	ENSMUST00000237369	14	ENSMUST00000235927	10	ENSMUST00000237369
1	ENSMUST00000235180	15	ENSMUST00000237442	1	ENSMUST00000237170	15	ENSMUST00000237814	10	ENSMUST00000238098
23	ENSMUST00000236215	16	ENSMUST00000235764	27	ENSMUST00000237874	16	ENSMUST00000237749	10	ENSMUST00000235828
25	ENSMUST00000235160	17	ENSMUST00000236950	30	ENSMUST00000237472	17	ENSMUST00000235957	12	ENSMUST00000237042
28	ENSMUST00000236591	17	ENSMUST00000238418	31	ENSMUST00000235764	21	ENSMUST00000236736	15	ENSMUST00000236504
29	ENSMUST00000235927	23	ENSMUST00000237060	35	ENSMUST00000236046	30	ENSMUST00000238222	15	ENSMUST00000238021
29	ENSMUST00000236925	23	ENSMUST00000235620	35	ENSMUST00000236687	31	ENSMUST00000237125	22	ENSMUST00000238288
2	ENSMUST00000235304	26	ENSMUST00000238151	39	ENSMUST00000236950	31	ENSMUST00000236330	23	ENSMUST00000235318
2	ENSMUST00000236824	28	ENSMUST00000236925	41	ENSMUST00000236209	35	ENSMUST00000238729	23	ENSMUST00000238267
2	ENSMUST00000235231	29	ENSMUST00000236873	45	ENSMUST00000237798	40	ENSMUST00000236898	2	ENSMUST00000238677
36	ENSMUST00000236950	29	ENSMUST00000237472	47	ENSMUST00000236030	45	ENSMUST00000235558	31	ENSMUST00000236414
37	ENSMUST00000235647	30	ENSMUST00000236303	49	ENSMUST00000237854	8	ENSMUST00000236824	32	ENSMUST00000237170
3	ENSMUST00000235957	30	ENSMUST00000237854	4	ENSMUST00000238288	9	ENSMUST00000236950	34	ENSMUST00000235648
3	ENSMUST00000237185	36	ENSMUST00000236186					36	ENSMUST00000235411
3	ENSMUST00000237146	37	ENSMUST00000237305					37	ENSMUST00000238331
40	ENSMUST00000237170	37	ENSMUST00000235518					37	ENSMUST00000237823
40	ENSMUST00000235620	3	ENSMUST00000238288					3	ENSMUST00000236873
40	ENSMUST00000235633	3	ENSMUST00000237603					40	ENSMUST00000238368
41	ENSMUST00000236195	46	ENSMUST00000237103					41	ENSMUST00000235135
45	ENSMUST00000236567	49	ENSMUST00000237742					44	ENSMUST00000236006
47	ENSMUST00000236873	7	ENSMUST00000237749					48	ENSMUST00000238306
47	ENSMUST00000236414	7	ENSMUST00000236480					49	ENSMUST00000235620
47	ENSMUST00000237587	9	ENSMUST00000235318						
7	ENSMUST00000238288								

Table 20. Unannotated differentially expressed transcripts in ^{16}O experiments at all time points. Each unannotated ENSEMBLE transcript ID is listed with the corresponding module number in the SOM Figure 13.

6.4.5 DIFFERENTIAL EXPRESSION ANALYSIS OF ^{28}SI REVEALS DYNAMIC TIME-DEPENDENT CHANGES IN INFLAMMATORY RESPONSE AT THE WHOLE TRANSCRIPTOME LEVEL

Transcriptional changes and altered pathways associated with proposed ^{28}Si induced hepatic carcinogenesis were evaluated using differential expression analysis of RNA-Seq data in ^{28}Si irradiated compared to non-irradiated control mice at 5 different time points (1mo, 2mo, 4mo, 9mo, and 12mo). Table 7 shows the total number of differentially expressed transcripts at each time point. IPA was used to functionally annotate and map the biological processes involving these differentially expressed transcripts (Figure 15). The analyses revealed that LXR/RXR is significantly affected at 1 month (activated), 2 months (directionality unknown), 4 months (inhibited), 9 months (activated), and 12 months (activated). Acute phase response signaling pathway demonstrated a different dynamic post ^{28}Si irradiation as compared to ^{56}Fe. In particular, it was significantly inhibited at 1, 2, 4, and 12 months and activated at 9 months. In addition, IL-8 signaling shows a pattern opposite to that of ^{16}O irradiation. Unlike ^{16}O irradiation, IL-8 signaling pathway is significantly activated at 1, 9 and 12 months, while it is inhibited at 4 months. Furthermore, PI3K/AKT signaling was significantly activated at 1, 4, and 9 months post ^{28}Si irradiation. This might suggest that ^{28}Si has an earlier cellular survival response compared to ^{56}Fe and ^{16}O. Additionally, the results show that aryl hydrocarbon receptor signaling is significantly inhibited at 2, 4, 9, and 12 months post ^{28}Si irradiation. Aryl hydrocarbon receptor (AHR) is a cytosolic protein associated chaperone and immunophilin-like protein. Upon ligand activation, AHR dissociates from the complex,

translocates into the nucleus and induces transcriptional activation of genes in various signaling pathways involved in cell cycle progression, tumorigenesis, apoptosis, and cell proliferation. [128-130]

The analyses revealed that BCR signaling was significantly affected at 1 month (inhibited), 2 months (activated), 4 months (inhibited), 9 months (activated), and 12 months (activated). This is also indicative of a stronger inhibitory apoptosis response later in time after ^{28}Si irradiation. In addition, the production of nitric oxide and reactive oxygen species in macrophages were significantly affected at all time points; specifically, at 1 month (activated), 2 months (activated), 9 months (activated), and 12 months (inhibited). The tumoricidal properties of macrophages are dependent on the production of reactive oxygen species (ROS). Production of ROS happens through the activation of the nicotinamide adenine diphosphate oxidase (NADPH oxidase), which is part of the electron transport chain. Factors such as bacterial products and metabolites can activate NADPH oxidase, which will lead to ROS production in macrophages and help defend against noxious stimuli. [131-133] The inhibition of ROS production at 12 months contributes to the carcinogenic process triggered by ^{28}Si irradiation. This process is especially pronounced during later time points when the immune response cannot properly regulate apoptosis or control tissue damage. Moreover, Insulin-like growth factor-1 (IGF-1) signaling, which promotes cell proliferation, growth, and survival, is significantly activated at 4, and 9 months. IGF-1 receptor is a transmembrane tyrosine kinase protein that activates many downstream pathways, which in turn induce genes that promote cell growth and differentiation, as well as pathways for cell survival [134-136]. IGF-1 targeted antibodies are currently under phase I clinical investigation as anticancer therapeutic drugs for

advanced or refractory solid tumors (NCT03746431). These pathways demonstrate a complex dynamic interplay with different immunological pathways after ^{28}Si irradiation, which could contribute to hepatic carcinogenic processes. A complete list of significantly impacted pathways ($-\log_{10}$(p-value)≥1.3) is provided in Tables 21, 22, 23, 24, and 25.

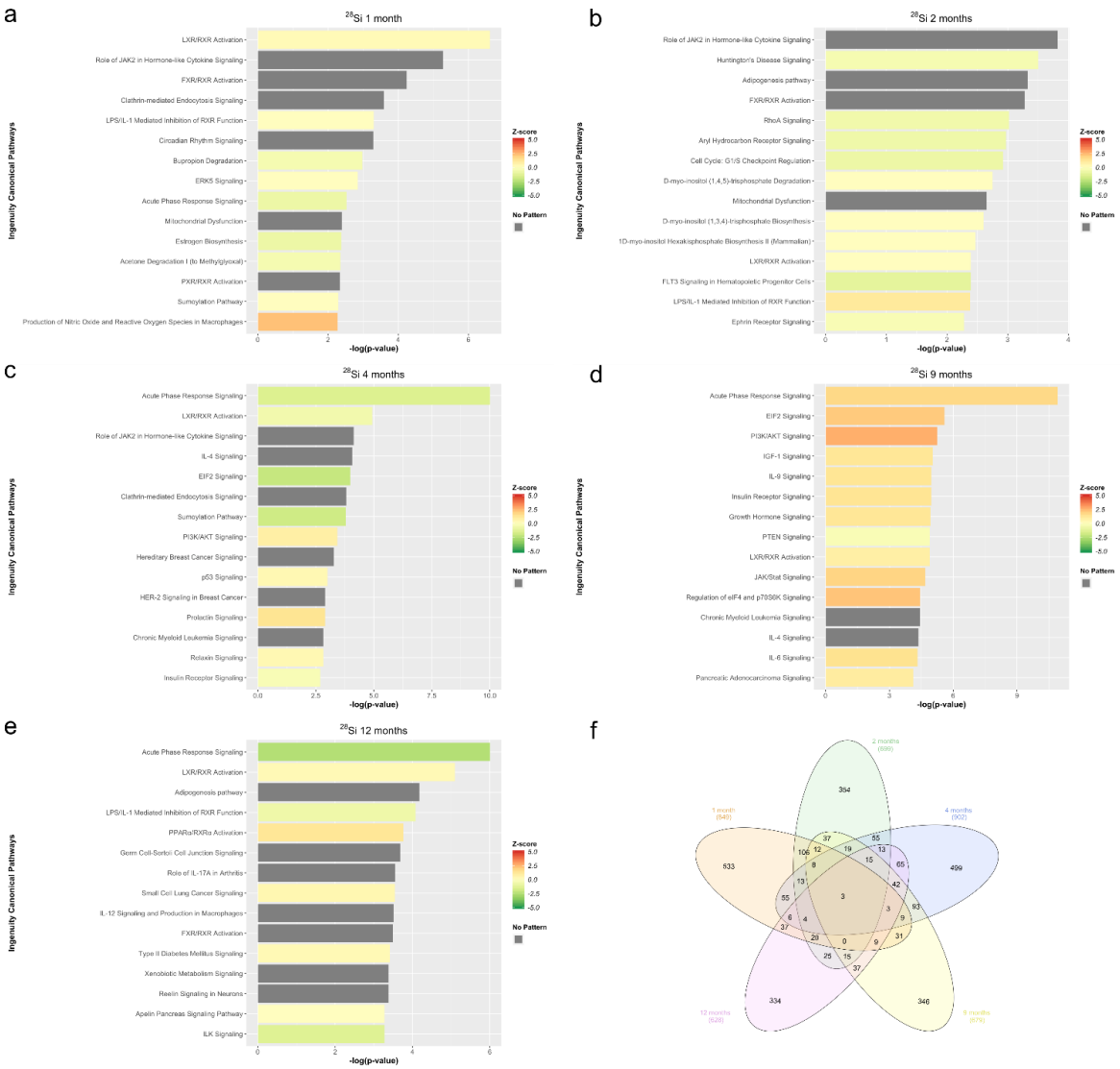

Figure 15. IPA of differentially expressed transcripts in ^{28}Si.

(a) Top pathways enrichment analysis at 1 month. **(b)** Top pathways enrichment analysis at 2 months. **(c)** Top pathways enrichment analysis at 4 months. **(d)** Top pathways enrichment analysis at 9 months. **(e)** Top pathways enrichment analysis at 12 months. **(f)**

The Venn Diagram shows shared and unique differentially expressed transcripts for all time points, in ^{28}Si irradiation compared to control.

Ingenuity Canonical Pathways	-log$_{10}$(p-value)	z-score	Molecules
LXR/RXR Activation	6.61	0.258	APOA2,APOA5,APOB,APOE,CD36,CLU,CYP7A1,FASN,HMGCR,IRF3,KNG1,LDLR,NFKB1,NR1H2,PLTP,SERPINF1,TF
Role of JAK2 in Hormone-like Cytokine Signaling	5.28	NA	SH2B1,SH2B2,SH2B3,SHC1,SIRPA,SOCS2,STAT1,TYK2
FXR/RXR Activation	4.24	NA	APOA2,APOB,APOE,CLU,CYP7A1,FASN,FETUB,G6PC3,KNG1,LIPC,PLTP,SCARB1,SERPINF1,TF
Clathrin-mediated Endocytosis Signaling	3.59	NA	ACTR3,AP1B1,APOA2,APOB,APOE,CD2AP,CLU,DNM2,F2,LDLR,MET,NUMB,PICALM,PROK1,RAB7A,TF
LPS/IL-1 Mediated Inhibition of RXR Function	3.3	0	ACSL3,ALAS1,APOE,CAT,CYP2B6,CYP2C8,CYP7A1,FABP5,FMO1,FMO2,LIPC,NDST1,NDST2,NR1H2,NR1I3,PLTP,SCARB1
Circadian Rhythm Signaling	3.29	NA	ARNTL,ATF2,CREB1,PER1,PER2,PER3
Bupropion Degradation	2.98	-0.447	CYP2B6,CYP2C8,CYP2E1,CYP2F1,POR
ERK5 Signaling	2.85	0	ATF2,CREB1,GAB1,MAPK7,RPS6KC1,WNK1,YWHAG,YWHAQ
Acute Phase Response Signaling	2.53	-0.816	APOA2,C1R,F2,HNRNPK,IKBKG,ITIH3,MAPK14,NFKB1,NR3C1,SERPINF1,SHC1,SOCS2,TF
Mitochondrial Dysfunction	2.39	NA	ATP5F1B,ATP5MC2,ATP5PB,ATPAF1,CAT,COX6B1,CYB5A,GPX4,NDUFA4,PARK7,PDHA1,PINK1,VDAC2
Estrogen Biosynthesis	2.37	-0.816	CYP2B6,CYP2C8,CYP2E1,CYP2F1,HSD17B12,POR
Acetone Degradation I (to Methylglyoxal)	2.35	-0.447	CYP2B6,CYP2C8,CYP2E1,CYP2F1,POR
PXR/RXR Activation	2.34	NA	ALAS1,CYP2B6,CYP2C8,CYP7A1,IGFBP1,NR1I3,NR3C1
Sumoylation Pathway	2.29	0	CEBPA,NFKB1,NR3C1,RHOBTB1,RHOT1,RPA1,SENP5,SP3,XIAP
Production of Nitric Oxide and Reactive Oxygen Species in Macrophages	2.27	2.309	APOA2,APOB,APOE,CAT,CLU,IKBKG,MAPK14,NFKB1,RHOBTB1,RHOT1,SIRPA,STAT1,TYK2
Ephrin B Signaling	2.2	1.342	ABI1,CAP1,CTNNB1,EPHB4,GNB1,GNB2,HNRNPK
Nicotine Degradation II	2.17	-0.378	CYP2B6,CYP2C8,CYP2E1,CYP2F1,FMO1,FMO2,POR

Actin Cytoskeleton Signaling	2.16	0.905	ACTN4,ACTR3,ARHGEF12,CYFIP1,F2,FLNA,GIT1,KNG1,MYH10,MYH14,PFN1,RDX,SHC1,TLN2
Role of PKR in Interferon Induction and Antiviral Response	2.16	NA	ATF2,IKBKG,MAPK14,NFKB1,STAT1
Adipogenesis pathway	2.16	NA	ARNTL,CEBPA,CTNNB1,EZH2,FGFR2,KMT2B,LPIN1,NOCT,PER2,RPS6KC1
PI3K/AKT Signaling	2.11	1.667	CTNNB1,GAB1,IKBKG,NFKB1,SHC1,SYNJ2,TSC1,TYK2,YWHAG,YWHAQ
ATM Signaling	2.09	0	ATF2,BRAT1,CREB1,GADD45G,HERC2,MAPK14,TDP1,USP7
NGF Signaling	2.03	0.333	ATF2,CREB1,GAB1,IKBKG,MAPK7,NFKB1,RPS6KC1,SHC1,SMPD4
IL-15 Production	2	NA	EPHB4,FGFR2,IRF3,KIT,MET,NFKB1,STAT1,TNK2,TYK2
SAPK/JNK Signaling	1.94	0.378	ATF2,GAB1,GNB1,HNRNPK,MAP4K3,MAPK8IP3,MINK1,SHC1
mTOR Signaling	1.9	0.378	DGKZ,EIF4A2,EIF4G1,EIF4G2,FKBP1A,PLD2,PROK1,RHOBTB1,RHOT1,RPS14,RPS6KC1,STK11,TSC1
iNOS Signaling	1.87	1.342	IKBKG,MAPK14,NFKB1,STAT1,TYK2
HIPPO signaling	1.86	0.447	AMOT,DLG1,ITCH,PARD3,Ppp1cc,YWHAG,YWHAQ
4-1BB Signaling in T Lymphocytes	1.85	0	ATF2,IKBKG,MAPK14,NFKB1
Cell Cycle: G2/M DNA Damage Checkpoint Regulation	1.84	NA	FBXL5,HIPK2,TRIP12,YWHAG,YWHAQ
Remodeling of Epithelial Adherens Junctions	1.79	-1	ACTN4,ACTR3,CTNNB1,DNM2,MET,RAB7A
DNA Methylation and Transcriptional Repression Signaling	1.76	NA	CHD4,H3F3A/H3F3B,MECP2,MTA1
TR/RXR Activation	1.74	NA	APOA5,CYP7A1,FASN,GPS2,LDLR,SCARB1,THRSP
IL-12 Signaling and Production in Macrophages	1.7	NA	APOA2,APOB,APOE,CLU,IKBKG,MAPK14,NFKB1,RAB7A,STAT1
Estrogen Receptor Signaling	1.68	NA	G6PC3,H3F3A/H3F3B,IGFBP1,MED23,NR3C1,RBFOX2,SHC1,TAF10,TAF6
Protein Kinase A Signaling	1.67	-1.069	ADCY9,AKAP1,ANAPC5,ATF2,CREB1,CTNNB1,FLNA,GNB1,GNB2,H3F3A/H3F3B,MYH10,NFAT5,NFKB1,Ppp1cc,PTCH1,PTPRC,PTPRJ,SIRPA,YWHAG,YWHAQ
Hypoxia Signaling in the Cardiovascular System	1.65	NA	ARNT,ATF2,CDC34,CREB1,P4HB,UBE2D3
Melanocyte Development and Pigmentation Signaling	1.62	0	ADCY9,ATF2,CREB1,KIT,RPS6KC1,SH2B2,SHC1
p38 MAPK Signaling	1.62	-0.378	ATF2,CREB1,H3F3A/H3F3B,HMGN1,MAPK14,PLA2G6,RPS6KC1,STAT1

Unfolded protein response	1.61	NA	CD82,CEBPA,HSPA5,P4HB,SYVN1
B Cell Receptor Signaling	1.58	-0.632	ATF2,BCL6,CREB1,GAB1,IKBKG,MAPK14,NFAT5,NFKB1,PTPRC,SHC1,SYNJ2
April Mediated Signaling	1.56	0	IKBKG,MAPK14,NFAT5,NFKB1
ILK Signaling	1.53	0.632	ACTN4,ATF2,CREB1,CTNNB1,FLNA,MYH10,MYH14,NFKB1,PROK1,RHOBTB1,RHOT1
PPARα/RXRα Activation	1.51	-1	ADCY9,APOA2,CD36,CKAP5,CYP2C8,FASN,IKBKG,MAPK14,MED23,NFKB1,SHC1
Role of BRCA1 in DNA Damage Response	1.5	NA	BABAM2,E2F8,RBL2,RPA1,SMARCA2,STAT1
B Cell Activating Factor Signaling	1.49	0	IKBKG,MAPK14,NFAT5,NFKB1
Atherosclerosis Signaling	1.49	NA	ABHD3,APOA2,APOB,APOE,CD36,CLU,NFKB1,PLA2G6
IL-22 Signaling	1.48	NA	MAPK14,STAT1,TYK2
Role of JAK1, JAK2 and TYK2 in Interferon Signaling	1.48	NA	NFKB1,STAT1,TYK2
D-myo-inositol (1,3,4)-trisphosphate Biosynthesis	1.48	NA	IPMK,SEC16A,SYNJ2
Apelin Adipocyte Signaling Pathway	1.48	-0.816	ADCY9,CAT,GPX1,GPX4,MAPK14,MAPK7
ERK/MAPK Signaling	1.48	0.333	ATF2,CREB1,ELF1,ELF4,H3F3A/H3F3B,PLA2G6,SHC1,STAT1,TLN2,YWHAG,YWHAQ
Nicotine Degradation III	1.46	-0.447	CYP2B6,CYP2C8,CYP2E1,CYP2F1,POR
PCP pathway	1.46	0.447	ATF2,DAAM1,LGR4,PFN1,PRICKLE1
tRNA Charging	1.46	-2.449	FARSA,FARSB,LARS2,MARS,Qars,TARS
Role of JAK family kinases in IL-6-type Cytokine Signaling	1.44	NA	MAPK14,STAT1,TYK2
Activation of IRF by Cytosolic Pattern Recognition Receptors	1.41	0.447	ATF2,IKBKG,IRF3,NFKB1,STAT1
1D-myo-inositol Hexakisphosphate Biosynthesis II (Mammalian)	1.39	NA	IPMK,SEC16A,SYNJ2
Epithelial Adherens Junction Signaling	1.38	NA	ACTN4,ACTR3,CTNNB1,EPN2,MET,MYH10,MYH14,PARD3,SSX2IP
BMP signaling pathway	1.37	0.816	ATF2,CHRD,CREB1,MAPK14,NFKB1,XIAP
Autophagy	1.36	NA	CTSH,CTSS,CTSV,MAP1LC3A,NBR1
BAG2 Signaling Pathway	1.36	0	HSPA5,MAPK14,NFKB1,PINK1
Mevalonate Pathway I	1.35	NA	HADHB,HMGCR,IDI1
FGF Signaling	1.33	-0.816	ATF2,CREB1,FGFR2,GAB1,MAPK14,MET
Pancreatic Adenocarcinoma Signaling	1.33	1.633	CYP2E1,E2F8,NFKB1,PLD2,PROK1,STAT1,TYK2

Table 21. Significant Pathways for differentially expressed transcripts in ^{28}Si vs. non-irradiated control at 1 month.

Ingenuity Canonical Pathways	-log$_{10}$(p-value)	z-score	Molecules
Role of JAK2 in Hormone-like Cytokine Signaling	3.82	NA	SH2B1,SH2B2,SH2B3,SHC1,SIRPA,STAT1
Huntington's Disease Signaling	3.5	-0.447	ATF2,ATP5F1B,ATP5PB,GNB1,GNB2,GPAA1,HDAC5,HDAC6,MAPK9,NCOR1,NCOR2,PDPK1,SGK1,SHC1,SIN3A,TCERG1
Adipogenesis pathway	3.33	NA	CEBPA,EZH2,FGFR2,HDAC5,HDAC6,KAT2A,KMT2B,PPIP5K1,RPS6KA1,SIN3A,TBL1XR1
FXR/RXR Activation	3.28	NA	APOA2,BAAT,FETUB,LIPC,MAPK9,NR0B2,PKLR,SAA1,SCARB1,SERPINF1,SLC22A7
RhoA Signaling	3.02	-0.632	ACTR3,ARHGEF1,BAIAP2,CDC42EP4,MPRIP,PFN1,RAPGEF6,SEPT2,SEPT9,TTN
Aryl Hydrocarbon Receptor Signaling	2.97	-0.707	ALDH2,ATR,CDKN1B,HSP90AB1,MGST1,NCOR2,NFIA,NFIX,NQO2,NR0B2,RBL2
Cell Cycle: G1/S Checkpoint Regulation	2.92	-0.816	ATR,CDKN1B,E2F3,HDAC5,HDAC6,RBL2,SIN3A
D-myo-inositol (1,4,5)-trisphosphate Degradation	2.75	0	INPP5A,INPP5D,SEC16A,SYNJ2
Mitochondrial Dysfunction	2.65	NA	ATP5F1B,ATP5PB,CAT,COX6B1,CYB5A,CYC1,GPX4,MAPK9,MT-ND4L,NDUFAF1,NDUFV1,PINK1
D-myo-inositol (1,3,4)-trisphosphate Biosynthesis	2.6	0	INPP5A,INPP5D,SEC16A,SYNJ2
1D-myo-inositol Hexakisphosphate Biosynthesis II (Mammalian)	2.47	0	INPP5A,INPP5D,SEC16A,SYNJ2
FLT3 Signaling in Hematopoietic Progenitor Cells	2.39	-1.134	ATF2,INPP5D,PDPK1,RPS6KA1,SHC1,STAT1,STAT2
LXR/RXR Activation	2.39	0	APOA2,APOA5,CD36,ECHS1,NCOR1,NCOR2,NR1H2,SAA1,SERPINF1
LPS/IL-1 Mediated Inhibition of RXR Function	2.38	1.134	ACOX2,ACSL3,ACSL4,ALAS1,ALDH2,CAT,LIPC,MAPK9,MGST1,NDST2,NR0B2,NR1H2,SCARB1
Ephrin Receptor Signaling	2.28	-0.333	ACTR3,ATF2,BCAR1,EPHB4,GNB1,GNB2,GRIN3A,PROK1,PXN,RAPGEF1,SHC1
Sirtuin Signaling Pathway	2.2	-0.277	ACLY,ATP5F1B,ATP5PB,CYC1,GABPB1,GABPB2,GLUD1,KAT2A,MT-ND4L,NDUFAF1,NDUFV1,NR1H2,PFKFB3,PFKM,POLR3D,STK11
Superpathway of D-myo-inositol (1,4,5)-trisphosphate Metabolism	2.14	0	INPP5A,INPP5D,SEC16A,SYNJ2
Actin Cytoskeleton Signaling	2.06	-1.265	ACTR3,ARHGEF1,BAIAP2,BCAR1,DIAPH1,FLNA,MPRIP,MYH14,PFN1,PXN,SHC1,TTN

NGF Signaling	2.04	0	ATF2,MAP3K13,Map3k7,MAPK9,PDPK1,RPS6KA1,SHC1,SMPD4
SAPK/JNK Signaling	1.89	0.816	ATF2,GNB1,HNRNPK,MAP3K13,MAPK8IP3,MAPK9,SHC1
Role of BRCA1 in DNA Damage Response	1.88	NA	ATR,E2F3,PBRM1,RBL2,SMARCC1,STAT1
Cyclins and Cell Cycle Regulation	1.85	NA	ATR,CDKN1B,E2F3,HDAC5,HDAC6,SIN3A
Calcium Signaling	1.8	0.816	ATF2,ATP2A2,CACNA1A,CALR,GRIA3,GRIN3A,HDAC5,HDAC6,MICU1,MYH14,NFAT5
Signaling by Rho Family GTPases	1.77	0.333	ACTR3,ARHGEF1,ARHGEF10,ARHGEF3,BAIAP2,CDC42EP4,GNB1,GNB2,MAPK9,PARD3,SEPT2,SEPT9
B Cell Receptor Signaling	1.74	0.333	ATF2,INPP5D,MAP3K13,Map3k7,MAPK9,NFAT5,PDPK1,SHC1,SYNJ2,TCF3
α-tocopherol Degradation	1.72	NA	CYP4F12,CYP4F3
Estrogen Receptor Signaling	1.72	NA	MED12,NCOR1,NCOR2,NR0B2,SHC1,TAF10,TAF6,TRRAP
Glutamate Receptor Signaling	1.71	NA	GNB1,GRIA3,GRIN3A,GRM8,SLC38A1
γ-linolenate Biosynthesis II (Animals)	1.71	NA	ACSL3,ACSL4,CYB5A
Glucocorticoid Receptor Signaling	1.68	NA	CEBPA,FKBP5,HSP90AB1,MAPK9,NCOR1,NCOR2,NFAT5,PBRM1,SGK1,SHC1,SMARCC1,STAT1,TAF10,TAF6,TAT
PPARα/RXRα Activation	1.67	0	ADCY4,APOA2,CD36,CKAP5,HSP90AB1,MED12,NCOR1,NCOR2,NR0B2,SHC1
Cdc42 Signaling	1.65	0	ACTR3,ATF2,BAIAP2,CDC42BPA,DIAPH1,MAPK9,MPRIP,PARD3,TNK2
Protein Kinase A Signaling	1.62	-0.302	ADCY4,ADD1,AKAP1,ANAPC5,ATF2,EYA3,FLNA,GNB1,GNB2,NFAT5,PPP1R10,PTPN4,PTPRJ,PXN,SIRPA,TCF3,TTN
RAR Activation	1.59	NA	ADCY4,AKR1C4,MAPK9,NCOR1,NCOR2,PBRM1,PDPK1,PML,SMARCC1,TNIP1
Insulin Receptor Signaling	1.59	-0.707	ACLY,INPP5D,PDPK1,PPP1R10,RAPGEF1,SGK1,SHC1,SYNJ2
Oxidative Phosphorylation	1.58	-1.134	ATP5F1B,ATP5PB,COX6B1,CYB5A,CYC1,MT-ND4L,NDUFV1
Phospholipase C Signaling	1.53	0.632	ADCY4,ARHGEF1,ARHGEF10,ARHGEF3,ATF2,GNB1,GNB2,HDAC5,HDAC6,MPRIP,NFAT5,SHC1
Breast Cancer Regulation by Stathmin1	1.53	NA	ADCY4,ARHGEF1,ARHGEF10,ARHGEF3,CDKN1B,E2F3,GNB1,GNB2,PPP1R10,SHC1

ATM Signaling	1.51	1.342	ATF2,ATR,HERC2,MAPK9,SMC2,TRRAP
Ephrin B Signaling	1.47	NA	EPHB4,GNB1,GNB2,HNRNPK,PXN
PTEN Signaling	1.43	0.378	BCAR1,CDKN1B,FGFR2,INPP5D,PDPK1,SHC1,SYNJ2
Integrin Signaling	1.42	-1.667	ACTR3,BCAR1,ITGA8,MPRIP,PFN1,PXN,RAPGEF1,SHC1,TNK2,TTN
Phagosome Maturation	1.42	NA	ATP6AP1,CALR,CTSH,CTSV,Dync1i2,DYNC1LI2,GPAA1,VPS33B
Assembly of RNA Polymerase III Complex	1.41	NA	GTF3C1,POLR3D
Chronic Myeloid Leukemia Signaling	1.4	NA	CDKN1B,E2F3,HDAC5,HDAC6,RBL2,SIN3A
Reelin Signaling in Neurons	1.38	NA	ARHGEF1,ARHGEF10,ARHGEF3,MAPK8IP3,MAPK9
FcγRIIB Signaling in B Lymphocytes	1.36	-1	CACNA1A,INPP5D,MAPK9,PDPK1,SHC1
Amyotrophic Lateral Sclerosis Signaling	1.35	1.342	CACNA1A,CAT,GRIA3,GRIN3A,PROK1,XIAP
3-phosphoinositide Degradation	1.35	0	INPP4A,INPP5D,PPIP5K1,PPP1R16B,PTPRJ,SIRPA,SYNJ2,UBLCP1
Type II Diabetes Mellitus Signaling	1.34	1	ACSL3,ACSL4,CACNA1A,CD36,MAPK9,PDPK1,PKLR,SMPD4
Apelin Adipocyte Signaling Pathway	1.33	-0.447	ADCY4,CAT,GPX4,MAPK9,MGST1
Production of Nitric Oxide and Reactive Oxygen Species in Macrophages	1.32	0.333	APOA2,CAT,IRF1,MAP3K13,Map3k7,MAPK9,PPP1R10,SIRPA,STAT1
Sertoli Cell-Sertoli Cell Junction Signaling	1.32	NA	ATF2,BCAR1,CLDN12,EPB41,MAP3K13,Map3k7,MAPK9,SPTAN1,TJP3
DNA Methylation and Transcriptional Repression Signaling	1.31	NA	ARID4B,CHD4,SIN3A
Sumoylation Pathway	1.3	0	CEBPA,MAPK9,PML,RCC1,SENP6,XIAP

Table 22. Significant Pathways for differentially expressed transcripts in ^{28}Si vs. non-irradiated control at 2 months.

Ingenuity Canonical Pathways	**-log$_{10}$(p-value)**	**z-score**	**Molecules**
Acute Phase Response Signaling	10	-1.5	APOA2,CFB,CP,F2,FGA,FN1,GRB2,HNRNPK,HP,IKBKB,IL1R1,ITIH2,ITIH3,ITIH4,JAK2,LBP,NR3C1,PIK3CD,SAA1,SAA2-SAA4,Saa3,SERPINA1,SERPINA3,SOCS2,SOCS3,TF

LXR/RXR Activation	4.93	-0.577	ABCG8,APOA2,APOA5,FGA,IL1R1,ITIH4,LBP,LPL,NCOR2,NR1H2,NR1H3,SAA1,SERPINA1,TF,TLR3
Role of JAK2 in Hormone-like Cytokine Signaling	4.13	NA	JAK2,SH2B1,SH2B3,SIRPA,SOCS2,SOCS3,STAT5A
IL-4 Signaling	4.07	NA	GRB2,HLA-A,INPP5B,INPP5D,JAK2,NFAT5,NR3C1,PIK3C2G,PIK3CD,SYNJ1,SYNJ2
EIF2 Signaling	3.98	-2.111	ACTB,EIF4G1,EIF4G3,GRB2,HSPA5,MT-TM,PIK3C2G,PIK3CD,PTBP1,RPL10A,RPL11,RPL12,RPL18A,RPL37,RPL38,RPS14,RPS15A,RPS19,XIAP
Clathrin-mediated Endocytosis Signaling	3.81	NA	ACTB,AP1G2,APOA2,ARRB1,CD2AP,F2,GRB2,MDM2,MET,PICALM,PIK3C2G,PIK3CD,PIP5K1C,RAB11A,SERPINA1,SYNJ1,TF
Sumoylation Pathway	3.8	-1.89	CEBPA,DNMT3A,MDM2,NR3C1,PML,RANGAP1,RCC1,RFC1,RHOBTB1,RHOT1,SENP6,XIAP
PI3K/AKT Signaling	3.42	0.832	CDKN1B,GRB2,IKBKB,INPP5B,INPP5D,ITGA3,JAK2,MDM2,PIK3CD,SYNJ1,SYNJ2,TSC1,YWHAG
Hereditary Breast Cancer Signaling	3.27	NA	ACTB,ARID1A,ATR,BRCA2,FANCM,GADD45G,HDAC10,HDAC6,PIK3C2G,PIK3CD,RAD50,RFC1,SMARCA2
p53 Signaling	3	0.378	ATR,COQ8A,GADD45G,MDM2,PIDD1,PIK3C2G,PIK3CD,PML,ST13,STAG1
Prolactin Signaling	2.9	1.414	GRB2,JAK2,NR3C1,PIK3C2G,PIK3CD,PRKCE,SOCS2,SOCS3,STAT5A
HER-2 Signaling in Breast Cancer	2.9	NA	CDKN1B,GRB2,MDM2,PARD3,PARD6A,PIK3C2G,PIK3CD,PRKCE,TSC1
Chronic Myeloid Leukemia Signaling	2.83	NA	CDKN1B,GRB2,HDAC10,HDAC6,IKBKB,MDM2,PIK3C2G,PIK3CD,STAT5A,TGFBR1
Relaxin Signaling	2.82	0.378	ADCY3,ADCY6,GNAI2,GNB1,GNG12,GUCY2C,NPR2,PDE1A,PDE4B,PDE4C,PDE5A,PIK3C2G,PIK3CD
Insulin Receptor Signaling	2.68	-0.302	ACLY,GRB10,GRB2,INPP5B,INPP5D,JAK2,PIK3C2G,PIK3CD,SOCS3,SYNJ1,SYNJ2,TSC1
TR/RXR Activation	2.66	NA	APOA5,DIO1,FGA,HP,MDM2,ME1,NCOR2,PIK3C2G,PIK3CD
PTEN Signaling	2.63	0.302	CDKN1B,FGFR3,GRB2,IKBKB,INPP5B,INPP5D,ITGA3,PIK3CD,SYNJ1,SYNJ2,TGFBR1

Growth Hormone Signaling	2.63	2.121	CEBPA,JAK2,PIK3C2G,PIK3CD,PRKCE,SOCS2,SOCS3,STAT5A
Tec Kinase Signaling	2.63	1	ACTB,GNAI2,GNB1,GNG12,GTF2I,ITGA3,JAK2,PIK3C2G,PIK3CD,PRKCE,RHOBTB1,RHOT1,STAT5A
Pancreatic Adenocarcinoma Signaling	2.59	-0.378	BRCA2,CDKN1B,GRB2,JAK2,MDM2,PIK3C2G,PIK3CD,PLD1,RALBP1,TGFBR1
Nitric Oxide Signaling in the Cardiovascular System	2.56	0.632	ATP2A2,ATP2A3,Calm1 (includes others),GUCY2C,ITPR1,PDE1A,PDE5A,PIK3C2G,PIK3CD,PRKCE
IL-9 Signaling	2.47	1	PIK3C2G,PIK3CD,SOCS2,SOCS3,STAT5A
Adipogenesis pathway	2.45	NA	ARNTL,ATG7,CEBPA,FGFR3,HDAC10,HDAC6,KAT6A,LPL,NOCT,PPIP5K1,SETDB1
Role of BRCA1 in DNA Damage Response	2.45	NA	ACTB,ARID1A,ATR,BRCA2,FANCM,RAD50,RFC1,SMARCA2
JAK/Stat Signaling	2.45	0.707	GRB2,JAK2,PIAS3,PIK3C2G,PIK3CD,SOCS2,SOCS3,STAT5A
Cardiac Hypertrophy Signaling (Enhanced)	2.36	0.962	ACVR2B,ADCY3,ADCY6,ATF2,ATP2A2,ATP2A3,Calm1 (includes others),DIAPH1,FGFR3,GNAI2,GNB1,HDAC10,HDAC6,IKBKB,IL1R1,ITGA3,ITPR1,JAK2,NFAT5,PDE1A,PDE4B,PDE4C,PDE5A,PIK3C2G,PIK3CD,PRKCE,TGFBR1
Phospholipase C Signaling	2.36	-0.302	ADCY3,ADCY6,ATF2,Calm1 (includes others),FCGR2A,GNB1,GNG12,GRB2,HDAC10,HDAC6,ITGA3,ITPR1,NFAT5,PLD1,PRKCE,RHOBTB1,RHOT1
D-myo-inositol (1,4,5)-trisphosphate Degradation	2.35	0	INPP5B,INPP5D,SYNJ1,SYNJ2
Cell Cycle: G1/S Checkpoint Regulation	2.31	1.633	ATR,CDKN1B,FBXL5,HDAC10,HDAC6,MDM2,RPL11
Ephrin Receptor Signaling	2.29	0.905	ABI1,ADAM10,ATF2,GNAI2,GNB1,GNG12,GRB2,ITGA3,ITSN1,JAK2,MAP4K4,PIK3C2G,SORBS1
Breast Cancer Regulation by Stathmin1	2.25	NA	ADCY3,ADCY6,Calm1 (includes others),CDKN1B,GNAI2,GNB1,GNG12,GRB2,ITPR1,PIK3C2G,PIK3CD,PRKCE,TUBB2A,UHMK1
Natural Killer Cell Signaling	2.25	NA	FCGR2A,GRB2,INPP5B,INPP5D,LAIR1,PIK3C2G,PIK3CD,PRKCE,SYNJ1,SYNJ2
Role of JAK1 and JAK3 in γc Cytokine Signaling	2.24	NA	FES,GRB2,JAK2,PIK3C2G,PIK3CD,SOCS3,STAT5A
Phagosome Formation	2.22	NA	C5AR1,FCGR2A,FN1,ITGA3,PIK3C2G,PIK3CD,PRKCE,RHOBTB1,RHOT1,TLR3
D-myo-inositol (1,3,4)-trisphosphate Biosynthesis	2.21	0	INPP5B,INPP5D,SYNJ1,SYNJ2

Role of NFAT in Regulation of the Immune Response	2.21	0	ATF2,Calm1 (includes others),FCGR2A,GNAI2,GNB1,GNG12,GRB2,HLA-A,IKBKB,ITPR1,NFAT5,PIK3C2G,PIK3CD
Renin-Angiotensin Signaling	2.17	0	ADCY3,ADCY6,ATF2,GRB2,ITPR1,JAK2,PIK3C2G,PIK3CD,PRKCE,SHF
Protein Ubiquitination Pathway	2.17	NA	BAG1,CUL2,DNAJB2,DNAJC12,DNAJC21,DNAJC5,HLA-A,HSPA5,MDM2,PAN2,UBE2M,UBE4A,USP15,USP19,USP34,USP45,XIAP
NRF2-mediated Oxidative Stress Response	2.15	NA	ACTB,DNAJB2,DNAJC21,DNAJC5,FKBP5,FMO1,GSTM4,Gstm6,KEAP1,MGST1,PIK3C2G,PIK3CD,PRKCE
Aryl Hydrocarbon Receptor Signaling	2.13	-1.134	ALDH2,ATR,CDKN1B,GSTM4,Gstm6,MDM2,MGST1,NCOR2,NEDD8,NFIA,TRIP11
Systemic Lupus Erythematosus In B Cell Signaling Pathway	2.13	-1.213	Calm1 (includes others),FCGR2A,GRB2,INPP5B,INPP5D,IRF5,JAK2,MAP4K4,NFAT5,PIK3C2G,PIK3CD,PRKCE,SHF,SYNJ1,SYNJ2,TBK1,TLR3
Thrombin Signaling	2.11	1.508	ADCY3,ADCY6,F2,GNAI2,GNB1,GNG12,GRB2,IKBKB,ITPR1,PIK3C2G,PIK3CD,PRKCE,RHOBTB1,RHOT1
PDGF Signaling	2.08	0	GRB2,INPP5B,INPP5D,JAK2,PIK3C2G,PIK3CD,SYNJ1,SYNJ2
Lipid Antigen Presentation by CD1	2.08	NA	AP1G2,CALR,CANX,PSAP
1D-myo-inositol Hexakisphosphate Biosynthesis II (Mammalian)	2.08	0	INPP5B,INPP5D,SYNJ1,SYNJ2
Iron homeostasis signaling pathway	2.07	NA	ATP6V0A1,CP,FBXL5,HBA1/HBA2,HP,JAK2,MMS19,NUBP2,SLC39A14,STAT5A,TF
DNA Double-Strand Break Repair by Homologous Recombination	2.07	NA	BRCA2,LIG1,RAD50
Calcium Transport I	2.07	NA	ATP2A2,ATP2A3,ATP2C1
PPARα/RXRα Activation	2.06	0	ACVR2B,ADCY3,ADCY6,APOA2,CKAP5,GRB2,IKBKB,IL1R1,JAK2,LPL,MAP4K4,NCOR2,TGFBR1
Caveolar-mediated Endocytosis Signaling	2.04	NA	ACTB,ARCN1,FLNA,FLOT2,HLA-A,ITGA3,ITSN1
Virus Entry via Endocytic Pathways	2.04	NA	ACTB,AP1G2,FLNA,HLA-A,ITGA3,ITSN1,PIK3C2G,PIK3CD,PRKCE
Germ Cell-Sertoli Cell Junction Signaling	2.03	NA	ACTB,CTNND1,EPN2,ITGA3,KEAP1,PIK3C2G,PIK3CD,RHOBTB1,RHOT1,SORBS1,TGFBR1,TUBB2A
Epithelial Adherens Junction Signaling	2.01	NA	ACTB,ACVR2B,CLIP1,CTNND1,EPN2,KEAP1,MET,PARD3,SORBS1,TGFBR1,TUBB2A
Huntington's Disease Signaling	2	0	ATF2,ATP5PF,CAPNS1,DNAJC5,GNB1,GNG12,GRB2,HDAC10,HDAC6,HSPA5,ITPR1,NCOR2,PIK3C2G,PIK3CD,PRKCE
Role of NFAT in Cardiac Hypertrophy	2	0.302	ADCY3,ADCY6,Calm1 (includes others),GNAI2,GNB1,GNG12,GRB2,HDAC10,HDAC6,ITPR1,PIK3C2G,PIK3CD,PRKCE,TGFBR1
iCOS-iCOSL Signaling in T Helper Cells	1.97	0	Calm1 (includes others),GRB2,HLA-A,IKBKB,INPP5D,ITPR1,NFAT5,PIK3C2G,PIK3CD

Actin Cytoskeleton Signaling	1.96	-0.905	ACTB,DIAPH1,F2,FLNA,FN1,GIT1,GNG12,GRB2,ITGA3,LBP,PIK3C2G,PIK3CD,PIP5K1C,TTN
FXR/RXR Activation	1.95	NA	ABCG8,APOA2,FGA,ITIH4,LPL,NR1H3,PKLR,SAA1,SERPINA1,TF
Leptin Signaling in Obesity	1.95	0.447	ADCY3,ADCY6,GRB2,JAK2,PIK3C2G,PIK3CD,SOCS3
ATM Signaling	1.95	-1	ATF2,ATR,BRAT1,GADD45G,HERC2,HP1BP3,MDM2,RAD50
Glucocorticoid Receptor Signaling	1.92	NA	ACTB,ARID1A,BAG1,CEBPA,CREBZF,FKBP5,GRB2,HSPA5,IKBKB,JAK2,NCOR2,NFAT5,NR3C1,PIK3C2G,PIK3CD,SMARCA2,STAT5A,TAT,TGFBR1
Erythropoietin Signaling	1.92	NA	GRB2,JAK2,PIK3C2G,PIK3CD,PRKCE,SOCS3,STAT5A
IL-3 Signaling	1.92	1.134	GRB2,INPP5D,JAK2,PIK3C2G,PIK3CD,PRKCE,STAT5A
3-phosphoinositide Degradation	1.88	0.302	CA3,INPP5B,INPP5D,MTM1,MTMR4,PPIP5K1,SET,SIRPA,SOCS3,SYNJ1,SYNJ2
LPS/IL-1 Mediated Inhibition of RXR Function	1.87	0	ABCG8,ACOX2,ALAS1,ALDH2,FMO1,GSTM4,Gstm6,HMGCS2,HS3ST6,IL1R1,LBP,MGST1,NR1H2,NR1H3
Antiproliferative Role of Somatostatin Receptor 2	1.87	0	CDKN1B,GNB1,GNG12,GUCY2C,NPR2,PIK3C2G,PIK3CD
TNFR2 Signaling	1.86	NA	IKBKB,TBK1,TNFAIP3,XIAP
Gαq Signaling	1.82	1	Calm1 (includes others),GNB1,GNG12,IKBKB,ITPR1,PIK3C2G,PIK3CD,PLD1,PRKCE,RHOBTB1,RHOT1
fMLP Signaling in Neutrophils	1.81	0.707	Calm1 (includes others),GNAI2,GNB1,GNG12,ITPR1,NFAT5,PIK3C2G,PIK3CD,PRKCE
Cellular Effects of Sildenafil (Viagra)	1.81	NA	ACTB,ADCY3,ADCY6,Calm1 (includes others),GUCY2C,ITPR1,PDE1A,PDE4B,PDE4C,PDE5A
Apelin Cardiomyocyte Signaling Pathway	1.78	1.414	ATP2A2,ATP2A3,GNAI2,ITPR1,PIK3C2G,PIK3CD,PRKCE,SLC9A8
RhoA Signaling	1.77	-2.121	ACTB,ARHGAP1,ARHGAP12,NRP2,PIP5K1C,PLD1,RAPGEF6,RHPN2,TTN
B Cell Receptor Signaling	1.77	-0.905	ATF2,Calm1 (includes others),FCGR2A,GRB2,IKBKB,INPP5B,INPP5D,NFAT5,PIK3C2G,PIK3CD,SYNJ1,SYNJ2
IL-6 Signaling	1.77	0	GRB2,IKBKB,IL1R1,JAK2,LBP,MAP4K4,PIK3C2G,PIK3CD,SOCS3
Superpathway of D-myo-inositol (1,4,5)-trisphosphate Metabolism	1.77	0	INPP5B,INPP5D,SYNJ1,SYNJ2
α-Adrenergic Signaling	1.76	1	ADCY3,ADCY6,Calm1 (includes others),GNAI2,GNB1,GNG12,ITPR1,PRKCE
Thrombopoietin Signaling	1.74	0.816	GRB2,JAK2,PIK3C2G,PIK3CD,PRKCE,STAT5A
Cardiac β-adrenergic Signaling	1.74	0	ADCY3,ADCY6,ATP2A2,ATP2A3,GNB1,GNG12,PDE1A,PDE4B,PDE4C,PDE5A
IGF-1 Signaling	1.74	0.378	GRB10,GRB2,JAK2,PIK3C2G,PIK3CD,SOCS2,SOCS3,YWHAG
Lysine Degradation II	1.69	NA	AADAT,AASDH,AASDHPPT
FGF Signaling	1.69	-1.134	ATF2,FGFR3,GRB2,ITPR1,MET,PIK3C2G,PIK3CD

Calcium-induced T Lymphocyte Apoptosis	1.65	0.816	ATP2A2,ATP2A3,Calm1 (includes others),HLA-A,ITPR1,PRKCE
CXCR4 Signaling	1.65	1.667	ADCY3,ADCY6,GNAI2,GNB1,GNG12,ITPR1,PIK3C2G,PIK3CD,PRKCE,RHOBTB1,RHOT1
Signaling by Rho Family GTPases	1.64	0	ACTB,CLIP1,GNAI2,GNB1,GNG12,ITGA3,PARD3,PARD6A,PIK3C2G,PIK3CD,PIP5K1C,PLD1,RHOBTB1,RHOT1
Superpathway of Inositol Phosphate Compounds	1.62	-0.277	CA3,INPP5B,INPP5D,MTMR4,PIK3C2G,PIK3CD,PIP5K1C,PPIP5K1,SET,SIRPA,SOCS3,SYNJ1,SYNJ2
Formaldehyde Oxidation II (Glutathione-dependent)	1.62	NA	ADH5,ESD
Synaptogenesis Signaling Pathway	1.61	0	ADCY3,ADCY6,AP1G2,ATF2,Calm1 (includes others),CTNND1,DNAJC5,GRB2,ITPR1,ITSN1,NRXN1,PIK3C2G,PIK3CD,PRKCE,SHF,STXBP1,STXBP6
3-phosphoinositide Biosynthesis	1.61	0.302	CA3,INPP5B,MTMR4,PIK3C2G,PIK3CD,PIP5K1C,PPIP5K1,SET,SIRPA,SOCS3,SYNJ1
Endothelin-1 Signaling	1.6	0.577	ADCY3,ADCY6,GNAI2,GRB2,GUCY2C,ITPR1,PIK3C2G,PIK3CD,PLD1,PRKCE,PTGS1,SHF
IL-8 Signaling	1.57	1.265	GNAI2,GNB1,GNG12,IKBKB,MAP4K4,PIK3C2G,PIK3CD,PLD1,PRKCE,RHOBTB1,RHOT1,TEK
IL-10 Signaling	1.57	NA	FCGR2A,IKBKB,IL1R1,LBP,MAP4K4,SOCS3
Sirtuin Signaling Pathway	1.55	0	ACLY,ACSS2,ADAM10,ARNTL,ATG7,ATP5PF,BECN1,GADD45G,GLUD1,HMGCS2,MT-ATP6,NDUFA4,NDUFAF1,NDUFV1,NR1H2,NR1H3,VDAC2
IL-1 Signaling	1.55	NA	ADCY3,ADCY6,GNAI2,GNB1,GNG12,IKBKB,IL1R1
Ephrin B Signaling	1.55	2	ABI1,GNAI2,GNB1,GNG12,HNRNPK,ITSN1
P2Y Purigenic Receptor Signaling Pathway	1.54	0	ADCY3,ADCY6,ATF2,GNAI2,GNB1,GNG12,PIK3C2G,PIK3CD,PRKCE
Th2 Pathway	1.54	0	ACVR2B,GRB2,HLA-A,JAK2,PIK3C2G,PIK3CD,SOCS3,STAT5A,TGFBR1
Endocannabinoid Developing Neuron Pathway	1.53	0	ADCY3,ADCY6,ATF2,CDKN1B,GNAI2,GNB1,PIK3C2G,PIK3CD
HOTAIR Regulatory Pathway	1.52	-1.265	ATG7,JARID2,KMT2A,MDM2,MET,PIK3C2G,PIK3CD,SETDB1,SUZ12,XIAP
Angiopoietin Signaling	1.47	0	GRB2,IKBKB,PIK3C2G,PIK3CD,STAT5A,TEK
Oxidative Phosphorylation	1.47	-2.121	ATP5PF,COX6B1,COX7A2,COX7B,MT-ATP6,NDUFA4,NDUFV1,SURF1
FAK Signaling	1.46	NA	ACTB,CAPNS1,GRB2,ITGA3,PIK3C2G,PIK3CD,TNS1
Gap Junction Signaling	1.46	NA	ACTB,ADCY3,ADCY6,GNAI2,GRB2,GUCY2C,ITPR1,NPR2,PIK3C2G,PIK3CD,PRKCE,TUBB2A
Mitochondrial Dysfunction	1.46	NA	ATP5PF,COX6B1,COX7A2,COX7B,MT-

			ATP6,NDUFA4,NDUFAF1,NDUFV1,OGDH,SURF1,VDAC2
Protein Kinase A Signaling	1.45	-0.243	ADCY3,ADCY6,ATF2,Calm1 (includes others),FLNA,GNAI2,GNB1,GNG12,ITPR1,NFAT5,NTN1,PDE1A,PDE4B,PDE4C,PDE5A,PRKCE,SIRPA,TGFBR1,TTN,YWHAG
Sperm Motility	1.45	0.816	Calm1 (includes others),ERBB4,FES,FGFR3,ITPR1,JAK2,MET,PDE1A,PDE4B,PDE4C,PRKCE,TEK,TNK2
Sphingosine-1-phosphate Signaling	1.44	1.134	ADCY3,ADCY6,GNAI2,PIK3C2G,PIK3CD,RHOBTB1,RHOT1,SMPD4
Fcγ Receptor-mediated Phagocytosis in Macrophages and Monocytes	1.42	-0.378	ACTB,FCGR2A,INPP5D,PIK3C2G,PLD1,PRKCE,RAB11A
Choline Biosynthesis III	1.42	NA	CHPT1,PHKA1,PLD1
Role of Tissue Factor in Cancer	1.42	NA	ARRB1,F2,FGA,ITGA3,JAK2,PIK3C2G,PIK3CD,STAT5A
CREB Signaling in Neurons	1.41	0	ADCY3,ADCY6,ATF2,Calm1 (includes others),GNAI2,GNB1,GNG12,GRB2,ITPR1,PIK3C2G,PIK3CD,PRKCE
Integrin Signaling	1.41	0.632	ACTB,ARF4,CAPNS1,GIT1,GRB2,ITGA3,PIK3C2G,PIK3CD,RHOBTB1,RHOT1,TNK2,TTN
Aldosterone Signaling in Epithelial Cells	1.41	0.447	DNAJB2,DNAJC12,DNAJC21,DNAJC5,HSPA5,ITPR1,PIK3C2G,PIK3CD,PIP5K1C,PRKCE
Neuregulin Signaling	1.4	0.816	CDKN1B,ERBB4,ERRFI1,GRB2,ITGA3,PRKCE,STAT5A
IL-7 Signaling Pathway	1.4	-0.816	CDKN1B,GRB2,MET,PIK3C2G,PIK3CD,STAT5A
Semaphorin Signaling in Neurons	1.4	NA	ARHGAP1,FES,MET,RHOBTB1,RHOT1
Fc Epsilon RI Signaling	1.4	0	GRB2,INPP5B,INPP5D,PIK3C2G,PIK3CD,PRKCE,SYNJ1,SYNJ2
Apelin Endothelial Signaling Pathway	1.4	0.707	ADCY3,ADCY6,Calm1 (includes others),GNAI2,PIK3C2G,PIK3CD,PRKCE,TEK
mTOR Signaling	1.4	0.816	EIF4G1,EIF4G3,PIK3C2G,PIK3CD,PLD1,PRKCE,RHOBTB1,RHOT1,RPS14,RPS15A,RPS19,TSC1
GP6 Signaling Pathway	1.38	0	ADAM10,Calm1 (includes others),COL27A1,FGA,ITPR1,PIK3C2G,PIK3CD,PRKCE
Role of JAK family kinases in IL-6-type Cytokine Signaling	1.37	NA	JAK2,SOCS3,STAT5A
Lysine Degradation V	1.37	NA	AADAT,AASDH,AASDHPPT
CD28 Signaling in T Helper Cells	1.37	-0.378	Calm1 (includes others),GRB2,HLA-A,IKBKB,ITPR1,NFAT5,PIK3C2G,PIK3CD
SAPK/JNK Signaling	1.37	-0.378	ATF2,GNB1,GRB2,HNRNPK,MAP4K4,PIK3C2G,PIK3CD
LPS-stimulated MAPK Signaling	1.36	0.447	ATF2,IKBKB,LBP,PIK3C2G,PIK3CD,PRKCE
PPAR Signaling	1.35	1.134	GRB2,IKBKB,IL1R1,MAP4K4,NCOR2,NR1H3,STAT5A
FLT3 Signaling in Hematopoietic Progenitor Cells	1.34	0	ATF2,GRB2,INPP5D,PIK3C2G,PIK3CD,STAT5A
IL-23 Signaling Pathway	1.32	1	JAK2,PIK3C2G,PIK3CD,SOCS3

Molecular Mechanisms of Cancer	1.32	NA	ADCY3,ADCY6,ATR,CDK9,CDKN1B,CTNND1,GNAI2,GRB2,ITGA3,JAK2,MDM2,PIK3C2G,PIK3CD,PRKCE,RALBP1,RHOBTB1,RHOT1,TGFBR1,XIAP
14-3-3-mediated Signaling	1.3	-0.378	CDKN1B,GRB2,PIK3C2G,PIK3CD,PRKCE,TSC1,TUBB2A,YWHAG
CCR3 Signaling in Eosinophils	1.3	NA	Calm1 (includes others),GNAI2,GNB1,GNG12,ITPR1,PIK3C2G,PIK3CD,PRKCE

Table 23. Significant Pathways for differentially expressed transcripts in ^{28}Si vs. non-irradiated control at 4 months.

Ingenuity Canonical Pathways	-log$_{10}$(p-value)	z-score	Molecules
Acute Phase Response Signaling	10.9	1.807	A2M,AKT3,APCS,APOA2,C1R,C4A/C4B,GRB2,HPX,IL1R1,IL33,ITIH3,ITIH4,JAK2,MAPK9,NR3C1,PIK3CA,PIK3CD,SAA1,Saa3,SERPINA3,SOCS2,SOCS3,STAT3,TF
EIF2 Signaling	5.58	2.121	AKT3,EIF2S3,EIF4G1,EIF4G3,EIF5,GRB2,MT-RNR1,MT-RNR2,MT-TM,MYCN,PABPC1,PIK3CA,PIK3CD,RPL10A,RPL18A,RPL38,RPS14,RPS15A,RPS3
PI3K/AKT Signaling	5.25	2.673	AKT3,CDKN1B,GRB2,GSK3A,HSP90AB1,INPPL1,ITGA3,JAK2,MDM2,PIK3CA,PIK3CD,SYNJ1,SYNJ2,TSC1
IGF-1 Signaling	5.04	1.265	AKT3,GRB10,GRB2,IGFBP1,IGFBP2,JAK2,PIK3CA,PIK3CD,PXN,SOCS2,SOCS3,STAT3
Insulin Receptor Signaling	4.97	1.387	ACLY,AKT3,GRB10,GRB2,GSK3A,INPPL1,JAK2,PIK3CA,PIK3CD,PPP1R10,SOCS3,SYNJ1,SYNJ2,TSC1
IL-9 Signaling	4.97	1.342	CISH,PIK3CA,PIK3CD,SOCS2,SOCS3,STAT3,STAT5A
Growth Hormone Signaling	4.93	1.265	A2M,CEBPA,JAK2,PIK3CA,PIK3CD,RPS6KA1,SOCS2,SOCS3,STAT3,STAT5A
LXR/RXR Activation	4.89	0.832	APOA2,C4A/C4B,CD14,CD36,HPX,IL1R1,IL33,ITIH4,NR1H2,PON3,RXRB,SAA1,TF
PTEN Signaling	4.89	-0.277	AKT3,CDKN1B,FGFR3,GRB2,GSK3A,INPPL1,ITGA3,MAGI1,MAST2,PIK3CA,PIK3CD,SYNJ1,SYNJ2
JAK/Stat Signaling	4.68	1.897	AKT3,CISH,GRB2,JAK2,PIK3CA,PIK3CD,SOCS2,SOCS3,STAT3,STAT5A

Regulation of eIF4 and p70S6K Signaling	4.45	2.236	AKT3,EIF2S3,EIF4G1,EIF4G3,GRB2,ITGA3,MT-RNR1,MT-RNR2,PABPC1,PIK3CA,PIK3CD,RPS14,RPS15A,RPS3
Chronic Myeloid Leukemia Signaling	4.43	NA	AKT3,CDKN1B,E2F3,GRB2,HDAC5,HDAC6,MDM2,PIK3CA,PIK3CD,RBL2,STAT5A
IL-4 Signaling	4.36	NA	AKT3,GRB2,INPPL1,JAK2,NFAT5,NR3C1,PIK3CA,PIK3CD,SYNJ1,SYNJ2
IL-6 Signaling	4.32	1.508	A2M,AKT3,CD14,GRB2,IL1R1,IL33,JAK2,MAPK9,PIK3CA,PIK3CD,SOCS3,STAT3
Pancreatic Adenocarcinoma Signaling	4.13	1	AKT3,CDKN1B,E2F3,GRB2,JAK2,MAPK9,MDM2,PIK3CA,PIK3CD,PLD1,STAT3
HGF Signaling	4.03	1.897	AKT3,DOCK1,ELF4,GRB2,ITGA3,Map3k7,MAPK9,PIK3CA,PIK3CD,PXN,STAT3
Role of JAK2 in Hormone-like Cytokine Signaling	3.85	NA	JAK2,SIRPA,SOCS2,SOCS3,STAT3,STAT5A
Prolactin Signaling	3.74	1.414	GRB2,JAK2,NR3C1,PIK3CA,PIK3CD,SOCS2,SOCS3,STAT3,STAT5A
HER-2 Signaling in Breast Cancer	3.74	NA	AKT3,CDKN1B,GRB2,GSK3A,MDM2,PARD3,PIK3CA,PIK3CD,TSC1
IL-22 Signaling	3.65	0.447	AKT3,MAPK9,SOCS3,STAT3,STAT5A
Role of JAK family kinases in IL-6-type Cytokine Signaling	3.56	NA	JAK2,MAPK9,SOCS3,STAT3,STAT5A
GM-CSF Signaling	3.53	2.121	AKT3,CAMK2G,CISH,GRB2,JAK2,PIK3CA,PIK3CD,STAT3
Acute Myeloid Leukemia Signaling	3.44	1	AKT3,ARAF,CEBPA,GRB2,PIK3CA,PIK3CD,PML,STAT3,STAT5A
HOTAIR Regulatory Pathway	3.28	0	AKT3,ATXN1,CDH1,DZIP3,KMT2A,MDM2,PIK3CA,PIK3CD,SETDB1,STAT3,STK38,SUZ12
CNTF Signaling	3.25	1.89	GRB2,JAK2,LIFR,PIK3CA,PIK3CD,RPS6KA1,STAT3
IL-23 Signaling Pathway	3.22	1.633	AKT3,JAK2,PIK3CA,PIK3CD,SOCS3,STAT3
mTOR Signaling	3.12	0.378	AKT3,EIF4G1,EIF4G3,MT-RNR1,MT-RNR2,PIK3CA,PIK3CD,PLD1,RPS14,RPS15A,RPS3,RPS6KA1,STK11,TSC1
ErbB2-ErbB3 Signaling	3.04	1.633	CDKN1B,GRB2,GSK3A,PIK3CA,PIK3CD,STAT3,STAT5A
Cancer Drug Resistance By Drug Efflux	3.04	NA	ABCC10,AKT3,ARAF,MDM2,PDK1,PIK3CA,PIK3CD
Telomerase Signaling	2.96	2.646	AKT3,ELF4,GRB2,HDAC5,HDAC6,HSP90AB1,PIK3CA,PIK3CD,TEP1

14-3-3-mediated Signaling	2.95	0	AKT3,CDKN1B,GRB2,GSK3A,MAPK9,PIK3CA,PIK3CD,RPS6KA1,STK11,TSC1
Paxillin Signaling	2.91	1	ACTN4,DOCK1,GIT2,GRB2,ITGA3,MAPK9,PIK3CA,PIK3CD,PXN
Role of JAK1 and JAK3 in γc Cytokine Signaling	2.89	NA	GRB2,JAK2,PIK3CA,PIK3CD,SOCS3,STAT3,STAT5A
SPINK1 General Cancer Pathway	2.89	1.134	AKT3,JAK2,Mt1,Mt2,PIK3CA,PIK3CD,STAT3
LPS/IL-1 Mediated Inhibition of RXR Function	2.88	0.816	ACSL1,ALDH3A2,CD14,CYP2A6 (includes others),CYP2B6,CYP2C8,FMO1,Gstm3,IL1R1,IL33,MAPK9,MGST1,NR1H2,SLC27A1
Adrenomedullin signaling pathway	2.85	1.387	AKT3,ARAF,CFH,GRB2,GSK3A,GUCY1B1,GUCY2C,IL33,ITPR1,MAPK9,PIK3CA,PIK3CD,RXRB
PXR/RXR Activation	2.85	NA	AKT3,ALDH3A2,CYP2A6 (includes others),CYP2B6,CYP2C8,IGFBP1,NR3C1
TR/RXR Activation	2.81	NA	AKR1C3,AKT3,COL6A3,MDM2,PIK3CA,PIK3CD,RXRB,TBL1XR1
Adipogenesis pathway	2.81	NA	CEBPA,FGFR3,GTF2H1,HDAC5,HDAC6,Kat6b,KAT7,RPS6KA1,SETDB1,TBL1XR1
Systemic Lupus Erythematosus Signaling	2.79	NA	AKT3,C6,C8B,CD2BP2,CD72,CREM,GRB2,HNRNPA2B1,IL33,NFAT5,PIK3CA,PIK3CD,PRPF3,PRPF40B
PDGF Signaling	2.78	1.414	GRB2,INPPL1,JAK2,PIK3CA,PIK3CD,STAT3,SYNJ1,SYNJ2
D-myo-inositol (1,4,5)-trisphosphate Degradation	2.77	0	INPPL1,SEC16A,SYNJ1,SYNJ2
FXR/RXR Activation	2.76	NA	AKT3,APOA2,C4A/C4B,HPX,IL33,ITIH4,MAPK9,PON3,SAA1,TF
Complement System	2.69	NA	C1R,C4A/C4B,C6,C8B,CFH
B Cell Receptor Signaling	2.66	1.155	AKT3,CAMK2G,GRB2,GSK3A,INPPL1,Map3k7,MAPK9,NFAT5,PIK3CA,PIK3CD,SYNJ1,SYNJ2
Inhibition of Angiogenesis by TSP1	2.64	-1	AKT3,CD36,CD47,GUCY1B1,MAPK9
D-myo-inositol (1,3,4)-trisphosphate Biosynthesis	2.63	0	INPPL1,SEC16A,SYNJ1,SYNJ2
FAK Signaling	2.61	NA	AKT3,DOCK1,GIT2,GRB2,ITGA3,PIK3CA,PIK3CD,PXN
Leptin Signaling in Obesity	2.58	1.89	AKT3,GRB2,JAK2,PIK3CA,PIK3CD,SOCS3,STAT3
EGF Signaling	2.55	2.449	AKT3,GRB2,ITPR1,PIK3CA,PIK3CD,STAT3
Erythropoietin Signaling	2.55	NA	AKT3,GRB2,JAK2,PIK3CA,PIK3CD,SOCS3,STAT5A

IL-3 Signaling	2.55	2.646	AKT3,GRB2,JAK2,PIK3CA,PIK3CD,STAT3,STAT5A
ERK/MAPK Signaling	2.53	1.508	ARAF,DOCK1,ELF4,GRB2,ITGA3,MYCN,PIK3CA,PIK3CD,PPP1R10,PXN,RPS6KA1,STAT3
IL-7 Signaling Pathway	2.51	1.134	AKT3,CDKN1B,GRB2,GSK3A,PIK3CA,PIK3CD,STAT5A
Antiproliferative Role of TOB in T Cell Signaling	2.49	NA	CDKN1B,PABPC1,PABPC4,RPS6KA1
1D-myo-inositol Hexakisphosphate Biosynthesis II (Mammalian)	2.49	0	INPPL1,SEC16A,SYNJ1,SYNJ2
Aryl Hydrocarbon Receptor Signaling	2.49	-1.89	AIP,ALDH3A2,CDKN1B,Gstm3,HSP90AB1,MDM2,MGST1,NFIB,RBL2,RXRB
Mouse Embryonic Stem Cell Pluripotency	2.47	2.121	AKT3,APC,GRB2,JAK2,LIFR,PIK3CA,PIK3CD,STAT3
FLT3 Signaling in Hematopoietic Progenitor Cells	2.42	1.89	AKT3,GRB2,PIK3CA,PIK3CD,RPS6KA1,STAT3,STAT5A
Docosahexaenoic Acid (DHA) Signaling	2.41	NA	AKT3,BID,GSK3A,PIK3CA,PIK3CD
Glucocorticoid Receptor Signaling	2.41	NA	A2M,AKT3,ANXA1,BAG1,CEBPA,GRB2,GTF2H1,HSP90AB1,JAK2,MAPK9,NFAT5,NR3C1,PIK3CA,PIK3CD,STAT3,STAT5A,TAT
Xenobiotic Metabolism Signaling	2.34	NA	AIP,ALDH3A2,CAMK2G,CYP2B6,CYP2C8,ESD,FMO1,Gstm3,HDAC5,HSP90AB1,Map3k7,MAPK9,MGST1,PIK3CA,PIK3CD
Myc Mediated Apoptosis Signaling	2.34	NA	AKT3,BID,GRB2,MAPK9,PIK3CA,PIK3CD
IL-17A Signaling in Airway Cells	2.3	1.633	AKT3,JAK2,MAPK9,PIK3CA,PIK3CD,STAT3
FGF Signaling	2.28	1.89	AKT3,FGFR3,GRB2,ITPR1,PIK3CA,PIK3CD,STAT3
Thrombopoietin Signaling	2.27	2.449	GRB2,JAK2,PIK3CA,PIK3CD,STAT3,STAT5A
Cell Cycle: G1/S Checkpoint Regulation	2.27	0	CDKN1B,E2F3,HDAC5,HDAC6,MDM2,RBL2
Glutamine Degradation I	2.26	NA	GLS,GLS2
Superpathway of D-myo-inositol (1,4,5)-trisphosphate Metabolism	2.16	0	INPPL1,SEC16A,SYNJ1,SYNJ2
ILK Signaling	2.15	1.265	ACTN4,AKT3,CDH1,DOCK1,FLNA,GSK3A,MAPK9,MYH10,PIK3CA,PIK3CD,PXN
Regulation of the Epithelial-Mesenchymal Transition Pathway	2.15	NA	AKT3,APC,ARAF,CDH1,FGFR3,GRB2,JAK2,PIK3CA,PIK3CD,STAT3,ZEB2
Sertoli Cell-Sertoli Cell Junction Signaling	2.14	NA	A2M,ACTN4,AKT3,CDH1,EPB41,EPN2,GSK3A,GUCY1B1,ITGA3,Map3k7,MAPK9
IL-15 Signaling	2.12	NA	AKT3,JAK2,PIK3CA,PIK3CD,STAT3,STAT5A
Glioma Signaling	2.12	1.342	AKT3,CAMK2G,E2F3,GRB2,MDM2,PIK3CA,PIK3CD,RBL2

PPARα/RXRα Activation	2.12	-2.333	AIP,APOA2,CD36,CKAP5,CYP2C8,GRB2,HSP90AB1,IL1R1,JAK2,MED12,SLC27A1
Actin Cytoskeleton Signaling	2.11	1.667	ACTN4,APC,CD14,DOCK1,FLNA,GRB2,ITGA3,MYH10,NCKAP1,PIK3CA,PIK3CD,PXN
Prostate Cancer Signaling	2.1	NA	AKT3,CDKN1B,GRB2,HSP90AB1,MDM2,PIK3CA,PIK3CD
Clathrin-mediated Endocytosis Signaling	2.1	NA	APOA2,EPS15,GAK,GRB2,MDM2,PICALM,PIK3CA,PIK3CD,SH3GL1,SYNJ1,TF
Role of NANOG in Mammalian Embryonic Stem Cell Pluripotency	2.1	2.646	AKT3,APC,GRB2,JAK2,LIFR,PIK3CA,PIK3CD,STAT3
Melanoma Signaling	2.1	2	AKT3,CDH1,MDM2,PIK3CA,PIK3CD
Estrogen Biosynthesis	2.1	-1.342	AKR1C3,CYP2A6 (includes others),CYP2B6,CYP2C8,HSD17B10
Glioblastoma Multiforme Signaling	2.09	2.333	AKT3,APC,CDKN1B,E2F3,GRB2,ITPR1,MDM2,PIK3CA,PIK3CD,TSC1
Small Cell Lung Cancer Signaling	2.06	1.342	AKT3,BID,CDKN1B,PIK3CA,PIK3CD,RXRB
ATM Signaling	2.06	-1.633	BID,HERC2,MAPK9,MDM2,MDM4,SMC2,TRRAP
p53 Signaling	2.03	-0.378	AKT3,COQ8A,MDM2,MDM4,PIK3CA,PIK3CD,PML
Fc Epsilon RI Signaling	2.02	1.414	AKT3,GRB2,INPPL1,MAPK9,PIK3CA,PIK3CD,SYNJ1,SYNJ2
TREM1 Signaling	2.01	2.449	AKT3,GRB2,JAK2,STAT3,STAT5A,TLR1
Germ Cell-Sertoli Cell Junction Signaling	2.01	NA	A2M,ACTN4,CDH1,EPN2,ITGA3,Map3k7,MAPK9,PIK3CA,PIK3CD,PXN
Non-Small Cell Lung Cancer Signaling	1.93	2.236	AKT3,GRB2,ITPR1,PIK3CA,PIK3CD,RXRB
Epithelial Adherens Junction Signaling	1.9	NA	ACTN4,AKT3,APC,CDH1,CLIP1,EPN2,MAGI1,MYH10,PARD3
Phagosome Maturation	1.87	NA	ATP6V0A1,ATP6V0C,CANX,CTSC,CTSH,Dync1i2,M6PR,PRDX1,VPS39
VEGF Signaling	1.86	1.633	ACTN4,AKT3,EIF2S3,GRB2,PIK3CA,PIK3CD,PXN
Endometrial Cancer Signaling	1.79	1.342	AKT3,CDH1,GRB2,PIK3CA,PIK3CD
NRF2-mediated Oxidative Stress Response	1.78	NA	DNAJB2,DNAJC21,DNAJC5,FMO1,Gstm3,MAPK9,MGST1,PIK3CA,PIK3CD,PRDX1
STAT3 Pathway	1.77	-0.378	CISH,FGFR3,IL1R1,JAK2,MAPK9,SOCS2,SOCS3,STAT3
Type II Diabetes Mellitus Signaling	1.77	0.447	ACSL1,AKT3,CD36,MAPK9,PIK3CA,PIK3CD,SLC27A1,SOCS2,SOCS3
IL-2 Signaling	1.76	2.236	AKT3,GRB2,PIK3CA,PIK3CD,STAT5A

Estrogen Receptor Signaling	1.76	NA	GRB2,GTF2H1,IGFBP1,MED12,MED13L,MED15,NR3C1,TRRAP
Nitric Oxide Signaling in the Cardiovascular System	1.74	2.646	AKT3,GUCY1B1,GUCY2C,HSP90AB1,ITPR1,PIK3CA,PIK3CD
Oncostatin M Signaling	1.72	2	GRB2,JAK2,STAT3,STAT5A
CD40 Signaling	1.71	0.447	MAPK9,PIK3CA,PIK3CD,STAT3,TNFAIP3
Aldosterone Signaling in Epithelial Cells	1.69	NA	DNAJB2,DNAJC12,DNAJC2,DNAJC21,DNAJC5,HSP90AB1,ITPR1,PIK3CA,PIK3CD
iCOS-iCOSL Signaling in T Helper Cells	1.66	1.633	AKT3,CAMK2G,GRB2,ITPR1,NFAT5,PIK3CA,PIK3CD
Endocannabinoid Developing Neuron Pathway	1.66	0.378	AKT3,ARAF,CDKN1B,MAPK9,PIK3CA,PIK3CD,STAT3
Role of Macrophages, Fibroblasts and Endothelial Cells in Rheumatoid Arthritis	1.66	NA	AKT3,APC,CAMK2G,CEBPA,IL1R1,IL33,JAK2,MAPK9,NFAT5,PIK3CA,PIK3CD,SOCS3,STAT3,TLR1
Regulation of Cellular Mechanics by Calpain Protease	1.65	NA	ACTN4,CDKN1B,GRB2,ITGA3,PXN
2-ketoglutarate Dehydrogenase Complex	1.64	NA	DLST,OGDH
RAR Activation	1.63	NA	AKR1C3,AKT3,GTF2H1,JAK2,MAPK9,PIK3CA,PIK3CD,PML,RXRB,STAT5A
Th17 Activation Pathway	1.61	1.633	HSP90AB1,IL1R1,JAK2,NFAT5,SOCS3,STAT3
NGF Signaling	1.59	1.134	AKT3,GRB2,Map3k7,MAPK9,PIK3CA,PIK3CD,RPS6KA1
Bupropion Degradation	1.58	NA	CYP2A6 (includes others),CYP2B6,CYP2C8
Role of Tissue Factor in Cancer	1.56	NA	AKT3,ITGA3,JAK2,PIK3CA,PIK3CD,RPS6KA1,STAT5A
NF-κB Signaling	1.54	0.333	AKT3,ARAF,FGFR3,IL1R1,IL33,PIK3CA,PIK3CD,TLR1,TNFAIP3
Cell Cycle: G2/M DNA Damage Checkpoint Regulation	1.53	1	MDM2,MDM4,RPS6KA1,TRIP12
Natural Killer Cell Signaling	1.52	NA	AKT3,GRB2,INPPL1,PIK3CA,PIK3CD,SYNJ1,SYNJ2
IL-10 Signaling	1.51	NA	CD14,IL1R1,IL33,SOCS3,STAT3
CD28 Signaling in T Helper Cells	1.51	1.89	AKT3,GRB2,ITPR1,MAPK9,NFAT5,PIK3CA,PIK3CD
Role of p14/p19ARF in Tumor Suppression	1.5	NA	MDM2,PIK3CA,PIK3CD
PAK Signaling	1.5	0.816	GRB2,ITGA3,MAPK9,PIK3CA,PIK3CD,PXN
Molecular Mechanisms of Cancer	1.49	NA	AKT3,APC,BID,CAMK2G,CDH1,CDK9,CDKN1B,E2F3,GRB2,GSK3A,ITGA3,JAK2,MAPK9,MDM2,PIK3CA,PIK3CD
Renin-Angiotensin Signaling	1.48	1.633	GRB2,ITPR1,JAK2,MAPK9,PIK3CA,PIK3CD,STAT3
Neuregulin Signaling	1.46	1	AKT3,CDKN1B,GRB2,HSP90AB1,ITGA3,STAT5A

Protein Ubiquitination Pathway	1.45	NA	BAG1,DNAJB2,DNAJC12,DNAJC2,DNAJC21,DNAJC5,HSP90AB1,MDM2,NEDD4L,UBE2M,USP24,USP8
Glutathione Redox Reactions I	1.43	NA	GPX1,GPX4,MGST1
Angiopoietin Signaling	1.43	NA	AKT3,GRB2,PIK3CA,PIK3CD,STAT5A
Ceramide Degradation	1.43	NA	ACER2,ASAH1
Systemic Lupus Erythematosus In B Cell Signaling Pathway	1.42	1.732	AKT3,CD72,GRB2,IL33,INPPL1,JAK2,NFAT5,PIK3CA,PIK3CD,STAT3,SYNJ1,SYNJ2
PPAR Signaling	1.41	-1.633	AIP,GRB2,HSP90AB1,IL1R1,IL33,STAT5A
Estrogen-Dependent Breast Cancer Signaling	1.41	2	AKT3,HSD17B10,PIK3CA,PIK3CD,STAT5A
VDR/RXR Activation	1.39	NA	CD14,CDKN1B,CEBPA,IGFBP1,RXRB
GDNF Family Ligand-Receptor Interactions	1.39	1	GRB2,ITPR1,MAPK9,PIK3CA,PIK3CD
3-phosphoinositide Degradation	1.38	0	INPP4A,INPPL1,MTM1,PPP1R16B,SIRPA,SOCS3,SYNJ1,SYNJ2
IL-17 Signaling	1.37	NA	AKT3,JAK2,MAPK9,PIK3CA,PIK3CD
Superpathway of Inositol Phosphate Compounds	1.37	1.265	INPPL1,PI4KB,PIK3CA,PIK3CD,PPP1R16B,SEC16A,SIRPA,SOCS3,SYNJ1,SYNJ2
PD-1, PD-L1 cancer immunotherapy pathway	1.36	-1.633	AKT3,CDKN1B,JAK2,PIK3CA,PIK3CD,STAT5A
Production of Nitric Oxide and Reactive Oxygen Species in Macrophages	1.35	1	AKT3,APOA2,JAK2,Map3k7,MAPK9,PIK3CA,PIK3CD,PPP1R10,SIRPA
Antiproliferative Role of Somatostatin Receptor 2	1.35	NA	CDKN1B,GUCY1B1,GUCY2C,PIK3CA,PIK3CD
Role of IL-17A in Arthritis	1.35	NA	MAPK9,PIK3CA,PIK3CD,RPS6KA1
HMGB1 Signaling	1.34	1.134	AKT3,IL1R1,IL33,Kat6b,KAT7,MAPK9,PIK3CA,PIK3CD
Th2 Pathway	1.33	2.449	GRB2,IL33,JAK2,PIK3CA,PIK3CD,SOCS3,STAT5A
Sumoylation Pathway	1.33	-1	CDH1,CEBPA,MAPK9,MDM2,NR3C1,PML
Colorectal Cancer Metastasis Signaling	1.32	1.897	AKT3,APC,CDH1,GRB2,JAK2,MAPK9,MSH3,PIK3CA,PIK3CD,STAT3,TLR1
Tec Kinase Signaling	1.32	1.414	GTF2I,ITGA3,JAK2,MAPK9,PIK3CA,PIK3CD,STAT3,STAT5A

Table 24. Significant Pathways for differentially expressed transcripts in ^{28}Si vs. non-irradiated control at 9 months.

Ingenuity Canonical Pathways	**-log$_{10}$(p-value)**	**z-score**	**Molecules**

Acute Phase Response Signaling	6	-2.53	C2,C4A/C4B,CP,HP,IL18,ITIH3,MAPK9,NFKB1,NR3C1,PIK3CD,PIK3CG,SAA1,Saa3,SERPINA1,SERPINE1,TCF3,TF
LXR/RXR Activation	5.1	0.302	C4A/C4B,CD36,IL18,LYZ,MLXIPL,NCOR2,NFKB1,NR1H2,RXRA,S100A8,SAA1,SERPINA1,TF
Adipogenesis pathway	4.18	NA	ERCC3,FGFR2,FGFR3,HDAC6,HDAC7,KDM1A,KMT2B,PPIP5K1,RPS6KA1,SAP130,SETDB1,SIN3A
LPS/IL-1 Mediated Inhibition of RXR Function	4.08	-0.707	ABCB11,ACSL1,ACSL4,ALAS1,CYP2B6,CYP2C8,GSTM4,GSTM5,Gstm6,IL18,LIPC,MAPK9,NR1H2,PPARGC1B,RXRA,SLC27A1
PPARα/RXRα Activation	3.76	1.265	ADCY4,ADIPOR2,CD36,CKAP5,CYP2C8,HELZ2,HSP90AB1,MED12,MED23,NCOR2,NFKB1,PRKAA1,RXRA,SLC27A1
Germ Cell-Sertoli Cell Junction Signaling	3.68	NA	ACTN4,CDH1,CTNND1,EPN2,FNBP1,MAP3K13,MAPK9,MYO7A,PIK3C3,PIK3CD,PIK3CG,PXN,RHOT1
Role of IL-17A in Arthritis	3.55	NA	ATF2,MAPK9,NFKB1,PIK3C3,PIK3CD,PIK3CG,RPS6KA1
Small Cell Lung Cancer Signaling	3.54	0.447	APAF1,MYC,NFKB1,PIK3C3,PIK3CD,PIK3CG,RXRA,SIN3A
IL-12 Signaling and Production in Macrophages	3.51	NA	IL18,LYZ,MAPK9,NFKB1,PIK3C3,PIK3CD,PIK3CG,PRKD3,RXRA,S100A8,SERPINA1
FXR/RXR Activation	3.49	NA	ABCB11,C4A/C4B,FETUB,IL18,LIPC,MAPK9,MLXIPL,RXRA,SAA1,SERPINA1,TF
Type II Diabetes Mellitus Signaling	3.41	0.333	ACSL1,ACSL4,ADIPOR2,CD36,MAPK9,NFKB1,PIK3C3,PIK3CD,PIK3CG,PRKAA1,PRKD3,SLC27A1
Reelin Signaling in Neurons	3.38	NA	ARHGEF2,ARHGEF3,ITGAL,MAPK8IP3,MAPK9,PIK3C3,PIK3CD,PIK3CG
Xenobiotic Metabolism Signaling	3.38	NA	ARNT,CYP2B6,CYP2C8,ESD,GSTM4,GSTM5,Gstm6,HSP90AB1,MAP3K13,MAPK9,NCOR2,NFKB1,PIK3C3,PIK3CD,PIK3CG,PRKD3,RXRA
ILK Signaling	3.27	-1.387	ACTN4,ATF2,CDH1,FNBP1,MAPK9,MYC,MYH10,NFKB1,PIK3C3,PIK3CD,PIK3CG,PXN,RHOT1
Apelin Pancreas Signaling Pathway	3.27	0	MAPK9,NFKB1,PIK3C3,PIK3CD,PIK3CG,PRKAA1
Apelin Endothelial Signaling Pathway	3.26	0.632	ADCY4,ARNT,Calm1 (includes others),MAPK9,NFKB1,PIK3

			C3,PIK3CD,PIK3CG,PRKAA1,PRKD3
Production of Nitric Oxide and Reactive Oxygen Species in Macrophages	3.25	-1.387	FNBP1,LYZ,MAP3K13,MAPK9,NFKB1,PIK3C3,PIK3CD,PIK3CG,PRKD3,RHOT1,S100A8,SERPINA1,TYK2
Chronic Myeloid Leukemia Signaling	3.22	NA	HDAC6,HDAC7,MECOM,MYC,NFKB1,PIK3C3,PIK3CD,PIK3CG,SIN3A
SAPK/JNK Signaling	3.22	0	ATF2,GNB1,MAP3K13,MAPK8IP3,MAPK9,MINK1,PIK3C3,PIK3CD,PIK3CG
Clathrin-mediated Endocytosis Signaling	3.21	NA	AP1G2,CD2AP,DNM2,EPS15,LYZ,MYO6,PICALM,PIK3C3,PIK3CD,PIK3CG,S100A8,SERPINA1,TF
Aryl Hydrocarbon Receptor Signaling	3.18	-1.134	APAF1,ARNT,GSTM4,GSTM5,Gstm6,HSP90AB1,MYC,NCOR2,NFIX,NFKB1,RXRA
IL-8 Signaling	3.06	-1.508	CDH1,FNBP1,GNB1,IRAK3,ITGAV,MAPK9,NFKB1,PIK3C3,PIK3CD,PIK3CG,PLD1,PRKD3,RHOT1
Leukocyte Extravasation Signaling	3.05	0	ACTN4,CLDN12,CTNND1,ITGAL,MAPK9,PIK3C3,PIK3CD,PIK3CG,PRKD3,PXN,RAPGEF4,SIPA1,TEC
Adrenomedullin signaling pathway	3.03	0.277	ADCY4,ARNT,Calm1 (includes others),CFH,GUCY2C,IL18,MAPK9,NFKB1,PIK3C3,PIK3CD,PIK3CG,RXRA,SHF
Pancreatic Adenocarcinoma Signaling	2.98	-1.134	BRCA2,MAPK9,NFKB1,PIK3C3,PIK3CD,PIK3CG,PLD1,SIN3A,TYK2
Nitric Oxide Signaling in the Cardiovascular System	2.95	0.333	Calm1 (includes others),GUCY2C,HSP90AB1,PDE1A,PIK3C3,PIK3CD,PIK3CG,PRKAA1,PRKD3
TR/RXR Activation	2.94	NA	COL6A3,DIO1,HP,NCOR2,PIK3C3,PIK3CD,PIK3CG,RXRA
Phospholipase C Signaling	2.9	1.941	ADCY4,ARHGEF2,ARHGEF3,ATF2,Calm1 (includes others),FCGR2A,FNBP1,GNB1,HDAC6,HDAC7,NFAT5,NFKB1,PLD1,PRKD3,RHOT1
mTOR Signaling	2.82	-1.897	ATG13,EIF4G1,EIF4G3,FNBP1,PIK3C3,PIK3CD,PIK3CG,PLD1,PRKAA1,PRKD3,RHOT1,RPS19,RPS6KA1
Tec Kinase Signaling	2.77	-0.632	FNBP1,GNB1,MAPK9,NFKB1,PIK3C3,PIK3CD,PIK3CG,PRKD3,RHOT1,TEC,TYK2
GP6 Signaling Pathway	2.65	1	ADAM10,Calm1 (includes others),COL4A1,COL4A5,COL6A3,PIK3C3,PIK3CD,PIK3CG,PRKD3

Molecular Mechanisms of Cancer	2.62	NA	ADCY4,APAF1,ARHGEF2,ARHGEF3,CDH1,CDK9,CTNND1,FNBP1,MAPK9,MYC,NFKB1,PIK3C3,PIK3CD,PIK3CG,PRKD3,RHOT1,SIN3A,TCF3,TYK2
Endocannabinoid Cancer Inhibition Pathway	2.61	0	ADCY4,ATF2,CDH1,MYC,PIK3C3,PIK3CD,PIK3CG,PRKAA1,TCF3,TCF7L2
Renin-Angiotensin Signaling	2.58	0.707	ADCY4,ATF2,MAPK9,NFKB1,PIK3C3,PIK3CD,PIK3CG,PRKD3,SHF
Colorectal Cancer Metastasis Signaling	2.58	-0.535	ADCY4,CDH1,FNBP1,GNB1,MAPK9,MYC,NFKB1,PIK3C3,PIK3CD,PIK3CG,RHOT1,TCF3,TCF7L2,TYK2
LPS-stimulated MAPK Signaling	2.56	-0.378	ATF2,MAPK9,NFKB1,PIK3C3,PIK3CD,PIK3CG,PRKD3
NF-κB Activation by Viruses	2.53	-0.378	ITGAL,ITGAV,NFKB1,PIK3C3,PIK3CD,PIK3CG,PRKD3
IL-23 Signaling Pathway	2.49	-0.447	NFKB1,PIK3C3,PIK3CD,PIK3CG,TYK2
Paxillin Signaling	2.44	-0.816	ACTN4,ITGAL,ITGAV,MAPK9,PIK3C3,PIK3CD,PIK3CG,PXN
CD40 Signaling	2.43	0	MAPK9,NFKB1,PIK3C3,PIK3CD,PIK3CG,TNFAIP3
Myc Mediated Apoptosis Signaling	2.43	NA	APAF1,MAPK9,MYC,PIK3C3,PIK3CD,PIK3CG
IL-4 Signaling	2.42	NA	HLA-A,NFAT5,NR3C1,PIK3C3,PIK3CD,PIK3CG,TYK2
IL-17A Signaling in Airway Cells	2.4	-0.816	MAPK9,NFKB1,PIK3C3,PIK3CD,PIK3CG,TYK2
HOTAIR Regulatory Pathway	2.39	-0.632	CDH1,KDM1A,MYC,NFKB1,PIK3C3,PIK3CD,PIK3CG,SETDB1,TCF3,TCF7L2
Role of p14/p19ARF in Tumor Suppression	2.39	0	PIK3C3,PIK3CD,PIK3CG,UBTF
Huntington's Disease Signaling	2.38	1.134	APAF1,ATF2,DNM2,GNB1,HDAC6,HDAC7,MAPK9,NCOR2,PIK3C3,PIK3CD,PIK3CG,PRKD3,SIN3A
RANK Signaling in Osteoclasts	2.36	0.378	Calm1 (includes others),MAP3K13,MAPK9,NFKB1,PIK3C3,PIK3CD,PIK3CG
P2Y Purigenic Receptor Signaling Pathway	2.36	1	ADCY4,ATF2,GNB1,MYC,NFKB1,PIK3C3,PIK3CD,PIK3CG,PRKD3
Signaling by Rho Family GTPases	2.35	-1.508	ARHGEF2,ARHGEF3,CDH1,FNBP1,GNB1,MAPK9,NFKB1,PARD3,PIK3C3,PIK3CD,PIK3CG,PLD1,RHOT1
Virus Entry via Endocytic Pathways	2.34	NA	AP1G2,DNM2,HLA-A,ITGAL,PIK3C3,PIK3CD,PIK3CG,PRKD3
B Cell Receptor Signaling	2.34	1	ATF2,Calm1 (includes others),FCGR2A,MAP3K13,MAPK9,NFAT5,NFKB1,PIK3C3,PIK3CD,PIK3CG,TCF3

HGF Signaling	2.32	0	ATF2,MAP3K13,MAPK9,PIK3C3,PIK3CD,PIK3CG,PRKD3,PXN
Gαq Signaling	2.31	0	Calm1 (includes others),FNBP1,GNB1,NFKB1,PIK3C3,PIK3CD,PIK3CG,PLD1,PRKD3,RHOT1
Acute Myeloid Leukemia Signaling	2.28	-0.378	MYC,NFKB1,PIK3C3,PIK3CD,PIK3CG,TCF3,TCF7L2
PXR/RXR Activation	2.27	NA	ABCB11,ALAS1,CYP2B6,CYP2C8,NR3C1,RXRA
Systemic Lupus Erythematosus In B Cell Signaling Pathway	2.26	0	Calm1 (includes others),FCGR2A,IL18,MCL1,MYC,NFAT5,NFKB1,PIK3C3,PIK3CD,PIK3CG,PRKD3,SHF,TBK1,TYK2
Prostate Cancer Signaling	2.21	NA	ATF2,HSP90AB1,NFKB1,PIK3C3,PIK3CD,PIK3CG,SIN3A
NGF Signaling	2.19	0	ATF2,MAP3K13,MAPK9,NFKB1,PIK3C3,PIK3CD,PIK3CG,RPS6KA1
eNOS Signaling	2.19	0.378	ADCY4,AQP8,Calm1 (includes others),DNM2,HSP90AB1,PIK3C3,PIK3CD,PIK3CG,PRKAA1,PRKD3
IL-9 Signaling	2.18	0	NFKB1,PIK3C3,PIK3CD,PIK3CG
Thyroid Cancer Signaling	2.18	NA	CDH1,MYC,RXRA,TCF3,TCF7L2
UVB-Induced MAPK Signaling	2.18	-0.447	MAPK9,PIK3C3,PIK3CD,PIK3CG,PRKD3
CXCR4 Signaling	2.14	-1.265	ADCY4,FNBP1,GNB1,MAPK9,PIK3C3,PIK3CD,PIK3CG,PRKD3,PXN,RHOT1
Caveolar-mediated Endocytosis Signaling	2.13	NA	DNM2,FLOT1,FLOT2,HLA-A,ITGAL,ITGAV
Glioma Invasiveness Signaling	2.13	-1.633	FNBP1,ITGAV,PIK3C3,PIK3CD,PIK3CG,RHOT1
fMLP Signaling in Neutrophils	2.13	1.414	Calm1 (includes others),GNB1,NFAT5,NFKB1,PIK3C3,PIK3CD,PIK3CG,PRKD3
Macropinocytosis Signaling	2.1	0.447	ABI1,ACTN4,PIK3C3,PIK3CD,PIK3CG,PRKD3
CD28 Signaling in T Helper Cells	2.09	0.378	Calm1 (includes others),HLA-A,MAPK9,NFAT5,NFKB1,PIK3C3,PIK3CD,PIK3CG
Phagosome Formation	2.09	NA	FCGR2A,FNBP1,MARCO,PIK3C3,PIK3CD,PIK3CG,PRKD3,RHOT1
Lymphotoxin β Receptor Signaling	2.08	-0.447	APAF1,NFKB1,PIK3C3,PIK3CD,PIK3CG
NF-κB Signaling	2.07	0	FGFR2,FGFR3,IL18,IRAK3,NFKB1,PIK3C3,PIK3CD,PIK3CG,TBK1,TNFAIP3
Fatty Acid Activation	2.05	NA	ACSL1,ACSL4,SLC27A1
Mouse Embryonic Stem Cell Pluripotency	2.02	-1.134	MYC,PIK3C3,PIK3CD,PIK3CG,TCF3,TCF7L2,TYK2

Epithelial Adherens Junction Signaling	2.02	NA	ACTN4,CDH1,CTNND1,EPN2,MYH10,MYO7A,PARD3,TCF3,TCF7L2
IL-17 Signaling	2	NA	ATF2,MAPK9,NFKB1,PIK3C3,PIK3CD,PIK3CG
Thrombin Signaling	1.97	-0.632	ADCY4,ARHGEF2,ARHGEF3,FNBP1,GNB1,NFKB1,PIK3C3,PIK3CD,PIK3CG,PRKD3,RHOT1
Gα12/13 Signaling	1.97	0	CDH1,MAPK9,NFKB1,PIK3C3,PIK3CD,PIK3CG,PXN,TEC
Complement System	1.96	-1	C2,C4A/C4B,CFH,MASP2
Stearate Biosynthesis I (Animals)	1.95	1.342	ACOT9,ACSL1,ACSL4,ELOVL1,SLC27A1
Role of NFAT in Regulation of the Immune Response	1.95	1.667	ATF2,Calm1 (includes others),FCGR2A,GNB1,HLA-A,NFAT5,NFKB1,PIK3C3,PIK3CD,PIK3CG
Cardiac Hypertrophy Signaling (Enhanced)	1.94	0.447	ADCY4,ATF2,Calm1 (includes others),DIAPH1,FGFR2,FGFR3,GNB1,HDAC6,HDAC7,IL18,MAP3K13,MAPK9,MYC,NFAT5,NFKB1,PDE1A,PIK3C3,PIK3CD,PIK3CG,PRKD3
Telomerase Signaling	1.94	-0.447	HDAC6,HDAC7,HSP90AB1,MYC,PIK3C3,PIK3CD,PIK3CG
Mitochondrial L-carnitine Shuttle Pathway	1.93	NA	ACSL1,ACSL4,SLC27A1
CNTF Signaling	1.92	-1.342	PIK3C3,PIK3CD,PIK3CG,RPS6KA1,TYK2
Nur77 Signaling in T Lymphocytes	1.92	NA	APAF1,Calm1 (includes others),HLA-A,RXRA,SIN3A
Cardiac Hypertrophy Signaling	1.9	0	ADCY4,ATF2,Calm1 (includes others),FNBP1,GNB1,MAP3K13,MAPK9,PIK3C3,PIK3CD,PIK3CG,RHOT1,RPS6KA1
Prolactin Signaling	1.9	-0.447	MYC,NR3C1,PIK3C3,PIK3CD,PIK3CG,PRKD3
Sumoylation Pathway	1.89	-0.447	CDH1,FNBP1,KDM1A,MAPK9,NFKB1,NR3C1,RHOT1
Osteoarthritis Pathway	1.89	0.333	ACVRL1,ATF2,FGFR3,MYBBP1A,NFKB1,PRKAA1,S100A8,SIK3,SLC39A8,TCF3,TCF7L2
Proline Degradation	1.87	NA	LOC102724788/PRODH,PRODH2
T Cell Receptor Signaling	1.87	NA	Calm1 (includes others),NFAT5,NFKB1,PIK3C3,PIK3CD,PIK3CG,TEC
Endometrial Cancer Signaling	1.86	-0.447	CDH1,MYC,PIK3C3,PIK3CD,PIK3CG
Regulation of the Epithelial-Mesenchymal Transition Pathway	1.86	NA	CDH1,FGFR2,FGFR3,NFKB1,PIK3C3,PIK3CD,PIK3CG,TCF3,TCF7L2,TYK2

HMGB1 Signaling	1.85	-1.414	FNBP1,IL18,MAPK9,NFKB1,PIK3C3,PIK3CD,PIK3CG,RHOT1,SERPINE1
Protein Kinase A Signaling	1.84	2.309	ADCY4,AKAP1,ANAPC5,ATF2,Calm1 (includes others),DUSP3,EYA3,GNB1,MYH10,NFAT5,NFKB1,PDE1A,PRKD3,PTPN21,PXN,TCF3,TCF7L2
Activation of IRF by Cytosolic Pattern Recognition Receptors	1.83	-0.447	ATF2,DDX58,MAPK9,NFKB1,TBK1
Role of Macrophages, Fibroblasts and Endothelial Cells in Rheumatoid Arthritis	1.81	NA	ATF2,Calm1 (includes others),IL18,IRAK3,MAPK9,MYC,NFAT5,NFKB1,PIK3C3,PIK3CD,PIK3CG,PRKD3,TCF3,TCF7L2
Glutamate Receptor Signaling	1.81	NA	Calm1 (includes others),GNB1,GRIK5,SLC1A4,SLC38A1
Aldosterone Signaling in Epithelial Cells	1.8	0	DNAJB2,DNAJC12,DNAJC2,HSP90AB1,HSPA4L,PIK3C3,PIK3CD,PIK3CG,PRKD3
FGF Signaling	1.8	0	ATF2,FGFR2,FGFR3,PIK3C3,PIK3CD,PIK3CG
ErbB2-ErbB3 Signaling	1.78	-1.342	MYC,PIK3C3,PIK3CD,PIK3CG,TYK2
γ-linolenate Biosynthesis II (Animals)	1.77	NA	ACSL1,ACSL4,SLC27A1
Choline Biosynthesis III	1.77	NA	CHPT1,PCYT1A,PLD1
Opioid Signaling Pathway	1.76	0.577	ADCY4,AP1G2,ATF2,Calm1 (includes others),GNB1,GRK6,MYC,NFKB1,PDE1A,PIK3CG,PRKD3,RPS6KA1
iCOS-iCOSL Signaling in T Helper Cells	1.76	1.134	Calm1 (includes others),HLA-A,NFAT5,NFKB1,PIK3C3,PIK3CD,PIK3CG
Endocannabinoid Developing Neuron Pathway	1.76	-0.378	ADCY4,ATF2,GNB1,MAPK9,PIK3C3,PIK3CD,PIK3CG
RAR Activation	1.75	NA	ADCY4,ERCC3,MAPK9,NCOR2,NFKB1,PIK3CD,PIK3CG,PRKD3,RXRA,TRIM24
Endothelin-1 Signaling	1.75	-0.632	ADCY4,GUCY2C,MAPK9,MYC,PIK3C3,PIK3CD,PIK3CG,PLD1,PRKD3,SHF
Docosahexaenoic Acid (DHA) Signaling	1.74	NA	APAF1,PIK3C3,PIK3CD,PIK3CG
Sirtuin Signaling Pathway	1.74	0.302	ACSS2,ADAM10,ATG13,CDH1,CYC1,GLUD1,MYC,NDUFAF1,NDUFV1,NFKB1,NR1H2,PFKM,PRKAA1,SIRT7
Thrombopoietin Signaling	1.73	-0.447	MYC,PIK3C3,PIK3CD,PIK3CG,PRKD3
Fatty Acid β-oxidation I	1.71	1	ACSL1,ACSL4,SCP2,SLC27A1
Acetate Conversion to Acetyl-CoA	1.68	NA	ACSL1,ACSS2
Remodeling of Epithelial Adherens Junctions	1.68	NA	ACTN4,CBLL1,CDH1,CTNND1,DNM2
SPINK1 General Cancer Pathway	1.68	-0.447	Mt2,PIK3C3,PIK3CD,PIK3CG,TYK2

IL-15 Production	1.67	NA	AATK,DYRK1A,FGFR2,FGFR3,NFKB1,TEC,TYK2
GNRH Signaling	1.65	0.707	ADCY4,ATF2,Calm1 (includes others),GNB1,MAP3K13,MAPK9,NFKB1,PRKD3,PXN
Melanocyte Development and Pigmentation Signaling	1.64	0	ADCY4,ATF2,PIK3C3,PIK3CD,PIK3CG,RPS6KA1
Bupropion Degradation	1.63	NA	CYP2B6,CYP2C8,POR
Th1 Pathway	1.63	-0.378	HLA-A,IL18,NFKB1,PIK3C3,PIK3CD,PIK3CG,TYK2
iNOS Signaling	1.62	NA	Calm1 (includes others),IRAK3,NFKB1,TYK2
Iron homeostasis signaling pathway	1.62	NA	ARNT,ATP6AP1,CP,FLVCR1,HP,TCIRG1,TF,TYK2
Cholecystokinin/Gastrin-mediated Signaling	1.62	-1.134	ATF2,FNBP1,IL18,MAPK9,PRKD3,PXN,RHOT1
IL-15 Signaling	1.61	NA	NFKB1,PIK3C3,PIK3CD,PIK3CG,TYK2
IL-6 Signaling	1.6	-0.378	IL18,MAPK9,MCL1,NFKB1,PIK3C3,PIK3CD,PIK3CG
p53 Signaling	1.6	0.816	APAF1,COQ8A,PIK3C3,PIK3CD,PIK3CG,STAG1
Ephrin A Signaling	1.59	NA	ADAM10,PIK3C3,PIK3CD,PIK3CG
Role of Pattern Recognition Receptors in Recognition of Bacteria and Viruses	1.59	0.378	DDX58,IL18,MAPK9,NFKB1,PIK3C3,PIK3CD,PIK3CG,PRKD3
Dendritic Cell Maturation	1.58	0.333	ATF2,FCGR2A,HLA-A,IL18,MAPK9,NFKB1,PIK3C3,PIK3CD,PIK3CG
Apoptosis Signaling	1.58	0	APAF1,LMNA,MCL1,NFKB1,RPS6KA1,SPTAN1
Glucocorticoid Receptor Signaling	1.57	NA	BAG1,ERCC3,HSP90AB1,MAPK9,NCOR2,NFAT5,NFKB1,NR3C1,PIK3C3,PIK3CD,PIK3CG,PRKAA1,SERPINE1,TAF1
CREB Signaling in Neurons	1.57	1	ADCY4,ATF2,Calm1 (includes others),GNB1,GRIK5,PIK3C3,PIK3CD,PIK3CG,PRKD3,RPS6KA1
Integrin Signaling	1.57	-1.265	ACTN4,ARF4,FNBP1,ITGAL,ITGAV,PIK3C3,PIK3CD,PIK3CG,PXN,RHOT1
Growth Hormone Signaling	1.54	-0.447	PIK3C3,PIK3CD,PIK3CG,PRKD3,RPS6KA1
Pyridoxal 5'-phosphate Salvage Pathway	1.54	0.447	DAPK1,DYRK1A,GRK6,MAPK9,PRKAA1
Relaxin Signaling	1.52	0.378	ADCY4,GNB1,GUCY2C,NFKB1,PDE1A,PIK3C3,PIK3CD,PIK3CG
Neuroinflammation Signaling Pathway	1.51	-0.577	ATF2,BACE1,HLA-A,IL18,IRAK3,MAPK9,NFAT5,NFKB1,PIK3C3,PIK3CD,PIK3CG,TBK1,TYK2
TNFR2 Signaling	1.51	NA	NFKB1,TBK1,TNFAIP3
Melanoma Signaling	1.51	NA	CDH1,PIK3C3,PIK3CD,PIK3CG

NRF2-mediated Oxidative Stress Response	1.5	NA	DNAJB2,GSTM4,GSTM5,Gstm6,MAPK9,PIK3C3,PIK3CD,PIK3CG,PRKD3
Role of NFAT in Cardiac Hypertrophy	1.5	0.707	ADCY4,Calm1 (includes others),GNB1,HDAC6,HDAC7,MAPK9,PIK3C3,PIK3CD,PIK3CG,PRKD3
Apelin Cardiomyocyte Signaling Pathway	1.49	-0.447	ARNT,MAPK9,PIK3C3,PIK3CD,PIK3CG,PRKD3
CD27 Signaling in Lymphocytes	1.48	1	APAF1,MAP3K13,MAPK9,NFKB1
Estrogen-Dependent Breast Cancer Signaling	1.48	0.447	ATF2,NFKB1,PIK3C3,PIK3CD,PIK3CG
Assembly of RNA Polymerase III Complex	1.46	NA	GTF3C1,GTF3C5
Erythropoietin Signaling	1.46	NA	NFKB1,PIK3C3,PIK3CD,PIK3CG,PRKD3
Non-Small Cell Lung Cancer Signaling	1.46	NA	PIK3C3,PIK3CD,PIK3CG,RXRA,SIN3A
Amyotrophic Lateral Sclerosis Signaling	1.45	0	ALS2,APAF1,GRIK5,PIK3C3,PIK3CD,PIK3CG
VEGF Signaling	1.45	-0.447	ACTN4,ARNT,PIK3C3,PIK3CD,PIK3CG,PXN
Sertoli Cell-Sertoli Cell Junction Signaling	1.45	NA	ACTN4,ATF2,CDH1,CLDN12,EPN2,MAP3K13,MAPK9,MYO7A,SPTAN1
Role of Osteoblasts, Osteoclasts and Chondrocytes in Rheumatoid Arthritis	1.44	NA	Calm1 (includes others),IL18,MAPK9,NFAT5,NFKB1,PIK3C3,PIK3CD,PIK3CG,TCF3,TCF7L2
4-1BB Signaling in T Lymphocytes	1.44	NA	ATF2,MAPK9,NFKB1
PD-1, PD-L1 cancer immunotherapy pathway	1.44	0.816	HLA-A,PDCD4,PIK3C3,PIK3CD,PIK3CG,TYK2
JAK/Stat Signaling	1.44	-0.447	NFKB1,PIK3C3,PIK3CD,PIK3CG,TYK2
IL-7 Signaling Pathway	1.44	-0.447	MCL1,MYC,PIK3C3,PIK3CD,PIK3CG
EIF2 Signaling	1.43	-0.378	ATF5,EIF2AK4,EIF4G1,EIF4G3,MYC,PIK3C3,PIK3CD,PIK3CG,RPL18A,RPS19
Antiproliferative Role of Somatostatin Receptor 2	1.42	0	GNB1,GUCY2C,PIK3C3,PIK3CD,PIK3CG
Neurotrophin/TRK Signaling	1.42	-0.447	ATF2,PIK3C3,PIK3CD,PIK3CG,RPS6KA1
Estrogen Receptor Signaling	1.41	NA	ERCC3,MED12,MED23,NCOR2,NR3C1,TAF1,TRRAP
PEDF Signaling	1.4	-0.447	NFKB1,PIK3C3,PIK3CD,PIK3CG,TCF7L2
FLT3 Signaling in Hematopoietic Progenitor Cells	1.38	-0.447	ATF2,PIK3C3,PIK3CD,PIK3CG,RPS6KA1
DNA Methylation and Transcriptional Repression Signaling	1.37	NA	MTA1,SAP130,SIN3A
Human Embryonic Stem Cell Pluripotency	1.37	NA	FGFR2,FGFR3,PIK3C3,PIK3CD,PIK3CG,TCF3,TCF7L2
HER-2 Signaling in Breast Cancer	1.36	NA	PARD3,PIK3C3,PIK3CD,PIK3CG,PRKD3
Ovarian Cancer Signaling	1.36	NA	BRCA2,PIK3C3,PIK3CD,PIK3CG,SIN3A,TCF3,TCF7L2
PI3K Signaling in B Lymphocytes	1.33	1.134	ATF2,ATF5,Calm1 (includes others),NFAT5,NFKB1,PIK3CD,PIK3CG

Rac Signaling	1.32	-0.447	NFKB1,PARD3,PIK3C3,PIK 3CD,PIK3CG,PLD1
Salvage Pathways of Pyrimidine Ribonucleotides	1.32	0	AK4,DAPK1,DYRK1A,GRK 6,MAPK9,PRKAA1
Breast Cancer Regulation by Stathmin1	1.31	NA	ADCY4,ARHGEF2,ARHGE F3,Calm1 (includes others),GNB1,PIK3C3,PIK3C D,PIK3CG,PRKD3
MIF-mediated Glucocorticoid Regulation	1.31	NA	CD74,NFKB1,NR3C1

Table 25. Significant Pathways for differentially expressed transcripts in ^{28}Si vs. non-irradiated control at 12 months.

6.4.6 IDENTIFICATION OF DYSREGULATED MOLECULAR PATHWAYS CORRESPONDING TO UNANNOTATED TRANSCRIPTS ASSOCIATED WITH ^{28}SI IRRADIATION, USING SOM

The above IPA analysis (Figure 15) resulted in a collection of 81 statistically significant high-quality functionally unannotated transcripts across all time points from ^{28}Si irradiated mice (Table 13). To characterize the unannotated transcripts, we obtained the $\log_2$ (fold change) expression values of significantly differentially expressed transcripts from ^{28}Si irradiation compared to non-irradiated control across 5 time points and applied the SOM machine learning algorithm. We next identified the modules from SOMs which contained the majority of unannotated transcripts and combined them to form larger clusters of similar transcription patterns for functionality analysis using IPA. We compared the identified 12 clusters across 5 time points using IPA (Figure 16f). Figure 6f shows the most significant pathways across all clusters. The activation z-scores were predicted for some of the clusters based on our observed data and the available literature. Even though the directionality could not be determined for some of these pathways, the significant

pathways included B cell signaling, hepatic fibrosis signaling, tec kinase signaling, neuroinflammation signaling, LXR/RXR activation, phospholipase C signaling, and the senescence pathway. A complete list of unannotated transcript ENSMBL IDs with their corresponding module numbers is provided in Table 26.

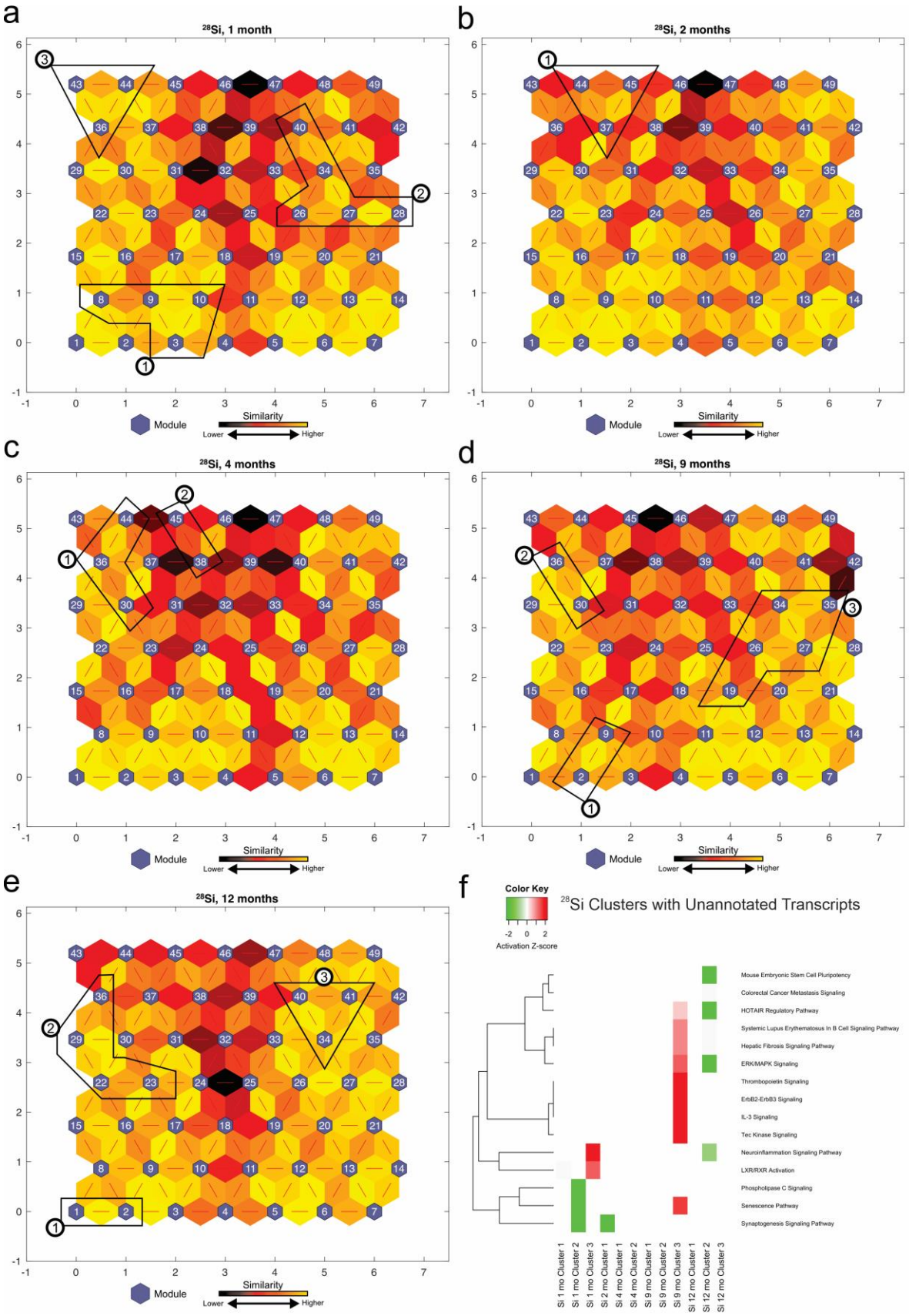
a
28Si, 1 month
b
28Si, 2 months
c
28Si, 4 months
d
28Si, 9 months
e
28Si, 12 months
Module
Similarity
Lower
Higher
f
Color Key
-2 0 2
Activation Z-score
28Si Clusters with Unannotated Transcripts
Mouse Embryonic Stem Cell Pluripotency
Colorectal Cancer Metastasis Signaling
HOTAIR Regulatory Pathway
Systemic Lupus Erythematosus In B Cell Signaling Pathway
Hepatic Fibrosis Signaling Pathway
ERK/MAPK Signaling
Thrombopoietin Signaling
ErbB2-ErbB3 Signaling
IL-3 Signaling
Tec Kinase Signaling
Neuroinflammation Signaling Pathway
LXR/RXR Activation
Phospholipase C Signaling
Senescence Pathway
Synaptogenesis Signaling Pathway
Si 1 mo Cluster 1
Si 1 mo Cluster 2
Si 1 mo Cluster 3
Si 2 mo Cluster 1
Si 4 mo Cluster 1
Si 4 mo Cluster 2
Si 9 mo Cluster 1
Si 9 mo Cluster 2
Si 9 mo Cluster 3
Si 12 mo Cluster 1
Si 12 mo Cluster 2
Si 12 mo Cluster 3

Figure 16. ^{28}Si analysis of self-organizing maps for each time point.

(a,b,c,d,e) Kohonen Self-Organizing Map (SOM) was applied to the differentially expressed (DE) transcripts obtained from the RNA-Seq data to identify coherent patterns of transcript expression at each time point, as well as patterns within the unannotated transcripts. The SOM clusters transcripts in each module according to $\log_2$(fold change) of the expression values. SOM clustering analysis demonstrates the distances between correlated transcript groups. The small blue hexagons are modules comprising transcripts with similar $\log_2$(fold change) expression patterns. The numbers of transcripts in each module are provided in Figure 17. Neighboring modules are connected with a red line. The colors of the lines connecting the modules indicate the similarity between modules: Lighter colors represent higher similarity, and darker colors represent lower similarity. **(f)** Expression patterns of unannotated transcripts were identified, and the corresponding modules (represented in circled numbers) were further analyzed by IPA. Only the most significant pathways across all clusters are shown with available color-coded activation z-scores. Inhibitory, activation, or unknown directionality z-scores corresponds to green, red, and white respectively. The entries with white color indicate the directionality could not be predicted based on the available data, yet the pathway is significantly identified by pathway analysis. The goal of the IPA downstream effects analysis is to identify functional pathways whose activity is expected to be increased or decreased, given the observed expression changes in a user's dataset (see Methods.)

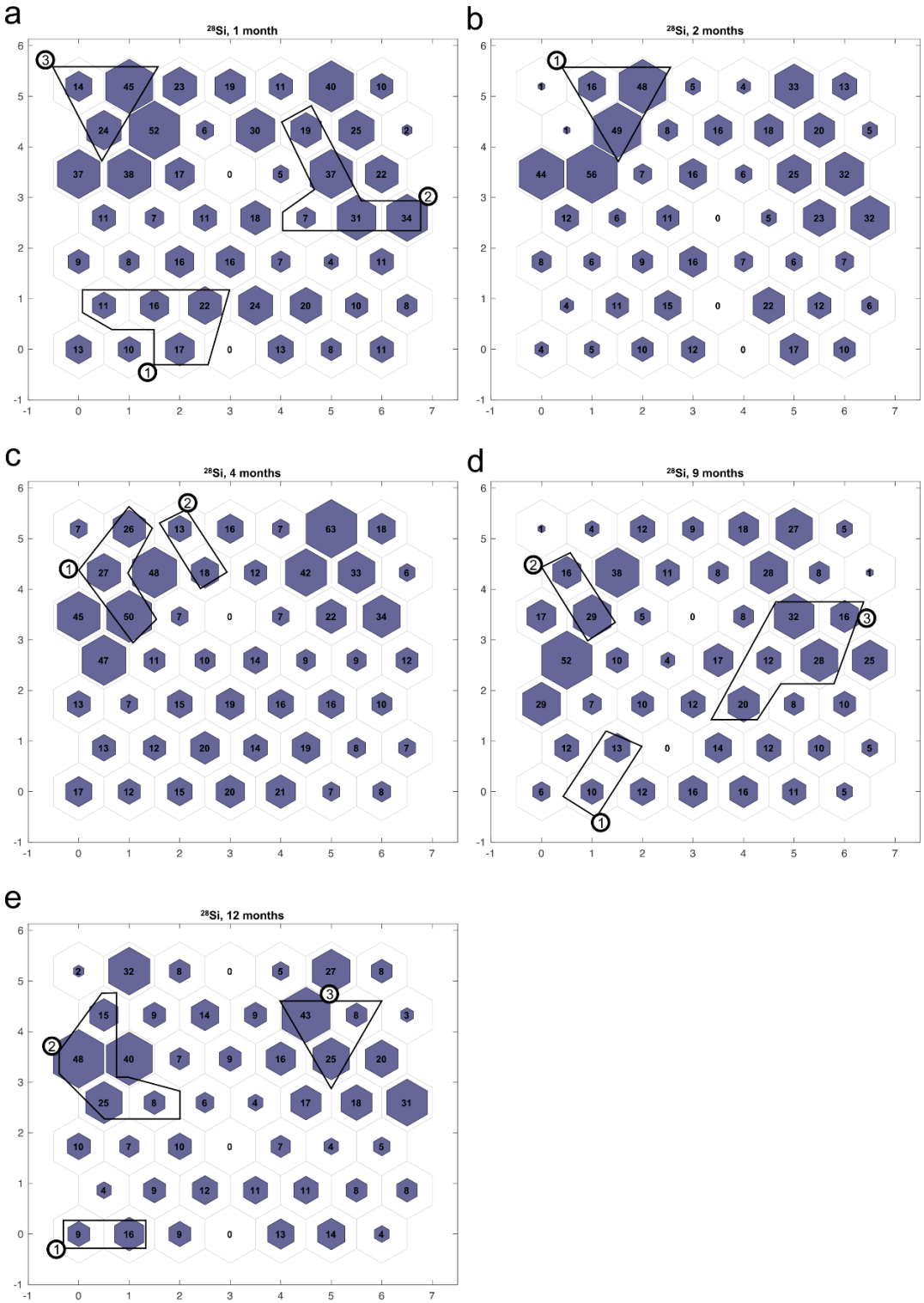

Figure 17. ^{28}Si Analysis of self-organizing maps for each time point.

(a,b,c,d,e) Kohonen Self-Organizing Map (SOM) was applied to the differentially expressed (DE) transcripts obtained from the RNA-Seq data to identify coherent patterns

of transcript expression at each time point, as well as patterns within the unmapped transcripts. The mapping clusters transcripts in each unit according to log_2(fold change) expression values for the transcripts in that unit. SOM clustering analysis demonstrates the distances between correlated transcript groups. The small blue hexagons are modules comprising transcripts with similar log_2(fold change) expression pattern. The numbers inside hexagons correspond to the number of transcripts in each module.

^{28}Si, 1 month		^{28}Si, 2 months		^{28}Si, 4 months		^{28}Si, 9 months		^{28}Si, 12 months	
Module	**Transcript Ensemble ID**	**Module**	**Transcript Ensemble ID**	**Module**	**Transcript Ensemble ID**	**Module**	**Transcript Ensemble ID**	**Module**	**Transcript Ensemble ID**
10	ENSMUST00000238749	29	ENSMUST00000235620	16	ENSMUST00000237125	19	ENSMUST00000237305	11	ENSMUST00000238098
11	ENSMUST00000237098	33	ENSMUST00000238125	1	ENSMUST00000237749	26	ENSMUST00000237358	13	ENSMUST00000235207
11	ENSMUST00000236403	35	ENSMUST00000237742	1	ENSMUST00000236336	27	ENSMUST00000236687	17	ENSMUST00000236414
26	ENSMUST00000236171	35	ENSMUST00000236925	20	ENSMUST00000237305	2	ENSMUST00000236504	1	ENSMUST00000238267
27	ENSMUST00000236591	37	ENSMUST00000237337	28	ENSMUST00000236046	2	ENSMUST00000238267	21	ENSMUST00000235620
28	ENSMUST00000235620	37	ENSMUST00000237529	30	ENSMUST00000236414	30	ENSMUST00000235318	22	ENSMUST00000237798
29	ENSMUST00000235647	37	ENSMUST00000237854	34	ENSMUST00000237854	30	ENSMUST00000236414	23	ENSMUST00000236171
34	ENSMUST00000237472	38	ENSMUST00000236006	36	ENSMUST00000235620	34	ENSMUST00000235927	29	ENSMUST00000235915
36	ENSMUST00000236546	3	ENSMUST00000236950	36	ENSMUST00000237499	35	ENSMUST00000238729	29	ENSMUST00000237823
3	ENSMUST00000236292	44	ENSMUST00000235929	36	ENSMUST00000238729	36	ENSMUST00000238021	29	ENSMUST00000238513
40	ENSMUST00000236873	45	ENSMUST00000235335	36	ENSMUST00000235411	47	ENSMUST00000236898	2	ENSMUST00000238288
43	ENSMUST00000238729	45	ENSMUST00000237478	38	ENSMUST00000237602	9	ENSMUST00000236950	2	ENSMUST00000235318
44	ENSMUST00000237337	45	ENSMUST00000237364	38	ENSMUST00000235332			34	ENSMUST00000235135
44	ENSMUST00000236215	6	ENSMUST00000238731	44	ENSMUST00000238021			36	ENSMUST00000236006
44	ENSMUST00000238271			44	ENSMUST00000238267			40	ENSMUST00000235648
47	ENSMUST00000238288			45	ENSMUST00000236794			41	ENSMUST00000238368
8	ENSMUST00000237749			48	ENSMUST00000236850			44	ENSMUST00000235411
8	ENSMUST00000237832							45	ENSMUST00000238021
9	ENSMUST00000236824							5	ENSMUST00000238677

Table 26. Unannotated differentially expressed transcripts in ^{28}Si across all time points. Each unannotated ENSEMBLE transcript ID is listed with the corresponding module number in the SOM Figure 16.

6.5 Discussion

Despite knowledge that deep spaceflight is associated with multiple carcinogenic processes, the different responses to HZE irradiation are still relatively unexplored. This study was designed to help identify the molecular mechanisms of HZE induced HCC focusing on transcription expression patterns at different time points after irradiation, and to elucidate novel unannotated transcripts that are significantly affected by HZE-irradiation. It has been hypothesized that a major driver of HZE induced carcinogenesis occurs through inflammatory responses, reactive oxygen species, and DNA damage. [137] Our results support an association between early proinflammatory response, downstream biomarkers of cytokine activity, and downregulation of such responses at later time points. The exact molecular factors that regulate these responses are not well defined, but HZE-irradiation engenders a complex immune response where directionality (activation/inhibition) cannot be predicted for some pathways.

We observed some significant commonly dysregulated immunological pathways in the HZE-irradiated mice, including PI3K signaling in B lymphocytes, acute phase response signaling, IL-8 signaling, IL-7 signaling, IL-3 signaling, and B cell receptor signaling. PI3K was mainly activated at later time points across all HZE ions. PI3K regulates numerous biological functions such as survival, differentiation, proliferation, migration, and metabolism. In the immune system, inhibited PI3K leads to immunodeficiency, whereas activation of this signaling cascade leads to leukemia and autoimmune responses. [135, 138, 139] The acute phase response signaling was activated at 1 month in ^{56}Fe but inhibited at this time point for both ^{16}O and ^{28}Si. This response is triggered by initiation of irradiation-induced tissue injury which leads to changes in concentration of several plasma

proteins as a result of significantly altered hepatic metabolism. [105, 106, 140] It has been previously shown that ^{16}O total body irradiation significantly decreases peripheral blood cell counts in mice as early as 2 weeks post irradiation, particularly white blood cells (WBC) and platelets (PLT). [95] This rapid deletion of peripheral WBC can be a potential contributor to an impaired acute phase response in ^{16}O and ^{28}Si irradiated mice through a similar mechanism. Additionally, IL-8 signaling was activated at 12 months post ^{56}Fe and ^{16}O irradiation, while it was inhibited in ^{28}Si. Given that IL-8 upregulates the expression of genes involved in tumor growth (EGFR, MMP2, MMP9), angiogenesis (VEGF), and cell proliferation through a metalloproteinase dependent pathway [117-119, 141, 142], its activation at 12 months post ^{56}Fe and^{16}O irradiation is in line with the tumor growth and spontaneous incidences of HCC seen previously. [7, 117-119, 142] It has been previously shown that ^{28}Si increases the levels of apoptotic cell death in the heart and bone marrow up to 6 months post-irradiation. [97] This chronic apoptotic response might be associated with the observed IL-8 suppression.

Nonetheless, as mentioned earlier, the focus of this study was limited to transcriptional changes induced in the liver by ^{56}Fe,^{16}O, and ^{28}Si irradiation at 5 different time points. Hence, it remains unclear how the detected changes reflect the magnitude of carcinogenic processes in the liver. In future studies, it is therefore important to investigate these differences by conducting a comparison both histologically and quantitively, in addition to measuring the different levels of enzymes/proteins responsible for the indicated pathways. A complete list of comparison analyses with predicted z-scores for significant pathways comparing between all HZE types of irradiated mice across all time points is provided Table 27.

Moreover, to assess the transcriptional pathways of our novel unannotated transcripts, we examined their activity patterns across 5 time points utilizing SOMs. To elucidate the biological functions associated with these transcript clusters, we then performed functional pathway analyses (Figure 9, 12, and 15). The deep mining of biological knowledge from these unannotated transcripts remains challenging due to the incompleteness of genome functional annotation. The SOM machine learning methodology takes advantage of already annotated and studied transcripts and pathways to infer the biological functions of the unannotated transcripts. Future studies should assess the transcriptional and regulatory activity of these unannotated transcripts using different techniques such as histone modifications (H3K4me3 and H3K27ac), which have been associated with activation of transcription and enhancer activity, respectively. [143, 144] Some of these unannotated transcripts may originate from enhancer regions or promotor upstream transcripts and thus play key regulatory roles in controlling gene expression following HZE irradiation, since they are significantly affected by irradiation. Additionally, aligning these significant unannotated transcripts to the human genome will help identify those that are conserved in humans. Even though, the precise functions of our unannotated transcripts remain to be elucidated, their significant changes post HZE-irradiation, their similar expression patterns with the annotated genes in specified modules and neighboring modules in the described SOMs, and their functional roles in transcription activity, organismal death, hepatic fibrosis signaling, and LXR/RXR signaling pathways, all provide compelling evidence to support further studies of the roles of these transcripts in the carcinogenic processes of HCC following low-dose HZE irradiation.

Canonical Pathways	^{56}Fe 1 mo	^{56}Fe 2 mo	^{56}Fe 4 mo	^{56}Fe 9 mo	^{56}Fe 12 mo	^{16}O 1 mo	^{16}O 2 mo	^{16}O 4 mo	^{16}O 9 mo	^{16}O 12 mo	^{28}Si 1 mo	^{28}Si 2 mo	^{28}Si 4 mo	^{28}Si 9 mo	^{28}Si 12 mo
PI3K Signaling in B Lymphocytes	-1.34	-0.71	-2.33	-1.13	1.89	-0.38	-2.24	1.00	-1.00	2.12	0.82	0.00	-0.38	1.89	1.13
Acute Phase Response Signaling	0.33	-1.67	-1.41	-1.07	-1.27	-1.34	-1.00	0.38	N/A	2.20	-0.82	-0.45	-1.50	1.81	-2.53
Synaptogenesis Signaling Pathway	-1.27	-0.91	-1.73	-0.78	1.34	-0.82	-1.13	0.71	-1.00	3.16	0.58	-1.27	0.00	1.90	0.91
Thrombin Signaling	-1.89	-1.63	-1.67	-0.91	1.13	-1.34	-1.00	1.34	-0.45	0.33	0.71	-0.82	1.51	1.63	-0.63
Protein Kinase A Signaling	-2.31	-1.94	-0.50	-0.30	0.00	-1.07	-1.67	0.54	-2.31	0.91	-1.07	-0.30	-0.24	-1.41	2.31
3-phosphoinositide Biosynthesis	-1.41	-1.00	1.63	0.00	2.65	0.00	0.00	1.89	1.34	2.12	1.63	0.45	0.30	1.89	0.45
fMLP Signaling in Neutrophils	-1.00	-1.63	-0.82	-1.13	2.24	-1.00	-2.24	N/A	N/A	1.34	1.00	N/A	0.71	2.00	1.41
Gαq Signaling	N/A	-1.63	-0.33	0.00	2.12	-1.13	-2.24	2.24	N/A	2.12	2.24	N/A	1.00	1.34	0.00
Role of NFAT in Regulation of the Immune Response	N/A	-1.00	-0.91	-0.63	2.12	-0.71	-1.34	2.65	-0.45	2.11	0.45	N/A	0.00	1.63	1.67
CREB Signaling in Neurons	-0.82	-0.45	-1.41	-0.30	2.24	-1.63	-2.00	N/A	-1.13	2.65	0.00	-0.82	0.00	1.13	1.00
Opioid Signaling Pathway	-1.27	1.41	-1.94	-0.83	1.67	-0.38	-0.38	0.38	-1.41	1.63	1.00	1.13	0.58	-0.82	0.58
Superpathway of Inositol Phosphate Compounds	-1.00	-1.51	1.13	0.00	2.65	0.00	0.82	1.41	1.34	2.12	1.00	0.33	-0.28	1.27	0.45
D-myo-inositol-5-phosphate Metabolism	-1.34	-1.00	2.00	0.82	2.24	-0.30	0.00	1.34	N/A	2.24	1.63	0.45	0.71	1.00	N/A
Phospholipase C Signaling	0.38	0.00	-0.63	0.00	1.67	-1.27	-1.90	2.24	0.00	0.58	1.00	0.63	-0.30	2.24	1.94
Apelin Endothelial Signaling Pathway	-2.00	-0.45	-1.63	-0.58	1.41	-2.00	-2.12	N/A	0.82	1.90	N/A	N/A	0.71	0.45	0.63
IL-8 Signaling	N/A	-1.41	-0.33	-1.67	1.00	-0.45	-0.38	1.63	-1.00	2.11	1.63	N/A	1.27	0.00	-1.51
CD28 Signaling in T Helper Cells	N/A	-0.71	-1.13	-1.41	1.41	-0.82	-1.34	1.34	N/A	2.12	1.34	0.00	-0.38	1.89	0.38
iCOS-iCOSL Signaling in T Helper Cells	N/A	-0.82	-0.82	-0.82	1.63	-0.82	N/A	2.24	-1.34	1.89	0.00	-1.00	0.00	1.63	1.13
D-myo-inositol (1,4,5,6)-Tetrakisphosphate Biosynthesis	-1.34	-0.71	2.00	0.82	2.24	0.00	0.00	1.34	N/A	2.24	1.13	0.45	0.71	1.00	N/A
D-myo-inositol (3,4,5,6)-tetrakisphosphate Biosynthesis	-1.34	-0.71	2.00	0.82	2.24	0.00	0.00	1.34	N/A	2.24	1.13	0.45	0.71	1.00	N/A
B Cell Receptor Signaling	-1.63	0.00	-1.21	-1.39	0.63	0.00	-1.13	0.71	-1.27	1.94	-0.63	0.33	-0.91	1.16	1.00
Role of NFAT in Cardiac Hypertrophy	-1.13	-1.34	-0.33	-0.78	1.89	-1.89	-0.45	0.82	-0.71	1.67	0.00	-0.45	0.30	1.13	0.71
Colorectal Cancer Metastasis Signaling	1.41	0.82	0.28	0.00	0.58	0.82	1.41	0.38	0.00	2.32	2.12	0.38	0.63	1.90	-0.54
Type II Diabetes Mellitus Signaling	N/A	-0.45	-0.45	-2.12	0.71	-1.00	0.45	2.00	-1.00	1.89	N/A	1.00	1.34	0.45	0.33
Adrenomedullin signaling pathway	-0.45	-1.89	-0.63	0.00	1.63	-2.00	-1.34	-0.38	0.38	2.14	0.00	N/A	-0.63	1.39	0.28
mTOR Signaling	-1.00	-0.45	0.00	-1.67	0.38	-0.45	-1.00	2.00	-1.89	0.38	0.38	0.45	0.82	0.38	-1.90
Neuroinflammation Signaling Pathway	0.91	-0.73	-1.41	-0.71	-0.91	0.63	-1.00	0.30	0.38	2.36	1.94	0.00	0.28	1.00	-0.58
Cardiac Hypertrophy Signaling (Enhanced)	-1.07	-0.66	0.00	-0.85	1.15	-0.47	-0.23	0.50	-2.00	1.96	1.16	0.83	0.96	0.73	0.45
AMPK Signaling	0.38	0.00	-1.13	0.63	0.82	0.38	-1.34	-1.34	1.60	1.41	0.00	-0.82	-1.63	1.13	-0.38
Glioblastoma Multiforme Signaling	-0.82	-1.63	-0.33	-0.38	-0.45	-0.45	0.45	1.63	-0.45	-0.38	1.00	N/A	0.71	2.33	-1.89
Aryl Hydrocarbon Receptor Signaling	-1.34	0.71	0.45	-1.41	N/A	-0.82	-0.71	0.82	0.00	0.30	1.34	-0.71	-1.13	-1.89	-1.13
Integrin Signaling	-1.34	-1.41	0.30	-1.16	-0.38	-0.33	0.45	0.00	-0.82	0.45	-0.33	-1.67	0.63	2.12	-1.27
P2Y Purigenic Receptor Signaling Pathway	-0.45	-1.00	-0.71	-1.00	2.45	N/A	N/A	1.00	-0.45	3.16	1.34	N/A	0.00	N/A	1.00
Nitric Oxide Signaling in the Cardiovascular System	N/A	N/A	-0.82	1.00	2.00	-1.00	0.00	0.45	1.63	2.00	N/A	0.00	0.63	2.65	0.33
3-phosphoinositide Degradation	-1.63	-0.33	1.63	0.00	1.89	-0.58	0.82	0.38	2.00	2.24	0.71	0.00	0.30	0.00	N/A
White Adipose Tissue Browning Pathway	1.00	-1.63	-1.00	0.63	1.34	1.00	N/A	N/A	0.00	1.41	0.82	0.00	-1.00	1.00	1.63
Production of Nitric Oxide and Reactive Oxygen Species in Macrophages	-0.38	-1.39	0.00	-0.63	0.30	1.00	-0.38	0.00	1.13	1.73	2.31	0.33	0.33	1.00	-1.39
Dendritic Cell Maturation	-1.34	-0.33	-0.91	-1.89	0.71	0.45	0.00	1.63	0.00	2.32	0.82	0.00	0.71	0.82	0.33

PI3K/AKT Signaling	-0.45	-0.30	0.00	0.38	-0.63	0.38	1.13	1.13	0.82	1.27	1.67	0.00	0.83	2.67	-0.45
Apelin Cardiomyocyte Signaling Pathway	-1.63	-1.41	-1.34	-1.41	1.00	N/A	N/A	N/A	N/A	2.00	N/A	N/A	1.41	1.34	-0.45
Mouse Embryonic Stem Cell Pluripotency	1.13	-0.82	-1.67	0.00	1.13	0.00	N/A	N/A	1.00	1.13	1.34	N/A	-0.45	2.12	-1.13
Systemic Lupus Erythematosus In B Cell Signaling Pathway	-0.38	0.00	-1.29	-1.16	0.63	0.63	-1.13	-0.30	-1.27	0.00	1.00	-1.13	-1.21	1.73	0.00
NF-κB Activation by Viruses	N/A	-1.34	-0.38	-1.89	0.71	-0.45	N/A	N/A	N/A	2.24	1.00	N/A	1.34	2.00	-0.38
ILK Signaling	1.34	0.71	-0.63	-0.63	0.45	0.00	0.00	0.45	1.34	2.11	0.63	0.38	-0.38	1.27	-1.39
Endocannabinoid Cancer Inhibition Pathway	-2.83	-0.38	0.00	0.30	-1.63	0.00	0.38	-0.38	1.13	-1.51	-0.38	-0.82	1.41	-0.45	0.00
Tec Kinase Signaling	N/A	N/A	1.89	-0.33	0.38	N/A	0.45	1.00	0.45	0.71	2.24	-1.00	1.00	1.41	-0.63
LXR/RXR Activation	1.73	-0.71	-1.51	1.16	0.00	2.53	0.00	0.38	1.00	-0.50	0.26	0.00	-0.58	0.83	0.30
Sirtuin Signaling Pathway	-2.00	0.83	0.00	1.00	-0.63	-0.38	-1.67	0.00	0.91	-1.73	0.28	-0.28	0.00	0.91	0.30
ERK/MAPK Signaling	-0.82	-0.38	-1.00	-0.28	-0.45	-0.38	1.00	-1.00	0.00	2.00	0.33	-1.00	0.00	1.51	-0.71
Osteoarthritis Pathway	0.45	0.71	1.41	0.82	0.38	0.71	1.41	-0.63	N/A	0.50	0.82	N/A	0.38	2.24	0.33
Relaxin Signaling	N/A	N/A	0.00	0.38	2.24	N/A	N/A	0.82	0.00	2.33	2.00	N/A	0.38	2.24	0.38
14-3-3-mediated Signaling	-1.34	-0.71	-0.45	-1.27	0.45	-1.34	0.00	N/A	-1.63	1.89	0.00	0.45	-0.38	0.00	-0.82
cAMP-mediated signaling	0.45	N/A	-1.00	0.71	N/A	0.00	-2.00	0.45	-1.67	2.24	N/A	-0.45	-0.33	-0.45	0.82
PPARα/RXRα Activation	0.33	-1.67	-0.33	-0.69	0.71	0.58	0.45	0.00	0.91	0.28	-1.00	0.00	0.00	-2.33	1.27
Ephrin Receptor Signaling	0.00	0.45	-0.30	-0.91	-0.45	1.00	0.00	1.00	-2.00	0.45	1.13	-0.33	0.91	1.13	0.45
RANK Signaling in Osteoclasts	N/A	-1.00	-1.00	-0.82	0.71	0.00	-0.82	1.00	N/A	1.90	1.00	0.00	-0.45	1.34	0.38
PKCθ Signaling in T Lymphocytes	N/A	-0.38	0.00	-1.00	1.63	0.00	N/A	1.63	-0.82	2.12	N/A	N/A	0.00	1.63	1.13
Growth Hormone Signaling	N/A	N/A	1.13	-1.27	-0.45	-1.00	N/A	2.24	-0.38	0.00	0.00	0.00	2.12	1.27	-0.45
Signaling by Rho Family GTPases	N/A	-0.71	0.38	-0.82	0.82	N/A	0.00	2.00	0.00	1.00	1.89	0.33	0.00	0.82	-1.51
Oxidative Phosphorylation	2.65	0.00	N/A	N/A	N/A	N/A	-0.82	N/A	1.63	N/A	-1.89	-1.13	-2.12	N/A	N/A
PEDF Signaling	N/A	-1.34	-0.71	-1.63	1.63	1.00	N/A	1.34	N/A	1.13	0.00	N/A	1.00	N/A	-0.45
eNOS Signaling	N/A	N/A	-0.82	-0.71	1.34	-0.45	-1.00	0.00	-0.82	1.63	0.45	N/A	-0.38	2.00	0.38
CXCR4 Signaling	N/A	0.00	0.33	-0.91	0.38	N/A	N/A	1.34	0.45	1.00	N/A	1.34	1.67	1.13	-1.27
Cardiac Hypertrophy Signaling	-0.45	0.00	0.00	0.00	1.34	-0.91	-1.13	0.71	-0.33	2.11	0.82	0.71	-0.30	0.82	0.00
Huntington's Disease Signaling	-1.00	0.00	0.00	-0.38	1.13	N/A	0.00	0.82	-1.34	1.41	N/A	-0.45	0.00	1.89	1.13
Actin Cytoskeleton Signaling	0.00	-0.71	0.00	0.00	0.82	-0.38	0.00	0.82	1.00	0.71	0.91	-1.27	-0.91	1.67	-0.38
Apelin Adipocyte Signaling Pathway	-1.34	0.82	-2.00	-0.33	-1.00	N/A	N/A	0.00	1.34	0.00	-0.82	-0.45	0.45	-1.00	N/A
FGF Signaling	N/A	-1.63	-1.67	-1.00	N/A	0.00	N/A	N/A	-1.00	0.38	-0.82	N/A	-1.13	1.89	0.00
Endothelin-1 Signaling	-1.13	-0.38	-1.34	-1.16	0.45	-0.45	N/A	0.45	-1.41	1.13	0.00	N/A	0.58	-0.33	-0.63
Leukocyte Extravasation Signaling	-0.45	0.71	-0.71	-1.94	0.00	0.00	1.13	-1.34	N/A	1.89	0.00	0.45	0.00	0.82	0.00
T Cell Exhaustion Signaling Pathway	N/A	1.00	0.33	1.00	-1.34	0.45	N/A	0.00	1.00	-2.45	1.00	N/A	0.00	0.38	0.45
PTEN Signaling	N/A	1.51	0.28	1.90	-0.33	0.00	-0.38	-1.13	1.34	0.30	-0.82	0.38	0.30	-0.28	0.45
LPS-stimulated MAPK Signaling	-1.00	-0.38	-1.13	-1.89	0.00	0.00	0.00	1.00	N/A	1.67	-0.45	N/A	0.45	1.00	-0.38
IL-7 Signaling Pathway	N/A	-2.45	-0.38	-0.63	N/A	N/A	N/A	N/A	-0.45	0.00	-1.00	-2.00	-0.82	1.13	-0.45
NGF Signaling	0.00	0.71	-0.71	-0.38	0.71	0.38	0.00	1.63	-0.45	2.83	0.33	0.00	0.00	1.13	0.00
STAT3 Pathway	N/A	-1.00	-0.71	-2.53	-1.34	N/A	N/A	N/A	N/A	-1.13	0.00	N/A	0.82	-0.38	-1.34
LPS/IL-1 Mediated Inhibition of RXR Function	0.63	0.38	0.00	0.45	0.00	0.33	2.00	-1.13	0.45	1.16	0.00	1.13	0.00	0.82	-0.71
Role of Pattern Recognition Receptors in Recognition of Bacteria and Viruses	-1.00	N/A	-1.63	-1.34	1.34	N/A	0.00	N/A	N/A	1.89	N/A	N/A	-0.45	1.00	0.38
Fc Epsilon RI Signaling	-1.00	0.00	-1.67	-1.90	0.45	N/A	N/A	0.00	-1.34	0.82	0.00	0.00	0.00	1.41	-0.45

Insulin Receptor Signaling	N/A	-0.38	-0.33	-2.11	-0.38	0.00	0.00	1.13	-1.41	-0.38	-0.45	-0.71	-0.30	1.39	N/A
Acute Myeloid Leukemia Signaling	N/A	N/A	-0.71	0.00	2.24	1.34	N/A	-0.82	-0.45	1.13	N/A	N/A	-0.82	1.00	-0.38
Pancreatic Adenocarcinoma Signaling	N/A	N/A	-0.71	-0.38	0.38	N/A	0.45	N/A	-0.45	2.33	1.63	N/A	-0.38	1.00	-1.13
IL-17A Signaling in Airway Cells	N/A	-1.63	-1.13	-0.82	-0.38	N/A	N/A	N/A	N/A	1.41	0.00	N/A	1.00	1.63	-0.82
Th2 Pathway	N/A	N/A	1.41	0.82	1.34	N/A	N/A	N/A	1.00	1.34	N/A	N/A	0.00	2.45	-0.45
IL-3 Signaling	N/A	N/A	0.38	0.00	1.00	0.00	N/A	N/A	N/A	1.63	N/A	-2.00	1.13	2.65	0.00
GP6 Signaling Pathway	N/A	N/A	-0.82	-1.13	1.63	-0.45	N/A	N/A	0.00	2.12	N/A	N/A	0.00	1.63	1.00
Cdc42 Signaling	0.00	0.71	0.38	-2.00	0.00	0.00	0.00	N/A	N/A	2.00	-1.00	0.00	1.63	-1.00	N/A
Amyotrophic Lateral Sclerosis Signaling	N/A	N/A	1.34	-1.00	1.63	N/A	N/A	N/A	-1.00	0.82	-1.00	1.34	-0.45	0.00	0.00
Cholecystokinin/Gastrin-mediated Signaling	-1.34	0.00	-0.82	-1.41	N/A	-1.00	0.00	N/A	N/A	0.71	-0.45	0.45	0.45	-0.82	-1.13
PPAR Signaling	1.00	-0.38	0.00	-0.71	-1.00	0.82	0.00	0.00	N/A	-1.00	N/A	0.45	1.13	-1.63	0.45
Gα12/13 Signaling	N/A	0.38	0.00	-1.41	0.71	0.00	0.00	N/A	-0.45	2.33	2.24	N/A	1.00	0.00	0.00
Renin-Angiotensin Signaling	N/A	0.00	-0.82	-1.00	0.45	N/A	-1.00	N/A	0.00	1.89	-1.00	N/A	0.00	1.63	0.71
EIF2 Signaling	0.00	0.00	-1.63	0.38	0.45	N/A	0.00	N/A	N/A	0.38	-1.00	N/A	-2.11	2.12	-0.38
NF-κB Signaling	N/A	-1.51	-0.91	-1.39	1.13	-1.00	0.38	0.00	-0.38	0.78	N/A	N/A	-0.63	0.33	0.00
NRF2-mediated Oxidative Stress Response	-0.45	0.38	-0.82	-1.13	-1.00	0.00	0.45	N/A	N/A	1.63	-1.41	-1.00	N/A	N/A	N/A
CDK5 Signaling	1.34	0.45	1.34	1.13	N/A	N/A	N/A	-1.00	N/A	N/A	1.00	-2.00	N/A	N/A	N/A
Endocannabinoid Developing Neuron Pathway	0.38	0.33	-1.67	-0.63	0.45	N/A	-0.45	0.45	-0.45	0.63	0.38	1.34	0.00	0.38	-0.38
GDNF Family Ligand-Receptor Interactions	N/A	N/A	-1.34	-1.13	N/A	N/A	N/A	N/A	-1.00	1.34	-1.00	N/A	N/A	1.00	-1.00
HMGB1 Signaling	N/A	-0.45	-0.82	-1.00	1.00	N/A	N/A	0.45	0.45	0.63	N/A	N/A	0.45	1.13	-1.41
Melanocyte Development and Pigmentation Signaling	1.00	0.00	-0.82	-0.33	N/A	0.00	N/A	1.00	-0.45	2.24	0.00	0.00	-0.82	1.00	0.00
Apoptosis Signaling	N/A	0.82	2.00	N/A	0.38	1.63	N/A	-0.82	-1.00	0.00	N/A	N/A	-1.00	N/A	0.00
Neurotrophin/TRK Signaling	N/A	N/A	-1.34	-0.45	N/A	N/A	N/A	N/A	-1.00	1.34	-1.00	0.00	-1.00	1.00	-0.45
Type I Diabetes Mellitus Signaling	N/A	-0.82	N/A	-1.63	-1.13	1.00	N/A	-0.38	N/A	0.00	0.45	N/A	1.34	-0.82	N/A
HOTAIR Regulatory Pathway	1.00	0.00	-0.82	-0.63	0.00	0.00	-0.71	0.00	-1.13	-0.83	-0.38	0.00	-1.27	0.00	-0.63
ATM Signaling	N/A	0.45	-0.45	-0.45	N/A	N/A	0.00	N/A	N/A	2.00	0.00	1.34	-1.00	-1.63	N/A
CD40 Signaling	N/A	-1.63	-2.12	-1.13	-0.82	N/A	N/A	-0.45	N/A	0.71	N/A	N/A	0.00	0.45	0.00
PD-1, PD-L1 cancer immunotherapy pathway	N/A	N/A	-0.38	1.13	0.00	N/A	N/A	-1.34	0.00	-1.13	N/A	N/A	-0.82	-1.63	0.82
Small Cell Lung Cancer Signaling	N/A	-1.34	-0.82	0.00	0.38	N/A	N/A	1.00	0.00	1.89	N/A	N/A	0.00	1.34	0.45
Pyridoxal 5'-phosphate Salvage Pathway	N/A	0.00	1.00	1.34	0.00	N/A	1.34	1.00	N/A	N/A	1.00	1.00	N/A	N/A	0.45
Fcγ Receptor-mediated Phagocytosis in Macrophages and Monocytes	N/A	N/A	0.00	-1.63	1.63	N/A	-1.00	N/A	N/A	N/A	2.00	N/A	-0.38	0.00	-0.45
Role of NANOG in Mammalian Embryonic Stem Cell Pluripotency	1.00	N/A	-0.45	0.00	N/A	N/A	N/A	N/A	0.45	1.00	0.45	N/A	0.00	2.65	-1.00
Prolactin Signaling	N/A	N/A	0.82	-1.39	-0.45	N/A	N/A	N/A	0.00	0.00	N/A	-1.00	1.41	1.41	-0.45
FLT3 Signaling in Hematopoietic Progenitor Cells	N/A	0.00	-1.00	0.00	N/A	0.00	N/A	N/A	0.00	2.00	-0.45	-1.13	0.00	1.89	-0.45
BMP signaling pathway	0.45	-0.45	-2.00	-0.82	N/A	N/A	-1.00	N/A	N/A	1.34	0.82	N/A	N/A	N/A	N/A
PAK Signaling	N/A	N/A	0.82	-1.41	-1.00	N/A	N/A	N/A	N/A	1.00	N/A	N/A	0.45	0.82	-1.34
GNRH Signaling	-0.38	0.00	0.00	-0.58	0.38	0.00	0.38	-0.45	-0.82	1.67	0.38	0.38	0.71	0.00	0.71
tRNA Charging	N/A	N/A	N/A	N/A	1.34	N/A	N/A	N/A	N/A	N/A	-2.45	-2.00	N/A	N/A	-1.00
Sphingosine-1-phosphate Signaling	-2.00	N/A	-0.82	0.00	0.00	N/A	N/A	1.13	N/A	0.00	N/A	N/A	1.13	N/A	-1.63

Gαs Signaling	N/A	N/A	-0.82	0.00	N/A	N/A	N/A	0.00	N/A	2.45	1.00	-0.45	0.00	N/A	2.00
SAPK/JNK Signaling	N/A	0.45	0.00	-1.13	0.00	0.00	N/A	0.00	-1.34	1.67	0.38	0.82	-0.38	0.45	0.00
JAK/Stat Signaling	N/A	N/A	0.00	-0.63	-0.71	N/A	N/A	1.00	0.45	0.30	0.45	N/A	0.71	1.90	-0.45
Wnt/β-catenin Signaling	N/A	0.82	0.00	N/A	0.00	1.41	2.00	-1.34	N/A	0.00	N/A	N/A	N/A	0.00	-1.00
PDGF Signaling	N/A	N/A	0.38	0.00	N/A	N/A	N/A	0.00	1.00	1.34	0.00	-1.00	0.00	1.41	-1.34
EGF Signaling	N/A	N/A	-1.63	-0.38	N/A	N/A	N/A	N/A	N/A	2.00	N/A	N/A	0.00	2.45	N/A
Antioxidant Action of Vitamin C	1.00	0.38	-0.82	N/A	0.00	0.00	N/A	N/A	N/A	-1.63	-1.63	N/A	-1.00	0.00	N/A
Calcium Signaling	-1.00	0.00	-2.45	0.45	N/A	-0.45	N/A	N/A	-0.45	N/A	N/A	0.82	-0.82	N/A	N/A
Estrogen-Dependent Breast Cancer Signaling	N/A	N/A	-1.00	-0.45	N/A	N/A	N/A	N/A	N/A	2.45	N/A	N/A	0.00	2.00	0.45
Rac Signaling	N/A	-1.00	0.00	-1.34	1.00	N/A	-0.45	N/A	N/A	1.63	N/A	N/A	0.00	0.45	-0.45
Lymphotoxin β Receptor Signaling	N/A	-1.00	-0.82	N/A	0.82	N/A	N/A	1.00	N/A	2.24	N/A	N/A	N/A	N/A	-0.45
Sumoylation Pathway	-0.82	N/A	N/A	N/A	N/A	N/A	N/A	-2.00	N/A	0.00	0.00	0.00	-1.89	-1.00	-0.45
p53 Signaling	N/A	N/A	0.82	1.34	0.38	N/A	N/A	0.45	0.45	-1.13	N/A	N/A	0.38	-0.38	0.82
Th17 Activation Pathway	N/A	-1.00	N/A	1.00	1.00	N/A	N/A	N/A	N/A	0.00	N/A	N/A	-1.00	1.63	-0.45
Glioma Signaling	N/A	N/A	-1.63	-1.13	N/A	N/A	N/A	N/A	-1.00	N/A	N/A	N/A	-0.45	1.34	0.45
IL-6 Signaling	N/A	-0.82	-0.38	-0.83	-0.33	N/A	N/A	0.00	N/A	1.50	0.00	N/A	0.00	1.51	-0.38
RhoA Signaling	0.00	-0.38	N/A	N/A	N/A	0.45	-0.38	-0.45	N/A	N/A	1.34	-0.63	-2.12	N/A	N/A
Salvage Pathways of Pyrimidine Ribonucleotides	N/A	-0.38	0.45	0.38	0.00	N/A	0.82	1.34	N/A	1.34	1.00	0.00	N/A	N/A	0.00
Endometrial Cancer Signaling	N/A	N/A	-1.00	-0.82	N/A	N/A	N/A	N/A	N/A	2.00	N/A	N/A	N/A	1.34	-0.45
Thrombopoietin Signaling	N/A	N/A	0.82	0.00	N/A	N/A	N/A	N/A	N/A	1.00	N/A	N/A	0.82	2.45	-0.45
VEGF Signaling	N/A	N/A	-0.45	0.00	0.00	N/A	N/A	N/A	N/A	2.00	N/A	N/A	-1.00	1.63	-0.45
ErbB Signaling	N/A	N/A	-0.82	-1.41	N/A	N/A	N/A	N/A	N/A	1.34	N/A	N/A	0.45	1.00	-0.45
Telomerase Signaling	N/A	N/A	-1.34	0.00	N/A	N/A	N/A	N/A	1.00	N/A	N/A	N/A	0.00	2.65	-0.45
UVB-Induced MAPK Signaling	N/A	N/A	-1.34	-1.63	N/A	N/A	N/A	N/A	N/A	2.00	N/A	N/A	N/A	N/A	-0.45
Corticotropin Releasing Hormone Signaling	-0.45	N/A	-0.82	0.33	N/A	N/A	N/A	0.00	1.00	1.00	-0.45	N/A	0.38	N/A	1.00
GM-CSF Signaling	N/A	N/A	0.00	-0.71	0.00	N/A	N/A	N/A	-0.45	1.63	N/A	N/A	-0.45	2.12	N/A
Superpathway of Cholesterol Biosynthesis	-2.45	N/A	N/A	N/A	N/A	-1.89	N/A	N/A	N/A	N/A	-1.00	N/A	N/A	N/A	N/A
Death Receptor Signaling	N/A	-1.34	1.00	N/A	0.00	0.45	N/A	-0.38	N/A	0.82	N/A	N/A	0.82	N/A	0.45
Nicotine Degradation II	-1.34	N/A	0.00	-0.45	-1.00	0.00	N/A	N/A	0.00	N/A	-0.38	N/A	N/A	-1.00	1.00
p38 MAPK Signaling	0.00	N/A	-1.00	0.00	N/A	0.00	N/A	-1.00	N/A	0.71	-0.38	N/A	-1.00	N/A	-1.00
HGF Signaling	N/A	0.00	0.00	-0.30	0.38	0.00	0.00	N/A	0.00	2.12	N/A	0.00	-0.38	1.90	0.00
UVC-Induced MAPK Signaling	-2.00	N/A	N/A	-2.00	N/A	N/A	1.00	N/A	N/A	N/A	N/A	N/A	N/A	N/A	N/A
Triacylglycerol Biosynthesis	-2.00	N/A	N/A	N/A	N/A	0.00	N/A	N/A	-2.00	N/A	-1.00	N/A	N/A	N/A	N/A
Melanoma Signaling	N/A	N/A	-0.45	-0.45	N/A	N/A	N/A	N/A	1.00	1.00	N/A	N/A	N/A	2.00	N/A
IL-23 Signaling Pathway	N/A	N/A	0.00	-0.45	0.45	N/A	N/A	N/A	N/A	0.82	N/A	N/A	1.00	1.63	-0.45
Acetone Degradation I (to Methylglyoxal)	-2.00	N/A	N/A	-1.34	N/A	-1.00	N/A	N/A	N/A	N/A	-0.45	N/A	N/A	N/A	N/A
Ephrin B Signaling	0.00	N/A	-1.00	-0.45	N/A	0.00	N/A	N/A	N/A	N/A	1.34	N/A	2.00	N/A	N/A
IGF-1 Signaling	N/A	N/A	0.00	-0.91	-0.82	N/A	N/A	N/A	0.00	0.38	N/A	N/A	0.38	1.27	-1.00
SPINK1 General Cancer Pathway	-1.00	N/A	0.00	-0.82	N/A	N/A	N/A	N/A	N/A	0.00	N/A	N/A	1.34	1.13	-0.45
April Mediated Signaling	N/A	-0.38	-1.00	N/A	0.00	-1.00	N/A	1.00	N/A	1.34	0.00	N/A	N/A	N/A	N/A
B Cell Activating Factor Signaling	N/A	-0.38	-1.00	N/A	0.00	-1.00	N/A	1.00	N/A	1.34	0.00	N/A	N/A	N/A	N/A

PCP pathway	N/A	N/A	-2.24	N/A	N/A	N/A	N/A	N/A	N/A	2.00	0.45	N/A	N/A	N/A	N/A
Wnt/Ca+ pathway	N/A	0.00	-2.24	N/A	N/A	-1.00	N/A	N/A	N/A	1.34	0.00	N/A	N/A	N/A	N/A
Role of RIG1-like Receptors in Antiviral Innate Immunity	N/A	-1.34	1.00	N/A	0.45	0.45	N/A	0.82	N/A	0.45	N/A	N/A	N/A	N/A	N/A
ErbB2-ErbB3 Signaling	N/A	N/A	0.45	0.00	N/A	N/A	N/A	N/A	1.00	N/A	N/A	N/A	0.00	1.63	-1.34
Cardiac β-adrenergic Signaling	N/A	N/A	1.00	1.00	N/A	N/A	N/A	-0.38	-1.00	N/A	N/A	-1.00	0.00	N/A	N/A
Cell Cycle: G1/S Checkpoint Regulation	N/A	N/A	N/A	-1.00	N/A	N/A	0.00	N/A	-0.45	0.45	N/A	-0.82	1.63	0.00	N/A
IL-9 Signaling	N/A	N/A	1.00	0.00	N/A	N/A	N/A	N/A	N/A	1.00	N/A	N/A	1.00	1.34	0.00
Paxillin Signaling	N/A	N/A	0.45	-0.63	-1.00	N/A	N/A	N/A	N/A	N/A	N/A	N/A	-0.45	1.00	-0.82
Inhibition of Angiogenesis by TSP1	N/A	N/A	N/A	-2.24	N/A	N/A	N/A	N/A	N/A	1.00	N/A	N/A	N/A	-1.00	N/A
Activation of IRF by Cytosolic Pattern Recognition Receptors	N/A	0.38	0.45	N/A	-0.82	0.45	0.00	0.45	N/A	0.71	0.45	0.00	N/A	N/A	-0.45
Agrin Interactions at Neuromuscular Junction	N/A	N/A	0.45	-1.34	-1.34	N/A	N/A	N/A	N/A	N/A	N/A	N/A	N/A	N/A	-1.00
Non-Small Cell Lung Cancer Signaling	N/A	N/A	-1.34	-0.45	N/A	N/A	N/A	N/A	N/A	N/A	N/A	N/A	0.00	2.24	N/A
Oncostatin M Signaling	N/A	N/A	1.00	1.00	N/A	N/A	N/A	N/A	N/A	N/A	N/A	N/A	N/A	2.00	N/A
IL-2 Signaling	N/A	N/A	-0.38	-0.38	N/A	N/A	N/A	N/A	0.00	1.00	N/A	N/A	0.00	2.24	N/A
Th1 Pathway	N/A	N/A	N/A	-0.71	-0.45	N/A	N/A	N/A	0.00	0.00	N/A	N/A	0.82	1.63	-0.38
VEGF Family Ligand-Receptor Interactions	N/A	N/A	-1.00	-0.82	N/A	N/A	N/A	N/A	N/A	N/A	N/A	N/A	0.00	2.00	0.00
Stearate Biosynthesis I (Animals)	N/A	N/A	N/A	-1.63	N/A	N/A	N/A	N/A	-0.82	N/A	N/A	N/A	N/A	N/A	1.34
TNFR2 Signaling	N/A	-0.45	1.00	N/A	1.00	N/A	N/A	N/A	N/A	1.34	N/A	N/A	N/A	N/A	N/A
CNTF Signaling	N/A	N/A	0.00	0.00	N/A	0.00	N/A	N/A	0.45	N/A	N/A	N/A	0.00	1.89	-1.34
TGF-β Signaling	N/A	N/A	-1.00	-1.00	N/A	N/A	N/A	N/A	N/A	1.63	N/A	N/A	N/A	N/A	N/A
CCR3 Signaling in Eosinophils	-1.00	N/A	-1.00	-1.63	N/A	N/A	N/A	N/A	N/A	N/A	N/A	N/A	N/A	N/A	0.00
Chemokine Signaling	-1.00	N/A	-1.00	-1.63	N/A	N/A	N/A	N/A	N/A	N/A	N/A	N/A	N/A	N/A	N/A
Superpathway of Geranylgeranyldiphosphate Biosynthesis I (via Mevalonate)	-2.24	N/A	N/A	N/A	N/A	-1.34	N/A	N/A	N/A	N/A	N/A	N/A	N/A	N/A	N/A
CD27 Signaling in Lymphocytes	N/A	0.45	N/A	N/A	0.00	0.00	0.00	0.45	N/A	1.63	N/A	N/A	N/A	N/A	1.00
iNOS Signaling	N/A	-1.34	N/A	N/A	0.00	N/A	N/A	N/A	N/A	0.82	1.34	N/A	N/A	N/A	N/A
Toll-like Receptor Signaling	N/A	-0.82	-1.00	N/A	N/A	N/A	N/A	0.00	N/A	0.63	N/A	N/A	-1.00	N/A	N/A
TNFR1 Signaling	N/A	0.45	0.00	N/A	1.00	0.00	N/A	0.00	N/A	2.00	0.00	N/A	N/A	N/A	N/A
TWEAK Signaling	N/A	-1.00	N/A	N/A	-0.45	-1.00	N/A	-1.00	N/A	N/A	N/A	N/A	N/A	N/A	N/A
Angiopoietin Signaling	N/A	0.45	0.00	1.00	1.00	-1.00	N/A	N/A	N/A	N/A	N/A	N/A	0.00	N/A	N/A
Glioma Invasiveness Signaling	N/A	N/A	-0.45	-1.34	N/A	N/A	N/A	N/A	N/A	N/A	N/A	N/A	N/A	N/A	-1.63
FcγRIIB Signaling in B Lymphocytes	N/A	N/A	N/A	-0.38	N/A	N/A	N/A	N/A	N/A	N/A	N/A	-1.00	0.00	1.00	-1.00
Mevalonate Pathway I	-2.00	N/A	N/A	N/A	N/A	-1.34	N/A	N/A	N/A	N/A	N/A	N/A	N/A	N/A	N/A
TREM1 Signaling	N/A	N/A	0.00	N/A	N/A	N/A	N/A	N/A	N/A	0.82	N/A	N/A	0.00	2.45	N/A
4-1BB Signaling in T Lymphocytes	N/A	0.00	-1.00	N/A	0.00	N/A	N/A	N/A	N/A	2.24	0.00	N/A	N/A	N/A	N/A
Leptin Signaling in Obesity	N/A	N/A	-0.45	0.00	0.00	N/A	N/A	N/A	N/A	0.45	N/A	N/A	0.45	1.89	N/A
Estrogen Biosynthesis	N/A	N/A	N/A	-1.00	N/A	0.00	N/A	N/A	N/A	N/A	-0.82	N/A	N/A	-1.34	N/A
Regulation of eIF4 and p70S6K Signaling	N/A	N/A	-0.45	-0.45	N/A	N/A	N/A	N/A	N/A	N/A	N/A	N/A	0.00	2.24	N/A
ERK5 Signaling	N/A	1.00	-1.00	N/A	N/A	N/A	0.00	N/A	-1.00	N/A	0.00	N/A	N/A	N/A	N/A
UVA-Induced MAPK Signaling	N/A	N/A	-1.00	-1.00	N/A	N/A	N/A	N/A	N/A	N/A	N/A	N/A	N/A	N/A	-1.00
Neuregulin Signaling	-0.45	N/A	0.00	-0.45	N/A	N/A	N/A	N/A	N/A	N/A	N/A	N/A	0.82	1.00	N/A

Macropinocytosis Signaling	N/A	N/A	N/A	-1.63	N/A	N/A	N/A	N/A	N/A	N/A	N/A	N/A	0.45	N/A	0.45
Induction of Apoptosis by HIV1	N/A	-0.45	N/A	N/A	0.00	N/A	1.00	-1.00	N/A	0.00	N/A	N/A	N/A	N/A	N/A
Nicotine Degradation III	N/A	N/A	N/A	-1.00	N/A	0.00	N/A	N/A	N/A	N/A	-0.45	N/A	N/A	N/A	1.00
Aldosterone Signaling in Epithelial Cells	N/A	-1.00	N/A	-1.00	N/A	N/A	N/A	N/A	N/A	N/A	N/A	N/A	0.45	N/A	0.00
HIPPO signaling	1.00	N/A	N/A	N/A	N/A	0.00	N/A	N/A	1.00	0.00	0.45	N/A	N/A	0.00	N/A
Antiproliferative Role of Somatostatin Receptor 2	N/A	N/A	0.00	-1.00	N/A	N/A	N/A	N/A	-1.00	0.45	N/A	N/A	0.00	N/A	0.00
MIF Regulation of Innate Immunity	N/A	N/A	N/A	N/A	N/A	N/A	N/A	N/A	N/A	2.24	N/A	N/A	N/A	N/A	N/A
ErbB4 Signaling	N/A	N/A	-0.45	-1.13	N/A	N/A	N/A	N/A	N/A	N/A	N/A	N/A	0.45	N/A	0.00
Cell Cycle: G2/M DNA Damage Checkpoint Regulation	N/A	N/A	N/A	N/A	N/A	N/A	N/A	0.00	N/A	1.00	N/A	N/A	N/A	1.00	N/A
Role of p14/p19ARF in Tumor Suppression	N/A	N/A	N/A	N/A	N/A	N/A	N/A	N/A	N/A	-2.00	N/A	N/A	N/A	N/A	0.00
Remodeling of Epithelial Adherens Junctions	N/A	-1.00	N/A	N/A	N/A	N/A	N/A	N/A	N/A	N/A	-1.00	N/A	N/A	N/A	N/A
Triacylglycerol Degradation	N/A	N/A	N/A	-0.45	N/A	N/A	N/A	N/A	0.45	N/A	N/A	-1.00	N/A	N/A	N/A
Sperm Motility	N/A	N/A	N/A	N/A	N/A	-1.00	N/A	N/A	N/A	N/A	N/A	N/A	0.82	N/A	N/A
Ovarian Cancer Signaling	N/A	N/A	-0.82	0.00	N/A	N/A	N/A	N/A	1.00	N/A	N/A	N/A	N/A	N/A	N/A
IL-1 Signaling	N/A	-0.38	N/A	0.00	0.00	N/A	N/A	0.00	N/A	1.13	N/A	N/A	N/A	N/A	N/A
Bupropion Degradation	N/A	N/A	N/A	-1.00	N/A	N/A	N/A	N/A	N/A	N/A	-0.45	N/A	N/A	N/A	N/A
Apelin Pancreas Signaling Pathway	N/A	N/A	N/A	0.00	1.00	N/A	N/A	N/A	0.00	0.45	N/A	N/A	N/A	N/A	0.00
VDR/RXR Activation	N/A	N/A	N/A	N/A	N/A	N/A	0.00	N/A	N/A	1.34	N/A	N/A	N/A	N/A	N/A
IL-22 Signaling	N/A	N/A	-0.45	-0.45	N/A	N/A	N/A	N/A	N/A	N/A	N/A	N/A	N/A	0.45	N/A
α-Adrenergic Signaling	N/A	N/A	N/A	N/A	N/A	N/A	N/A	N/A	N/A	N/A	N/A	N/A	1.00	N/A	N/A
Phosphatidylcholine Biosynthesis I	N/A	1.00	N/A	N/A	N/A	N/A	N/A	N/A	N/A	N/A	N/A	N/A	N/A	N/A	N/A
Fatty Acid β-oxidation I	N/A	0.00	N/A	N/A	N/A	N/A	N/A	N/A	N/A	N/A	N/A	N/A	N/A	N/A	1.00
Glycolysis I	N/A	1.00	N/A	N/A	N/A	N/A	N/A	N/A	N/A	N/A	N/A	N/A	N/A	N/A	N/A
Complement System	N/A	N/A	N/A	N/A	N/A	N/A	N/A	N/A	N/A	N/A	N/A	N/A	N/A	N/A	-1.00
Amyloid Processing	N/A	N/A	-1.00	N/A	N/A	N/A	N/A	N/A	N/A	N/A	N/A	N/A	N/A	N/A	N/A
Regulation of Cellular Mechanics by Calpain Protease	N/A	N/A	0.00	N/A	N/A	N/A	1.00	N/A	N/A	N/A	N/A	N/A	0.00	N/A	N/A
Retinol Biosynthesis	N/A	N/A	N/A	0.45	N/A	N/A	N/A	N/A	0.45	N/A	N/A	N/A	N/A	N/A	N/A
Calcium-induced T Lymphocyte Apoptosis	N/A	N/A	N/A	N/A	N/A	N/A	N/A	N/A	N/A	N/A	N/A	N/A	0.82	N/A	N/A
FAT10 Cancer Signaling Pathway	N/A	0.00	0.00	N/A	0.45	0.00	N/A	N/A	N/A	N/A	N/A	N/A	N/A	N/A	N/A
GPCR-Mediated Nutrient Sensing in Enteroendocrine Cells	N/A	N/A	N/A	-0.38	N/A	N/A	N/A	N/A	N/A	N/A	N/A	N/A	0.00	N/A	N/A
Regulation of the Epithelial-Mesenchymal Transition Pathway	N/A	N/A	N/A	N/A	N/A	N/A	N/A	N/A	N/A	N/A	N/A	N/A	N/A	N/A	N/A
CDP-diacylglycerol Biosynthesis I	N/A	N/A	N/A	N/A	N/A	N/A	N/A	N/A	N/A	N/A	N/A	N/A	N/A	N/A	N/A
Pregnenolone Biosynthesis	N/A	N/A	N/A	N/A	N/A	N/A	N/A	N/A	N/A	N/A	N/A	N/A	N/A	N/A	N/A
Cyclins and Cell Cycle Regulation	N/A	N/A	N/A	N/A	N/A	N/A	N/A	N/A	N/A	N/A	N/A	N/A	N/A	N/A	N/A
Xenobiotic Metabolism Signaling	N/A	N/A	N/A	N/A	N/A	N/A	N/A	N/A	N/A	N/A	N/A	N/A	N/A	N/A	N/A
Ephrin A Signaling	N/A	N/A	N/A	N/A	N/A	N/A	N/A	N/A	N/A	N/A	N/A	N/A	N/A	N/A	N/A
Sertoli Cell-Sertoli Cell Junction Signaling	N/A	N/A	N/A	N/A	N/A	N/A	N/A	N/A	N/A	N/A	N/A	N/A	N/A	N/A	N/A
D-myo-inositol (1,4,5)-trisphosphate Degradation	N/A	N/A	N/A	N/A	N/A	N/A	N/A	N/A	N/A	N/A	N/A	0.00	0.00	0.00	N/A
Protein Ubiquitination Pathway	N/A	N/A	N/A	N/A	N/A	N/A	N/A	N/A	N/A	N/A	N/A	N/A	N/A	N/A	N/A
Altered T Cell and B Cell Signaling in Rheumatoid Arthritis	N/A	N/A	N/A	N/A	N/A	N/A	N/A	N/A	N/A	N/A	N/A	N/A	N/A	N/A	N/A

IL-15 Signaling	N/A	N/A	N/A	N/A	N/A	N/A	N/A	N/A	N/A	N/A	N/A	N/A	N/A	N/A	N/A
Hepatic Cholestasis	N/A	N/A	N/A	N/A	N/A	N/A	N/A	N/A	N/A	N/A	N/A	N/A	N/A	N/A	N/A
DNA Double-Strand Break Repair by Homologous Recombination	N/A	N/A	N/A	N/A	N/A	N/A	N/A	N/A	N/A	N/A	N/A	N/A	N/A	N/A	N/A
Maturity Onset Diabetes of Young (MODY) Signaling	N/A	N/A	N/A	N/A	N/A	N/A	N/A	N/A	N/A	N/A	N/A	N/A	N/A	N/A	N/A
Role of PKR in Interferon Induction and Antiviral Response	N/A	N/A	N/A	N/A	N/A	N/A	N/A	N/A	N/A	N/A	N/A	N/A	N/A	N/A	N/A
Cancer Drug Resistance By Drug Efflux	N/A	N/A	N/A	N/A	N/A	N/A	N/A	N/A	N/A	N/A	N/A	N/A	N/A	N/A	N/A
Systemic Lupus Erythematosus Signaling	N/A	N/A	N/A	N/A	N/A	N/A	N/A	N/A	N/A	N/A	N/A	N/A	N/A	N/A	N/A
MIF-mediated Glucocorticoid Regulation	N/A	N/A	N/A	N/A	N/A	N/A	N/A	N/A	N/A	N/A	N/A	N/A	N/A	N/A	N/A
Glycerol Degradation I	N/A	N/A	N/A	N/A	N/A	N/A	N/A	N/A	N/A	N/A	N/A	N/A	N/A	N/A	N/A
Factors Promoting Cardiogenesis in Vertebrates	N/A	N/A	N/A	N/A	N/A	N/A	N/A	N/A	N/A	N/A	N/A	N/A	N/A	N/A	N/A
Reelin Signaling in Neurons	N/A	N/A	N/A	N/A	N/A	N/A	N/A	N/A	N/A	N/A	N/A	N/A	N/A	N/A	N/A
α-tocopherol Degradation	N/A	N/A	N/A	N/A	N/A	N/A	N/A	N/A	N/A	N/A	N/A	N/A	N/A	N/A	N/A
Fatty Acid Activation	N/A	N/A	N/A	N/A	N/A	N/A	N/A	N/A	N/A	N/A	N/A	N/A	N/A	N/A	N/A
G Protein Signaling Mediated by Tubby	N/A	N/A	N/A	N/A	N/A	N/A	N/A	N/A	N/A	N/A	N/A	N/A	N/A	N/A	N/A
TR/RXR Activation	N/A	N/A	N/A	N/A	N/A	N/A	N/A	N/A	N/A	N/A	N/A	N/A	N/A	N/A	N/A
Ubiquinol-10 Biosynthesis (Eukaryotic)	N/A	N/A	N/A	N/A	N/A	N/A	N/A	N/A	N/A	N/A	N/A	N/A	N/A	N/A	N/A
FAK Signaling	N/A	N/A	N/A	N/A	N/A	N/A	N/A	N/A	N/A	N/A	N/A	N/A	N/A	N/A	N/A
Bladder Cancer Signaling	N/A	N/A	N/A	N/A	N/A	N/A	N/A	N/A	N/A	N/A	N/A	N/A	N/A	N/A	N/A
Phenylalanine Degradation I (Aerobic)	N/A	N/A	N/A	N/A	N/A	N/A	N/A	N/A	N/A	N/A	N/A	N/A	N/A	N/A	N/A
CTLA4 Signaling in Cytotoxic T Lymphocytes	N/A	N/A	N/A	N/A	N/A	N/A	N/A	N/A	N/A	N/A	N/A	N/A	N/A	N/A	N/A
Chronic Myeloid Leukemia Signaling	N/A	N/A	N/A	N/A	N/A	N/A	N/A	N/A	N/A	N/A	N/A	N/A	N/A	N/A	N/A
Role of JAK1 and JAK3 in γc Cytokine Signaling	N/A	N/A	N/A	N/A	N/A	N/A	N/A	N/A	N/A	N/A	N/A	N/A	N/A	N/A	N/A
Glutamate Receptor Signaling	N/A	N/A	N/A	N/A	N/A	N/A	N/A	N/A	N/A	N/A	N/A	N/A	N/A	N/A	N/A
Tight Junction Signaling	N/A	N/A	N/A	N/A	N/A	N/A	N/A	N/A	N/A	N/A	N/A	N/A	N/A	N/A	N/A
Natural Killer Cell Signaling	N/A	N/A	N/A	N/A	N/A	N/A	N/A	N/A	N/A	N/A	N/A	N/A	N/A	N/A	N/A
RAR Activation	N/A	N/A	N/A	N/A	N/A	N/A	N/A	N/A	N/A	N/A	N/A	N/A	N/A	N/A	N/A
Autophagy	N/A	N/A	N/A	N/A	N/A	N/A	N/A	N/A	N/A	N/A	N/A	N/A	N/A	N/A	N/A
Estrogen Receptor Signaling	N/A	N/A	N/A	N/A	N/A	N/A	N/A	N/A	N/A	N/A	N/A	N/A	N/A	N/A	N/A
Adipogenesis pathway	N/A	N/A	N/A	N/A	N/A	N/A	N/A	N/A	N/A	N/A	N/A	N/A	N/A	N/A	N/A
Cell Cycle Regulation by BTG Family Proteins	N/A	N/A	N/A	N/A	N/A	N/A	N/A	N/A	N/A	N/A	N/A	N/A	N/A	N/A	N/A
Lysine Degradation II	N/A	N/A	N/A	N/A	N/A	N/A	N/A	N/A	N/A	N/A	N/A	N/A	N/A	N/A	N/A
Regulation of IL-2 Expression in Activated and Anergic T Lymphocytes	N/A	N/A	N/A	N/A	N/A	N/A	N/A	N/A	N/A	N/A	N/A	N/A	N/A	N/A	N/A
Th1 and Th2 Activation Pathway	N/A	N/A	N/A	N/A	N/A	N/A	N/A	N/A	N/A	N/A	N/A	N/A	N/A	N/A	N/A
Proline Degradation	N/A	N/A	N/A	N/A	N/A	N/A	N/A	N/A	N/A	N/A	N/A	N/A	N/A	N/A	N/A
Tetrahydrofolate Salvage from 5,10-methenyltetrahydrofolate	N/A	N/A	N/A	N/A	N/A	N/A	N/A	N/A	N/A	N/A	N/A	N/A	N/A	N/A	N/A
DNA Methylation and Transcriptional Repression Signaling	N/A	N/A	N/A	N/A	N/A	N/A	N/A	N/A	N/A	N/A	N/A	N/A	N/A	N/A	N/A
D-myo-inositol (1,3,4)-trisphosphate Biosynthesis	N/A	N/A	N/A	N/A	N/A	N/A	N/A	N/A	N/A	N/A	N/A	0.00	0.00	0.00	N/A
IL-12 Signaling and Production in Macrophages	N/A	N/A	N/A	N/A	N/A	N/A	N/A	N/A	N/A	N/A	N/A	N/A	N/A	N/A	N/A
IL-17A Signaling in Fibroblasts	N/A	N/A	N/A	N/A	N/A	N/A	N/A	N/A	N/A	N/A	N/A	N/A	N/A	N/A	N/A
Tetrapyrrole Biosynthesis II	N/A	N/A	N/A	N/A	N/A	N/A	N/A	N/A	N/A	N/A	N/A	N/A	N/A	N/A	N/A
Assembly of RNA Polymerase III Complex	N/A	N/A	N/A	N/A	N/A	N/A	N/A	N/A	N/A	N/A	N/A	N/A	N/A	N/A	N/A

G-Protein Coupled Receptor Signaling	N/A	N/A	N/A	N/A	N/A	N/A	N/A	N/A	N/A	N/A	N/A	N/A	N/A	N/A	N/A
γ-linolenate Biosynthesis II (Animals)	N/A	N/A	N/A	N/A	N/A	N/A	N/A	N/A	N/A	N/A	N/A	N/A	N/A	N/A	N/A
Thyroid Cancer Signaling	N/A	N/A	N/A	N/A	N/A	N/A	N/A	N/A	N/A	N/A	N/A	N/A	N/A	N/A	N/A
T Cell Receptor Signaling	N/A	N/A	N/A	N/A	N/A	N/A	N/A	N/A	N/A	N/A	N/A	N/A	N/A	N/A	N/A
Axonal Guidance Signaling	N/A	N/A	N/A	N/A	N/A	N/A	N/A	N/A	N/A	N/A	N/A	N/A	N/A	N/A	N/A
Ketogenesis	N/A	N/A	N/A	N/A	N/A	N/A	N/A	N/A	N/A	N/A	N/A	N/A	N/A	N/A	N/A
Oxidative Ethanol Degradation III	N/A	N/A	N/A	N/A	N/A	N/A	N/A	N/A	N/A	N/A	N/A	N/A	N/A	N/A	N/A
MSP-RON Signaling Pathway	N/A	N/A	N/A	N/A	N/A	N/A	N/A	N/A	N/A	N/A	N/A	N/A	N/A	N/A	N/A
Lysine Degradation V	N/A	N/A	N/A	N/A	N/A	N/A	N/A	N/A	N/A	N/A	N/A	N/A	N/A	N/A	N/A
Apelin Cardiac Fibroblast Signaling Pathway	N/A	N/A	N/A	N/A	N/A	N/A	N/A	N/A	N/A	N/A	N/A	N/A	N/A	N/A	N/A
IL-17A Signaling in Gastric Cells	N/A	N/A	N/A	N/A	N/A	N/A	N/A	N/A	N/A	N/A	N/A	N/A	N/A	N/A	N/A
Nur77 Signaling in T Lymphocytes	N/A	N/A	N/A	N/A	N/A	N/A	N/A	N/A	N/A	N/A	N/A	N/A	N/A	N/A	N/A
Cleavage and Polyadenylation of Pre-mRNA	N/A	N/A	N/A	N/A	N/A	N/A	N/A	N/A	N/A	N/A	N/A	N/A	N/A	N/A	N/A
Lipid Antigen Presentation by CD1	N/A	N/A	N/A	N/A	N/A	N/A	N/A	N/A	N/A	N/A	N/A	N/A	N/A	N/A	N/A
Formaldehyde Oxidation II (Glutathione-dependent)	N/A	N/A	N/A	N/A	N/A	N/A	N/A	N/A	N/A	N/A	N/A	N/A	N/A	N/A	N/A
Semaphorin Signaling in Neurons	N/A	N/A	N/A	N/A	N/A	N/A	N/A	N/A	N/A	N/A	N/A	N/A	N/A	N/A	N/A
Circadian Rhythm Signaling	N/A	N/A	N/A	N/A	N/A	N/A	N/A	N/A	N/A	N/A	N/A	N/A	N/A	N/A	N/A
Iron homeostasis signaling pathway	N/A	N/A	N/A	N/A	N/A	N/A	N/A	N/A	N/A	N/A	N/A	N/A	N/A	N/A	N/A
Atherosclerosis Signaling	N/A	N/A	N/A	N/A	N/A	N/A	N/A	N/A	N/A	N/A	N/A	N/A	N/A	N/A	N/A
2-ketoglutarate Dehydrogenase Complex	N/A	N/A	N/A	N/A	N/A	N/A	N/A	N/A	N/A	N/A	N/A	N/A	N/A	N/A	N/A
Role of BRCA1 in DNA Damage Response	N/A	N/A	N/A	N/A	N/A	N/A	N/A	N/A	N/A	N/A	N/A	N/A	N/A	N/A	N/A
Ceramide Degradation	N/A	N/A	N/A	N/A	N/A	N/A	N/A	N/A	N/A	N/A	N/A	N/A	N/A	N/A	N/A
Coagulation System	N/A	N/A	N/A	N/A	N/A	N/A	N/A	N/A	N/A	N/A	0.00	N/A	N/A	N/A	N/A
BAG2 Signaling Pathway	N/A	N/A	N/A	N/A	N/A	N/A	N/A	N/A	N/A	N/A	N/A	0.00	N/A	N/A	N/A
Hereditary Breast Cancer Signaling	N/A	N/A	N/A	N/A	N/A	N/A	N/A	N/A	N/A	N/A	N/A	N/A	N/A	N/A	N/A
Assembly of RNA Polymerase II Complex	N/A	N/A	N/A	N/A	N/A	N/A	N/A	N/A	N/A	N/A	N/A	N/A	N/A	N/A	N/A
Myc Mediated Apoptosis Signaling	N/A	N/A	N/A	N/A	N/A	N/A	N/A	N/A	N/A	N/A	N/A	N/A	N/A	N/A	N/A
IL-17 Signaling	N/A	N/A	N/A	N/A	N/A	N/A	N/A	N/A	N/A	N/A	N/A	N/A	N/A	N/A	N/A
Glutathione Redox Reactions I	N/A	N/A	N/A	N/A	N/A	N/A	N/A	N/A	N/A	N/A	N/A	N/A	N/A	N/A	N/A
Telomere Extension by Telomerase	N/A	N/A	N/A	N/A	N/A	N/A	N/A	N/A	N/A	N/A	N/A	N/A	N/A	N/A	N/A
HER-2 Signaling in Breast Cancer	N/A	N/A	N/A	N/A	N/A	N/A	N/A	N/A	N/A	N/A	N/A	N/A	N/A	N/A	N/A
Valine Degradation I	N/A	N/A	N/A	N/A	N/A	N/A	N/A	N/A	N/A	N/A	N/A	N/A	N/A	N/A	N/A
Human Embryonic Stem Cell Pluripotency	N/A	N/A	N/A	N/A	N/A	N/A	N/A	N/A	N/A	N/A	N/A	N/A	N/A	N/A	N/A
Gap Junction Signaling	N/A	N/A	N/A	N/A	N/A	N/A	N/A	N/A	N/A	N/A	N/A	N/A	N/A	N/A	N/A
FXR/RXR Activation	N/A	N/A	N/A	N/A	N/A	N/A	N/A	N/A	N/A	N/A	N/A	N/A	N/A	N/A	N/A
Caveolar-mediated Endocytosis Signaling	N/A	N/A	N/A	N/A	N/A	N/A	N/A	N/A	N/A	N/A	N/A	N/A	N/A	N/A	N/A
Ethanol Degradation IV	N/A	N/A	N/A	N/A	N/A	N/A	N/A	N/A	N/A	N/A	N/A	N/A	N/A	N/A	N/A
BER pathway	N/A	N/A	N/A	N/A	N/A	N/A	N/A	N/A	N/A	N/A	N/A	N/A	N/A	N/A	N/A
Dopamine Receptor Signaling	N/A	N/A	N/A	N/A	N/A	N/A	N/A	N/A	N/A	N/A	N/A	N/A	N/A	N/A	N/A
IL-4 Signaling	N/A	N/A	N/A	N/A	N/A	N/A	N/A	N/A	N/A	N/A	N/A	N/A	N/A	N/A	N/A
Transcriptional Regulatory Network in Embryonic Stem Cells	N/A	N/A	N/A	N/A	N/A	N/A	N/A	N/A	N/A	N/A	N/A	N/A	N/A	N/A	N/A
Mitochondrial L-carnitine Shuttle Pathway	N/A	N/A	N/A	N/A	N/A	N/A	N/A	N/A	N/A	N/A	N/A	N/A	N/A	N/A	N/A
Glutamine Degradation I	N/A	N/A	N/A	N/A	N/A	N/A	N/A	N/A	N/A	N/A	N/A	N/A	N/A	N/A	N/A

Role of Oct4 in Mammalian Embryonic Stem Cell Pluripotency	N/A	N/A	N/A	N/A	N/A	N/A	N/A	N/A	N/A	N/A	N/A	N/A	N/A	N/A	N/A
IL-10 Signaling	N/A	N/A	N/A	N/A	N/A	N/A	N/A	N/A	N/A	N/A	N/A	N/A	N/A	N/A	N/A
Germ Cell-Sertoli Cell Junction Signaling	N/A	N/A	N/A	N/A	N/A	N/A	N/A	N/A	N/A	N/A	N/A	N/A	N/A	N/A	N/A
Prostate Cancer Signaling	N/A	N/A	N/A	N/A	N/A	N/A	N/A	N/A	N/A	N/A	N/A	N/A	N/A	N/A	N/A
Phosphatidylglycerol Biosynthesis II (Non-plastidic)	N/A	N/A	N/A	N/A	N/A	N/A	N/A	N/A	N/A	N/A	N/A	N/A	N/A	N/A	N/A
Epithelial Adherens Junction Signaling	N/A	N/A	N/A	N/A	N/A	N/A	N/A	N/A	N/A	N/A	N/A	N/A	N/A	N/A	N/A
Phagosome Maturation	N/A	N/A	N/A	N/A	N/A	N/A	N/A	N/A	N/A	N/A	N/A	N/A	N/A	N/A	N/A
Clathrin-mediated Endocytosis Signaling	N/A	N/A	N/A	N/A	N/A	N/A	N/A	N/A	N/A	N/A	N/A	N/A	N/A	N/A	N/A
Superpathway of D-myo-inositol (1,4,5)-trisphosphate Metabolism	N/A	N/A	N/A	N/A	N/A	N/A	N/A	N/A	N/A	N/A	N/A	0.00	0.00	0.00	N/A
Histidine Degradation VI	N/A	N/A	N/A	N/A	N/A	N/A	N/A	N/A	N/A	N/A	N/A	N/A	N/A	N/A	N/A
Unfolded protein response	N/A	N/A	N/A	N/A	N/A	N/A	N/A	N/A	N/A	N/A	N/A	N/A	N/A	N/A	N/A
Role of JAK1, JAK2 and TYK2 in Interferon Signaling	N/A	N/A	N/A	N/A	N/A	N/A	N/A	N/A	N/A	N/A	N/A	N/A	N/A	N/A	N/A
Antiproliferative Role of TOB in T Cell Signaling	N/A	N/A	N/A	N/A	N/A	N/A	N/A	N/A	N/A	N/A	N/A	N/A	N/A	N/A	N/A
PXR/RXR Activation	N/A	N/A	N/A	N/A	N/A	N/A	N/A	N/A	N/A	N/A	N/A	N/A	N/A	N/A	N/A
Cellular Effects of Sildenafil (Viagra)	N/A	N/A	N/A	N/A	N/A	N/A	N/A	N/A	N/A	N/A	N/A	N/A	N/A	N/A	N/A
Mitochondrial Dysfunction	N/A	N/A	N/A	N/A	N/A	N/A	N/A	N/A	N/A	N/A	N/A	N/A	N/A	N/A	N/A
Breast Cancer Regulation by Stathmin1	N/A	N/A	N/A	N/A	N/A	N/A	N/A	N/A	N/A	N/A	N/A	N/A	N/A	N/A	N/A
Role of Macrophages, Fibroblasts and Endothelial Cells in Rheumatoid Arthritis	N/A	N/A	N/A	N/A	N/A	N/A	N/A	N/A	N/A	N/A	N/A	N/A	N/A	N/A	N/A
Role of JAK2 in Hormone-like Cytokine Signaling	N/A	N/A	N/A	N/A	N/A	N/A	N/A	N/A	N/A	N/A	N/A	N/A	N/A	N/A	N/A
Role of IL-17A in Arthritis	N/A	N/A	N/A	N/A	N/A	N/A	N/A	N/A	N/A	N/A	N/A	N/A	N/A	N/A	N/A
Calcium Transport I	N/A	N/A	N/A	N/A	N/A	N/A	N/A	N/A	N/A	N/A	N/A	N/A	N/A	N/A	N/A
Role of Tissue Factor in Cancer	N/A	N/A	N/A	N/A	N/A	N/A	N/A	N/A	N/A	N/A	N/A	N/A	N/A	N/A	N/A
Erythropoietin Signaling	N/A	N/A	N/A	N/A	N/A	N/A	N/A	N/A	N/A	N/A	N/A	N/A	N/A	N/A	N/A
Docosahexaenoic Acid (DHA) Signaling	N/A	N/A	N/A	N/A	N/A	N/A	N/A	N/A	N/A	N/A	N/A	N/A	N/A	N/A	N/A
Choline Biosynthesis III	N/A	N/A	N/A	N/A	N/A	N/A	N/A	N/A	N/A	0.00	N/A	N/A	N/A	N/A	N/A
Phagosome Formation	N/A	N/A	N/A	N/A	N/A	N/A	N/A	N/A	N/A	N/A	N/A	N/A	N/A	N/A	N/A
Role of JAK family kinases in IL-6-type Cytokine Signaling	N/A	N/A	N/A	N/A	N/A	N/A	N/A	N/A	N/A	N/A	N/A	N/A	N/A	N/A	N/A
HIF1α Signaling	N/A	N/A	N/A	N/A	N/A	N/A	N/A	N/A	N/A	N/A	N/A	N/A	N/A	N/A	N/A
Role of Osteoblasts, Osteoclasts and Chondrocytes in Rheumatoid Arthritis	N/A	N/A	N/A	N/A	N/A	N/A	N/A	N/A	N/A	N/A	N/A	N/A	N/A	N/A	N/A
1D-myo-inositol Hexakisphosphate Biosynthesis II (Mammalian)	N/A	N/A	N/A	N/A	N/A	N/A	N/A	N/A	N/A	N/A	N/A	0.00	0.00	0.00	N/A
GADD45 Signaling	N/A	N/A	N/A	N/A	N/A	N/A	N/A	N/A	N/A	N/A	N/A	N/A	N/A	N/A	N/A
Hypoxia Signaling in the Cardiovascular System	N/A	N/A	N/A	N/A	N/A	N/A	N/A	N/A	N/A	N/A	N/A	N/A	N/A	N/A	N/A
Molecular Mechanisms of Cancer	N/A	N/A	N/A	N/A	N/A	N/A	N/A	N/A	N/A	N/A	N/A	N/A	N/A	N/A	N/A
IL-15 Production	N/A	N/A	N/A	N/A	N/A	N/A	N/A	N/A	N/A	N/A	N/A	N/A	N/A	N/A	N/A
Virus Entry via Endocytic Pathways	N/A	N/A	N/A	N/A	N/A	N/A	N/A	N/A	N/A	N/A	N/A	N/A	N/A	N/A	N/A
Graft-versus-Host Disease Signaling	N/A	N/A	N/A	N/A	N/A	N/A	N/A	N/A	N/A	N/A	N/A	N/A	N/A	N/A	N/A
Hepatic Fibrosis / Hepatic Stellate Cell Activation	N/A	N/A	N/A	N/A	N/A	N/A	N/A	N/A	N/A	N/A	N/A	N/A	N/A	N/A	N/A
Glucocorticoid Receptor Signaling	N/A	N/A	N/A	N/A	N/A	N/A	N/A	N/A	N/A	N/A	N/A	N/A	N/A	N/A	N/A

Biotin-carboxyl Carrier Protein Assembly	N/A	N/A	N/A	N/A	N/A	N/A	N/A	N/A	N/A	N/A	N/A	N/A	N/A	N/A	N/A
Acetate Conversion to Acetyl-CoA	N/A	N/A	N/A	N/A	N/A	N/A	N/A	N/A	N/A	N/A	N/A	N/A	N/A	N/A	N/A

Table 27. A complete list of predicted z-scores for significantly altered pathways in all HZE irradiated mice across all time points. NA indicates that the directionality for the significant pathway could not be predicted based on the available literature and observed data.

6.6 Conclusions

^{56}Fe,^{16}O, and ^{28}Si are all major HZE contributors in the space radiation environment, yet the differences in biological effects (both acute and chronic) of these HZE ions after total body irradiation in mice remain largely unexplored. To understand the molecular mechanisms of HZE-induced HCC, we investigated the effects of ^{56}Fe,^{16}O, and ^{28}Si ions irradiation on transcript expression utilizing RNA-Seq data collected from the livers of mice at 5 different time points post-irradiation. Our findings revealed an early activation of proinflammatory response along with various cytokine activities, and inhibition of these responses at later time points post-irradiation. Additionally, our results revealed a number of unannotated transcripts that were significantly affected post low-dose HZE irradiation, and their associations with specific functional pathways. Taken together, these findings provide leads regarding potentially important new transcripts and transcriptional products, which could lead to identification of novel countermeasures and therapeutic targets. Identification of novel transcriptional products may be accomplished by *in silico* translation of unannotated transcripts into amino acid sequences which can be used to search Data Independent Acquisition (DIA) proteomics datasets from similar studies. This will enable the identification of novel transcriptional products.

6.7 Availability of Data and Materials

The data discussed in this chapter have been deposited in NCBI's Gene Expression Omnibus (Nia et al., 2020) and are accessible through GEO Series accession number GSE146254. (https://www.ncbi.nlm.nih.gov/geo/query/acc.cgi?acc=GSE146254).

7 CHAPTER 4: ^{137}CS Γ RAY AND ^{28}SI IRRADIATION INDUCED MURINE HEPATOCELLULAR CARCINOMA LIPID CHANGES IN LIVER ASSESSED BY MALDI-MSI COMBINED WITH SPATIAL SHRUNKEN CENTROID CLUSTERING ALGORITHM

7.1 Abstract

The characterization of lipids by Matrix-Assisted Laser Desorption Ionization Mass Spectrometry Imaging (MALDI-MSI) is of great interest because not only are lipids important structural molecules in both the cell and internal organelle membranes, but they are also important signaling molecules. MALDI-MSI combined with spatial image segmentation has been previously used to identify tumor heterogeneities within tissues with distinct anatomical regions such as brain. However, there has been no systematic study utilizing MALDI-MSI combined with spatial image segmentation assessing the tumor microenvironment in the liver. Here, we present that image segmentation can be used to assess the tumor microenvironment in the liver. In particular, to better understand the molecular mechanisms of irradiation-induced hepatic carcinogenesis, we used MALDI-MSI in the negative ion mode to identify lipid changes 12 months post exposure to low dose ^{28}Si and ^{137}Cs γ ray irradiation. We report here the changes in lipid profiles of murine liver tissues after exposure to irradiation, analyzed using Spatial Shrunken Centroid Clustering Algorithm. These findings provide valuable information as astronauts will be exposed to high-charge, high-energy (HZE) and low energy gamma ray irradiation during deep space travel. Even at low doses, exposure to these irradiations can lead to cancer. Previous studies infer that irradiation of mice with low-dose HZE particles induces

oxidative damage and micro-environmental changes that are thought to play roles in the pathophysiology of hepatocellular carcinoma (HCC).

Keywords: Mass Spectrometry Imaging, Lipid, Tumor Microenvironment, Irradiation-induced Hepatocellular Carcinoma, Small Molecule Imaging, Laser Desorption Ionization

7.2 Introduction

The primary goal of NASA's space irradiation research is to assess the health effects of deep space irradiation on astronauts, in order to provide risk prediction and to develop preventive measures against diseases that would further slow space exploration. The irradiation encountered in space is a form of galactic cosmic rays (GCR), which include low energy gamma rays (^{137}Cs γ) and particle nuclei of HZE (Z>13), and other ions that are created during interactions within the spacecraft. [145] Even at low doses, exposure to HZE, such as ^{28}Si as well as low energy ^{137}Cs γ rays, can lead to cancer. [6] Previous studies have shown that irradiation of mice with low dose HZE significantly increases the incidence of HCC. [7] Current literature supports that irradiation of mice induces oxidative damage and micro-environmental changes that are thought to play roles in the pathophysiology of HCC. [7, 8] Tumor heterogeneity is now considered a key factor in the prognosis and clinical outcomes of patients, and the way they respond to chemotherapy. [146-150] Understanding the molecular basis and characterization of tumor heterogeneity is an important step to shed light on how HZE and ^{137}Cs γ ray irradiation induce liver tumors or HCC.

Mass Spectrometry Imaging (MSI) is a powerful tool that has been extensively utilized in cancer research to characterize heterogeneities, due to its exceptional advantage

of maintaining the spatial organization of cells when analyzing tissue specimens. This allows researchers to conduct an in-depth analysis of the molecular content of their specimens. MALDI-MSI has indeed been able to characterize relevant tumor populations within cancer tissues. [151-157] It has also been exploited for identification of novel biomarkers as well as early detection and recognition of micro-environmental changes in lipid profiles. [22-26] The high abundance of various lipids in biological tissues has rendered MALDI-MSI a suitable method to detect these changes. Lipids are the main constituents of membranes in cells, as well as of internal organelles. Most membranes are lipid bilayers composed of different classes of lipids such as phospholipids, cholesterol, sphingolipids, triglycerides, and etc. The method has been shown to identify and quantify (relative to control) polar lipids per sample, providing information on the structural integrity of cells and the potential state of cellular communication. [27-29, 158] Changes in lipid expression have been shown to be involved in numerous pathological states. [30-34]

Each MALDI-MSI experiment produces a distribution of complex lipids in tissue, a wealth of information that requires extensive effort and time to analyze. The complexity and size of this data requires use of data reduction methods and more automated approaches to provide useful information. Various tools and image segmentation methods have been used to segment MALDI-MSI images, based on the characteristic masses for specific tissue regions.[159-162] Here we use Cardinal R package [163], an open-source R-based software package developed specifically for MALDI-MSI, to segment liver tissues based on their characteristic masses, and to further detect the significant lipid differences between non-irradiated controls and irradiated liver tissues from the tumor specimens. The Cardinal

R package has been used in the context of brain tissue as a tool to segment different anatomical regions with different spectral characteristics. [164] However, multivariate statistical techniques and model-based image segmentation has not found application in liver tissue, due to liver tissue's homogeneous nature, as opposed to brain, which has distinct anatomical regions. Analyzing liver spectra is often quite tedious due to the large and homogeneous nature of this tissue, and due to the biological and technical variation in intensities of spectral features. Using statistical inference is crucial for differentiating the systematic signals in the spectra from the noise, and for further performing an unbiased statistical comparison between different experimental conditions.

To better understand the molecular mechanisms of low energy ^{137}Cs γ rays as well as HZE, in particular ^{28}Si irradiation, induced hepatic carcinogenesis, we used MALDI-MSI in negative ion mode to identify changes in lipid profiles from the tumor specimens in the livers of C3H/HeNCrl mice, compared to non-irradiated controls using Spatial Shrunken Centroid Clustering Algorithm.

7.3 Methods

7.3.1 Animal Experiment

C3H/HeNCrl mice purchased from Charles River (Wilmington, MA) were used in this experiment. Mice were used for this study because they have been shown in the past to be a good experimental model for liver carcinogenesis. Strains used were based on a previous study which demonstrated that C3H/HeNCrl mice are sensitive to the induction of HCC after exposure to a dose of 0.2 Gy of 600 MeV/n ^{56}Fe. [7] Tumor induction studies and studies of molecular changes in the irradiated tissues can only be conducted in whole

animals. *In vivo* studies are necessary to study the microenvironmental effects of HZE exposure because computer models or cell culture are inadequate based on extensive literature searches. Conducted studies were approved by the institutional animal care and use committees (IACUCs) that are charged with evaluating the appropriateness of the use of animals in specific experiments and the numbers of animals requested for each group. The numbers of animals used were based on the expected numbers of irradiation-related tumors that would develop if animals were allowed to live out their lifespan. Power calculations for numbers in this study are based on chi-square test for comparing two proportions, controlling two-sided significance level at 0.05 or with 95% confidence about our results, and with 80% power.

Serial sacrifice study consisted of 7 (2 per treatment and 3 control) male C3H/HeNCrl mice 360 days post-exposure to HZE ^{28}Si irradiation (0.2 Gy) (n=2), ^{137}Cs γ rays (1.0 Gy) (n=2), and non-irradiated/sham-irradiated control (n=3). The mice were shipped from the vendor to Brookhaven National Laboratories (BNL) and housed at the BNL animal facility until the time of irradiation at the NASA Space Radiation Laboratory (NSRL). Following irradiation, the animals were shipped to the UTMB Animal Resources Center (ARC), quarantined for one month and then maintained in the ARC for the duration of the experiment. Animals were housed in sterile cages with free access to food and water. Facilities at both BNL and UTMB are fully AAALAC accredited which ensured adequacy of all animal care issues at both animal facilities. At 12 months, animals from each treatment group and control were randomly selected and euthanized by using CO_2 asphyxiation as per current AVMA guidelines for euthanasia. Prior to euthanasia animals were weighed and weight recorded. Post euthanasia, tissues of the left lobe of livers were

collected, snap-frozen on either dry ice or liquid nitrogen and stored at -80ºC until tissues could be extracted for MALDI-MSI. Livers were sampled by taking two 10 μm slices using a cryotome at -20°C.

7.3.2 MALDI-MSI EXPERIMENT

7.3.2.1 Sample Preparation and Histological Annotation

In the present study, 2 tumor samples from biological replicates of C3H/HeNCrl mice irradiated with ^{137}Cs γ rays (1.0 Gy), 2 tumor samples from biological replicates of C3H/HeNCrl mice irradiated with 350 MeV/n ^{28}Si (0.2 Gy), and 3 healthy samples from biological replicates of C3H/HeNCrl mice in non-irradiated/sham-irradiated control, were collected 12 months post-irradiation. Left lobes of the livers were harvested, frozen in liquid nitrogen vapor and stored at -80°C. All tissue samples were sectioned at 10 μm thickness using a Leica CM1950 cryostat (Leica Microsystems GmbH, Wetzlar, Germany) at -20°C and thaw mounted onto indium tin oxide (ITO) coated glass slides, (ITO glass, Type II, 0.7mm) (Hudson Surface Technology, Inc., West New York, NJ ; cat. # PL-IC-000010-P100 (formerly PSI 1207000)). Each tissue slice for MALDI imaging was followed by a slice collected for morphological/immunocytochemical staining (H&E staining) and mounted on a regular Superfrost™ Plus microscope slide (Fisher Scientific, Pittsburgh, PA; cat. # 12-550-15). Each slide was stored in a 50 ml plastic conical tube at -80°C. A detailed histological analysis of the cryosections was performed by an experienced pathologist (HSL) post acquisition hematoxylin and eosin (H&E) staining. Before matrix application, the slides were transferred to -20°C for 20 minutes and then placed into a vacuum desiccator for approximately 25 minutes.

7.3.2.2 MALDI Matrix Application and Mass Spectrometry Imaging

1,5-Diaminonaphthalene (DHB) (MilliporeSigma, St. Louis. MO; cat.# 149357) was applied by sublimation under vacuum using a procedure similar to that described by Wildburger (2017). [165] Sublimation of DHB was performed for 1 min at 120°C under 10-15 mTorr. Matrix coating density was approximately 500 μg/cm^2. After that, the slide was placed in a 50 ml plastic conical tube at −80°C. Prior to MALDI imaging, the slides were transferred to -20°C for 20 minutes, and then quickly transferred into a vacuum desiccator and brought to room temperature under vacuum for approximately 10 minutes. An Ultraflextreme MALDI-TOF/TOF MS (Bruker Daltonics, Billerica, MA) equipped with a smartbeam Nd: YAG 355 nm laser was utilized for MALDI analysis. The laser was operated at 250 Hz in negative ion reflector mode. Mass spectra were collected with a pulsed ion extraction time of 80 ns, an accelerating voltage of 20.0 kV, an extraction voltage of 17.90 kV, a lens voltage of 7.80 kV, and a reflector voltage of 21.15 kV. The laser spot size was set at medium focus (~50 μm laser spot diameter), and laser power was optimized at the start of each run and then fixed for the whole experiment. The mass spectra data were acquired over a mass range of m/z 400-1600 Da. Mass calibration was performed prior to data acquisition using Bruker Peptide Calibration Standard II (Bruker Daltonics, Billerica, MA) as an external standard. For mass spectrometry analysis, imaging spatial resolution was set to 100 μm. Each spectrum was a sum of 500 laser shots. Regions of interest were manually defined in the flexImaging 3.0.54 software, using a scan of the slide with the tissue sections acquired at 1200 dpi using an Epson 3170 photo scanner. MALDI mass spectra were processed with the total ion current (TIC) normalization, and the signal intensity of each imaging data was represented as the normalized intensity.

7.3.3 DATA ANALYSIS

7.3.3.1 Image Pre-processing

It is necessary to use appropriate pre-processing steps in oder to derive reliable conclusions and to obtain maximal biological information from MALDI-MSI data. In order to improve signal quality and compress the raw data acquired into a list of valuable peaks associated with relevant *m/z* values for further analysis, we used the Cardinal R package [163] to perform all preprocessing data. This includes normalization based on the total ion count (TIC), spectra smoothing, baseline correction, peak detection and spectra alignment.

7.3.3.2 Image Segmentation

We used the spatial shrunken centroids clustering algorithm provided in Cardinal R package [163], a model-based unsupervised image segmentation technique using adaptive weights that preserve edges between segments. The spatial shrunken centroids clustering algorithm uses a statistical regularization to enforce feature sparsity. As a result, the analysis automatically identifies informative *m/z* values and partitions the observations within a dataset into segments. The pixels in the dataset are partitioned according to their *m/z* similarity, expressed by their chemical and/or biological properties. [166] In particular, the parameters are *r* (the neighborhood smoothing radius), *k* (he initial number of segments /clusters), and *s* (the shrinkage parameter). We selected a set of parameters to get sharp/not pixelated segments with sharp edges (r=6, k=5, s=3). We then exported each segment with its corresponding list of *m/z,* and t-score, which is an enrichment score that is calculated based on the abundancy of specific *m/z* values in the corresponding segment compared to

other segments. In this analysis, the segmentation was performed on one slide/image with 7 different specimens on it partitioned toegher. In particular, the samples were 2 biological replicates from liver tumor section in ^{28}Si irradiated, 2 biological replicates from liver tumor section in ^{137}Cs γ rays irradiated, and 3 biological replicates from non-tumor liver section in non-irradiated/sham-irradiated control mice.

7.3.3.3 Statistical Comparison and MALDI-MSI Visualizations

After image segmentation, we picked the highly enriched up-regulated *m/z,* as well as down-regulated *m/z,* features in segment 1 (core tumor regions), compared to segment 3 (healthy non-irradiated control) using their t-score enrichment values. Evaluation of t-scores from core tumor regions in irradiated liver sections compared to non-irradiated healthy control and healthy-looking non-core tumor regions revealed peaks that could discriminate between different segments based on their corresponding t-scores. These peaks were also confirmed using flexImaging 3.0.54 (Bruker Daltonics, Billerica, MA), by visualizing the hotspots and differences between the segments. Despite the unquestionable advantages of visualization software in visualizing the spatial distribution and relative abundance of *m/z* directly, the visualized features are often complex and easy to miss, which makes analysis and interpretation challenging. Therefore, using a model-based approached and t-score enrichment values allowed us to detect different features in a more systematic matter, as opposed to purely relying on the qualitative visualization of hot spots.

7.3.4 MS/MS Validation of Selected *m/z*-Values

On-tissue MS/MS fragmentation spectra of the lipid species of interest were acquired using the Ultraflextreme mass spectrometer in negative ion LIFT mode. The laser

was operated at 1000 Hz; each MS-MS spectrum was a sum of 1500 shots for precursor ions and 5000-10000 shots for product ions, respectively. MS/MS spectra in the reflector mode were acquired with a pulsed ion extraction time of 80 ns, an accelerating voltage of 7.5 kV, an extraction voltage of 6.8 kV, a lens voltage of 3.5 kV, a reflector voltage of 29.5 kV, a lift 1 voltage of 19.00 kV, and a lift 2 voltage of 3.7 kV. Preliminary assignments for the detected lipid species and their identification by MS/MS spectra were performed using the LIPID MAPS Structure Database , Human Metabolome Database, and Swiss Lipids.

7.3.5 Lipids Identifications

The selected parent ions with significant differences between irradiated core tumor region compared to healthy non-irradiated control were analyzed via direct MS/MS and were then manually searched for in the LIPID Metabolites and Pathway Strategy structure database using negative ion mode (LIPID MAPS Structure Database) Search results were further filtered by eliminating matches outside a mass error range of 100 ppm, thus reducing the potential for false positives.

7.4 Results

7.4.1 Screening of lipid biomarkers in ^{137}Cs γ ray irradiated tumor, ^{28}Si irradiated tumor compared to healthy non-irradiated control tissues

2 tumor liver slices from biological replicates of ^{28}Si irradiated, 2 tumor liver slices from biological replicates of ^{137}Cs γ ray irradiated, and 3 healthy non-tumor liver slices

from biological replicates of non-irradiated control were measured using MALDI-MSI and evaluated using the Spatial Shrunken Centroid Clustering Algorithm as shown in Figure 18. The image segmentation analysis was oriented to identify significant mass signatures in the irradiated tumor regions compared to healthy non-irradiated control. Figure 18 shows the different segmentations that resulted from spatial heterogeneities within the specimens. In particular, in tumor specimens (^{137}Cs γ ray and ^{28}Si irradiated), segment 1 (orange) originated from the sections of tumor/HCC that represented as the most disease looking segment histologically (H&E staining), also visible on the slide prepared for MALDI by naked eyes. This observation possibly represents the tumor initiation region (core tumor) where the initial cells transformed by a switching event common to all malignancies, to malignant cells. Table 28 shows the identified signature *m/z*-values with their corresponding t-scores in the irradiated core tumor segments (segment 1/orange) and the healthy segments which included non-irradiated control segments and the healthy-looking part of the tumor segments (segment 3/green).

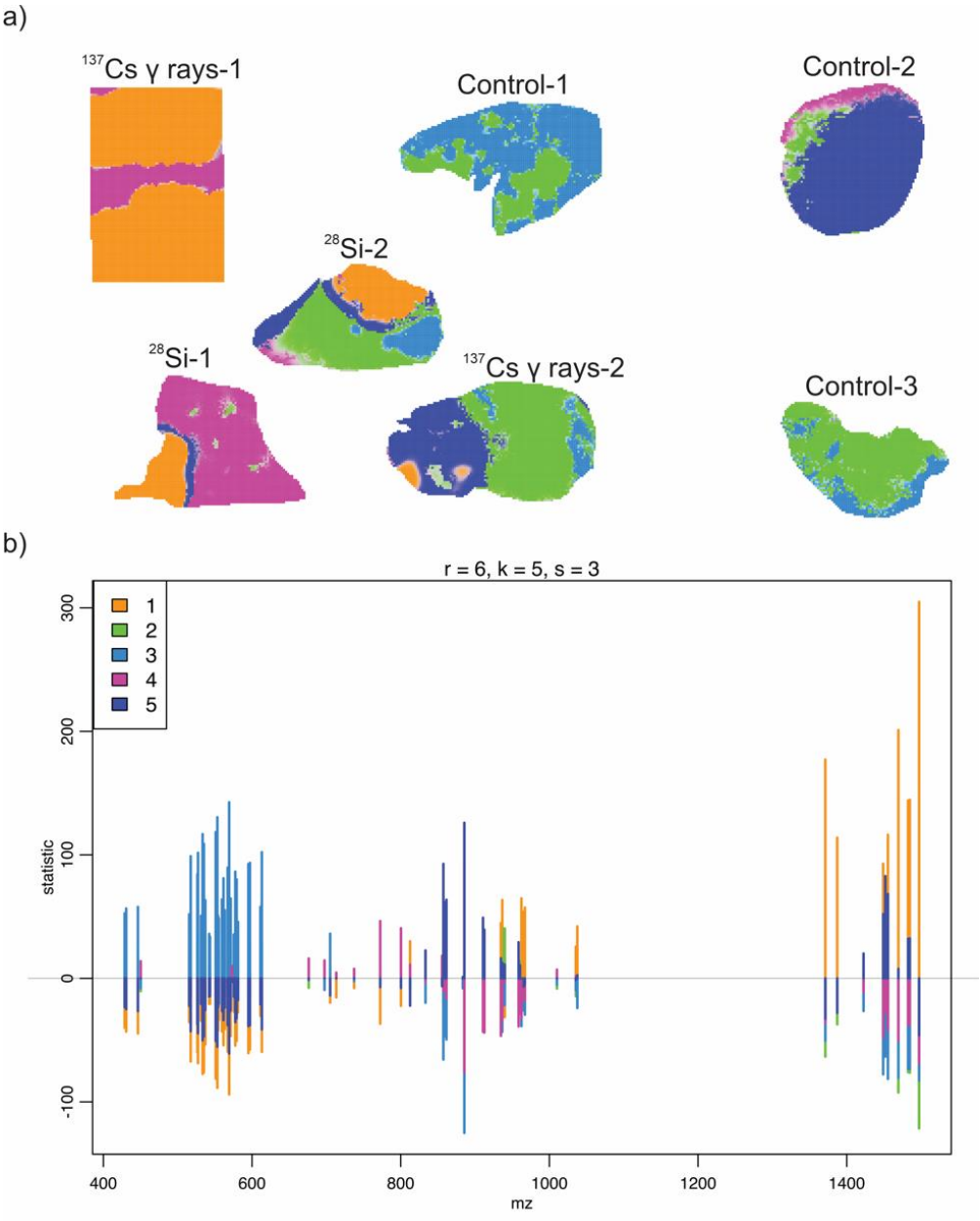

Figure 18. Segmentation result of the MALDI-MSI dataset using the Spatial Shrunken Centroid Clustering Algorithm.

a) There are 2 biological replicates from tumor sections of ^{28}Si irradiated, 2 biological replicates from tumor sections of ^{137}Cs γ rays irradiated, and 3 biological replicates from healthy non-irradiated control murine liver tissues. The segmentation with Spatial Shrunken Centroids and Structurally Adaptive distance selected 5 tissue segments that are color coded. The colors correspond to numbers in the bottom figure legend b which represent segment 1 (orange), 2 (green), 3 (light blue), 4 (pink), and 5 (dark blue). Segment 1 (orange) shows the core tumor/HCC region on each tumor specimen where the disease looking part of the specimen was observed both histologically (H&E staining) and visible

by naked eye on the MALDI slide. Segment 2 (green), Segment 3 (light blue), and Segment 4 (pink) shows healthy looking part of the tumor sections as well as in control sections. Segment 5 (dark blue) shows a transition looking part of the specimens in which the tissue looks neither completely healthy nor tumor looking. **(b)** The t-statistics quantified the relative importance of the peaks in each segment. The spectra show that segment 1 (orange/core tumor) is enriched (upregulated) mainly in higher *m/z*-values (~1400) and downregulated in lower *m/z*-values (<600). Conversely, healthy parts of the tumor sections from irradiated and healthy non-irradiated specimens show upregulation of lower *m/z*-values (<600).

m/z Detected	**t-score in Non-irradiated Healthy Control**	**t-score in Irradiated Core Tumor**	**Up/Down Regulated in Tumor vs. Control**	**Identified Lipid**
533.48	42.33	-77.41	Down	PA(14:1(9Z)/10:0) or Isomer PA(10:0/14:1(9Z))
535.11	43.67	-76.21	Down	PA(25:0/0:0)
537.09	26.77	-53.50	Down	PG(15:1(9Z)/4:0) or PG(P-16:0/4:0)
551.06	47.62	-81.27	Down	PE(2 3:0/0:0)
553.11	51.72	-88.72	Down	PG(10:0/10:0) or Isomer PG(12:0/8:0) and PS(20:0/0:0)
567.1	32.33	-59.24	Down	PS(16:0/4:0)
569.1	54.51	-94.01	Down	PS(22:6(4Z,7Z,10Z,13Z,16Z,19Z)/0:0)
579.07	25.83	-50.63	Down	PG(18:1(11E)/4:0)
595.11	33.57	-60.59	Down	PS(23:0/0:0)
611.11	11.09	-30.47	Down	PS(2:0/22:6(4Z,7Z,10Z,13Z,16Z,19Z))
613.13	29.62	-59.52	Down	Mixture of PA(20:3(8Z,11Z,14Z)/10:0) and PS(20:5(5Z,8Z,11Z,14Z,17Z)/4:0)
705.12	7.77	-19.68	Down	PE(21:0/12:0) or Isomer PE(12:0/21:0)
885.38	-39.73	92.24	Up	PI(18:0/20:4(5Z,8Z,11Z,14Z))
1370.52	-63.40	177.15	Up	Ganglioside GM2 GalNAcβ1-4(NeuGcα2-3)Galβ1-4Glcβ-Cer (undetermined tail)
1454.73	-72.08	116.29	Up	Ganglioside GM2 GalNAcβ1-4(NeuGcα2-3)Galβ1-4Glcβ-Cer (d18:1/22:0)
1482.76	-75.94	143.95	Up	Ganglioside GM2 GalNAcβ1-4(NeuGcα2-3)Galβ1-4Glcβ-Cer (undetermined tail)
1484.74	-76.40	144.59	Up	Ganglioside GM2 GalNAcβ1-4(NeuGcα2-3)Galβ1-4Glcβ-Cer (undetermined tail)
1497.71	-121.51	304.79	Up	Ganglioside GM2 GalNAcβ1-4(NeuGcα2-3)Galβ1-4Glcβ-Cer (undetermined tail)

Table 28. Identified signature m/z-values with their corresponding t-scores in segment 1/orange which represented the core-tumor in irradiated specimens vs. healthy segments 2/green which were identified in all control specimens as well as healthy parts of the tumor specimens. Identified Lipid column shows lipids that were identified by manual searching of on-tissue MS/MS fragmentations (100 ppm accuracy) of the corresponding m/z-values.

7.4.2 UPREGULATION OF HIGHER M/Z-VALUES AND DOWNREGULATION OF LOWER M/Z-VALUES FROM MICE LIVERS IN IRRADIATED TUMOR/HCC VS. HEALTHY SEGMENTS

Our findings show that irradiation induced HCC results in upregulation of lipids with higher masses and downregulation of lipids with lower masses in the liver. In particular, most upregulated peaks (Table 28) correspond to a mouse analogue (*N*-Glycolylneuraminic acid/Neu5Gc) of human GM2 (N-acetylneuraminic acid/Neu5Ac), a type of ganglioside with one sialic acid, as determined by *m/z* matches to lipid masses in the Lipid Maps Database and MS/MS fragmentations. The increased levels of the mouse analogue of GM2 post-exposure to low doses of HZE irradiation, in particular ^{28}Si (0.2 Gy), and low energy^{137}Cs γ ray (1.0 Gy) irradiation, appears to be a novel finding, as we know of no reports in the literature identifying higher levels of these GM2 analogues in mice in association with HCC. Additionally, downregulation of PA, PG, PS, and PE lipids was observed. Specifically, PA, phosphatidic acid, which can have many different combinations of fatty acids of varying lengths and saturation, was downregulated. PAs are important for biosynthesis of triacylglycerols and phospholipids and many other lipids, and their physical properties influence membrane curvature. They are maintained at low

concentration in order to act as a signaling molecule; [167-169] PG, phosphatidylglycerol which indirectly activates lipid-gated ion channels; [170] PS, phosphatidylserine, a component of the cell membrane which plays a key role in cell cycle signaling, and apoptosis; [171, 172] and finally, PE, phosphatidylethanolamine, a class of phospholipids found in biological membranes which play a role in the secretion of lipoproteins in the liver. [173, 174]

7.5 Discussion

Our study demonstrates for the first time that MALDI-MSI combined with unsupervised image segmentation can identify *m/z* changes in a homogenous tissue; specifically, liver where the distinct anatomical structures are challenging to identify, as opposed to tissues like brain, where different anatomical features are recognized relatively easily. Although unquestionably advantageous, the routinely used gene-expression profiling and proteomics methods not only require considerable amounts of tissue material, but use tissue homogenates which would negatively influence the diagnostic characterization based on tissue heterogeneity. On the other hand, MALDI-MSI segmentations of the liver would allow for a more specific identification of location of biological regions, leading to a better definition of *m/z* signatures obtained to describe tumor heterogeneity. The different segments identified in tumor sections (Figure 18) demonstrate the distinct heterogeneities and chemical properties within the tumor microenvironments. These heterogeneities are crucial to identify different subtypes of irradiation-induced HCC, each of which could have potentially different prognoses and require different approaches in clinical management.

Alterations in lipid metabolism and regulation are hallmarks of cancer which affect cellular function and growth. [175] The MALDI-MSI analysis of the livers in this study identified a 1454.73 *m/z* peak (Table 28) that corresponds to a glycosphingolipid (GSL) belonging to the ganglioside subfamily, shown in Figure 19. This GSL is upregulated in irradiated liver samples in contrast to control. This GSL is analogous to human GM2 (molecules only differ an OH or H on a terminal sugar). Several studies have described an association between increased level of GM2 and HCC in humans. One such study reported 20-100X increased levels of GM2 in sera from patients with HCC. [176] Additionally, peaks 551.06 and 705.12 identified as PEs were downregulated in core tumor regions. Previous studies have demonstrated a decrease in PC/PE ratio to be associated with hepatocyte nodules in rat livers. [177, 178] This might be due to decreased synthesis of PC, or decreased conversion of PE to PC following inactivation of the enzyme (PMET) responsible for the conversion of PE to PC. [179] The observation suggests that PE synthesis might be downregulated locally in tissues, regardless of this ratio. The decreased observed ratio could potentially be due to decreased PC synthesis through pathways (Kennedy pathway) not dependent upon PE to PC conversion. [180] Moreover, peaks 533.48, 535.11, and 613.13 identified as PAs were also downregulated in core tumor regions. Since PAs can act as lipid ligands which gate ion channels, this finding can help guide our understanding of lipid signaling cascades and their roles in the carcinogenic process of irradiation-induced HCC.

These novel findings on the lipid species post-exposure to low doses of ^{28}Si and ^{137}Cs γ rays support the strong potential of exploring these lipid species as early biomarkers of HCC risk in astronauts during deep space travel. In future works, the incorporation of

targeted gene expression, proteomics and comprehensive ultra-high resolution lipidomic arrays is planned to allow for identification of enzymes involved in the synthesis of these lipids, validate the potential identified biomarkers, and possibly determine targets for mediation of irradiation-induced HCC.

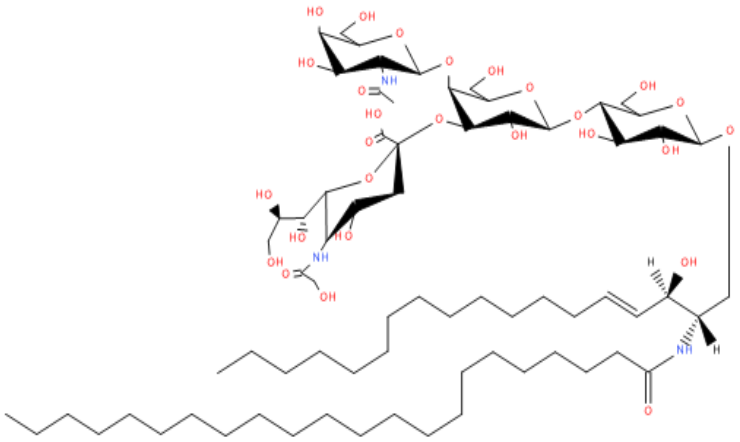

Figure 19. Structural formula of GalNAcβ1-4(NeuGcα2-3)Galβ1-4Glcβ-Cer (d18:1/22:0)

7.6 Conclusions

This investigation shows that even though MALDI-MSI datasets are complex and high dimensional and especially difficult to interpret quantitively in homogenous tissues such as liver, segmentation can provide a unique way to depict the complex lipid heterogeneity of liver tissues in one image. Utilizing the Spatial Shrunken Centroid Clustering Algorithm enabled us to extract meaningful information from the raw measurements by reducing dimensionality and identifying region-specific *m/z*-changes in irradiated vs. non-irradiated control mice liver tissues. We collected MS/MS data and refined the identification of the lipid species found in the study and have assigned lipid species identifications based on Lipid Maps Database searching of MS/MS fragmentations.

This approach has allowed us to reliably identify a number of lipid ion species (Table 1) whose levels were significantly changed in irradiated tumor/HCC compared to healthy non-irradiated controls, based on both signal intensity and spatial distribution. In particular, we have confirmed the identity of *N*-Glycolylneuraminic acid/Neu5Gc. Its upregulation is of special interest because the human analogue (N-acetylneuraminic acid/Neu5Ac) is elevated in patients with HCC. Comparative analysis of this data enabled us to get a better systematic picture of the oncogenic transformation and cancer progression induced by HZE and γ-ray irradiation in mice livers. Understanding this process and its mechanisms is critical to the safety of future manned spaceflights. Since lipids serve as an excellent source of information on various cellular signaling processes, and thus cancerous growth, our assigned lipid species can further be explored in future studies as potential biomarkers of HCC risk in astronauts during deep space travel. An attractive medical translation would be using lipid arrays in which the aforementioned potential lipids are immobilized and probed with astronauts' sera for the presence of immune reactivities against these lipids. [181]

8 CHAPTER 5: CONCLUSIONS

8.1 New Results of this Work

In this dissertation, we have shed light on the carcinogenic process of irradiation-induced HCC utilizing RNA-Seq and MALDI-MSI.

1. In Chapter 2, we offered a new analytical pipeline to study the RNA-Seq dataset of ^{56}Fe irradiated compared to non-irradiated control mice liver tissues. This pipeline allowed us to determine gene interaction modules that were more biologically interpretable than those produced by existing methods.

2. In Chapter 3, we performed a comparative transcriptomic analysis in a mouse model for irradiation-induced cancer using the RNA-Seq data from HZE irradiated (^{56}Fe, ^{16}O, and ^{28}Si) mice liver tissues compared to non-irradiated control. We have demonstrated the shared mechanisms, as well as their unique dynamic time dependent immunological responses, post-exposure to irradiation. Additionally, using the SOM machine learning algorithm, we were able to infer the biological functions of the unannotated transcripts that were significantly affected post-exposure to HZE.

3. In Chapter 4, we investigated the changes in lipid profiles of liver tissues after exposure to HZE, in particular, ^{28}Si and low energy ^{137}Cs γ rays, in a more HCC susceptible mice strain. Our findings demonstrated a handful of potential candidates as biomarkers of irradiation-induced HCC, which included upregulation in mice of a human GM2 analogue previously implicated in patients with HCC.

8.2 A Few Notes on the Importance of these Results

In Chapter 2, we discussed a new pipeline that combines the adjacency matrix notion of WGCNA with Modularity Maximization methods to find modules that are involved in various biological pathways of ^{56}Fe irradiation-induced HCC. Even though RNA-Seq has been the tool of choice for large-scale transcriptomics, it has unmet bioinformatics challenges that need to be addressed to make *de novo* discovery possible and to allow scientists to extract meaningful biological information. Differential co-expression analysis can identify significant co-expression modules that are affected by a treatment condition or disease. These modules are then used to find genes/transcripts underlying the differences between sample conditions. [182-187] WGCNA, one of the first co-expression tools used on RNA-Seq data, has been utilized in finding associations between modules and biological functions. [182, 188, 189] The utilization of WCGNA in our dataset resulted in a large number of unassigned transcripts, and modules with too many transcripts, which made biological interpretation more difficult. The nove discussed WGCNA-M pipeline allowed us to reduce the number of unassigned transcripts while maintaining an optimal number of modules. This method provides an additional avenue to explore various RNA-Seq datasets, and can be applied to other omics datasets, such as those produced by proteomics and lipidomics experiments. Biological processes are carried out by modules of interacting molecules. Genes with similar expression display an increased likelihood of being associated with a common functional module, following the guilt-by-association principle. However, although co-expression methods confer insights about most genes in an assigned module, assuming they are functionally related, it is important to remember the possibility that not every entity in a particular module is associated with the specific functions for

which it is enriched. Biological validation of the functionality of target genes is integral, prior to making conclusions regarding genes in the same modules.

In Chapter 3, we explored the effects of HZE on hepatic carcinogenesis by comparative transcriptomics analysis. Additionally, we utilized SOMs to identify functional associations for transcripts significantly affected by HZE, but that were unannotated by IPA. It is important to note that we used average-sized SOMs (n=16) since we also performed the analysis on the differentially expressed transcripts. One can also perform SOMs analysis with larger map sizes on all expressed transcripts. It has been previously reported that SOMs with maps sizes of greater than 100 modules can capture a variety of patterns that may not be otherwise revealed, and that such SOMs can show emergent behavior. [190, 191] For this study, we aimed to focus on finding a rather smaller list of candidates that can be validated in the future, for use as irradiation countermeasures. Consequently, we limited our SOM analysis to the list of differentially expressed transcripts. Subsequent mining and re-analyses of these datasets will allow users to extend the analysis and extract groups of transcripts that have implications not only for irradiation-induced HCC but other types of irradiation that show similar biological effects.

In Chapter 4, we utilized MALDI-MSI with the Spatial Shrunken Centroid Clustering Algorithm to identify lipid species affected by ^{28}Si and ^{137}Cs γ ray irradiation. Since lipids serve as an excellent source of information on various cellular signaling processes, and thus cancerous growth, our assigned lipid species can further be explored in future studies as potential biomarkers of HCC risk in astronauts during deep space travel. An attractive medical translation would be using lipid arrays in which the aforementioned

potential lipids are immobilized and probed with astronauts' sera for the presence of immune reactivities against these lipids. [181]

In conclusion, this dissertation aimed to determine the specific effects that low-dose HZE and ^{137}Cs γ ray irradiation have on biochemical pathways implicated in the development of HCC, and to identify potential countermeasures as novel therapeutic targets. The acquisition of this information was a critical first step in determining changes that occur at the molecular level in response to these irradiations. The presented findings on the effects of low-dose HZE and ^{137}Cs γ ray irradiation on hepatic carcinogenesis helped identify the micro-environmental changes in pathways and lipids that lead to irradiation-induced HCC. Additionally, we developed an analytical pipeline that can be applied to perform similar analyses based on relevant gene expression data.

8.3 Future Works

Several exciting research avenues can be pursued in the future. The long-term objective of the parent study (NNX15AD65G) was to understand the molecular mechanisms underlying HZE and ^{137}Cs γ ray irradiation-induced HCC and liver damage. The different ions that makeup the GCR spectrum have unique effects on gene expression patterns. [192] Our findings on the unique pathways and genes impacted by different ions will allow the development of targeted interventions to counteract irradiation-induced liver damage. The next step is to test potential therapeutic countermeasures identified from this work. Another possible next step is to study the differences in gene expression and lipid species identified from this dissertation and conduct global methylation studies. It has been

shown that exposure to irradiation is associated with changes in methylation status and the specific effects exhibit tissue, gender and strain specificity. [193-198]

9 REFERENCES

1. White RJ, Averner M: **Humans in space**. *Nature* 2001, **409**(6823):1115-1118.
2. Cucinotta FA, Durante M: **Cancer risk from exposure to galactic cosmic rays: implications for space exploration by human beings**. *The Lancet Oncology* 2006, **7**(5):431-435.
3. Hayatsu K, Hareyama M, Kobayashi S, Yamashita N, Sakurai K, Hasebe N: **HZE Particle and Neutron Dosages from Cosmic Rays on the Lunar Surface**. 2009, **78**(Suppl.A):149-152.
4. Hamilton SA, Pecaut MJ, Gridley DS, Travis ND, Bandstra ER, Willey JS, Nelson G, Bateman TA: **A murine model for bone loss from therapeutic and space-relevant sources of radiation**. *Journal of Applied Physiology* 2006, **101**(3):789-793.
5. Cucinotta FA, Wu H, Shavers MR, George K: **Radiation dosimetry and biophysical models of space radiation effects**. *Gravitational and Space Biology* 2003, **16**(2):11-19.
6. Wakeford R: **The cancer epidemiology of radiation**. 2004, **23**(38):6404-6428.
7. Weil MM, Bedford JS, Bielefeldt-Ohmann H, Ray FA, Genik PC, Ehrhart EJ, Fallgren CM, Hailu F, Battaglia CL, Charles B *et al*: **Incidence of acute myeloid leukemia and hepatocellular carcinoma in mice irradiated with 1 GeV/nucleon (56)Fe ions**. *Radiat Res* 2009, **172**(2):213-219.
8. Weil MM, Ray FA, Genik PC, Yu Y, McCarthy M, Fallgren CM, Ullrich RL: **Effects of 28Si Ions, 56Fe Ions, and Protons on the Induction of Murine Acute Myeloid Leukemia and Hepatocellular Carcinoma**. *PLoS ONE* 2014, **9**(8):e104819.
9. Burns FJ, Jin Y, Koenig KL, Hosselet S: **The low carcinogenicity of electron radiation relative to argon ions in rat skin**. *Radiation research* 1993, **135**(2):178-188.
10. Alpen E, Powers-Risius P, Curtis S, DeGuzman R: **Tumorigenic potential of high-Z, high-LET charged-particle radiations**. *Radiation research* 1993, **136**(3):382-391.
11. Dicello JF, Christian A, Cucinotta F, Gridley D, Kathirithamby R, Mann J, Markham A, Moyers M, Novak G, Piantadosi S: **In vivo mammary tumourigenesis in the Sprague–Dawley rat and microdosimetric correlates**. *Physics in Medicine & Biology* 2004, **49**(16):3817.
12. Blakely EA, Kronenberg A: **Heavy-ion radiobiology: new approaches to delineate mechanisms underlying enhanced biological effectiveness**. *Radiation research* 1998, **150**(5s):S126-S145.
13. Sutherland BM, Bennett PV, Sidorkina O, Laval J: **Clustered DNA damages induced in isolated DNA and in human cells by low doses of ionizing radiation**. *Proceedings of the National Academy of Sciences* 2000, **97**(1):103-108.
14. Gulston M, de Lara C, Jenner T, Davis E, O'Neill P: **Processing of clustered DNA damage generates additional double-strand breaks in mammalian cells post-irradiation**. *Nucleic acids research* 2004, **32**(4):1602-1609.

15. Rydberg B, Cooper B, Cooper PK, Holley WR, Chatterjee A: **Dose-dependent misrejoining of radiation-induced DNA double-strand breaks in human fibroblasts: experimental and theoretical study for high-and low-LET radiation**. *Radiation research* 2005, **163**(5):526-534.
16. Guo J, Zeitlin C, Wimmer-Schweingruber RF, Hassler DM, Ehresmann B, Köhler J, Böhm E, Böttcher S, Brinza D, Burmeister S: **MSL-RAD radiation environment measurements**. *Radiation protection dosimetry* 2015, **166**(1-4):290-294.
17. Weil MM, Ray FA, Genik PC, Yu Y, McCarthy M, Fallgren CM, Ullrich RL: **Effects of 28Si ions, 56Fe ions, and protons on the induction of murine acute myeloid leukemia and hepatocellular carcinoma**. *PloS one* 2014, **9**(7):e104819.
18. Covelli V, Di Majo V, Coppola M, Rebessi S: **Neutron carcinogenesis in mice: A study of the dose-response curves**. *Radiation research* 1991, **128**(1s):S114-S116.
19. Spitz DR, Azzam EI, Li JJ, Gius D: **Metabolic oxidation/reduction reactions and cellular responses to ionizing radiation: a unifying concept in stress response biology**. *Cancer Metastasis Rev* 2004, **23**(3-4):311-322.
20. Schonfeld SJ, Bhatti P, Brown EE, Linet MS, Simon SL, Weinstock RM, Hutchinson AA, Stovall M, Preston DL, Alexander BH *et al*: **Polymorphisms in oxidative stress and inflammation pathway genes, low-dose ionizing radiation, and the risk of breast cancer among US radiologic technologists**. *Cancer Causes Control* 2010, **21**(11):1857-1866.
21. Zhao W, Robbins ME: **Inflammation and chronic oxidative stress in radiation-induced late normal tissue injury: therapeutic implications**. *Curr Med Chem* 2009, **16**(2):130-143.
22. Aichler M, Walch A: **MALDI Imaging mass spectrometry: current frontiers and perspectives in pathology research and practice**. *Lab Invest* 2015, **95**(4):422-431.
23. Cornett DS, Reyzer ML, Chaurand P, Caprioli RM: **MALDI imaging mass spectrometry: molecular snapshots of biochemical systems**. *Nat Methods* 2007, **4**(10):828-833.
24. Eriksson C, Masaki N, Yao I, Hayasaka T, Setou M: **MALDI Imaging Mass Spectrometry-A Mini Review of Methods and Recent Developments**. *Mass Spectrom (Tokyo)* 2013, **2**(Spec Iss):S0022.
25. Walch A, Rauser S, Deininger SO, Hofler H: **MALDI imaging mass spectrometry for direct tissue analysis: a new frontier for molecular histology**. *Histochem Cell Biol* 2008, **130**(3):421-434.
26. Franck J, Arafah K, Elayed M, Bonnel D, Vergara D, Jacquet A, Vinatier D, Wisztorski M, Day R, Fournier I *et al*: **MALDI imaging mass spectrometry: state of the art technology in clinical proteomics**. *Mol Cell Proteomics* 2009, **8**(9):2023-2033.
27. Angel PM, Spraggins JM, Baldwin HS, Caprioli R: **Enhanced sensitivity for high spatial resolution lipid analysis by negative ion mode matrix assisted laser desorption ionization imaging mass spectrometry**. *Anal Chem* 2012, **84**(3):1557-1564.

28. Murphy RC, Hankin JA, Barkley RM: **Imaging of lipid species by MALDI mass spectrometry**. *J Lipid Res* 2009, **50 Suppl**:S317-322.
29. Fuchs B, Suss R, Schiller J: **An update of MALDI-TOF mass spectrometry in lipid research**. *Prog Lipid Res* 2011, **50**(1):132.
30. Liu Y, Chen Y, Momin A, Shaner R, Wang E, Bowen NJ, Matyunina LV, Walker LD, McDonald JF, Sullards MC *et al*: **Elevation of sulfatides in ovarian cancer: an integrated transcriptomic and lipidomic analysis including tissue-imaging mass spectrometry**. *Mol Cancer* 2010, **9**:186.
31. Farooqui AA: **Lipid mediators in the neural cell nucleus: their metabolism, signaling, and association with neurological disorders**. *Neuroscientist* 2009, **15**(4):392-407.
32. Lin ME, Herr DR, Chun J: **Lysophosphatidic acid (LPA) receptors: signaling properties and disease relevance**. *Prostaglandins Other Lipid Mediat* 2010, **91**(3-4):130-138.
33. Hu C, van der Heijden R, Wang M, van der Greef J, Hankemeier T, Xu G: **Analytical strategies in lipidomics and applications in disease biomarker discovery**. *J Chromatogr B Analyt Technol Biomed Life Sci* 2009, **877**(26):2836-2846.
34. Watson AD: **Thematic review series: systems biology approaches to metabolic and cardiovascular disorders. Lipidomics: a global approach to lipid analysis in biological systems**. *J Lipid Res* 2006, **47**(10):2101-2111.
35. Ritchie ME, Phipson B, Wu D, Hu Y, Law CW, Shi W, Smyth GK: **limma powers differential expression analyses for RNA-sequencing and microarray studies**. *Nucleic Acids Res* 2015, **43**(7):e47.
36. Barabasi AL, Oltvai ZN: **Network biology: understanding the cell's functional organization**. *Nature reviews Genetics* 2004, **5**(2):101-113.
37. Hartwell LH, Hopfield JJ, Leibler S, Murray AW: **From molecular to modular cell biology**. *Nature* 1999, **402**(6761 Suppl):C47-52.
38. Zhang B, Horvath S: **A general framework for weighted gene co-expression network analysis**. *Statistical applications in genetics and molecular biology* 2005, **4**:Article17.
39. Eisen MB, Spellman PT, Brown PO, Botstein D: **Cluster analysis and display of genome-wide expression patterns**. *Proceedings of the National Academy of Sciences of the United States of America* 1998, **95**(25):14863-14868.
40. Stuart JM, Segal E, Koller D, Kim SK: **A gene-coexpression network for global discovery of conserved genetic modules**. *Science (New York, NY)* 2003, **302**(5643):249-255.
41. Langfelder P, Horvath S: **WGCNA: an R package for weighted correlation network analysis**. *BMC Bioinformatics* 2008, **9**(1):559.
42. Langfelder P, Zhang B, Horvath S: **Defining clusters from a hierarchical cluster tree: the Dynamic Tree Cut package for R**. *Bioinformatics (Oxford, England)* 2008, **24**(5):719-720.
43. Jiang B, Gribskov M: **Assessment of subnetwork detection methods for breast cancer**. *Cancer informatics* 2014, **13**(Suppl 6):15-23.
44. Newman MEJ: **Detecting community structure in networks**. *The European Physical Journal B - Condensed Matter* 2004, **38**(2):321-330.

45. Danon L, Díaz-Guilera A, Duch J, Arenas A: **Comparing community structure identification**. *Journal of Statistical Mechanics: Theory and Experiment* 2005, **2005**(09):P09008-P09008.
46. Fortunato S: **Community detection in graphs**. *Physics Reports* 2010, **486**(3-5):75-174.
47. Girvan M, Newman MEJ: **Community structure in social and biological networks**. *Proceedings of the National Academy of Sciences* 2002, **99**(12):7821-7826.
48. Newman MEJ: **The Structure and Function of Complex Networks**. *SIAM Review* 2003, **45**(2):167-256.
49. Newman ME, Girvan M: **Finding and evaluating community structure in networks**. *Phys Rev E Stat Nonlin Soft Matter Phys* 2004, **69**(2 Pt 2):026113.
50. Fortunato S, Barthelemy M: **Resolution limit in community detection**. *Proceedings of the National Academy of Sciences* 2007, **104**(1):36-41.
51. Ronhovde P, Nussinov Z: **Local resolution-limit-free Potts model for community detection**. *Physical Review E* 2010, **81**(4).
52. Arenas A, Fernández A, Gómez S: **Analysis of the structure of complex networks at different resolution levels**. *New Journal of Physics* 2008, **10**(5):053039.
53. Aldecoa R, Marín I: **Deciphering Network Community Structure by Surprise**. 2011, **6**(9):e24195.
54. Chen T, Singh P, Bassler KE: **Network community detection using modularity density measures**. *Journal of Statistical Mechanics: Theory and Experiment* 2018, **2018**(5):053406.
55. Cucinotta FA, Durante M: **Cancer risk from exposure to galactic cosmic rays: implications for space exploration by human beings**. *Lancet Oncol* 2006, **7**(5):431-435.
56. Durante M, Cucinotta FA: **Heavy ion carcinogenesis and human space exploration**. *Nature reviews Cancer* 2008, **8**(6):465-472.
57. Yu MW, Lien JP, Chiu YH, Santella RM, Liaw YF, Chen CJ: **Effect of aflatoxin metabolism and DNA adduct formation on hepatocellular carcinoma among chronic hepatitis B carriers in Taiwan**. *Journal of hepatology* 1997, **27**(2):320-330.
58. de Martel C, Ferlay J, Franceschi S, Vignat J, Bray F, Forman D, Plummer M: **Global burden of cancers attributable to infections in 2008: a review and synthetic analysis**. *The Lancet Oncology* 2012, **13**(6):607-615.
59. El-Serag HB: **Hepatocellular Carcinoma**. *New England Journal of Medicine* 2011, **365**(12):1118-1127.
60. Leach JK, Van Tuyle G, Lin PS, Schmidt-Ullrich R, Mikkelsen RB: **Ionizing radiation-induced, mitochondria-dependent generation of reactive oxygen/nitrogen**. *Cancer research* 2001, **61**(10):3894-3901.
61. Andrews S: **FastQC**. In., 0.11.8 edn; 2018.
62. Dobin A, Davis CA, Schlesinger F, Drenkow J, Zaleski C, Jha S, Batut P, Chaisson M, Gingeras TR: **STAR: ultrafast universal RNA-seq aligner**. *Bioinformatics (Oxford, England)* 2013, **29**(1):15-21.

63. Frankish A, Diekhans M, Ferreira A-M, Johnson R, Jungreis I, Loveland J, Mudge JM, Sisu C, Wright J, Armstrong J *et al*: **GENCODE reference annotation for the human and mouse genomes**. *Nucleic Acids Research* 2018, **47**(D1):D766-D773.
64. Team RC: **R: A language and enviornment for statistical computing**. In. Vienna, Austria: R Foundation for Statistical Computing.
65. Robinson MD, McCarthy DJ, Smyth GK: **edgeR: a Bioconductor package for differential expression analysis of digital gene expression data**. *Bioinformatics (Oxford, England)* 2010, **26**(1):139-140.
66. McCarthy DJ, Chen Y, Smyth GK: **Differential expression analysis of multifactor RNA-Seq experiments with respect to biological variation**. *Nucleic Acids Res* 2012, **40**(10):4288-4297.
67. Cox DR, Reid N: **Parameter Orthogonality and Approximate Conditional Inference**. *Journal of the Royal Statistical Society Series B (Methodological)* 1987, **49**(1):1-39.
68. Lun ATL, Chen Y, Smyth GK: **It's DE-licious: A Recipe for Differential Expression Analyses of RNA-seq Experiments Using Quasi-Likelihood Methods in edgeR**. In: *Statistical Genomics: Methods and Protocols.* Edited by Mathé E, Davis S. New York, NY: Springer New York; 2016: 391-416.
69. Lund Steven P, Nettleton D, McCarthy Davis J, Smyth Gordon K: **Detecting Differential Expression in RNA-sequence Data Using Quasi-likelihood with Shrunken Dispersion Estimates**. In: *Statistical applications in genetics and molecular biology.* vol. 11; 2012.
70. Phipson B, Lee S, Majewski IJ, Alexander WS, Smyth GK: **ROBUST HYPERPARAMETER ESTIMATION PROTECTS AGAINST HYPERVARIABLE GENES AND IMPROVES POWER TO DETECT DIFFERENTIAL EXPRESSION**. *The annals of applied statistics* 2016, **10**(2):946-963.
71. Love MI, Huber W, Anders S: **Moderated estimation of fold change and dispersion for RNA-seq data with DESeq2**. *Genome Biology* 2014, **15**(12):550.
72. Treviño S, Nyberg A, Del Genio CI, Bassler KE: **Fast and accurate determination of modularity and its effect size**. *Journal of Statistical Mechanics: Theory and Experiment* 2015, **2015**(2):P02003.
73. Bhavnani SK, Chen T, Ayyaswamy A, Visweswaran S, Bellala G, Rohit D, Kevin EB: **Enabling Comprehension of Patient Subgroups and Characteristics in Large Bipartite Networks: Implications for Precision Medicine**. *AMIA Joint Summits on Translational Science proceedings AMIA Joint Summits on Translational Science* 2017, **2017**:21-29.
74. Krämer A, Green J, Pollard J, Jr, Tugendreich S: **Causal analysis approaches in Ingenuity Pathway Analysis**. *Bioinformatics* 2013, **30**(4):523-530.
75. Rand WM: **Objective Criteria for the Evaluation of Clustering Methods**. *Journal of the American Statistical Association* 1971, **66**(336):846-850.
76. Hubert L, Arabie P: **Comparing partitions**. *Journal of Classification* 1985, **2**(1):193-218.
77. Chauhan R, Ravi J, Datta P, Chen T, Schnappinger D, Bassler KE, Balázsi G, Gennaro ML: **Reconstruction and topological characterization of the sigma**

factor regulatory network of Mycobacterium tuberculosis. *Nature Communications* 2016, **7**:11062.
78. Azzam EI, Jay-Gerin JP, Pain D: **Ionizing radiation-induced metabolic oxidative stress and prolonged cell injury**. *Cancer letters* 2012, **327**(1-2):48-60.
79. Turrens JF, Alexandre A, Lehninger AL: **Ubisemiquinone is the electron donor for superoxide formation by complex III of heart mitochondria**. *Archives of biochemistry and biophysics* 1985, **237**(2):408-414.
80. Nohl H: **A novel superoxide radical generator in heart mitochondria**. *FEBS letters* 1987, **214**(2):269-273.
81. Boveris A, Chance B: **The mitochondrial generation of hydrogen peroxide. General properties and effect of hyperbaric oxygen**. *Biochemical Journal* 1973, **134**(3):707.
82. Cadenas E, Davies KJ: **Mitochondrial free radical generation, oxidative stress, and aging**. *Free radical biology & medicine* 2000, **29**(3-4):222-230.
83. Babior BM: **NADPH Oxidase: An Update**. *Blood* 1999, **93**(5):1464.
84. Los M, Schenk H, Hexel K, Baeuerle PA, Dröge W, Schulze-Osthoff K: **IL-2 gene expression and NF-kappa B activation through CD28 requires reactive oxygen production by 5-lipoxygenase**. *The EMBO journal* 1995, **14**(15):3731-3740.
85. Behrmann I, Smyczek T, Heinrich PC, Schmitz-Van de Leur H, Komyod W, Giese B, Müller-Newen G, Haan S, Haan C: **Janus Kinase (Jak) Subcellular Localization Revisited THE EXCLUSIVE MEMBRANE LOCALIZATION OF ENDOGENOUS JANUS KINASE 1 BY CYTOKINE RECEPTOR INTERACTION UNCOVERS THE Jak· RECEPTOR COMPLEX TO BE EQUIVALENT TO A RECEPTOR TYROSINE KINASE**. *Journal of Biological Chemistry* 2004, **279**(34):35486-35493.
86. Rahmani B, Zimmermann MT, Grill DE, Kennedy RB, Oberg AL, White BC, Poland GA, McKinney BA: **Recursive Indirect-Paths Modularity (RIP-M) for Detecting Community Structure in RNA-Seq Co-expression Networks**. *Front Genet* 2016, **7**:80.
87. Bell AW, Deutsch EW, Au CE, Kearney RE, Beavis R, Sechi S, Nilsson T, Bergeron JJM: **A HUPO test sample study reveals common problems in mass spectrometry–based proteomics**. *Nature Methods* 2009, **6**(6):423-430.
88. Liu H, Sadygov RG, Yates JR: **A Model for Random Sampling and Estimation of Relative Protein Abundance in Shotgun Proteomics**. *Analytical Chemistry* 2004, **76**(14):4193-4201.
89. White MY, Brown DA, Sheng S, Cole RN, O'Rourke B, Van Eyk JE: **Parallel Proteomics to Improve Coverage and Confidence in the Partially Annotated Oryctolagus cuniculus Mitochondrial Proteome**. 2011, **10**(2):M110.004291-M004110.
90. Goh WWB, Lee YH, Chung M, Wong L: **How advancement in biological network analysis methods empowers proteomics**. 2012, **12**(4-5):550-563.
91. Lay JO, Liyanage R, Borgmann S, Wilkins CL: **Problems with the "omics"**. *TrAC Trends in Analytical Chemistry* 2006, **25**(11):1046-1056.

92. Navas-Iglesias N, Carrasco-Pancorbo A, Cuadros-Rodríguez L: **From lipids analysis towards lipidomics, a new challenge for the analytical chemistry of the 21st century. Part II: Analytical lipidomics**. 2009, **28**(4):393-403.
93. Limoli CL, Giedzinski E, Baure J, Rola R, Fike JR: **Redox changes induced in hippocampal precursor cells by heavy ion irradiation**. *Radiat Environ Biophys* 2007, **46**(2):167-172.
94. Raber J, Yamazaki J, Torres ERS, Kirchoff N, Stagaman K, Sharpton T, Turker MS, Kronenberg A: **Combined Effects of Three High-Energy Charged Particle Beams Important for Space Flight on Brain, Behavioral and Cognitive Endpoints in B6D2F1 Female and Male Mice**. *Frontiers in Physiology* 2019, **10**.
95. Chang J, Luo Y, Wang Y, Pathak R, Sridharan V, Jones T, Mao XW, Nelson G, Boerma M, Hauer-Jensen M *et al*: **Low Doses of Oxygen Ion Irradiation Cause Acute Damage to Hematopoietic Cells in Mice**. 2016, **11**(7):e0158097.
96. Impey S, Jopson T, Pelz C, Tafessu A, Fareh F, Zuloaga D, Marzulla T, Riparip L-K, Stewart B, Rosi S *et al*: **Short- and long-term effects of 56Fe irradiation on cognition and hippocampal DNA methylation and gene expression**. 2016, **17**(1).
97. Tungjai M, Whorton EB, Rithidech KN: **Persistence of apoptosis and inflammatory responses in the heart and bone marrow of mice following whole-body exposure to 28Silicon (28Si) ions**. 2013, **52**(3):339-350.
98. Chen S, Ren C, Zhai J, Yu J, Zhao X, Li Z, Zhang T, Ma W, Han Z, Ma C: **CAFU: a Galaxy framework for exploring unmapped RNA-Seq data**. *Brief Bioinform* 2019.
99. Simon LM, Karg S, Westermann AJ, Engel M, Elbehery AHA, Hense B, Heinig M, Deng L, Theis FJ: **MetaMap: An atlas of metatranscriptomic reads in human disease-related RNA-seq data**. *GigaScience* 2018.
100. Whitacre LK, Tizioto PC, Kim J, Sonstegard TS, Schroeder SG, Alexander LJ, Medrano JF, Schnabel RD, Taylor JF, Decker JE: **What's in your next-generation sequence data? An exploration of unmapped DNA and RNA sequence reads from the bovine reference individual**. *BMC Genomics* 2015, **16**:1114.
101. Jin M, Liu H, He C, Fu J, Xiao Y, Wang Y, Xie W, Wang G, Yan J: **Maize pan-transcriptome provides novel insights into genome complexity and quantitative trait variation**. *Sci Rep* 2016, **6**:18936.
102. Kazemian M, Ren M, Lin JX, Liao W, Spolski R, Leonard WJ: **Comprehensive assembly of novel transcripts from unmapped human RNA-Seq data and their association with cancer**. *Mol Syst Biol* 2015, **11**(8):826.
103. Laine VN, Gossmann TI, van Oers K, Visser ME, Groenen MAM: **Exploring the unmapped DNA and RNA reads in a songbird genome**. *BMC Genomics* 2019, **20**(1):19.
104. Pennica D, Kohr WJ, Fendly BM, Shire SJ, Raab HE, Borchardt PE, Lewis M, Goeddel DV: **Characterization of a recombinant extracellular domain of the type 1 tumor necrosis factor receptor: evidence for tumor necrosis factor-alpha induced receptor aggregation**. *Biochemistry* 1992, **31**(4):1134-1141.

105. Mitani K, Fujita H, Kappas A, Sassa S: **Heme oxygenase is a positive acute-phase reactant in human Hep3B hepatoma cells**. *Blood* 1992, **79**(5):1255-1259.
106. Mueller CR: **The down-regulation of albumin transcription during regeneration is due to the loss of HNF-1 and the D-site transcription factors**. *DNA Cell Biol* 1992, **11**(7):559-566.
107. Mukwaya A, Lennikov A, Xeroudaki M, Mirabelli P, Lachota M, Jensen L, Peebo B, Lagali N: **Time-dependent LXR/RXR pathway modulation characterizes capillary remodeling in inflammatory corneal neovascularization**. *Angiogenesis* 2018, **21**(2):395-413.
108. Kliewer SA, Umesono K, Noonan DJ, Heyman RA, Evans RM: **Convergence of 9-cis retinoic acid and peroxisome proliferator signalling pathways through heterodimer formation of their receptors**. 1992, **358**(6389):771-774.
109. Hughes AR, Putney JW, Jr.: **Metabolism and functions of inositol phosphates**. *Biofactors* 1988, **1**(2):117-121.
110. Reddy JK, Goel SK, Nemali MR, Carrino JJ, Laffler TG, Reddy MK, Sperbeck SJ, Osumi T, Hashimoto T, Lalwani ND: **Transcription regulation of peroxisomal fatty acyl-CoA oxidase and enoyl-CoA hydratase/3-hydroxyacyl-CoA dehydrogenase in rat liver by peroxisome proliferators**. 1986, **83**(6):1747-1751.
111. Guo B, Rothstein TL: **B Cell Receptor (BCR) Cross-Talk: IL-4 Creates an Alternate Pathway for BCR-Induced ERK Activation That Is Phosphatidylinositol 3-Kinase Independent**. 2005, **174**(9):5375-5381.
112. Kiyokawa H, Busquets X, Powell CT, Ngo L, Rifkind RA, Marks PA: **Cloning of a D-type cyclin from murine erythroleukemia cells**. 1992, **89**(6):2444-2447.
113. Bredt DS, Snyder SH: **Isolation of nitric oxide synthetase, a calmodulin-requiring enzyme**. 1990, **87**(2):682-685.
114. Altmann M, Sonenberg N, Trachsel H: **Translation in Saccharomyces cerevisiae: initiation factor 4E-dependent cell-free system**. 1989, **9**(10):4467-4472.
115. Castrillo A, Tontonoz P: **Nuclear receptors in macrophage biology: at the crossroads of lipid metabolism and inflammation**. *Annu Rev Cell Dev Biol* 2004, **20**:455-480.
116. Joseph SB, Castrillo A, Laffitte BA, Mangelsdorf DJ, Tontonoz P: **Reciprocal regulation of inflammation and lipid metabolism by liver X receptors**. *Nature Medicine* 2003, **9**(2):213-219.
117. Cohen S: **Cell mediated immunity and the inflammatory system**. 1976, **7**(3):249-264.
118. Detmers PA, Lo SK, Olsen-Egbert E, Walz A, Baggiolini M, Cohn ZA: **Neutrophil-activating protein 1/interleukin 8 stimulates the binding activity of the leukocyte adhesion receptor CD11b/CD18 on human neutrophils**. *J Exp Med* 1990, **171**(4):1155-1162.
119. Smith WB, Gamble JR, Clark-Lewis I, Vadas MA: **Interleukin-8 induces neutrophil transendothelial migration**. *Immunology* 1991, **72**(1):65-72.
120. Levin AA, Sturzenbecker LJ, Kazmer S, Bosakowski T, Huselton C, Allenby G, Speck J, Ratzeisen C, Rosenberger M, Lovey A *et al*: **9-Cis retinoic acid**

stereoisomer binds and activates the nuclear receptor RXRα. 1992, **355**(6358):359-361.
121. Edwards CK, 3rd, Lorence RM, Dunham DM, Arkins S, Yunger LM, Greager JA, Walter RJ, Dantzer R, Kelley KW: **Hypophysectomy inhibits the synthesis of tumor necrosis factor alpha by rat macrophages: partial restoration by exogenous growth hormone or interferon gamma**. *Endocrinology* 1991, **128**(2):989-986.
122. Kim JB, Spiegelman BM: **ADD1/SREBP1 promotes adipocyte differentiation and gene expression linked to fatty acid metabolism**. 1996, **10**(9):1096-1107.
123. Tang QQ, Lane MD: **Role of C/EBP homologous protein (CHOP-10) in the programmed activation of CCAAT/enhancer-binding protein-beta during adipogenesis**. 2000, **97**(23):12446-12450.
124. Choy L, Derynck R: **Transforming Growth Factor-β Inhibits Adipocyte Differentiation by Smad3 Interacting with CCAAT/Enhancer-binding Protein (C/EBP) and Repressing C/EBP Transactivation Function**. *Journal of Biological Chemistry* 2003, **278**(11):9609-9619.
125. Sawyers CL, Callahan W, Witte ON: **Dominant negative MYC blocks transformation by ABL oncogenes**. 1992, **70**(6):901-910.
126. Towatari M, Adachi K, Kato H, Saito H: **Absence of the human retinoblastoma gene product in the megakaryoblastic crisis of chronic myelogenous leukemia**. *Blood* 1991, **78**(9):2178-2181.
127. Gishizky ML, Cortez D, Pendergast AM: **Mutant forms of growth factor-binding protein-2 reverse BCR-ABL-induced transformation**. 1995, **92**(24):10889-10893.
128. Ali R, Sauerbier W: **Effects of Ultraviolet Irradiation and Postirradiation Incubation on Heterogeneous Nuclear RNA Size in Murine Cells**. 1978, **22**(3):393-411.
129. Kaartinen V, Voncken JW, Shuler C, Warburton D, Bu D, Heisterkamp N, Groffen J: **Abnormal lung development and cleft palate in mice lacking TGF–β3 indicates defects of epithelial–mesenchymal interaction**. 1995, **11**(4):415-421.
130. Bissonnette RP, Brunner T, Lazarchik SB, Yoo NJ, Boehm MF, Green DR, Heyman RA: **9-cis retinoic acid inhibition of activation-induced apoptosis is mediated via regulation of fas ligand and requires retinoic acid receptor and retinoid X receptor activation**. 1995, **15**(10):5576-5585.
131. Sakamoto W, Fujie K, Handa H: **Inhibition of prostaglandin E2 and superoxide anion production in rat peritoneal macrophages by the calcium antagonists nifedipine and nisoldipine**. *Arzneimittelforschung* 1991, **41**(8):781-785.
132. Collart MA, Belin D, Vassalli JD, de Kossodo S, Vassalli P: **Gamma interferon enhances macrophage transcription of the tumor necrosis factor/cachectin, interleukin 1, and urokinase genes, which are controlled by short-lived repressors**. *J Exp Med* 1986, **164**(6):2113-2118.
133. Nathan CF, Murray HW, Wiebe ME, Rubin BY: **Identification of interferon-gamma as the lymphokine that activates human macrophage oxidative metabolism and antimicrobial activity**. *J Exp Med* 1983, **158**(3):670-689.

134. Baker SJ, Kerppola TK, Luk D, Vandenberg MT, Marshak DR, Curran T, Abate C: **Jun is phosphorylated by several protein kinases at the same sites that are modified in serum-stimulated fibroblasts**. 1992, **12**(10):4694-4705.
135. Myers MG, Backer JM, Sun XJ, Shoelson S, Hu P, Schlessinger J, Yoakim M, Schaffhausen B, White MF: **IRS-1 activates phosphatidylinositol 3'-kinase by associating with src homology 2 domains of p85**. 1992, **89**(21):10350-10354.
136. De Leon DD, Wilson DM, Powers M, Rosenfeld RG: **Effects of Insulin-Like Growth Factors (IGFs) and IGF Receptor Antibodies on the Proliferation of Human Breast Cancer Cells**. 1992, **6**(4):327-336.
137. Sridharan DM, Asaithamby A, Bailey SM, Costes SV, Doetsch PW, Dynan WS, Kronenberg A, Rithidech KN, Saha J, Snijders AM *et al*: **Understanding Cancer Development Processes after HZE-Particle Exposure: Roles of ROS, DNA Damage Repair and Inflammation**. *Radiation Research* 2015, **183**(1):1-26.
138. Tamir I, Cambier JC: **Antigen receptor signaling: integration of protein tyrosine kinase functions**. 1998, **17**(11):1353-1364.
139. Kurosaki T: **GENETIC ANALYSIS OF B CELL ANTIGEN RECEPTOR SIGNALING**. *Annual Review of Immunology* 1999, **17**(1):555-592.
140. Pennica D, Kohr WJ, Fendly BM, Shire SJ, Raab HE, Borchardt PE, Lewis M, Goeddel DV: **Characterization of a recombinant extracellular domain of the type 1 tumor necrosis factor receptor: evidence for tumor necrosis factor .alpha. induced receptor aggregation**. *Biochemistry* 1992, **31**(4):1134-1141.
141. Li A, Dubey S, Varney ML, Dave BJ, Singh RK: **IL-8 Directly Enhanced Endothelial Cell Survival, Proliferation, and Matrix Metalloproteinases Production and Regulated Angiogenesis**. *The Journal of Immunology* 2003, **170**(6):3369-3376.
142. Itoh Y, Joh T, Tanida S, Sasaki M, Kataoka H, Itoh K, Oshima T, Ogasawara N, Togawa S, Wada T: **IL-8 promotes cell proliferation and migration through metalloproteinase-cleavage proHB-EGF in human colon carcinoma cells**. 2005.
143. Bernstein BE, Kamal M, Lindblad-Toh K, Bekiranov S, Bailey DK, Huebert DJ, McMahon S, Karlsson EK, Kulbokas EJ, Gingeras TR *et al*: **Genomic Maps and Comparative Analysis of Histone Modifications in Human and Mouse**. *Cell* 2005, **120**(2):169-181.
144. Heintzman ND, Stuart RK, Hon G, Fu Y, Ching CW, Hawkins RD, Barrera LO, Van Calcar S, Qu C, Ching KA *et al*: **Distinct and predictive chromatin signatures of transcriptional promoters and enhancers in the human genome**. *Nature Genetics* 2007, **39**(3):311-318.
145. Guo J, Zeitlin C, Wimmer-Schweingruber RF, Hassler DM, Ehresmann B, Kohler J, Bohm E, Bottcher S, Brinza D, Burmeister S *et al*: **MSL-RAD radiation environment measurements**. *Radiat Prot Dosimetry* 2015, **166**(1-4):290-294.
146. Dagogo-Jack I, Shaw AT: **Tumour heterogeneity and resistance to cancer therapies**. *Nature Reviews Clinical Oncology* 2018, **15**(2):81-94.
147. McGranahan N, Swanton C: **Clonal Heterogeneity and Tumor Evolution: Past, Present, and the Future**. *Cell* 2017, **168**(4):613-628.
148. Jamal-Hanjani M, Wilson GA, McGranahan N, Birkbak NJ, Watkins TBK, Veeriah S, Shafi S, Johnson DH, Mitter R, Rosenthal R *et al*: **Tracking the**

Evolution of Non–Small-Cell Lung Cancer. *New England Journal of Medicine* 2017, **376**(22):2109-2121.
149. Nowell P: **The clonal evolution of tumor cell populations**. *Science* 1976, **194**(4260):23-28.
150. Piotrowska Z, Niederst MJ, Karlovich CA, Wakelee HA, Neal JW, Mino-Kenudson M, Fulton L, Hata AN, Lockerman EL, Kalsy A *et al*: **Heterogeneity Underlies the Emergence of EGFRT790 Wild-Type Clones Following Treatment of T790M-Positive Cancers with a Third-Generation EGFR Inhibitor**. *Cancer Discovery* 2015, **5**(7):713-722.
151. Seeley EH, Caprioli RM: **MALDI imaging mass spectrometry of human tissue: method challenges and clinical perspectives**. 2011, **29**(3):136-143.
152. Drake RR, Powers TW, Jones EE, Bruner E, Mehta AS, Angel PM: **MALDI Mass Spectrometry Imaging of N-Linked Glycans in Cancer Tissues**. *Adv Cancer Res* 2017, **134**:85-116.
153. Dekker TJA, Balluff BD, Jones EA, Schöne CD, Schmitt M, Aubele M, Kroep JR, Smit VTHBM, Tollenaar RAEM, Mesker WE *et al*: **Multicenter Matrix-Assisted Laser Desorption/Ionization Mass Spectrometry Imaging (MALDI MSI) Identifies Proteomic Differences in Breast-Cancer-Associated Stroma**. 2014, **13**(11):4730-4738.
154. Buck A, Halbritter S, Späth C, Feuchtinger A, Aichler M, Zitzelsberger H, Janssen K-P, Walch A: **Distribution and quantification of irinotecan and its active metabolite SN-38 in colon cancer murine model systems using MALDI MSI**. *Analytical and Bioanalytical Chemistry* 2015, **407**(8):2107-2116.
155. Willems SM, Van Remoortere A, Van Zeijl R, Deelder AM, McDonnell LA, Hogendoorn PC: **Imaging mass spectrometry of myxoid sarcomas identifies proteins and lipids specific to tumour type and grade, and reveals biochemical intratumour heterogeneity**. 2010, **222**(4):400-409.
156. Jones EA, Van Remoortere A, Van Zeijl RJM, Hogendoorn PCW, Bovée JVMG, Deelder AM, McDonnell LA: **Multiple Statistical Analysis Techniques Corroborate Intratumor Heterogeneity in Imaging Mass Spectrometry Datasets of Myxofibrosarcoma**. *PLoS ONE* 2011, **6**(9):e24913.
157. Balluff B, Frese CK, Maier SK, Schöne C, Kuster B, Schmitt M, Aubele M, Höfler H, Deelder AM, Heck A, Jr. *et al*: **De novo discovery of phenotypic intratumour heterogeneity using imaging mass spectrometry**. 2015, **235**(1):3-13.
158. Fuchs B, Suss R, Schiller J: **An update of MALDI-TOF mass spectrometry in lipid research**. *Prog Lipid Res* 2010, **49**(4):450-475.
159. Mann HB, Whitney DR: **On a Test of Whether one of Two Random Variables is Stochastically Larger than the Other**. *The Annals of Mathematical Statistics* 1947, **18**(1):50-60.
160. Hanselmann M, Kirchner M, Renard BY, Amstalden ER, Glunde K, Heeren RMA, Hamprecht FA: **Concise Representation of Mass Spectrometry Images by Probabilistic Latent Semantic Analysis**. *Analytical Chemistry* 2008, **80**(24):9649-9658.
161. Diehl HC, Beine B, Elm J, Trede D, Ahrens M, Eisenacher M, Marcus K, Meyer HE, Henkel C: **The challenge of on-tissue digestion for MALDI MSI- a**

comparison of different protocols to improve imaging experiments. *Anal Bioanal Chem* 2015, **407**(8):2223-2243.
162. Gut Y, Boiret M, Bultel L, Renaud T, Chetouani A, Hafiane A, Ginot Y-M, Jennane R: **Application of chemometric algorithms to MALDI mass spectrometry imaging of pharmaceutical tablets**. 2015, **105**:91-100.
163. Bemis KD, Harry A, Eberlin LS, Ferreira C, van de Ven SM, Mallick P, Stolowitz M, Vitek O: **Cardinal: an R package for statistical analysis of mass spectrometry-based imaging experiments**. *Bioinformatics* 2015, **31**(14):2418-2420.
164. Fülöp A, Sammour DA, Erich K, Von Gerichten J, Van Hoogevest P, Sandhoff R, Hopf C: **Molecular imaging of brain localization of liposomes in mice using MALDI mass spectrometry**. *Scientific Reports* 2016, **6**(1):33791.
165. Wildburger NC, Wood PL, Gumin J, Lichti CF, Emmett MR, Lang FF, Nilsson CL: **ESI–MS/MS and MALDI-IMS Localization Reveal Alterations in Phosphatidic Acid, Diacylglycerol, and DHA in Glioma Stem Cell Xenografts**. *Journal of Proteome Research* 2015, **14**(6):2511-2519.
166. Tibshirani R, Hastie T, Narasimhan B, Chu G: **Diagnosis of multiple cancer types by shrunken centroids of gene expression**. *Proceedings of the National Academy of Sciences* 2002, **99**(10):6567-6572.
167. Robinson CV, Rohacs T, Hansen SB: **Tools for Understanding Nanoscale Lipid Regulation of Ion Channels**. *Trends in Biochemical Sciences* 2019, **44**(9):795-806.
168. Comoglio Y, Levitz J, Kienzler MA, Lesage F, Isacoff EY, Sandoz G: **Phospholipase D2 specifically regulates TREK potassium channels via direct interaction and local production of phosphatidic acid**. 2014, **111**(37):13547-13552.
169. Welti R: **Profiling Membrane Lipids in Plant Stress Responses. ROLE OF PHOSPHOLIPASE Dalpha IN FREEZING-INDUCED LIPID CHANGES IN ARABIDOPSIS**. 2002, **277**(35):31994-32002.
170. Yang SF, Freer S, Benson A: **Transphosphatidylation by phospholipase D**. *Journal of Biological Chemistry* 1967, **242**(3):477-484.
171. Kannan M, Riekhof WR, Voelker DR: **Transport of phosphatidylserine from the endoplasmic reticulum to the site of phosphatidylserine decarboxylase2 in yeast**. *Traffic* 2015, **16**(2):123-134.
172. Vickers NJ: **Animal Communication: When I'm Calling You, Will You Answer Too?** *Current Biology* 2017, **27**(14):R713-R715.
173. Wellner N, Diep TA, Janfelt C, Hansen HS: **N-acylation of phosphatidylethanolamine and its biological functions in mammals**. *Biochimica et Biophysica Acta (BBA)-Molecular and Cell Biology of Lipids* 2013, **1831**(3):652-662.
174. Vance JE: **Phosphatidylserine and phosphatidylethanolamine in mammalian cells: two metabolically related aminophospholipids**. *J Lipid Res* 2008, **49**(7):1377-1387.
175. Das UN, Madhavi N, Kumar GS, Padma M, Sangeetha P: **Can tumour cell drug resistance be reversed by essential fatty acids and their metabolites?** 1998, **58**(1):39-54.

176. Higashi H, Hirabayashi Y, Hirota M, Matsumoto M, Kato S: **Detection of ganglioside GM2 in sera and tumor tissues of hepatoma patients**. *Jpn J Cancer Res* 1987, **78**(12):1309-1313.
177. Abel S, Smuts CM, de Villiers C, Gelderblom WCA: **Changes in essential fatty acid patterns associated with normal liver regeneration and the progression of hepatocyte nodules in rat hepatocarcinogenesis**. *Carcinogenesis* 2001, **22**(5):795-804.
178. Abel S, De Kock M, Smuts C, De Villiers C, Swanevelder S, Gelderblom W: **Dietary modulation of fatty acid profiles and oxidative status of rat hepatocyte nodules: Effect of different n− 6/n− 3 fatty acid ratios**. *Lipids* 2004, **39**(10):963-976.
179. Tessitore L, Sesca E, Vance DE: **Inactivation of phosphatidylethanolamine N-methyltransferase-2 in aflatoxin-induced liver cancer and partial reversion of the neoplastic phenotype by PEMT transfection of hepatoma cells**. *International journal of cancer* 2000, **86**(3):362-367.
180. Gibellini F, Smith TK: **The Kennedy pathway-De novo synthesis of phosphatidylethanolamine and phosphatidylcholine**. *IUBMB Life* 2010:n/a-n/a.
181. Kanter JL, Narayana S, Ho PP, Catz I, Warren KG, Sobel RA, Steinman L, Robinson WH: **Lipid microarrays identify key mediators of autoimmune brain inflammation**. *Nature Medicine* 2006, **12**(1):138-143.
182. Langfelder P, Luo R, Oldham MC, Horvath S: **Is my network module preserved and reproducible?** *PLoS computational biology* 2011, **7**(1).
183. Amar D, Safer H, Shamir R: **Dissection of regulatory networks that are altered in disease via differential co-expression**. *PLoS computational biology* 2013, **9**(3).
184. Hu R, Qiu X, Glazko G, Klebanov L, Yakovlev A: **Detecting intergene correlation changes in microarray analysis: a new approach to gene selection**. *BMC bioinformatics* 2009, **10**(1):20.
185. Kostka D, Spang R: **Finding disease specific alterations in the co-expression of genes**. *Bioinformatics* 2004, **20**(suppl_1):i194-i199.
186. Hudson NJ, Reverter A, Dalrymple BP: **A differential wiring analysis of expression data correctly identifies the gene containing the causal mutation**. *PLoS computational biology* 2009, **5**(5).
187. Pierson E, Koller D, Battle A, Mostafavi S, Consortium G: **Sharing and specificity of co-expression networks across 35 human tissues**. *PLoS computational biology* 2015, **11**(5).
188. Yang Y, Han L, Yuan Y, Li J, Hei N, Liang H: **Gene co-expression network analysis reveals common system-level properties of prognostic genes across cancer types. Nat Commun. 2014; 5: 3231**. In.
189. Kogelman LJ, Cirera S, Zhernakova DV, Fredholm M, Franke L, Kadarmideen HN: **Identification of co-expression gene networks, regulatory genes and pathways for obesity based on adipose tissue RNA Sequencing in a porcine model**. *BMC medical genomics* 2014, **7**(1):57.
190. Mortazavi A, Pepke S, Jansen C, Marinov GK, Ernst J, Kellis M, Hardison RC, Myers RM, Wold BJ: **Integrating and mining the chromatin landscape of cell-**

type specificity using self-organizing maps. *Genome Research* 2013, **23**(12):2136-2148.
191. Ultsch A: **Data mining and knowledge discovery with emergent self-organizing feature maps for multivariate time series**. In: *Kohonen maps.* Elsevier; 1999: 33-45.
192. Ding L-H, Park S, Peyton M, Girard L, Xie Y, Minna JD, Story MD: **Distinct transcriptome profiles identified in normal human bronchial epithelial cells after exposure to γ-rays and different elemental particles of high Z and energy**. *BMC genomics* 2013, **14**(1):372.
193. Miousse IR, Chang J, Shao L, Pathak R, Nzabarushimana É, Kutanzi KR, Landes RD, Tackett AJ, Hauer-Jensen M, Zhou D: **Inter-strain differences in LINE-1 DNA methylation in the mouse hematopoietic system in response to exposure to ionizing radiation**. *International journal of molecular sciences* 2017, **18**(7):1430.
194. Koturbash I, Miousse IR, Sridharan V, Nzabarushimana E, Skinner CM, Melnyk SB, Pavliv O, Hauer-Jensen M, Nelson GA, Boerma M: **Radiation-induced changes in DNA methylation of repetitive elements in the mouse heart**. *Mutation Research/Fundamental and Molecular Mechanisms of Mutagenesis* 2016, **787**:43-53.
195. Wang J, Zhang Y, Xu K, Mao X, Xue L, Liu X, Yu H, Chen L, Chu X: **Genome-wide screen of DNA methylation changes induced by low dose X-ray radiation in mice**. *PloS one* 2014, **9**(3).
196. Newman MR, Sykes PJ, Blyth BJ, Bezak E, Lawrence MD, Morel KL, Ormsby RJ: **The methylation of DNA repeat elements is sex-dependent and temporally different in response to X radiation in radiosensitive and radioresistant mouse strains**. *Radiation research* 2014, **181**(1):65-75.
197. Prior S, Miousse IR, Nzabarushimana E, Pathak R, Skinner C, Kutanzi KR, Allen AR, Raber J, Tackett AJ, Hauer-Jensen M: **Densely ionizing radiation affects DNA methylation of selective LINE-1 elements**. *Environmental research* 2016, **150**:470-481.
198. Kennedy E, Powell D, Li Z, Bell J, Barwick B, Feng H, McCrary M, Dwivedi B, Kowalski J, Dynan W: **Galactic cosmic radiation induces persistent epigenome alterations relevant to human lung cancer**. *Scientific reports* 2018, **8**(1):1-14.

10 VITA

BIOGRAPHICAL

Anna M. Nia
U.S. Citizen
Email: anna.nia@ucla.edu
Email: amnia@utmb.edu
Cell: +1-310-467-8324
ORCID ID: 0000-0003-2757-7267
https://orcid.org/0000-0003-2757-7267
Google Scholar Profile:
https://scholar.google.com/citations?user=ahhZ6awAAAAJ&hl=en

PRESENT POSITION

Aug 2015 - Present: **M.D.-Ph.D. Candidate**, School of Medicine and Department of Molecular Biophysics
University of Texas Medical Branch (UTMB), Galveston, TX, USA

EDUCATION

Aug 2015 - Present: **M.D.-Ph.D Candidate**, Medicine and Ph.D. in Molecular Biophysics
University of Texas Medical Branch (UTMB), Galveston, TX, USA
Ph.D. Thesis Advisor: Dr. Mark Emmett

Sep 2013 - Aug 2015: **M.S.,** Bioengineering
University of California, Los Angeles (UCLA), Los Angeles, CA, USA
Master's Thesis Advisor: Dr. Alan Garfinkel

Sep 2008 - Dec 2012: **B.S.,** Major in Neuroscience, Minor in Biomedical Research
Departmental Highest Honors, Magna Cum Laude, College Honors
University of California, Los Angeles (UCLA), Los Angeles, CA, USA
Undergraduate Thesis Advisor: Dr. Felix Schweizer

PUBLICATIONS

[6] **Nia, A.M.,** Chen, T., Barnette, B.L., Khanipov, K., Ullrich, R., Bhavnani, S., Emmett, M.R. (2020), "Efficient Identification of Multiple Pathways: RNA-Seq Analysis of Livers from ^{56}Fe Ion Irradiated Mice", *BMC Bioinformatics*, DOI: 10.1186/s12859-020-3446-5
Retrieved from https://bmcbioinformatics.biomedcentral.com/articles/10.1186/s12859-020-3446-5?utm_source=other&utm_medium=other&utm_content=null&utm_campaign=BSCN_2_DD01_CN_bmcso_article_paid_XMOL

[5] **Nia, A.M.,** Zavlin, D. (2019). "The Burden of Physicians' Administrative Workload Affects Clinical and Scientific Mentoring" *AMEE MedEdPublish*, DOI: 10.15694/mep.2019.000074.1
Retrieved from https://www.mededpublish.org/manuscripts/2318

[4] **Nia, A.M.,** Branch, D.W., Maynard, K., Frank, T., Zavlin, D., Patterson, J.T., Lall, R.R. (2019). "Metabolic Syndrome Associated with Increased Rates of Medical Complications Following Intracranial Tumor Resection" *World Neurosurgery*, PMID: 30878753, DOI: 10.1016/j.wneu.2019.03.046
Retrieved from https://www.sciencedirect.com/science/article/pii/S1878875019306734?via%3Dihub

[3] Zavlin, D., Chegireddy, V., Nguyen-Lee, J.J., Shih, L., **Nia A.M.,** Friedman, J.D., Echo, A. (2018). "Training E_ects of Visual Stroboscopic Impairment on Surgical Performance: A Randomized-Controlled Trial." *Journal of Surgical Education*, PMID: 30131280, DOI: 10.1016/j.jsurg.2018.07.018.
Retrieved from https://www.sciencedirect.com/science/article/pii/S1931720418304057?via%3Dihub

[2] Zavlin, D., Chegireddy, V., Boukovalas, S., **Nia, A.M.,** Branski, L.K., Friedman, J.D., Echo, A. (2018). "Multi-Institutional Analysis of Independent Predictors for Burn Mortality in the United States." *Burns & Trauma*, PMID: 30151396, DOI: 10.1186/s41038-018-0127-y
Retrieved from https://burnstrauma.biomedcentral.com/articles/10.1186/s41038-018-0127-y

[1] **Nia, A.M.** (2015). "Multi Negative Feedback Loops and Nonlinear Time-Delays in a Mathematical Model of Bone Morphogenetic Protein (BMP) Signaling in Vascular Endothelial Cells." *eScholarship*, UCLA, ProQuest ID: Nia_ucla_0031N_13904. Merritt ID: ark:/13030/m5vx3bjw.
Retrieved from https://escholarship.org/uc/item/5m96170m

SUBMITTED FOR PUBLICATION

[3] **Nia, A.M.,** Khanipov, K., Barnette, B.L., Ullrich, R., Golovko, G., Emmett, M.R. (2020), "Comparative RNA-Seq Transcriptome Analyses Reveal Dynamic Time-Dependent Effects of ^{56}Fe, ^{16}O, and ^{28}Si Irradiation on the Induction of Murine Hepatocellular Carcinoma", *BMC Genomics,* DOI: 10.21203/rs.3.rs-17127/v1
Retrieved from https://www.researchsquare.com/article/rs-17127/v1

[2] **Nia, A.M.,** Branch, D.W., Maynard, K., Frank, T., Guillet, J.Y., Patterson, J.T., Lall, R.R. (2020), "How the Elderly Fare After Brain Tumor Surgery Compared to Younger Patients: A National Surgical Quality Improvement Program Analysis of 30,183 Cases", *Journal of Clinical Neuroscience*

[1] Golovko, G., Khanipov, K., Albayrak, L., **Nia, A.M.,** Duarte, R.S.A., Chumakov, S., Fofanov, Y., (2020), "Identification of Multidimensional Boolean Patterns in Microbial Communities", *Microbiome*

ABSTRACTS AND RESEARCH PRESENTATIONS

[25] **Nia, A.M.** (presenting author), Allison, R., Branch, D.W., Khanipov, K., Golovko, G., Guillet, J.Y., Patterson, J.T., Lall, R.R., "Using Machine Learning Algorithms for Prediction of Postoperative Length of Hospital Stay and Discharge Disposition After Craniotomy for Resection of Craniopharyngiomas in Adults: A National Surgical Quality Improvement Program Analysis of 2011 to 2017" Poster Presentation, American Association of Neurological Surgeons, Boston, MA, April 2020

[24] Golovko, G. (presenting author), Khanipov, K., **Nia, A.M.,** Evangelista, L., Fofanov, Y., "Methodology and Infrastructure of Integrating Multi-Omics Data with EMR to Advance Precision Medicine Research " Oral Presentation, Association for Clinical and Translational Science, Data Science Session, Washington, DC, April 2020

[23] Khanipov, K. (presenting author), Golovko, G., **Nia, A.M.,** Evangelista, L., Fofanov, Y., "Interactions of the Infant Nasopharyngeal Microbiota and Subjects' Clinical Traits in Development of Viral Upper Respiratory Tract Infections and Acute Otitis Media " Poster Presentation, Association for Clinical and Translational Science, Data Science Session, Washington, DC, April 2020

[22] Ali, A. (presenting author), Moth, J.L., McFarland, J.R., Crandall, C.K., Sweeney, M., **Nia, A.M.,** Miles, B.L., Korst, G., Hrushka J.M., Merrill, A.D., Allison, R.Z., "Impact of Hard Hats for Little Heads in L.A. Morgan Elementary School" Poster Presentation, Public Health Symposium, The University of Texas Medical Branch, Galveston, TX, April 2020

[21] **Nia, A.M.** (presenting author), Khanipov, K., Golovko, G., "Effects of Injectable, Erythropoietin and Glucocorticoids Combinational Therapy on Erythrocyte Sedimentation Rate Following Spinal Cord Injury" Poster Presentation, Association for Clinical and Translational Science, Data Science Session, Washington, DC, April 2020

[20] **Nia, A.M.** (presenting author), Chen, T., Barnette, B., Khanipov, K., Ullrich, R., Bhavnani, S., Emmett, M.R., "Application of Modularity Maximization Algorithm for RNA-Seq Analysis of Livers from ^{56}Fe Ion Irradiated Mice" Poster Presentation, NASA Human Research Program Investigator's Conference, Galveston, TX, January 2020

[19] **Nia, A.M.** (presenting author), Branch, D.W., Maynard, K., Frank, T., Guillet, J.Y., Patterson, J.T., Lall, R.R., "Complications and Total Length of Hospital Stay after Craniotomy for Tumor in Elderly Patients: A National Surgical Quality Improvement Program Analysis of 30,183 Patients from 2008 to 2016" Poster Presentation, American Association of Neurological Surgeons, San Diego, CA, April 2019

[18] Zavlin, D. (presenting author), Chegireddy, V., Nguyen-lee, J.J., Shih, L., **Nia, A.M.,** Friedman, J.D., Echo, A. "E_ects of Limited Visual Input on Surgical Performance: a Randomized-Controlled Trial" Poster Presentation, The Society of American Gastrointestinal and Endoscopic Surgeons, Baltimore, MD, April 2019

[17] Chegireddy, V. (presenting author), Zavlin, D., Nguyen-lee, J.J., Shih, L., **Nia, A.M.,** Friedman, J.D., Echo, A. "Effects of Limited Visual Input on Surgical Performance: a Randomized-Controlled Trial" Oral Presentation, American Society for Reconstructive Microsurgery, Palm Desert, CA, February 2019

[16] Emmett, M.R. (presenting author), Barnette, B.L., **Nia, A.M.,** Strain, S.K., Lichti, C.F., Yu, Y., Ullrich, R.L., "Molecular Biosynthetic Pathway Alterations Induced By Low Dose, High Charge, High-Energy Ions (HZE): A Multi-Omics Study of HZE-Induced Hepatocelullar Carcinoma (HCC)" Poster Presentation, NASA Human Research Program Investigator's Conference, Galveston, TX, January 2019

[15] Barnette, B.L. (presenting author), **Nia, A.M.,** Strain, S.K., Lichti, C.F., Yu, Y., Ullrich, R.L., Emmett, M.R. "An Integrated Omics Approach to Define the Molecular Mechanisms Induced by Low Dose, High-Energy, High Charge Ions (HZE) in Relation to Hepatocellular Carcinoma (HCC)" Poster Presentation, NASA Human Research Program Investigator's Conference, Galveston, TX, January 2019

[14] **Nia, A.M.** (presenting author), Shavkunov, A., Ullrich, R.L., Emmett, M.R. "Radiation Induced Lipid Changes in Liver by MALDI Imaging Combined with Spatial Shrunken Centroid Clustering" Poster Presentation, NASA Human Research Program Investigator's Conference, Galveston, TX, January 2019

[13] Barnette, B.L. (presenting author), **Nia, A.M.,** Strain, S.K., Lichti, C.F., Yu, Y., Ullrich, R.L., Emmett, M.R. "An Integrated Omics Approach to Define the Molecular Mechanisms Induced by Low Dose, High-Energy, High Charge Ions (HZE) in Relation to Hepatocellular Carcinoma (HCC)" Poster Presentation, University of Texas Medical Branch, Department of Biochemistry and Molecular Biology Annual Retreat, Galveston, TX, October 2018

[12] **Nia, A.M.** (presenting author), Barnette, B.L., Strain, S.K., Lichti, C.F., Yu, Y., Ullrich, R., Emmett, M.R. "Computational Mathematics Assimilation of Large Multi-Omics Datasets" Poster Presentation, University of Texas Medical Branch, Department of Biochemistry and Molecular Biology Annual Retreat, Galveston, TX, October 2018

[11] **Nia, A.M.** (presenting author), Branch, D.W., Maynard, K., Frank, T., Patterson, J.T., Lall, R.R., "Ramifications of Metabolic Syndrome on Intracranial Tumor Resections in the United States" Oral Presentation, Tumor Session, Congress of Neurological Surgeons, Houston, TX, October 2018

[10] Steinberg, A.J. (presenting author), Zavlin, D., Chegireddy, V., **Nia, A.M.,** Ellsworth, W.A. "Impact of Breast Ptosis on Contralateral Prophylactic Mastectomy and Postoperative Morbidity during Microsurgical Reconstruction." Oral Presentation, Texas Society of Plastic Surgeons, San Antonio, TX, September 2018

[9] **Nia, A.M.** (presenting author), Barnette, B.L., Strain, S.K., Lichti, C.F., Yu, Y., Ullrich, R., Emmett, M.R. "Computational Mathematics Assimilation of Large Multi-Omics Datasets" Poster Presentation, Informatics Session, American Society of Mass Spectrometry, San Diego, CA, June 2018

[8] Barnette, B.L. (presenting author), **Nia, A.M.,** Strain, S.K., Lichti, C.F., Yu, Y., Ullrich, R., Emmett, M.R. "An Integrated Omics Approach to Define the Molecular Mechanisms of Galactic Cosmic Ray Induced Hepatocellular Carcinoma" Poster Presentation, System Biology Session, American Society of Mass Spectrometry, San Diego, CA, June 2018

[7] Zavlin, D. (presenting author), Chegireddy, V., Nguyen-lee, J.J., Shih, L., **Nia, A.M.,** Friedman, J.D., Echo, A. "E_ects of Limited Visual Input on Surgical Performance: a Randomized-Controlled Trial." Oral Presentation, Houston Methodist Bookout Symposium, Houston, TX, June 2018

[6] Barnette, B.L. (presenting author), **Nia, A.M.,** Strain, S.K., Lichti, C.F., Yu, Y., Ullrich, R., Emmett, M.R. "An Integrated Omics Approach to Define the Molecular Mechanisms of Hepatocellular Carcinoma (HCC) Induced by Low Dose, High-Energy, High Charge Ions (HZE)" Oral Presentation, NASA Human Research Program Investigator's Conference, Galveston, TX, January 2018

[5] **Nia, A.M.** (presenting author), Guo, Y., Guihard, P., Bostrom, K., Garfinkel, A., "Multi-Negative Feedback Loops and Nonlinear Time-Delays in a Mathematical Model of Bone Morphogenetic Protein (BMP) Signaling in Vascular Endothelial Cells" Poster Presentation, American Physician Scientists Association (APSA), Texas A&M Health Science Center, College Station, TX, October 2015

[4] **Nia, A.M.** (presenting author), Caputo, A, Schweizer, F.E. "Role of SNAP-25 Ubiquitination in Neurotransmitter Release" Poster Presentation, 15th Annual Science Poster Session, University of California, Los Angeles (UCLA), Los Angeles, CA, May 2012

[3] **Nia, A.M.** (presenting author), Caputo, A, Schweizer, F.E. "Role of SNAP-25 Ubiquitination in Neurotransmitter Release" Poster Presentation, 13th Annual Neuroscience Poster Session, University of California, Los Angeles (UCLA), Los Angeles, CA, May 2012

[2] **Nia, A.M.** (presenting author), Caputo, A, Schweizer, F.E. "Strategies to Study the Role of Fast Dynamic Ubiquitination at Synapses" Oral Presentation, 37th West Coast Biological Sciences Research Conference, Loyola Marymount University, Los Angeles, CA, April 2012

[1] Caputo, A, (presenting author), **Nia, A.M.,** Schweizer, F.E. "Strategies to Study the Role of Fast Dynamic Ubiquitination at Synapses" Poster Presentation, Department of Neurobiology Retreat, University of California, Los Angeles (UCLA), Los Angeles, CA, March 2012